2008

CHARACTERISATION OF LATENT INFECTIONS IN AQUATIC CYANOBACTERIA AND MICROALGAE

LOHR, JAYME ELIZABETH

CHARACTERISATION OF LATENT INFECTIONS IN AQUATIC CYANOBACTERIA AND MICROALGAE

by

JAYME ELIZABETH LOHR

A thesis submitted to the University of Plymouth
in partial fulfilment for the degree of

DOCTOR OF PHILOSOPHY

School of Biological Sciences
Faculty of Science

April 2008

ABSTRACT

Characterisation of latent infections in aquatic cyanobacteria and microalgae

Jayme Elizabeth Lohr

Aquatic photosynthetic microorganisms were surveyed (algae and cyanobacteria) for novel lysogenic/latent viruses and new methodology was established, using a variety of techniques such as AFC, electron microscopy, and molecular tools. The first study assessed *Symbiodinium* sp. cultures as a model system to investigate the induction of potential latent viruses. The study of *Symbiodinium* sp. showed that ca. 37% of the strains tested had a group of filamentous VLPs that is inducible by UV-C treatment. Extrapolation of this virus-host interaction and its effects on zooxanthellae viability provides a novel link to the impact of latent infection on symbiotic dinoflagellates of cnidarians and the subsequent disruption of the reef ecosystems. The second study examined the interaction of a freshwater cyanobacterium and its inducible VLPs. The work carried out on *Pseudanabaena*, strain PPt10905 suggests that this freshwater cyanobacterium harbours a prophage. An unusual interaction was observed in this freshwater cyanobacterium, where the abundance of carboxysome-like particles increased 10 times in heat-treated cultures. The cyanobacterium PPt10905, its inducible VLPs and the co-occurring increase in carboxysomes could be a new mechanism in which lysogeny benefits freshwater cyanobacteria, possibly increasing the host's photosynthetic efficiency. Finally, the third study investigated the presence of latent viruses in the Plymouth culture collection of marine algae. The characterisation and isolation of inducible viruses from this algal culture collection has revealed much novel information on the prevalence of latent viruses in algae. From the 30 algal species examined in this study, over 35% appear to contain an inducible infectious agent. AFC and TEM images have confirmed the presence of VLPs, and thin sections of UV-induced cultures further supported the presence of VLPs in the UV-induced cultures. This work's contribution increases the knowledge of latent and temperate viruses of aquatic microbes, which are underrepresented in previous studies. Additionally, this research established novel techniques for the study of unique biological interactions between aquatic viruses and their hosts that will facilitate and improve subsequent investigation of similar systems.

TABLE OF CONTENTS

LIST OF TABLES

LIST OF FIGURES

LIST OF ABBREVIATIONS

AFC	Analytical flow cytometry
AU	Arbitrary units
BLAST	Basic Alignment Search Tool
bp	Base pair
CCMP	Center for Culture of Marine Phytoplankton
CTAB	Cetyl trimethyl ammonium bromide
dH_2O	Deionised water
ddH_2O	MilliQ water
DNA	Deoxyribonucleic acid
EDTA	Ethylenediaminetetraacetic acid
FISH	Fluorescent *in situ* hybridisation
GLF	Green fluorescence
HAB	Harmful algal bloom
ICTV	International Committee on Taxonomy of Viruses
ITS	Internal transcribed spacer region
kbp	Kilobase
mRNA	messenger RNA
PAR	Photosynthetic Active Radiation
PCC	Plymouth Culture Collection
PCR	Polymerase Chain Reaction
PEG	Polyethylene glycol
PFGE	Pulsed Field Gel Electrophoresis
RNA	Ribonucleic acid
rRNA	Ribosomal RNA
RuBP	Ribulose-1, 5-bisphosphate

SDS	Sodium dodecyl sulfate
SSC	Side scatter
TAE	Tris acetate EDTA
TBE	Tris boric acid EDTA
TEM	Transmission Electron Microscopy
UV	Ultraviolet light
VLP	Virus-like particle

ACKNOWLEDGEMENTS

I would like to thank my advisors, Colin Munn and Willie Wilson who gave me the opportunity to work on this truly exciting research project. They have been a great help all along and taught me discipline and rigor in my work. I enjoyed our discussions and the fact that I was always treated as a colleague even when I was a junior graduate student.

Next, I would like to thank my colleagues at Plymouth Marine Laboratory, Claire Evans and Mike Allen who have always been very accessible and made me feel welcome during my time in the UK. I would like to especially thank Glen Harper and the University of Plymouth electron microscopy laboratory for their help and I will always be grateful to them for introducing me to the Friday fish "n" chips with a pint.

Finally, I would like to thank my family for all their support. I would have never been able to carry on if it wasn't for the continual support and encouragement of my family. The countless hours speaking on the phone made the homesick feeling more bearable.

AUTHOR'S DECLARATION

At no time during the registration for the degree of Doctor of Philosophy has the author been registered for any other University award without prior agreement of the Graduate Committee.

Word count of main body of thesis: 48,498

Signed Jaime John

Date 10/9/2008

CHAPTER 1 Introduction

1.1 The global importance of aquatic viruses

Viruses are the most abundant biological entities on the planet (Rohwer & Edwards, 2002). Most organisms appear to be susceptible to at least one type of virus, which suggests that viruses have an immense diversity. In aquatic environments, viruses are ubiquitous and highly abundant (Bergh *et al.*, 1989; Wommack & Colwell, 2000). Investigations have only recently begun to examine the plethora and diversity of aquatic viruses. Much research has focused on the abundance and diversity of viruses in the oceans, where thousands of genotypes and millions of virus particles have been observed (Bergh *et al.*, 1989; Breitbart *et al.*, 2002). The roles and impacts of the billions of aquatic viruses remain largely unknown, leaving many aspects of aquatic viruses yet to be revealed.

1.1.1 Development of aquatic virus research

The increased knowledge of aquatic viruses may be attributed to the application of powerful new tools and improved techniques for their detection, enumeration and molecular manipulation. The introduction of direct counts, through epifluorescence microscopy, drastically changed the outlook on the importance of viruses by revealing that culture-based techniques had greatly underestimated the number of viruses present in the environment (Noble & Fuhrman, 1998; Wen *et al.*, 2004). Electron microscopy further emphasised the prevalence of viruses when Bergh and coworkers used transmission electron microscopy to show that there are ca. 10 million virus-like particles (VLPs) per ml of seawater (Bergh *et al.*, 1989). Electron microscopy is now routinely used to examine morphological diversity and can provide evidence of viruses in infected cells. Detection, enumeration and measurement of size distributions through the use of analytical flow cytometry (AFC) and pulsed field gel electrophoresis (PFGE)

have also greatly contributed to the knowledge of viruses present in aquatic environments. AFC provides a tool to examine virus-host interaction (Brussaard *et al.*, 2000). AFC not only allows for the detection and enumeration of groups of viruses, it also provides the means to enumerate and monitor the fluorescence of algal hosts (Marie *et al.*, 1999). Size fractionation of viral genomes by PFGE allows changes in viral communities to be monitored and assessed by unique banding patterns (Steward *et al.*, 2000; Wommack *et al.*, 1999).

Molecular techniques such as polymerase chain reaction (PCR) amplification supplied a direct screening method for the presence of specific viruses, while providing insight into the diversity and structure of virus populations. PCR offers rapid amplification and identification of specific gene fragments from different genera of viruses and natural virus communities. DNA polymerase and the major capsid proteins are just a couple of examples of routinely used marker molecules for examining genetic relatedness and inferring phylogenetic relationships among viruses (Chen & Suttle, 1996; Graves & Meints, 1992; Schroeder *et al.*, 2003). Another molecular marker is the RNA-dependent RNA polymerase which has been successfully used to reveal an unexpected large diversity of RNA viruses in the coastal ocean (Culley *et al.*, 2003). Most recently, metagenomics and whole genome sequencing are providing even more insight into the evolution and functions of viruses (Breitbart & Rohwer, 2005; Desnues *et al.*, 2008). Full genome sequencing of viruses provides insights into genome organisation and function among viruses revealing potential links in viral evolution (Allen *et al.*, 2006; Chen & Lu, 2002). Metagenomic studies, or the complete sequencing of every biological entity present in a sample, have identified thousands of viral types never before isolated, giving a glimpse of the potential viruses remaining to be discovered (Edwards & Rohwer, 2005).

1.1.2 Viral Dynamics

Viruses are active and important components of aquatic systems. Viruses can maintain host community diversity by altering the population density of bacteria and algae and/or selecting for certain species (Muhling *et al.*, 2005). The impact of viral lysis on the population dynamics of primary producers and heterotrophic prokaryotes influences the fluxes of organic matter in the microbial loop (Filippini *et al.*, 2006). Viral lysis in aquatic environments reduces the comsumption of primary producers and heterotrophic prokaryotes by grazers and increases the pool of dissolved organic matter, leading to an altered view of the traditional food webs (Fuhrman, 1999; Suttle, 2005). The introduction of viruses into the microbial loop, the virus shunt, diverts and redistributes the flux of organic matter, shifting the food web dynamics (Suttle, 2005; Weinbauer, 2004; Wilhelm & Suttle, 1999) (Figure 1.1).

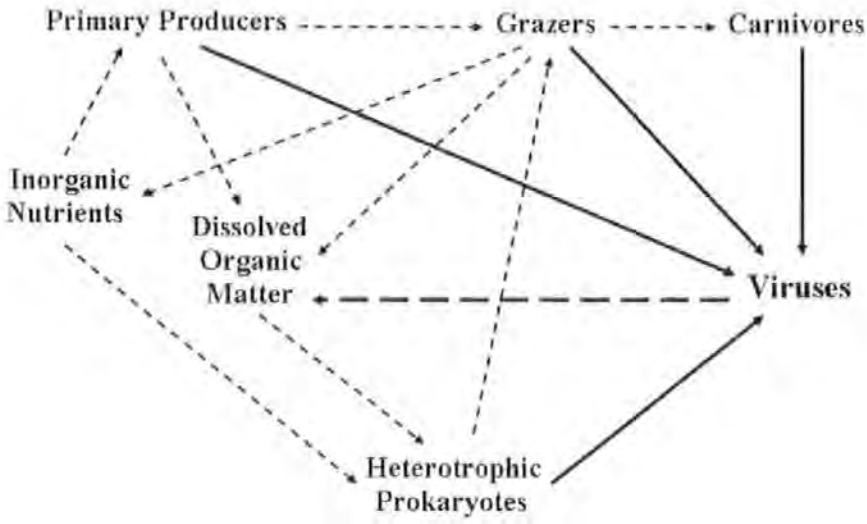

Figure 1.1. Microbial loop with virus shunt; modified from Wilhelm and Suttle (1999).

1.2 Capsid structure and symmetry

Viruses are composed of a nucleic acid genome surrounded by a protein coat (capsid) and replicate as obligate intracellular parasites by taking over the biosynthetic functions within a host cell (Wagner & Hewlett, 2004). The majority of viruses fit into two structural classes based on their capsid structure: icosahedral viruses and helical viruses. The more complex viruses and enveloped viruses use a combination of these symmetries to build parts of their protein shell.

A complete infective virus particle is known as a virion (Wagner & Hewlett, 2004). It consists of nucleic acid surrounded by a capsid. Viral genomes generally code for few proteins to build a capsid, and one or several similar proteins associate into structural units, capsomers. The capsid together with its enclosed nucleic acid is referred to as the nucleocapsid (Wagner & Hewlett, 2004). The capsid shape serves as the basis for morphological distinction. The basic structural forms of viruses are detailed below.

1.2.1 Icosahedral symmetry

Icosahedral capsid symmetry consists of capsomers arranged in a regular geometrical pattern which may be rotated to give a number of identical appearances. An icosahedron is composed of 20 identical facets, each an equilateral triangle, with 12 vertices at the corners (Knipe & Howley, 2001). There is an axis of five-fold rotational symmetry through the centre of each vertex, an axis of three-fold rotational symmetry through the centre of each face and an axis of two-fold rotational symmetry through the centre of each edge to make up the 5:3:2 rotational symmetry shown in figure 1.2 (Dimmock *et al.*, 2001). The capsid is assembled from one or more repeating subunits of viral proteins. The size of capsid varies depending on the size and number of capsomers arranged on the faces of the icosahedron.

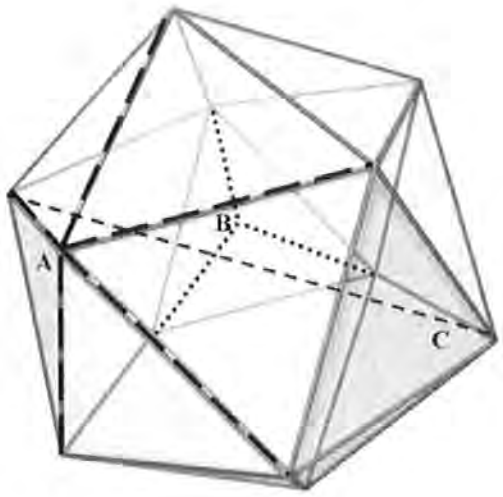

Figure 1.2. The illustration shows the axis of five-fold rotational symmetry (A) at each vertex, the axis of three-fold rotational symmetry (B) through the centre of each face and the axis of two-fold rotational symmetry (C) through the centre of each edge (Modified from Dimmock *et al.*, 2001).

1.2.2 Helical symmetry

Helical symmetry is the simplest way to arrange the multiple, identical protein subunits in the capsid (Dimmock *et al.*, 2001). Rotational symmetry is used to arrange the irregularly shaped proteins around a central axis by stacking repeated components with a constant relationship to one another into a coiled structure to form a helix. A helix can be defined mathematically by two parameters: diameter (amplitude) and the distance covered by each complete turn of the helix (pitch), as shown in figure 1.3 (Knipe & Howley, 2001). The virus genome is bound in the centre of the protein helix by charge interactions.

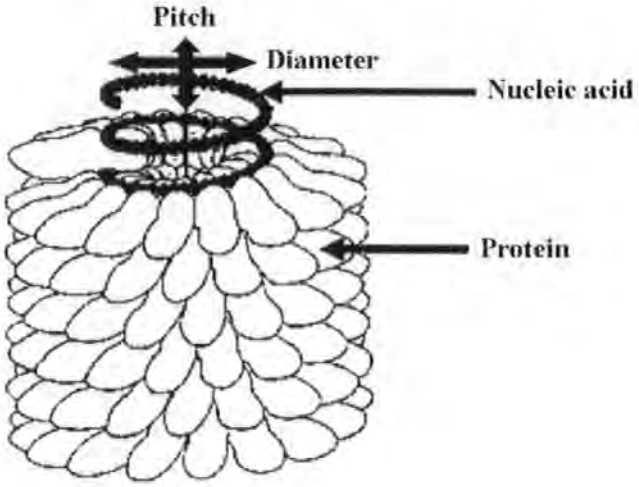

Figure 1.3. The illustration shows the coiling of the helical structure in relation to the pitch and diameter (Modified from Dekker, 1978).

1.2.3 Enveloped viruses

Enveloped viruses have distinct advantages over 'naked' virus particles (Section 1.2.1 and 1.2.2). In 'naked' viruses the capsid proteins are directly exposed to the environment while enveloped viruses are protected by a membrane envelope derived from the host (Dimmock *et al.*, 2001). The enveloped viruses surround themselves in a form of one of the cell membranes or use cytoplasmic membranes or nuclear membranes (Dimmock *et al.*, 2001). This strategy of enveloped viruses allows the viruses to exit the host without destruction of its host. The structure of enveloped viruses may be based on icosahedral or helical symmetry which is formed before, or as, the virus leaves the cell. The site of assembly varies for different viruses; however, enveloped viruses generally use cellular membranes as assembly sites. The virus is transported to the cell surface and subsequently released in a vacuole (Figure 1.4).

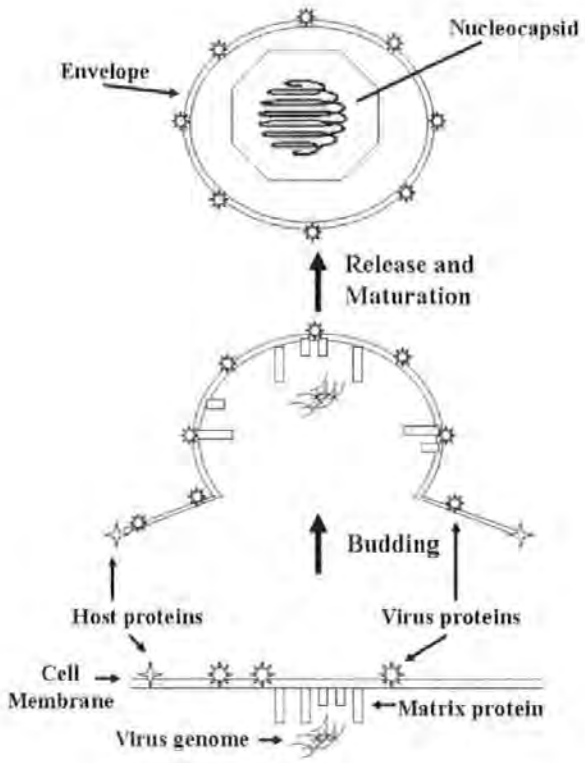

Figure 1.4. The illustration shows the formation of an enveloped virus (Modified from Cann, 2001).

1.2.4 Complex viruses

The particle structure of complex viruses has structural similarities to helical and/or icosahedral symmetry. Many viruses of bacteria (bacteriophage) typically have a complex structure consisting of an icosahedral head and a helical tail (Dimmock *et al.*, 2001). These viruses may possess extra structures such as protein tails and tail fibres. There are separate assembly pathways for the head and tail sections of the particle, which come together at a late stage in the infection cycle to make up the virion (Figure 1.5) (Knipe & Howley, 2001).

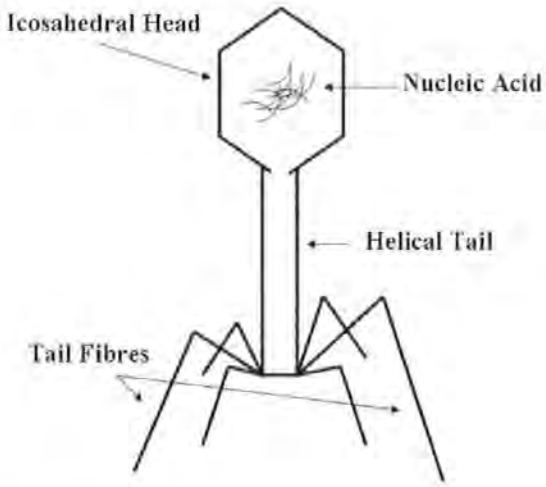

Figure 1.5. Illustration showing the structure of a complex virus (T-even bacteriophage) (adapted from Leiman *et al.*, 2004).

1.3 Replication strategies

Viruses can be classified into seven classes based on their genome types (double-stranded, ds, or single-stranded, ss DNA or RNA) and replication strategies, the Baltimore classification (Baltimore, 1971). The seven classes are: dsDNA viruses (class I), ssDNA viruses (class II), dsRNA viruses (class III), ssRNA viruses with (+) sense genome, (class IV), ssRNA viruses with (-) sense genome (class V), ssRNA viruses with a DNA intermediate (class VI), and dsDNA viruses with a RNA intermediate (class VII).

The Baltimore classification is based on the way in which viruses synthesise messenger RNA (mRNA) (Dimmock *et al.*, 2001). As the viruses do not contain the molecules necessary to translate mRNA, they must rely on the host organism to generate positive strand mRNAs in order to produce proteins and replicate themselves (Dimmock *et al.*, 2001). In dsDNA virus replication, either stand can be used to translate the mRNA. Replication of ssDNA viruses involves the formation of a (-) sense strand, which serves as a template for (+) strand synthesis. The dsRNA viruses have segmented genomes; each segment is transcribed separately to produce monocistronic mRNAs. Translation in

ssRNA viruses with (+) sense genomes form a polyprotein product, which is subsequently cleaved to form the mature proteins. The first step in replication of ssRNA viruses with (-) sense genome is transcription by virus-encoded RNA-dependent RNA polymerase to produce monocistronic mRNAs, which serve as the template for genome replication. In ssRNA viruses with a DNA intermediate, the diploid genome is used as the template for reverse transcription. Reverse transcription is also used by dsDNA viruses with a RNA intermediate, however this occurs inside the virus particle on maturation.

In aquatic environments, most of the replication types have been found. Class I is the most common while no example of Class VII are known in aquatic phytoplankton. Table 1.1 lists examples of several of the replication strategies found in aquatic viruses.

Table 1.1. Replication strategies found in viruses of aquatic phytoplankton. *Not of aquatic origin.

Class	Genome type/replication strategy	Family	Example
I	dsDNA	*Phycodnaviridae*	*Emiliania huxleyi* virus 86 (Schroeder *et al.*, 2002)
II	ssDNA	*Circoviridae*	*Chaetoceros salsugineum* CsNIV (Nagasaki *et al.*, 2005)
III	dsRNA	*Reoviridae*	*Micromonas pusilla* MpRNAV-01B (Brussaard *et al.*, 2004a)
IV	ssRNA (+) sense	*Dicistroviridae*	*Rhizosolenia setigera* RsRNAV (Nagasaki *et al.*, 2004)
V	ssRNA (-) sense	*Marnaviridae*	*Heterosigma akashiwo* HaRNAV (Lang *et al.*, 2004)
VI	ssRNA with DNA intermediate	*Pseudoviridae*	*Volvox carteri Osser virus* (Lindauer *et al.*, 1993)
VII	dsDNA with RNA intermediate	*Caulimoviridae*	*Blueberry red ringspot virus* (Glasheen *et al.*, 2002)*

1.4 Taxonomy

Viruses can be grouped by the hosts they infect, their size, shape and type of infectious lifecycle and/or nucleic acid type. Advances in technology have slowly changed the way viruses are classified. Traditionally, viruses were classified by physical characteristics, type of host and/or type of infection. More recently, morphology of the viruses has been used as a way to classify viruses and even more recently genome similarities have been used to differentiate viruses (Rohwer & Edwards, 2002).

A viral species was formally defined by van Regenmortel as '...a polythetic class of viruses that constitutes a replicating lineage and occupies a particular ecological niche' (van Regenmortel, 1990). The International Committee on Taxonomy of Viruses (ICTV) (Murphy *et al.*, 1995) use this definition for the classification of viruses. A drawback to this formal definition is the requirement that the virus be in culture. Genomic data of viruses are not compatible with the ICTV definition to describe viral species. New terms are continually being established to encompass the data from molecular based viral classification. A viral 'genotype', for example, is one way to distinguish groups of viruses based on sequence similarities (Breitbart *et al.*, 2002). Group and subgroup designations which are comparable to families and subfamilies in the ICTV system have been described to classify viruses of bacteria based on their genomes (Rohwer & Edwards, 2002). Classic definitions and descriptions are slowly changing and will eventually evolve to integrate viral species based on genomic data.

1.4.1 Bacteriophages

Bacteriophages (commonly referred to as phages) are viruses of prokaryotes and include viruses of eubacteria (Calendar, 2006). Traditionally characterised by morphotypes and host genera, bacteriophages are the largest of all virus groups by the number of descriptions (Ackermann, 2001). Phages belonging to 13 virus families are known to

infect over 140 bacterial genera (Calendar, 2006). In the order Caudovirales, *Myoviridae*, *Siphoviridae* and *Podoviridae* represent the three main families of tailed dsDNA phages (96-97%) and polyhedral, filamentous, and pleomorphic phages representing the remaining 3–4% belong to 10 families (Ackermann, 2007) (Figure 1.6). To date there are over two hundred complete phage genomes (Genbank, April 2007). The three main families, *Myoviridae*, *Siphoviridae* and *Podoviridae* differ mainly in head and tail morphology. The family *Myoviridae* is characterised by rigid contractile tails (80-450 nm). The head is separated from tail by a neck, consisting of a central tube and a contractile sheath. Another distinct characteristic of *Myoviridae* are their long tail fibers. The family *Siphoviridae* has a flexible, non-contractile tail (65-570 nm) and short tail fibers. The distinguishing characteristic of *Podoviridae* is a short (<20 nm) or non-existent tail. Phage heads generally have icosahedral symmetry or symmetry which is derived from a basic icosahedral structure. The head diameters range in size from 50-200 nm; *Myoviridae* typically have a larger head diameter (80-200 nm) than *Siphoviridae* (ca. 60 nm) (Proctor, 1997). Aquatic cyanophages (viruses of cyanobacteria) have been identified from the three main morphological families *Myoviridae*, *Siphoviridae* and *Podoviridae* (Safferman *et al.*, 1983; Suttle & Chan, 1993).

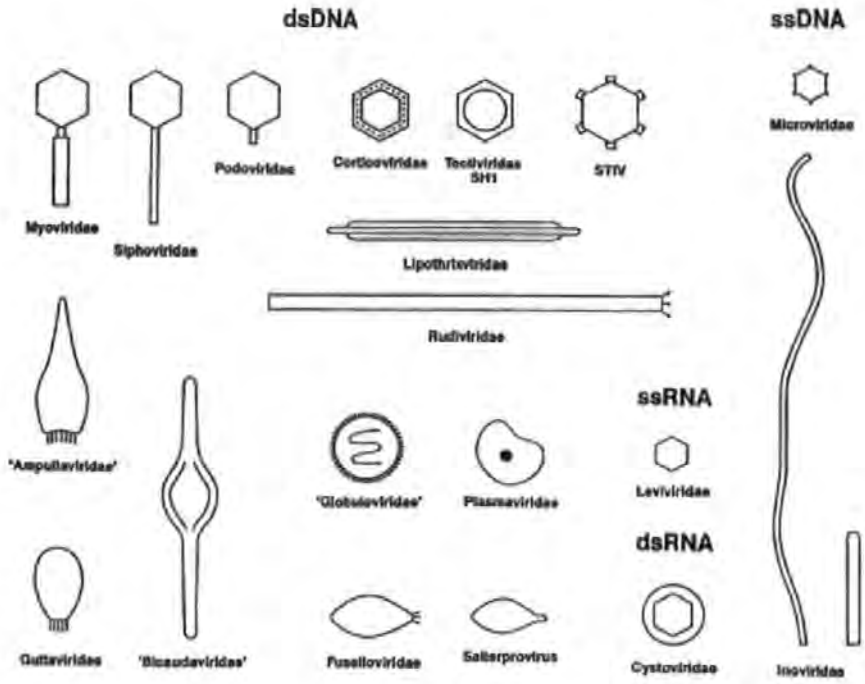

Shape	Nucleic acid	Virus group	Particulars	Example
Tailed	DNA, 2, L	*Myoviridae*	tail contractile	T4
		Siphoviridae	tail long, noncontractile	λ
		Podoviridae	tail short	T7
Polyhedral	DNA, 1, C	*Microviridae*	conspicuous capsomers	ϕX174
	2, C, S	*Corticoviridae*	complex capsid, lipids	PM2
	2, L	*Tectiviridae*	inner lipid vesicle, pseudotail	PRD1
	2, L	SHI, group*	inner lipid vesicle	SH1
	2, C	STV1 group*	turret-shaped protrusions	STIV
	RNA, 1, L	*Leviviridae*	poliovirus-like	MS2
	2, L, seg	*Cystoviridae*	envelope, lipids	ϕ6
Filamentous	DNA, 1, C	*Inoviridae*	a. long filaments	fd
			b. short rods	MVL1
	2, L	*Lipothrixviridae*	envelope, lipids	TTV1
	2, L	*Rudiviridae*	TMV-like	SIRV-1
Pleomorphic	DNA, 2, C, S	*Plasmaviridae*	envelope, lipids, no capsid	L2
	2, C, S	*Fuselloviridae*	same, lemon-shaped	SSV1
	2, L, S	*Salterprovirus*	same, lemon-shaped	His1
	2, C, S	*Guttaviridae*	droplet-shaped	SNDV
	2, L	*Ampullaviridae**	bottle-shaped	ABV
	2, C	*Bicaudaviridae**	two-tailed, growth cycle	ATV
	2, L	*Globuloviridae**	paramyxovirus-like	PSV

C Circular; *L* linear; *S* superhelical; *seg* segmented; *1* single-stranded; *2* double-stranded
*Awaiting classification

Figure 1.6. Drawings of bacteriophage morphotypes and a list describing the bacteriophage groups (Reproduced from Ackermann, 2007).

1.4.2 Algal viruses

Viruses of algae have few morphological known types. The majority of algal viruses described to date are members of the *Phycodnaviridae*, which is a family of large dsDNA viruses with an isocohedral shape. This family contains six genera and range in size from 100-400 nm (Table 1.2).

Marnaviridae is the second family of algal viruses. The family *Marnaviridae* consists of ssRNA viruses that are icosahedral with a diameter ~25 nm (Table 1.2). A number of RNA viruses of algae have recently been isolated and characterised (Lang *et al.*, 2004; Tai *et al.*, 2003; Tomaru *et al.*, 2004). There is one exception of an algal RNA virus that is not in the family *Marnaviridae*. *Micromonas pusilla* is susceptible to a dsRNA virus (65–80 nm) which has been placed in the family of plant viruses, *Reoviridae* (Brussaard *et al.*, 2004a) (Table 1.2).

Table 1.2. Examples of algal viruses. Data abstracted from http://www.ncbi.nlm.nih.gov/ICTVdb/Ictv/index.htm.

Genus	Species type	Strains	Particle diameter (nm)	Genome size (kbp)
Marnavirus	*Heterosigma akashiwo RNA virus*	HaRNAV-SOG263		9
Chlorovirus	*Paramecium bursaria Chlorella virus* (NC64A and phi viruses*)	PBCV-AL1A, PBCV-AL2C, PBCV-BJ2C, PBCV-CA1A, PBCV-CA1D, PBCV-CA2A, PBCV-CA4A, PBCV-CA4B, PBCV-CVBII, PBCV-CVK2, PBCV-CVU1, PBCV-IL2A, PBCV-IL2B, PBCV-IL3A, PBCV-IL3B, PBCV-IL5-2s1, PBCV-MA1D, PBCV-MA1E, PBCV-NC1A, PBCV-NC1B, PBCV-NC1C, PBCV-NC1D, PBCV-NE8A, PBCV-NE8D, PBCV-NY2A, PBCV-NY2B, PBCV-NY2C, PBCV-NY2F, PBCV-NYb1, PBCV-NYs1, PBCV-SC1A, PBCV-SC1B, PBCV-SH6A, PBCV-XZ5C, PBCV-XY6E, PBCV-XZ3A, PBCV-XZ4A, PBCV-XZ4C, PBCV-A1, PBCV-B1, PBCV-G1, PBCV-M1, PBCV-R1	190	300-370
	Hydra viridis Chlorella virus	HVCV-1, HVCV-2, HVCV3		
Prasinovirus	*Micromonas pusilla virus*	MpV-SP1, MpV-SP2, MpV-GM1, MpV-PB6, MpV-PB7, MpV-PB8, MpV-PL1, MpV-SG1	115-120	200-560
Prymnesiovirus	*Chysochromulina brevifilum virus*	CbV-PW1, CbV-PW3	120-160	485-510
	Phaeocystis globosa virus	PgV-01T, PgV-02T, PgV-03T, PgV-04T, PgV-05T, PgV-06T, PgV-07T, PgV-09T, PgV-10T, PgV-11T, PgV-12T, PgV-13T, PgV-14T, PgV-15T, PgV-16T, PgV-17T, PgV-18T		
Phaeovirus	*Ectocarpus fasciculatus virus*	EfV-a	130-200	130-200
	Ectocarpus siliculosus virus	EsV-1, EsV-a		
	Feldmannia irregularisvirus	FiV-a		
	Feldmannia spp. *virus*	FsV, FsV-a		
	Hincksia hinckiae virus	HhV-a		
	Myriotrichia clavaeformis virus	McV-a		
	Pilayella littoralis virus	PIV-a		
Raphidovirus	*Heterosigma akashiwo virus*	HaV01, HaV02, HaV03, HaV04, HaV05, HaV06, HaV07, HaV08, HaV09, HaV10, HaV11, HaV12, HaV13, HaV14, HaV15	202	294
Coccolithovirus	*Emiliania huxleyi virus*	EhV-84, EhV-86, EhV-88, EhV-163, EhV-201, EhV-202, EhV-203, EhV-205, EhV-207, EhV-208, EhV-99B1, EhV-KB1, EhV-2KB2	160-200	407-415

1.5 Life cycles

The main types of viral infections are lytic, lysogenic, latent, pseudolysogenic and chronic (Dimmock *et al.*, 2001) (Figure 1.7). The lytic cycle is typically considered the main method of viral replication; however, these cycles are somewhat interchangeable under certain conditions, such as temperature variations, exposure to UV irradiation, and/or exposure to chemical agents (Cann, 2001). The specificity of host ranges found in viruses can be limited to infecting individuals of a single subspecies, to the ability to infect more than one related species or even genus (Ackermann & DuBow, 1987; Fuhrman & Suttle, 1993).

Viruses have evolved to take advantage of receptor molecules present on the host's cell surface as attachment sites (Dimmock *et al.*, 2001). Viral binding sites may be found in specific places, bacteriophage tails, or distributed over the entire viral surface (Ackermann *et al.*, 1998). The specific binding of viral attachment proteins interact in a similar manner as ligands and bind to a specific receptor expressed on the surface of the host cell (Hurst, 2000). The surface-bound virus penetrates the host cellular membrane to deliver its genetic material into the cell (Strauss & Strauss, 2001). The virus then utilises the host cell's metabolic machinery to replicate.

1.5.1 Lytic

Lytic (virulent) viruses infect a host, replicate and are released by lysis of the host cell. A lytic virus reproduces rapidly after infecting a cell. Once inside the host cell the virus' nucleic acid uses the host cell's machinery to make large amounts of viral components. In the case of DNA viruses, the host DNA-dependent RNA polymerase transcribes the viral DNA into (mRNA) molecules (Hurst, 2000). RNA viruses use RNA-dependent RNA polymerase (RDRP) to transcribe the viral RNA into DNA, which is then transcribed into mRNA (Section 1.3). After many copies of viral components, such as

the genome and the capsids are made, the components are assembled into complete viruses. Upon lyses of the host, the infective viruses are then free to encounter a new host.

In a typical lytic life cycle, two essential classes of genes are expressed in phases described as described as early and late. Expression of early genes is generally involved in regulating transcription and the replication of the viral genome. The late genes produce the structural proteins, such as viral capsid proteins, which can then be assembled into new virus particles (Hurst, 2000).

1.5.2 Lysogeny/latency

A lysogenic infection occurs when a viral genome integrates itself into a host (prophage) after entry and replicates along with the host. This phenomenon is particularly well known in bacteriophages; phages with this property are known as temperate. The prophages remain dormant until the lytic cycle is induced by a physical (UV irradiation) or chemical agent (Mitomycin C) (Jiang & Paul, 1994; Jiang & Paul, 1998; Paul & Jiang, 2001).

A lysogenic/latent state may be advantageous to the survival of a virus. Under conditions where the host population is small the lysogenised/latent viruses are protected from the environment while the host slowly replicates and passes on the virus genome to its progeny.

Lysogeny has been documented in both marine and freshwater systems. Studies on the prevalence of lysogeny in marine environments have shown that up to ca. 40% of bacteria are potential lysogens (Cochran & Paul, 1998; Jiang & Paul, 1998; Ohki & Fujita, 1996; Tapper & Hicks, 1998). While lysogeny does not exert a huge influence on host population size, it does impact distribution of genetic and phenotypic characteristics (Wommack & Colwell, 2000). For example, the manifestation of

lysogeny can lead to lysogenic conversion due to the presence of a temperate phage, which can convert an innocuous bacterium into a pathogenic form. This has been demonstrated in the case of the *Vibrio harveyi* bacterium, where infection by the temperate phage, VHML, alters colony morphology and causes the bacterium to produce an exotoxin which can be lethal to fish and invertebrates (Oakey & Owens, 2000). While it is well documented that lysogens are prevalent in aquatic environments their potential roles have been minimally investigated.

A lytic or lysogenic life cycle, in the case of Lambda, is determined by the concentration of the repressor protein and the CRO protein (Calendar, 2006). The CRO protein inhibits the production of the repressor and favors the lytic life cycle. Under conditions where the production of the repressor is favored, high levels of the repressor protein, cI, accumulate and a lysogenic life cycle is established. The cI protein binds to both the left and right promoters and represses transcription of the immediate early genes. Adverse conditions, such as increased temperature or exposure to UV irradiation, terminate repression through induction. When the infected host cell is damaged it undergoes an SOS response, several genes are expressed that aid in repairing damaged DNA. The protease activity, from expression of RecA, cleaves cI which initiates the lytic cycle.

Latent infections in eukaryotic viruses can down regulate their own transcription in a similar manner, through latency-associated transcripts (Mu *et al.*, 2007). Latency in eukaryotic algae is more complex than lysogeny in prokaryotes. While phages integrate into the host genome of prokaryotes, viruses causing a latent infection in eukaryotic algae may integrate themselves into the chloroplast, mitochondrial or host genome (Alberts *et al.*, 1994; Delaroque *et al.*, 1999). Investigations of latency in algae are mainly limited to macroalgae. The first latent virus of an alga was the *Ectocarpus siliculosus* virus (EsV) (Kapp, 1998). Since the discovery of EsV, latent viruses of other

brown algae have been isolated and described (Henry & Meints, 1992). Although much work has been done on viruses of macroalgae, latency in unicellular algae has not been formally addressed to date.

1.5.3 Pseudolysogeny/Chronic infections

Phages may replicate through four major life cycles: lytic, lysogenic, pseudolysogenic, and by chronic infection. Pseudolysogeny is a less well-defined type of virus–host interaction in prokaryotes. There are several definitions of pseudolysogeny. Ackermann first described pseudolysogeny as a phenomenon where there is a constant production of virus (Ackermann, 1987). In this state, viral propagation is not stimulated with inducing agents and remains in a carrier state with no integration into the host's cellular replicons; viral progeny are propagated and released while the host organism remains relatively unaffected (Fuhrman & Suttle, 1993; Williamson *et al.*, 2001; Zingone *et al.*, 2006). Other definitions describe pseudolysogeny as transient lysogeny in which there is a loss of viable or detectable prophage while some resistance to full lytic phage development is retained. (Furman,1999; Khemayan *et al.*, 2006).

One explanation of this phenomenon suggests that perhaps the host is not optimal for the virus and although infection occurs, the host-virus compatibility are not ideal. This may be due to weak or poor repression of phage DNA transcription caused by a defective repressor protein (Williamson *et al.*, 2001). Other explanations are that there is a combination of either sensitive and resistant hosts or perhaps a mixture of virulent and latent viruses. Environmental conditions, such as limited nutrients, have also been proposed as a factor leading to pseudolysogeny, where the phage "waits" in an inactive state until environmental conditions are more favorable and normal viral activity returns (Ripp & Miller, 1997). Although the definition of this unusual state has not yet been

fully agreed upon, there are a few examples of pseudolysogeny found in the marine environment (Khemayan *et al.*, 2006; Lohr *et al.*, 2005; Williamson *et al.*, 2001). Chronic infections have been described in prokaryotes and eukaryotes alike. During a chronic infection there is a stable relationship in which host cells and virus titres both increase and there is a constant production of virus (Ackermann, 1987). Chronically infecting viruses can release progeny without killing their host. To release virions located in the prokaryotic or eukaryotic cell cytoplasm without disrupting the cell membrane, the virus buds through the host membrane(s). The chronic cycle has been best described for the filamentous phage of *Escherichia coli*, for example phage M13 (Cann, 2001). In eukaryotes, chronic infections are best describe for clinical viruses, such as herpesviruses (Knipe & Howley, 2001), while in algae this type of virus-host interaction remains to be observed.

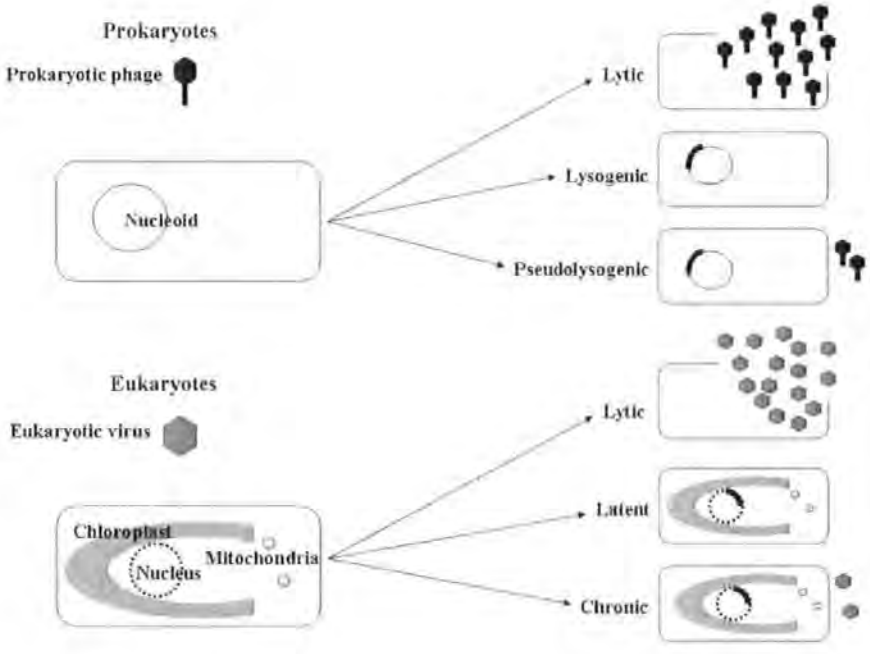

Figure 1.7. Virus lifecycles (adapted from Fuhrman & Suttle, 1993).

1.5.4 Gene transfer

Viruses can instigate the exchange of genetic material. Transduction occurs when host DNA is mistakenly packaged into the viral capsid during viral production and subsequently is incorporated into a new host cell. Generalised transduction occurs in lytic and lysogenic viruses, while specialised transduction occurs only in lysogenic viruses (Kokjohn, 1989; Miller, 2001). Specialised transduction transfers specific genes located near the integration site while generalised transduction can transfer DNA from any location from the host. It has been estimated that in the world's oceans phages transduce 10^{28} bp of DNA each year (Paul *et al.*, 2002).

Genome sequencing of aquatic viruses has revealed several examples of gene transfer. For example, genes related to photosynthesis have been identified in the genomes of cyanophages infecting *Synechococcus* spp. (Bailey *et al.*, 2004; Mann, 2003; Millard *et al.*, 2004) and *Prochlorococcus marinus* (Lindell *et al.*, 2005). The extra genes carried within the viral genome may be expressed by the host. These genes can change the phenotypic characteristics of the host. Expression of virally encoded genes can be beneficial to the virus, allowing the host to survive longer and produce more virus particles (Bailey *et al.*, 2004).

1.6 Nature of known aquatic viruses

In general, the principles of viral dynamics in aquatic systems are similar in marine and freshwater environments. Distribution of viruses and viral abundance in aquatic environments depend on a multitude of factors: blooms, sedimentation, water mixing, breakdown of VLPs due to light, time, and temperature which may all contribute to the distribution and abundance of viruses. Viral abundance in aquatic systems can range from tens to millions per ml (Bergh *et al.*, 1989; Hennes *et al.*, 1995), while the precise distribution of viruses is less defined.

1.6.1 Freshwater viruses

Large volumes of freshwater are scattered all over the globe, from lakes and ponds. In lakes and ponds, viruses terminate blooms while in other cases the viruses themselves can potentially harm humans. Enterobacteria are of significant interest in relation to human health. While many enterobacteriophages found in freshwater systems have been studied in great detail and have contributed greatly to the knowledge of phages, here the focus will be on viruses of photosynthetic hosts.

Freshwater photosynthetic hosts such as cyanobacteria and algae are of great importance in freshwater systems. Cyanobacteria and algae supplement aquatic environments by generating O_2, reducing levels of CO_2 and producing organic matter that is then available to other organisms.

Cyanobacteria and their cyanophages have been investigated in several freshwater systems. LPP-1 was the first reported freshwater cyanophage (Safferman & Morris, 1963). Since this first report, studies have examined viruses infecting many freshwater cyanobacteria, such as *Microcystis* spp., *Anabaena* spp., *Nostoc* spp., *Synechococcus* spp. and *Anacystis* spp. (Baker *et al.*, 2006; Safferman *et al.*, 1972; Tucker & Pollard, 2005). During the last few years molecular markers, such as the major capsid protein gene, have been employed to detect and examine cyanophage diversity in freshwater systems, revealing high diversity (Baker *et al.*, 2006; Dorigo *et al.*, 2004). While most investigations of freshwater cyanophage employed just a few cyanobacterial hosts and their lytic viruses, there is only one report of a freshwater lysogenic cyanophage (Lee *et al.*, 2006).

The first algal virus was isolated more than 20 years ago; this algal virus, PBCV-1, infected a symbiotic *Chlorella*-like alga isolated from *Paramecium bursaria* (van Etten *et al.*, 1982). Viruses infecting *P. bursaria Chlorella* strains have been characterised in detail (van Etten *et al.*, 1991) and the diversity of freshwater *Chlorella* viruses have

been recently examined in natural communities and in other hosts (Bubeck & Pfitzner, 2005; Cho *et al.*, 2002). Despite this, there is little information available on viruses which infect eukaryotic algae in freshwater systems.

1.6.2 Marine viruses

Phycoviruses (viruses of eukaryotic algae) and cyanophages are ubiquitous in the world's oceans (Fuhrman, 1999; Suttle, 2005). The photosynthetic hosts of these viruses contribute to primary production of the oceans. Phytoplankton blooms influence global biogeochemical cycling and they can have both environmental and economic impacts (Munn, 2004). It is well established that viruses play an important role in population dynamics and community composition of marine phytoplankton (Brussaard, 2004a; Larsen *et al.*, 2001; Schroeder *et al.*, 2003; Suttle, 2000).

Cyanobacteria are abundant in the world's oceans, particularly those from the genera *Synechococcus* and *Prochlorococcus*. Many cyanophages of *Synechococcus* and *Prochlorococcus* have been studied in detail and genomes of cyanophage P-SSP7, P-SSM2 and P-SSM4 (*Prochlorococcus*) (Sullivan *et al.*, 2005) and S-PM2 (Mann *et al.*, 2005) and P60 (Chen & Lu, 2002) (*Synechococcus*) and Syn9 (Weigele *et al.*, 2007) have been fully sequenced. Marine cyanophages have been isolated for several other cyanobacteria such as *Phormidium persicinum* (Ohki & Fujita, 1996), *Phormidium ubcinatum* (Bisen *et al.*, 1986) and *Trichodesmium* spp. (Ohki, 1999).

Many viruses that infect marine algae have been reported. Algal viruses have been described for the smallest alga, *Ostreococcus tauri* (O'Kelly *et al.*, 2003) as well as the macroalga *Ectocarpus* spp. (Muller *et al.*, 1996), and *Feldmannia* spp. (Henry & Meints, 1992). Phycoviruses have been isolated for most groups of marine algae and are extremely well studied as many of the host species form massive blooms. Phycoviruses of several bloom-forming algae have been isolated and identified, for example

Emiliania huxleyi (Schroeder *et al.*, 2002; Wilson *et al.*, 2002), *Aureococcus anophagefferens* (Milligan & Cosper, 1994), *Micromonas pusilla* (Suttle *et al.*, 1991), *Phaeocystis pouchetii* (Jacobsen *et al.*, 1996), *Rhodomonas* spp. (Suttle *et al.*, 1991), *Heterosigma akashiwo* (Nagasaki *et al.*, 1999)), *Hymenomonas carterae* (Pienaar, 1976), *Chrysochromulina* spp. (Suttle & Chan, 1995), *Cryptomonas* spp. (Pienaar, 1976), *Pyramimonas orientalis* (Pienaar, 1976) and *Platymonas* spp. (Pearson & Norris, 1974). Marine phycoviruses in two genera have been fully sequenced, *Emiliania huxleyi virus* 86 (Wilson, 2005) and *Ectocarpus siliculosus virus* 1 (Delaroque *et al.*, 2001). These complete genomes offer the first glimpse into the diversity and evolutionary history of the phycoviruses.

1.7 Aims and objectives

The overall aim of this project was to expand the current knowledge of lysogenic/latent viruses from aquatic environments. The overall objective is therefore to survey potential hosts (algae and cyanobacteria) from aquatic environments for novel lysogenic/latent viruses. The objectives can be summarised in 3 main statements:

1) To investigate potential latent systems

2) To examine the induction process

3) To isolate and characterise potential latent viruses.

This work has been further divided into three sections with similar aims applied to different aquatic systems.

1.7.1 Do zooxanthellae harbour latent viruses?

The hypothesis that zooxanthellae (symbiotic dinoflagellates of corals and other animals) harbour latent viruses has been suggested in previous studies where VLPs associated with heat-shocked zooxanthellae and corals have been demonstrated (Davy *et*

al., 2006; Wilson *et al.*, 2001; Wilson *et al.*, 2005). In these previous studies, the host of the VLPs could not be determined, mainly due to the complexity of the associated microbes. Assessment of *Symbiodinium* spp. cultures has been used here as a model system to investigate the induction of potential latent viruses. The unique host-virus system described here provides insight into the role of latent infections in zooxanthellae through environmentally-regulated viral induction mechanisms.

Specific aims were:

1) To determine if zooxanthellae are susceptible to latent infections utilising *Symbiodinium* spp. cultured *in vitro* in order to simplify the complexity found in whole organisms containing symbionts

2) To determine the conditions under which potential latent viruses can be induced

3) To isolate and characterise inducible VLPs

1.7.2 What are the potential interactions of inducible VLPs from a freshwater cyanobacterium?

Lysogeny has been well documented in heterotrophic bacteria, and there have been several investigations documenting prophage induction in filamentous forms of cyanobacteria (Cannon *et al.*, 1971; Ohki & Fujita, 1996; Padan *et al.*, 1972). Lytic cyanophages have been the focus of most investigations, while very little work has been performed on freshwater temperate cyanophages (Lee *et al.*, 2006). The unusual interaction of a freshwater cyanobacterium and its inducible VLPs are described here.

Specific aims were:

1) To optimise the production of inducible VLPs from the freshwater cyanobacterium, *Pseudanabaena* spp.

2) To isolate and characterise inducible VLPs

1.7.3 Are latent viruses prevalent in algal culture collections?

Most of our knowledge of algal viruses is from studies of viruses which have been isolated and purified in the laboratory. Several of the well studied algal viruses are the viral isolates which infect freshwater endosymbiotic *Chlorella*-like algae (van Etten *et al.*, 2002), the viruses of the bloom-forming *Emiliania huxleyi* (Wilson, 2005), the viruses infecting the harmful bloom-causing alga, *Phaeocystis globosa* (Brussaard *et al.*, 2004b), the ssRNA virus of the toxic bloom forming alga, *Heterosigma akashiwo* (Lang *et al.*, 2004) and the dsRNA virus of the marine photosynthetic flagellate *Micromonas pusilla* (Attoui *et al.*, 2006; Brussaard *et al.*, 2004b). The host organisms have been selected by culture conditions and only viruses which cause lysis of specific cultivatable strains have been examined. In this study several strains of pico- and nano-algae have been assessed for potential latent viruses. The characterisation and isolation of inducible viruses from this algal culture collection has revealed much information on the prevalence of latent viruses in algae and is the first study looking at the frequency of latent algal viruses.

Specific aims were:

1) To investigate the prevalence of inducible latent viruses in algae

2) To characterise potential virus-host interactions

3) To isolate and characterise inducible VLPs

CHAPTER 2 Methods and Materials

2.1 Cultures

2.1.1 Zooxanthellae

During this study, 16 strains of *Symbiodinium* species isolated from a variety of cnidarian hosts were maintained in culture (Table 2.1). The isolate strains 12, 61, 104, 133, 135, 141, 152, 185, 203, 292, 368, 379, 383, 385 were obtained from a collection held at the Marine Biological Association (Plymouth, England) and are described in a previous study (LaJeunesse, 2001). A further two strains (200X and 200Y) were isolated from *Acropora formosa*. The zooxanthellae were grown in ASP-8A medium with antibiotics (Table 2.2) and subcultured monthly. All media components were purchased from Sigma-Aldrich Co. (Dorset, UK). Algal cultures were grown under a light:dark cycle of 16:8 h at 26°C. The light irradiance applied was 40-50 μmol quanta $m^{-2}s^{-1}$(Photosynthetic Active Radiation) The main zooxanthellae isolate used in this study (strain 292) has been deposited at the Center for Culture of Marine Phytoplankton (CCMP, http://ccmp.bigelow.org) as strain CCMP 2465; several of the other strains have also been deposited at CCMP.

Table 2.1. List of zooxanthellae strains showing original isolate number designation, CCMP designation, host origin, clade/ITS type, symbiont species and accession number.

Isolate number	CCMP number	Host origin	Clade/ITS type	Symbiont species	Accession number
12	2463	*Aiptasia tagetes* (sea anemone)	B1	*Symbiodinium* species	n/a
61	2464	*Cassiopeia xamachana* (jellyfish)	A1	*Symbiodinium microadriaticum*	AF333505
104	n/a	*Heliopor* species (coral)	A2	n/a	n/a
133	2455	*Meandrina meandrites* (coral)	F2	*Symbiodinium* species	AF333516
135	2468	*Montipora verrucosa* (coral)	F1	*Symbiodinium kawagutii*	AF333517
141	2459	*Oculina diffusa* (coral)	B2.1	*Symbiodinium* species	AF333513
152	2466	*Discosoma sancti-thomae* (coral)	C1	*Symbiodinium goreaui*	AF333515
185	2461	*Zoanthus sociatus* (sea anemone)	A2	*Symbiodinium pilosum*	AF333506
203	n/a	*Hippopus hippopus* (giant clam)	C2	*Symbiodinium* species	AF333518
292	2465	*Tridacna maxima* (giant clam)	A3	*Symbiodinium* species	n/a
368	n/a	*Linuche unguiculata* (jellyfish)	A4	*Symbiodinium linucheae*	AF333509
379	2456	*Plexaura homamalla* (sea fan)	A4	*Symbiodinium* species	n/a
383	n/a	*Anthropleura elegantissima* (sea anemone)	E1	*Symbiodinium californium*	AF334659
385	2462	*Dichotomi* species (jellyfish)	B3	*Symbiodinium* species	AF333514
200X	n/a	*Acropora formosa* (coral)	n/a	n/a	n/a
200Y	n/a	*Acropora formosa* (coral)	n/a	n/a	n/a

Table 2.2. ASP-8A medium.

Compound	Stock solution (g/l)	Quantity in 1 l of dH_2O
Sodium Chloride (NaCl)	-	25 g
Potassium Chloride (KCl)	70	10 ml
Magnesium Sulfate ($MgSO_4$)	450	20 ml
Calcium Chloride ($CaCl_2$)	110	10 ml
PII Metal Solution	Table 2.2 (c)	10 ml
Tris Base, pH 9.0 ($C_4H_{11}NO_3$)	100	10 ml
Nitrilotriacetic Acid ($C_6H_9NO_6$)	30	1 ml
Ammonium Nitrate (NH_4NO_3)	1	1 ml
Sodium Nitrate ($NaNO_3$)	50	1 ml
Potassium Dihydrogen Phosphate (KH_2PO_4)	10	1 ml
8A Vitamin Solution	Table 2.2 (b)	0.5 ml
Vitamin B_{12}	10 µg/ml	0.1 ml
Antibiotic Solution	Table 2.2 (a)	1 ml

Table 2.2 (a). ASP-8A antibiotic solution.

Compound	Stock Solution (mg/ml)	Quantity in 100 ml of dH_2O, working stock (ml)
Polymyxin	0.9	1
Streptomycin	33	10
Penicillin	5.8	2.24
Neomycin	20	1
Erythromycin	100	1

Table 2.2 (b). ASP-8A vitamin solution.

Compound	Quantity in 1 l dH_2O, 8A Vitamin Solution (g/l)
p-Aminobenzoic Acid	0.04
Biotin	0.002
Vitamin B_{12}	0.002
Choline Dihydrogen Citrate	2
Folic Acid	0.01
Folinic Acid	0.0008
Inositol	4
Nicotinic Acid	0.4
Orotic Acid	0.08
d-Pantothenic Acid	0.4
Pyridoxamine	0.08
Pyridoxine	0.16
Putrescine	0.16
Riboflavin	0.02
Thiamine	0.8
Thymine	3.2

Table 2.2 (c). ASP-8A PII trace metal solution.

Compound	Quantity in 1 l dH_2O, PII Trace Metal Solution (g/l)
Cobalt (II) Sulfate Heptahydrate ($CoSO_4$)	0.0048
Ferric Chloride ($FeCl_3$)	0.049
Ethylenediaminetetraacetic Acid ($C_{10}H_{16}N_2O_8$)	1
Boric Acid (H_3BO_3)	1.14
Manganese Sulphate ($MnSO_4$)	0.164
Zinc Sulfate ($ZnSO_4$)	0.022

2.1.2 Cyanobacterium

The cyanobacterium, *Pseudanabaena* spp. PPt10905, was isolated from a water sample collected at a depth of 0.5 meters from Priest Pot at the head of Esthwaite Water in the English Lake District (10/9/02). The cyanobacterium was grown in BG-11 medium (Table 2.3) and subcultured fortnightly. Cultures were grown under a light:dark cycle of 16:8 h at 26°C. The light irradiance applied was 40-50 µmol quanta $m^{-2}s^{-1}$(PAR).

Table 2.3. BG-11 medium.

Compound	Stock solution (g/l)	Quantity in 1 l of dH_2O
Sodium Nitrate ($NaNO_3$)	300	5 ml
Potassium Phosphate (K_2HPO_4)	40	1 ml
Magnesium Sulphate ($MgSO_4 \cdot 7(H_2O)$)	75	1 ml
Calcium Chloride ($CaCl_2$)	36	1 ml
Citric Acid ($C_6H_8O_7$)	6	1 ml
Ferric Ammonium Citrate ($C_6H_{11}FeNO_7$)	6	1 ml
Sodium Carbonate (Na_2CO_3)	20	1 ml
Ethylenediaminetetraacetic Acid ($C_{10}H_{16}N_2O_8$)	1	1 ml
A6 Microelements	Table 2.3 (a)	1 ml

Table 2.3 (a). A6 microelements.

Compound	Quantity in 1 l dH_2O, A6 Microelements (g/l)
Orthoboric Acid (H_3BO_3)	2.86
Manganese Chloride ($MnCl_2$)	1.81
Zinc Sulphate ($ZnSO_4 \cdot 7H_2O$)	0.222
Sodium Molybdate ($NaMoO_4$)	0.391
Copper Sulphate ($CuSO_4$)	0.079
Cobalt II Nitrate ($Co(NO_3)_2$)	0.049

2.1.3 Plymouth Culture Collection (PCC) of Marine Algae

During this study, 49 strains of pico and nano phytoplankton obtained from the Plymouth Culture Collection (PCC) of Marine Algae (http://www.mba.ac.uk/education/education_outreach.php?culturecollection) were maintained in culture (Table 2.4). The algal cultures were grown in F/2 medium (Table 2.5) with a light:dark cycle of 16:8 h at 15°C and subcultured monthly. The light irradiance applied was 50-100 µmol quanta $m^{-2}s^{-1}$(PAR).

Table 2.4. List of Plymouth culture collection algal strains.

PCC Designation	Division	Class	Species
83	Chlorophyta	Chlorophyceae	*Dunaliella tertiolecta*
85	Chlorophyta	Chlorophyceae	*Chorella stigmatophora*
430	Chlorophyta	Chlorophyceae	*Dunaliella minuta*
491	Chlorophyta	Chlorophyceae	*Chlamydomona concordia*
272	Chlorophyta	Prasinophyceae	*Tetraselmis tetrathele*
299	Chlorophyta	Prasinophyceae	*Pyraminonas urceolata*
315	Chlorophyta	Prasinophyceae	*Tetraselmis* spp.
456	Chlorophyta	Prasinophyceae	*Tetraselmis rubens*
492	Chlorophyta	Prasinophyceae	*Pyraminonas panceae*
511A	Chlorophyta	Prasinophyceae	*Tetraselmis* spp.
512	Chlorophyta	Prasinophyceae	*Tetraselmis* spp.
570	Chlorophyta	Prasinophyceae	*Tetraselmis marina ?*
591	Chromophyta	Eustigmatophyceae	*Nannochloropsis salina*
663	Chromophyta	Eustigmatophyceae	*Nannochloropsis oculata*
23	Cryptophyta	Cryptophyceae	*Cryptomonas appendiculata*
29	Cryptophyta	Cryptophyceae	*Cryptomonas maculata*
157	Cryptophyta	Cryptophyceae	*Hemiselmis virescens*
412	Cryptophyta	Cryptophyceae	*Cryptomonas calceiformis*
8	Haptophyta	Prymnesiophyceae	*Isochrysis aff. galbana*
75	Haptophyta	Prymnesiophyceae	*Pavlova lutheri*
93	Haptophyta	Prymnesiophyceae	*Pavlova gyrans*
133	Haptophyta	Prymnesiophyceae	*Imantonia rotunda*
154	Haptophyta	Prymnesiophyceae	*Pavlova salina*
156	Haptophyta	Prymnesiophyceae	*Pleurochrysis carterae*
162	Haptophyta	Prymnesiophyceae	*Ochrosphaera neapolitana*
240	Haptophyta	Prymnesiophyceae	*Isochrysis* spp.
341	Haptophyta	Prymnesiophyceae	*Ochrosphaera ?*
351	Haptophyta	Prymnesiophyceae	*Cricosphaera ?*
377	Haptophyta	Prymnesiophyceae	*Chrysotila stipitata*
378 (1)	Haptophyta	Prymnesiophyceae	*Pleurochrysis carterae*
434 (5)	Haptophyta	Prymnesiophyceae	*Ochisphaera ?*
471	Haptophyta	Prymnesiophyceae	*Pavlova pinguis*
475	Haptophyta	Prymnesiophyceae	*Chrysotila lamellosa*
484	Haptophyta	Prymnesiophyceae	*Pavlova* spp.
486	Haptophyta	Prymnesiophyceae	*Pavlova aff. salina*
506A	Haptophyta	Prymnesiophyceae	*Isochrysis* spp.
508	Haptophyta	Prymnesiophyceae	*Apistonema* spp.
515	Haptophyta	Prymnesiophyceae	*Pavlova virescens*
527	Haptophyta	Prymnesiophyceae	*Prymnesium patelliferum*
536	Haptophyta	Prymnesiophyceae	*Hymenosa globosa*
554	Haptophyta	Prymnesiophyceae	*Pavlova aff. lutheri*
562	Haptophyta	Prymnesiophyceae	*Isochrysis* spp.
564	Haptophyta	Prymnesiophyceae	*Dicrateria inornata*
565	Haptophyta	Prymnesiophyceae	*Isochrysis galbana*
568	Haptophyta	Prymnesiophyceae	*Pleurochrysis* spp.
577	Haptophyta	Prymnesiophyceae	*Imantonia rotunda ?*
598	Haptophyta	Prymnesiophyceae	*Prymnesium* spp.
472	Rhodophyta	Rhodophyceae	*Rhodosorus marinus*
539	Rhodophyta	Rhodophyceae	*Porphridium purpureum*

Table 2.5. F/2 medium, made up in 0.2 μm filtered seawater.

Compound	Stock solution (g/l)	Quantity in 1 l of seawater
Sodium Nitrate ($NaNO_3$)	75	1 ml
Sodium Dihydrogen Phosphate (NaH_2PO_4)	5	1 ml
F/2 Trace Metal Solution	Table 2.5 (a)	1 ml
F/2 Vitamin Solution	Table 2.5 (b)	0.5 ml

Table 2.5 (a). F/2 trace metal solution.

Compound	Stock solution (g/l)	Quantity in 1 l of dH_2O, Trace Metal Solution
Ferric Chloride ($FeCl_3$)	-	3.15 g
Ethylenediaminetetraacetic Acid ($C_{10}H_{16}N_2O_8$)	-	4.36 g
Copper (II) Sulfate ($CuSO_4$)	9.8	1 ml
Sodium Molybdate (Na_2MoO_4)	6.3	1 ml
Zinc Sulfate ($ZnSO_4$)	22	1 ml
Cobalt (II) Chloride ($CoCl_2$)	10	1 ml
Manganese Chloride ($MnCl_2$)	180	1 ml

Table 2.5 (b). F/2 vitamin solution.

Compound	Stock solution (g/l)	Quantity in 1 l of dH_2O, Vitamin Solution
Vitamin B_{12} (cyanocobalamin)	1	1 ml
Biotin	0.1	10 ml
Thiamine · HCl	-	200 mg

2.2 Induction conditions

The zooxanthellae, algae and cyanobacterium were induced by exposure to physical and chemical stresses. The methodologies varied and are detailed below.

2.2.1 Zooxanthellae induction

The 16 zooxanthellae cultures were initially exposed to three experimental treatments: an elevated temperature of 34°C, direct exposure to UV-C radiation of 254 nm and exposure to Mitomycin C (Fisher) at a concentration of 1 µg/ml

The initial host concentrations in all cases were ca. 10^5 ml^{-1}. The cultures (50 ml) were monitored daily for cell lysis and cell counts were made using a Reichert Bright-Line haemocytometer. UV-C irradiation was the induction method used in the subsequent induction experiments.

Triplicate exponentially growing cultures were exposed for 2 min in open Petri dishes, to UV-C light (254 nm) from a Chromato-Vue transilluminator (model TM-20) which was placed upside down 12 cm above the Petri dishes to allow direct irradiation (Figure 2.1). After exposure, the cultures were transferred back into flasks and maintained at 26°C with irradiance on a 16:8 h light:dark cycle. Samples for enumeration of zooxanthellae and VLPs were collected daily for one week.

Zooxanthellae were enumerated immediately by analytical flow cytometry (Section 2.3) and 1 ml aliquots were fixed in 0.5% v/v gluteraldehyde, stored at room temperature for 30 min, snap frozen in liquid nitrogen, and stored at -80°C until processed for enumeration of VLPs and bacteria (Section 2.3).

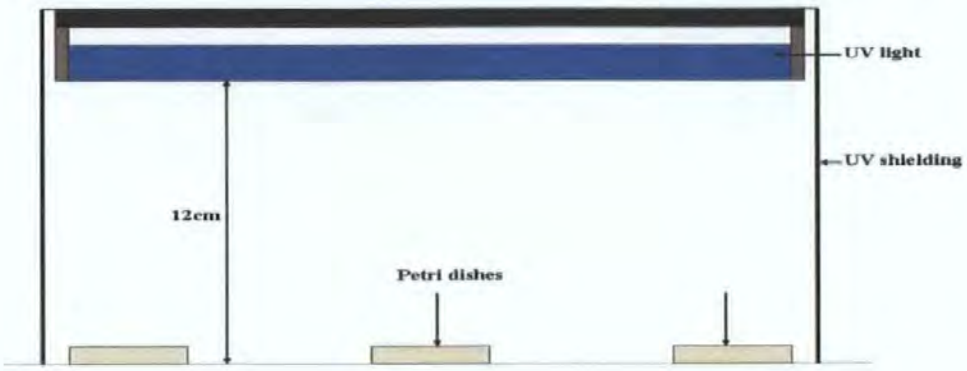

Figure 2.1. Setup of UV-C light for induction.

2.2.2 Cyanobacterium induction

Triplicate exponentially growing cultures (100 ml, ca. 10^5 cells ml^{-1}) were heat shocked at 34°C with irradiance maintained on a 16:8 h light:dark cycle. Samples for the enumeration of the cyanobacterium and VLPs were collected daily for two weeks. The cyanobacteria were enumerated immediately using a haemocytometer (Section 2.3) and 1 ml aliquots were fixed in 0.5% v/v gluteraldehyde, stored at room temperature for 30 min, snap frozen in liquid nitrogen, and stored at -80°C until processed for enumeration of VLPs (Section 2.3).

2.2.3 PCC phytoplankton induction

Triplicate exponentially growing cultures (50 ml, ca. 10^5 cells ml^{-1}) were exposed for 1 min , in open Petri dishes, to UV-C light (254 nm) (Phillips TUV15W G15T8) which was mounted 12 cm above the Petri dishes to allow direct irradiation. After exposure, the cultures were transferred back into flasks and maintained at 15°C with irradiance on a 16:8 h light:dark cycle. Samples for enumeration of algae and VLPs were collected daily for one week. Algae were enumerated immediately by analytical flow cytometry (Section 2.3) and 1 ml aliquots were fixed in 0.5% v/v gluteraldehyde, stored at room

temperature for 30 min, snap frozen in liquid nitrogen, and stored at -80°C until processed for enumeration of VLPs and bacteria (Section 2.3).

2.3 Enumeration of hosts, VLPs and bacteria

Cell numbers of the zooxanthellae (initial induction assessment) and the cyanobacterium were estimated by haemocytometry. A drop of well-mixed suspension was pipetted onto a Reichert Bright-line haemocytometer and counted under a light microscope at 400x magnification. Triplicate counts for each sample were averaged. Depending on the cell density, cells were counted in 5 random central grids or all cells in the 25 central grids were counted (Figure 2.2).

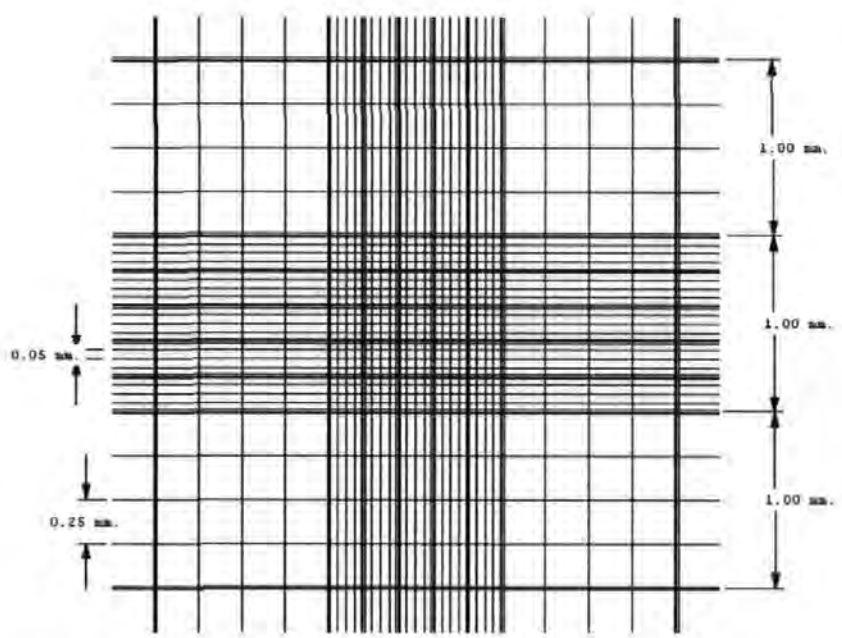

Figure 2.2. Haemocytometer grid.

Zooxanthellae, algae and all VLPs and bacterial counts (excluding PPt10905) were made using analytical flow cytometry (AFC). All analyses were performed on a Becton Dickinson FACScan flow cytometer using Cellquest software. For enumeration of live algae, undiluted and/or 1:10 dilutions of samples were run for 2 min on a high flow rate

of ca. 50-70 µl min^{-1} with the discriminator set on red fluorescence. For VLP and bacterial enumeration, counts were performed on fixed samples diluted from 1:10 to 1:1000 in TE buffer (10 mM Tris, 1 mM EDTA, pH 8.0) filtered to 50 kDa using tangential flow filtration (Vivaflow® flip flow, Section 2.5.1). The samples were stained for 10-15 min at 80°C with 10^{-5} dilution of SYBRgreen I stain (Molecular Probes) and allowed to cool for 5 min. The samples were analysed for 2 min at a low flow rate of ca. 30 µl min^{-1} with the discriminator set on green fluorescence (Marie *et al.*, 1999).

Algae were enumerated from plots of forward scatter versus red fluorescence and VLPs and bacteria were enumerated from plots of side scatter versus green fluorescence. Calibration of the flow rates were measured volumetrically, and performed before each analysis and for each flow rate setting.

2.4 Transmission Electron Microscopy (TEM)

Samples potentially containing VLPs were filtered through 0.45 µm filter units (Whatman) with a BD Plastipak® sterile 10 ml syringe to remove debris and large cells. Aliquots were fixed in 0.5 % v/v gluteraldehyde, stored at room temperature for 30 min and snap frozen in liquid nitrogen. 'Spot' grids were prepared by placing the grid onto 15-30 µl of fixed suspension for 30 min. Excess liquid was removed with filter paper. Dilute samples were centrifuged onto grids for 1 h at 100,000 x *g* using a Beckman L8-M ultracentrifuge. TEM grids were stained with a drop of 2% w/v uranyl acetate placed on the grid and wicked off immediately; a further drop was left for 30 seconds then wicked off. The grids were then washed with dH_2O and left to air dry before being stored in a grid box.

For preparation of thin sections, 10 ml of culture was pelleted by centrifugation at 10,000 x *g* for 5 min. The pellet was resuspended, washed and re-pelleted twice in

sterile culture medium. Molten agar (2 % Fisher brand agar) was added to the washed pellet and allowed to set; excess agar was trimmed from the agar plug. Embedded cells were fixed in 1 % v/v gluteraldehyde. The agar plugs were post-fixed in a 4 % w/v osmium tetroxide solution mixed 1:1 with sterile culture medium for 1-2 h at room temperature, followed by 2 washes in sterile medium. The agar plugs were dehydrated in an ascending ethanol series (30 % to 100 %) for at least 15 min each and kept overnight in 100 % ethanol. The agar plugs were then infiltrated with resin (TAAB Laboratories Equipment Ltd.) The resin percentage was increased every 12-24 h (30 % v/v to 100 % v/v) and maintained in fresh 100 % resin for an additional 24 h. Agar plugs and 100 % resin were transferred to pre-shaped moulds and dried overnight at 60°C. The blocks were mounted and cut into sections of 70-80 nm thickness on a Reichert-Jung Ultracut Microtome and floated onto TEM grids. Thin sections floated onto TEM grids were stained first with 2% w/v uranyl acetate in 70% v/v ethanol for 15 min, washed in dH_2O, and further stained in Reynolds lead citrate for 15 min, followed by a further rinse in dH_2O.

To visualise the VLPs, prepared grids and thin sections were examined under a transmission electron microscope. Samples were analysed with a JEOL 200 CX TEM (Magnification 0.8-600x 10^3) at 160 kV. Photographs were taken at magnifications between 5-50 x 10^3.

2.5 Concentration of VLPs

2.5.1 Tangential flow filtration

Tangential flow filtration was used to concentrate lysates (500 ml - 2 l) to ca. 50 ml with 50 kDa MWCO cutoff cartridges (Vivaflow® flip flow) (Figure 2.3). The pump was used to generate flow through the channel between the membrane surfaces. The tangentially pumped fluid was recirculated along the surface of the membrane, while the

applied pressure forced a portion of the fluid through the membrane to the filtrate side. The retentate containing the viruses was reduced in volume, concentrating the viruses.

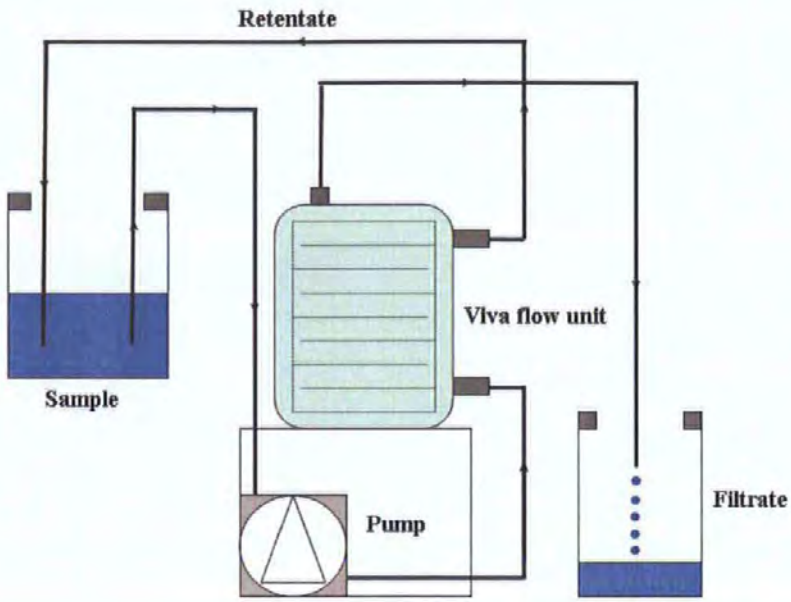

Figure 2.3. Vivaflow system.

2.5.2 QuikStand filtration system

The QuikStand filtration system was used to concentrate lysates (1-8 l) to ca. 200 ml. The QuikStand filtration is based on a hollow fibre cartridge and works under the same premise as Vivaflow® flip flow cartridges (Section 2.5.1). The hollow fibre filtration cartridge consists of a bundle of parallel tubules in which the liquid recirculates through, while permeate is pushed through the membrane pores (Figure 2.4).

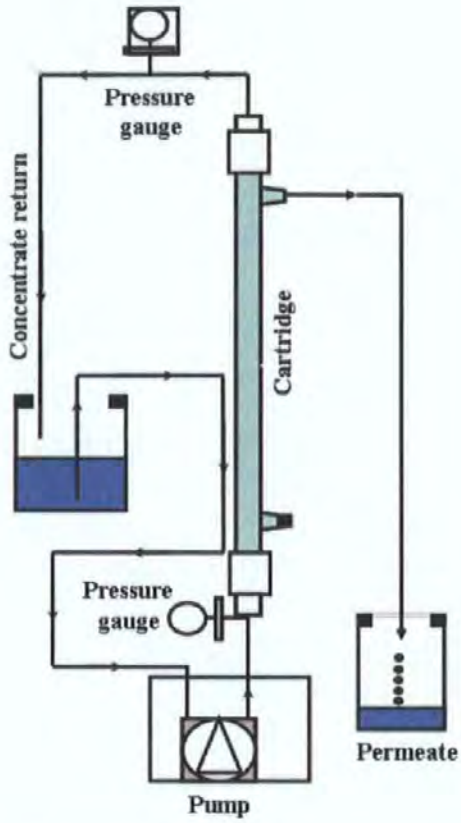

Figure 2.4. QuikStand filtration system.

2.5.3 Polyethylene glycol (PEG) precipitation

PEG precipitation was used to concentrate lysates (<200 ml) to ca. 1-3 ml. DNase I and RNase were added to the lysate to a final concentration of 1 µg/ml and incubated for 30 min at room temperature. NaCl was added to a final concentration of 1 M and PEG 8000 was added to a final concentration of 10% w/v, this was left on ice for at least 2 h and then centrifuged at 11,000 x *g* for 10 min. The supernatant was decanted and remaining liquid was allowed to drain from pellet for 5 min. The pellet was resuspended in SM buffer (0.1 M NaCl, 8 mM $MgSO_4$, 50 mM Tris-HCl, 0.005% w/v glycerol). PEG was removed by dialysis (Fisher, 14 kDa MWCO) overnight in SM buffer, with two buffer changes.

2.5.4 Ultracentrifugation

Ultracentrifugation was used to concentrate lysates (<50 ml) to ca. 0.5-3 ml, using a Beckman L8-M ultracentrifuge (SW28 rotor) run at 100,000 x *g* for 4 h. The supernatant was decanted and the pellet was resuspended to desired volume in SM buffer.

2.5.5 CsCl gradients

CsCl gradients were prepared by layering CsCl made up in TE buffer (10 mM Tris, 1 mM EDTA) at densities of 1.0, 1.2, 1.4, and 1.6 g cm^{-3}. Concentrated VLPs were added to the 1.0 g cm^{-3} layer, final volume 3 ml. The gradient was centrifuged at 100,000 x *g* for 2 h at 20°C, with the deceleration set at 8, in a Beckman L8-M ultracentrifuge (SW40 Ti rotor). Translucent white band(s) were removed by piercing the ultracentrifuge tube just below the band(s) to separate the aliquots. Aliquots were dialysed (Fisher, 14 kDa MWCO) overnight against a 1 l volume of TE buffer at 4°C, the TE buffer was changed twice. The dialysed VLP concentrate was stored at 4°C until further analysis.

2.6 Isolation of VLPs

2.6.1 Isolation of VLPs from zooxanthellae

VLPs were isolated from the lysates (1-8 l) of zooxanthellae cultures 96 h after exposure to UV light. Debris, bacteria and algal cells were removed by filtering through 0.45 µm pore size, 47 mm diameter filters (PALL Corp.). VLPs from the supernatants were concentrated by tangential flow filtration to ca. 50 ml (Section 2.5.1) and ultracentrifugation (Section 2.5.4) to a volume of ca. 3 ml. VLPs were further purified and concentrated on a CsCl gradient (Section 2.5.5).

2.6.2 Isolation of VLPs from cyanobacteria and PCC phytoplankton

VLPs from cyanobacteria and algal cultures were concentrated from 1-5 l of 0.2 µm filtered lysates using the QuikStand filtration system and concentrated to ca, 200 ml (Section 2.5.2). PEG precipitation further concentrated the lysates to ca. 1-3 ml (Section 2.5.3).

2.7 Extraction of nucleic acid

2.7.1 Algal DNA extractions

Exponentially growing host cells (10 ml) were pelleted, rinsed with sterile medium and repelleted. The pellet was resuspended in 1ml of lysis buffer (100 mM Tris, pH 8.0, 30 mM EDTA, 2 M NaCl, 30 mM EDTA, 10 mg/ml Proteinase K, 2 % w/v CTAB (cetyl trimethyl ammonium bromide), 2 % w/v PVPP, 2 % v/v 2-mercaptoethanol) and incubated at 42°C for 90 min. After the incubation, an equal volume of chloroform:isoamyl alcohol (24:1) was added and mixed by inverting several times. The organic and aqueous layers were separated by centrifugation at 6,000 x *g* for 10 min. The chloroform:isoamyl alcohol extraction step was repeated until the interface was clean (ca. 3x). DNA was precipitated from the top aqueous layer with the addition of 0.5x volume of 7.5 M ammonium acetate and 2 volumes of 100 % ethanol and kept at 4°C for at least 1 h. The DNA was pelleted by centrifugation at 16,000 x *g* for 30 min and then washed with 70% v/v ethanol. The DNA was pelleted by centrifugation at 16,000 x *g* for 15 min and the supernatant was decanted. The pellet was air dried and resuspended in 50 µl of ddH_2O.

2.7.2 Viral RNA extractions

RNA extractions were performed on aliquots of concentrated VLPs from CCMP 2465 (140 µl) obtained from bands in CsCl gradients using the QIAamp Viral RNA Mini Kit (Qiagen), according to the manufacturer's instructions.

2.7.3 Viral DNA extractions

For DNA extraction of concentrated VLPs a CTAB extraction method was used. For 1 ml of concentrate, 500 µl of prewarmed (55°C) lysis buffer (0.5% w/v SDS, 20 µg/ml proteinase K) was added and mixed by inverting. This mixture was incubated at 55°C for 1 h and mixed every 10 min. After the incubation was complete, 80 µl 5M NaCl and 150 µl prewarmed CTAB solution (2% w/v CTAB, 1.4 8M NaCl, 20 mM EDTA, 100 mM Tris) was added and incubated at 60 °C for 15 min. Chloroform:Isoamyl alcohol (24:1) extraction were performed as previously stated (Section 2.7.1). DNA was precipitated by the addition of 0.6 volume isopropanol. The contents were mixed by inverting and left at room temperature for 30 min. The DNA by centrifugation at 16,000 x *g* for 30 min, rinsed with 70% v/v ethanol and centrifuged for an additional 15 min. The pellet was air dried and resuspended in 50 µl of ddH_2O.

2.7.4 RNase and DNase treatments

The nucleic acid extracted from the VLPs was subjected to RNase and DNase treatments. 15 µl of the nucleic acid preparation was treated with 1 µl of RNase or DNase (Promega) containing 1x enzyme buffer supplied by the manufacturer (final volume 20 µl). The reactions were incubated at room temperature for 2 h.

2.8 Pulsed field gel electrophoresis (PFGE)

Lysates embedded in agarose and DNA extracted from the VLPs were examined with PFGE. Concentrated VLPs were prepared for PFGE according to a method described by Wommack *et al.*, 1999. Equal volumes (Wommack *et al.*, 1999) of molten 1.5% incert agarose (Biorad) and concentrated VLPs in SM Buffer were mixed by pipetting the mixture a few times in 2 ml microfuge tube. The mixture was aliquoted into plug moulds (BioRad). The agarose in plug moulds was solidified at -20°C for 2 min. Agarose plugs were incubated in 2 ml of Proteinase K solution (250 mM EDTA, 1% w/v SDS, 1 mg/ml Proteinase K) overnight at room temperature, in the dark. The Proteinase K digestion buffer was washed from the plugs with three rinses (30 min each rinse) in TE 20:50 (20 mM Tris, 50 mM EDTA, pH 8.0). Plugs were stored at 4°C in TE 20:50.

Gels containing 1 % (w/v) Biorad PFGE agarose were prepared by adding solid agarose to 0.5x TBE and heating to boiling point in a microwave oven. After cooling to approximately 45°C, the gel was poured into a casting tray containing a well-forming comb and left to solidify at room temperature for 15 min and then placecd at 4°C for 30 min. Agarose plugs were placed in the wells and sealed in with 2 % agarose. Liquid samples containing 1x loading buffer were loaded into wells after the addition of prechilled (4°C) 0.5x TBE tank buffer.

Electrophoresis conditions were 6 V/cm with an angle of 120°. The switch times and length of the runs varied and are specified in each figure showing the PFGE images. Gels were stained with ethidium bromide and visualised by UV excitation. Band sizes were estimated using a 0.05–1 Mb lambda ladder (BioRad) and/or a 0.2–2.2 Mb *S. cerevisiae* ladder (BioRad).

2.9 Polymerase chain reaction (PCR)

PCR was used to amplify fragments inserted in clones and to test DNA for amplification of algal virus or cyanophage specific genes. The reaction conditions varied between samples and are detailed below.

The PCR reaction mixtures contained ca. 100 ng of template DNA (depending on the source), 1x PCR buffer, 1-4 mM $MgCl_2$, 1 unit of *Taq* polymerase (Promega), 10 mM of each of the deoxynucleotide triphosphates and 10-50 pmol of each primer (Table 2.6) to a final volume of 50 µl. Where cells were used as a source of DNA template, a colony was resuspended in 5 µl high-purity water (MilliQ) and incubated at 95°C for 5 min. This lysed cell suspension was added directly to the PCR reaction mixture as template.

Table 2.6. List of primers used in this study.

Primer	Size	Primer sequence
M13F	18 bp	5' GTAAAACGACGGCCAGTG 3'
M13R	19 bp	5' GGAAACAGCTATGACCATG 3'
SL1	21 bp	5' CAGTCCAGTTACGCTGGAGTC 3'
SR1	25 bp	5' CTTTCTGCTGGAGGGGTCAGGTATG 3'
POL	17 bp	5' [G/C][A/T][A/G]TCIGT[A/G]TCICC[A/G]TA 3'
AVS	23 bp	5' GA[A/G]GGIGCIACIGTI[T/C]TIGA[T/C]GC 3'

All PCR reactions were performed in a PTC-200 cycling system (MJ Research). For amplification from colonies, thermal cycling was initiated with denaturation at 94°C for 1 min, annealing at 55°C for 1 min and extension at 72°C for 3 min for 30 cycles with final extension at 72°C for 10 min and held at 4°C. For amplification with DNA polymerase primers thermal cycling was initiated with denaturation at 95°C for 3 min, then 30 cycles of denaturing at 95°C for 30 seconds, annealing at 48°C for 60 seconds, and extension at 72°C for 90 seconds, with a final extension time at 72°C for 5 min.

2.9.1 Electrophoresis

Gels containing 1 % (w/v) agarose were prepared by adding solid agarose (Fisher) to 1 × TAE (40 mM Tris-acetate, 1 mM EDTA) and heating to boiling point in a microwave oven. After cooling to approximately 45°C, ethidium bromide was added to a final concentration of 0.5 µg/ml and the gel poured into a casting tray containing well-forming combs and left to solidify at room temperature. DNA samples containing 1x loading buffer (0.4% w/v orange G, 0.03% w/v bromophenol blue, 0.03% w/v xylene cyanol FF, 15% w/v Ficoll 400, 10 mM Tris-HCl (pH 7.5) and 50 mM EDTA (pH 8.0)) were loaded into wells. Electrophoresis was performed at a constant voltage of 100 V for 45 mins in 1 × TAE tank buffer. DNA bands were visualised by placing the gel on a UV transilluminator. Band sizes were estimated using 100 bp ladder (Promega) and/or lambda DNA cut with *Hind*III.

2.9.2 Gel Purification of DNA

DNA bands amplified by PCR were excised from the agarose gel using a scalpel. DNA was then extracted and purified from the agarose using Wizard® SV Gel and PCR Clean-Up kit (Promega) using the manufacturer's instructions. Samples were eluted in 30 µl of nuclease-free water and stored at -20°C.

2.9.3 Sequencing reactions

Sequencing reactions were carried out using a BigDye® Terminator v3.1 kit (Applied Biosystems). Reactions were set up as follows: 0.1-0.3 µg template, 5 µl 5x BigDye buffer, 3.2 pmol of primer and 1 µl BigDye Ready Reaction mix to a total volume of 20 µl.

Sequencing reactions were initiated with denaturation at 96°C for 1 min, followed by 25 cycles of 96°C for 10 seconds, 50°C for 5 seconds, 60°C for 4 min and held at 4°C until further processing.

The sequencing reactions were cleaned up using ethanol precipitation. 5 µl of 125 mM EDTA was added to the sequencing reactions and centrifuged briefly in a microfuge, next 60 µl of ice cold 100% ethanol was added and left at room temperature for 15 min in the dark. The tubes were centrifuged for 15 min at 6000 x *g* and the supernatant was removed. 65 µl of ice cold 70 % v/v ethanol was added and then centrifuged for 30 min at 6000 x *g*. The ethanol was pipetted off and the pellet was air dried. DNA samples were resuspended in 10 µl of HiDi® formamide (Applied Biosystems).

2.10 Cloning

2.10.1 Preparation of DNA for cloning

Prior to cloning, genomic DNA (Section 2.7.3) was fragmented. The DNA was fragmented by digestion with restriction enzymes or sonication. Restriction enzyme digestions were set up in accordance to the manufacturers' instructions with slight modification in the incubation times to optimise the fragment sizes (Table 2.7). All restriction enzymes were purchased from Promega (Southampton, UK).

Table 2.7. Restriction enzymes.

Enzyme	Cut site
*BamH*I	G^GATCC
*Eco*RV	GAT^ACT
*Hae*III	GG^CC
*Hha*I	GCG^C
*Hind*III	A^AGCTT
*Kpn*I	GGTAC^C
*Mbo*II	GAAGA(N)$_8$^
*Rsa*I	GT^AC
*Sau*3AI	N^GATCN
*Sma*I	CCC^GGG
*Spe*I	A^CTAGT
*Xba*I	T^CTAGA

To produce fragments in the desired size range, the DNA was sonicated. The time of sonication was optimised to obtain fragments of the desired size.

Sheared and digested DNA was blunt-ended prior to ligation using Mung bean nuclease, *Pfu* or Blunt end repair kit (Lucigen) according to the manufacturer's instructions. Fragmented DNA was run on agarose gels, stained with ethidium bromide and visualised with a dark reader (Clare Chemical Research Ltd.). Fragments of desired size were excised from the gel (Section 2.9.4).

2.10.2 Cloning

Cloning was carried out using a Zero Blunt® TOPO® PCR Cloning Kit (Invitrogen) and a Lucigen pSMART LCKan kit. The blunt ended fragments were ligated into the Zero Blunt vector or the pSMART vectors respectively. The ligation reactions were transformed into One Shot® Chemically Competent *E. coli* or E. cloni 10G Chemically Competent Cells or according to the manufacturers' instruction. Transformants were spread onto Luria-Bertani (LB) plates with 50 µg/ml of Kanamycin or yeast tryptone (YT) plates with 30 µg/ml of kanamycin (Table 4) and incubated overnight at 37°C.

Table 2.8. Composition of cloning media.

Medium	Quantity in 1 l of medium
Luria-Bertani broth	10 g Tryptone 5 g Yeast extract 10 g NaCl
Luria-Bertani Agar	10 g Tryptone 5 g Yeast Extract 10 g NaCl 15 g Agar
SOC	20 g Tryptone 5 g Yeast extract 0.5 g NaCl 10 ml 1 M $MgCl_2$ 10 ml 1 M $MgSO_4$ 2 ml 20% (w/v) Glucose
Yeast tryptone broth	8 g Tryptone 5 g Yeast extract 5 g NaCl
Yeast tryptone agar	8 g Tryptone 5 g Yeast extract 5 g NaCl 15 g Agar

2.10.3 Screening and sequencing

To screen for inserts, small amounts of each clone were picked into 5 µl of molecular grade water and heated to 94°C for 5 min then cooled to 4°C. PCR amplification was performed using the vector primers (Section 2.7). PCR products were treated with ExoSAP-IT (USB Corporation), 1 µl ExoSAP-IT was added to 2.5 µl PCR product and incubated at 37°C for 15 min, 80°C for 15 min and then held at 4°C. ExoSAP-IT treated PCR products were used for sequencing reactions (Section 2.7.1)

For larger inserts, plasmids were prepared for sequencing using Wizard® *Plus* SV Minipreps DNA Purification System (Promega) according to manufacturer's instructions.

Sequencing was performed through Plymouth Marine Laboratory on an ABI 3100 automated sequencer (Applied Biosystems). Clones were sequenced with plasmid forward and reverse primers, M13F and M13R for fragments cloned into the Zero Blunt vector (Invitrogen). The primers SL1 and SR2 were used for fragments in Lucigen pSMART HCKan plasmid.

2.10.4 Sequence analysis

Consensus sequences were assembled using SeqMan (DNASTAR) and PhredPhrap software (Ewing & Green, 1998). The BLAST (Basic Local Alignment Search Tool) programs, Blastn, Blastx, Blastp and PSI-BLAST were used to compare continuous sequences (contigs) to nucleotide and amino acid databases (Altschul *et al.*, 1997). Top BLAST hits to the non-redundant GenBank data set and top BLAST hits to the non-redundant GenBank data set restricted to virus sequences were complied. Searches for open reading frames (ORFs), were performed online with the WebGeneMark.hmm software (Besemer & Borodovsky, 1999). These predicted genes were compared against sequences in GenBank. A hit was considered significant if it had an *E* value of <0.001.

CHAPTER 3 Latent viruses of zooxanthellae

3.1 Introduction

Dinoflagellates are considered to be amongst the most primitive of the eukaryotes with fossil records dating back to the Triassic age (Peters *et al.*, 2005). Most dinoflagellates are unicellular, photosynthetic algae found in many aquatic environments; the majority of species are marine, but they are also common in freshwater lakes, rivers and bogs. The free-living phytoplankton are some of the major primary producers in the oceans. However, at high concentrations many species form harmful blooms. While not all dinoflagellate blooms are dangerous, some species produce neurotoxins that can have detrimental effects on fish, marine mammals and humans (Miller & Belas, 2003).

Dinoflagellates contain chlorophylls *a* and *c* and fucoxanthin, as well as various other accessory pigments. Chloroplasts are enveloped by three rather than two membranes, which has led to suggestions that the chloroplasts (plastids) in dinoflagellates were originally symbiotic algae that evolved by tertiary endosymbiosis (Morden & Sherwood, 2002). Movement of dinoflagellates is facilitated by two dissimilar flagella which propel the cells in a whirling motion; the name dinoflagellate refers to the Greek word *dinos* meaning whirling.

Some dinoflagellate species are endosymbionts of a wide variety of marine animals, including scleractinian corals, softcorals, molluscs, sea anemones, gorgonians, sponges, and foraminifera (Rowan, 1998; Trench, 1993). All symbionts have been placed in the genus *Symbiodinium* and are called zooxanthellae when observed within the host tissues. By far the best-understood zooxanthellae are those associated with cnidarians. The association of the endosymbionts is mutually beneficial to both organisms and the symbiosis with zooxanthellae is believed to explain the success of reef-building corals in nutrient-poor tropical seas (Glynn *et al.*, 1991). The zooxanthellae release photosynthetic products to their hosts, providing an important source of organic carbon

and nitrogen for host metabolism, growth and reproduction (Davy *et al.*, 1996; Muscatine, 1990; Wang & Douglas, 1998). In return, the host provides protection to the dinoflagellate.

Symbionts can be horizontally or laterally acquired by the host organism and in some cases there is specificity between host and *Symbiodinium* clade. Clade types are groupings of divergent lineages of *Symbiodinium* and within each clade are numerous closely related types or species (Rowan & Powers, 1991). Some of these clades contain one or more described species while other clades have no formally described species. There are currently eleven named species in the genus *Symbiodinium*, ten of which have been described based on the morphological description of cultured isolates (Table 3.1).

Table 3.1. Named *Symbiodinium* species, clade affiliation and host organism of isolation (LaJeunesse, 2001).

Organism	Clade	Host
Symbiodinium microadriaticum	A1	Jellyfish (*Cassiopeia xamachana, C. andromeda*), coral (*Stylophora pistillata, Acropora valida*)
Symbiodinium pilosum	A2	Zoanthid (*Zoanthus sociatus*)
Symbiodinium kawagutii	F1	Coral (*Montipora capitata*)
Symbiodinium goreaui	C1	Anemone (*Ragactis lucida*)
Symbiodinium californium	B4 aka E1	Anemone (*Anthopleura elegantissima*)
Symbiodinium corculorum	A2	Clam (*Corculorum cardissa*)
Symbiodinium meandrinae	A2	Coral (*Meandrina meandrites*)
Symbiodinium pulchrorum	B	Anemone (*Aiptasia* spp.)
Symbiodinium bermudense	B	Anemone (*Aiptasia pallida*)
Symbiodinium cariborum	A1.1	Jellyfish (*Cassiopeia frondosa*), Anenome (*Condylactis gigantea*)
Symbiodinium muscatinei	B4 aka E	Anemone (*Anthopleura elegantissima*)

Symbiodinium taxonomy is predominantly based on molecular phylogenetics (Baker, 2003; LaJeunesse, 2001). Nuclear (rDNA) and chloroplast (cpDNA) ribosomal DNA phylogenies divide the genus into eight highly divergent lineages, or clades (Clades A through H). The internal transcribed spacer region (ITS) (Hunter *et al.*, 1997) is a less conserved portion of the rDNA which provides higher levels of variation and resolution than 18S rDNA and 23S rDNA (Coffroth & Santos, 2005; LaJeunesse, 2001; van Oppen *et al.*, 2001).

The ecological dominance and the distribution of clades differ throughout the world's oceans and closely related symbionts are found in unrelated hosts (Baker & Rowan, 1997; Baker, 2003; Carlos *et al.*, 1999; LaJeunesse *et al.*, 2003; Rowan & Powers, 1991). Clade A are found in scleractinian corals, octocorals, hydrocorals, clams, anemones and zoanthids. Most hosts of clade A zooxanthellae are found in the Caribbean, but they are also found in the Great Barrier Reef, the Red Sea and the western Pacific. Clade B are commonly found in Caribbean gorgonians, but they have been isolated from Atlantic stony coral, Hawaiian Aiptasia anemones, the coral *Pocillopora damicornis* and Great Barrier Reef *Acropora* species. Clade C is considered a pandemic generalist. Clade D is found in corals in the West Pacific. Clade E is not known to occur in corals, but rather in anemones; the two named members in this clade, *S. muscatinei* and *S. californium* are found in the host *Anthopleura*. Members of this clade are sometimes listed as belonging to Clade B. Clades A-D have been the focus of more interest while clades F, G and H are not as well described.

Zooxanthellae are known to have differing susceptibilities to stresses (Baker, 2003). While species may be in the same clade, this does not necessarily infer that they are physiologically similar to one another. However, there seem to be common traits among *Symbiodinium* clades. The two most common trends exhibited in clades are tolerances to irradiance and temperature (Rowan & Knowlton, 1995). Some zooxanthellae clades are more tolerant of high light intensity and/or thermal variations. Symbionts of clades A and B are found in areas with higher irradiance while clade C is generally found in areas with lower light intensities (Rowan *et al.*, 1997). Symbionts in clade D appear to be the most tolerant of elevated temperatures and are generally the dominant clade on reefs which have experienced temperature-related bleaching (Baker *et al.*, 2004; Fabricius *et al.*, 2004; Glynn *et al.*, 2001).

Reef-building corals associate with a diverse array of eukaryotic and prokaryotic microbes. The coral colony has been modeled as a holobiont comprising multispecies mutualisms consisting of the coral animal, endosymbiotic dinoflagellates (zooxanthellae), bacteria, fungi, protozoa, endolithic algae and other unknown components (Rohwer *et al.*, 2002). The disruption of any of these components may cause physiological changes that result in coral disease or death. Disruption of the zooxanthellae-host symbiosis (bleaching), can lead to expulsion of zooxanthellae from the host and/or a decline in the zooxanthellae photosynthetic pigment (Glynn *et al.*, 1991; Jones, 1997). Zooxanthellae have been shown to undergo necrosis, apoptosis and lysis during bleaching (Banin, 2000; Strychara *et al.*, 2004). The expulsion of *Symbiodinium* cells may help corals adapt to changing environmental conditions by allowing symbiont populations to redistribute themselves allowing more tolerant clades to repopulate (Baker, 2001; Buddemeier & Fautin, 1993). After a bleaching event, if the symbiont – host relationship is not recovered the coral will not survive (Szmant & Gassman, 1990).

Coral bleaching has increased in frequency and intensity in the last two decades, leading to mass mortality of corals and a consequent reduction in the biodiversity of reefs (Brown, 1997; Szmant & Gassman, 1990). Bleaching has been observed in over 50 countries and in the three major oceans (Wilkinson, 1998). Many environmental factors have been linked to coral bleaching; these include elevated and reduced temperature (Fitt *et al.*, 2001), exposure to ultraviolet radiation (Jokiel, 1990), and bacterial infections (Ben-Haim *et al.*, 2003; Kushmaro *et al.*, 1997). However the underlying cause of bleaching and the mechanisms involved remain largely unknown.

The random mosaic patterns often seen during bleaching are difficult to attribute to the effect of temperature stress alone as neighboring regions of the colony must be exposed to the same conditions (Hayes & Bush, 1990). One explanation for the patchy spatial

distribution of coral bleaching involves localised infections. Bacterial infection by *Vibrio* spp. has been shown to be responsible for some types of coral bleaching (Ben-Haim *et al.*, 2003; Rosenberg & Ben-Haim, 2002; Toren *et al.*, 1998).

Another explanation may be that susceptible strains of zooxanthellae may harbour a latent infection. There are relatively few reports on viruses of dinoflagellates (Franca, 1976; Nagasaki *et al.*, 2003; Onji *et al.*, 2003; Sicko-Goad & Walker, 1979; Tarutani *et al.*, 2001) and less still on the presence of viruses in zooxanthellae. Previous studies in this laboratory have shown that zooxanthellae and corals produce VLPs upon exposure to temperature stress and elevated temperature (Davy *et al.*, 2006; Wilson *et al.*, 2001; Wilson *et al.*, 2005), suggesting that zooxanthellae harbour latent viruses. While the previous studies strongly suggest stressed corals and zooxanthellae harbour latent infections, the VLPs observed have not been characterised as the host of the VLPs produced upon exposure to heat stress were not identified.

This study utilises *Symbiodinium* spp. cultured *in vitro* to simplify the complexity found in whole organisms containing symbionts, in order to determine whether VLPs are induced by exposure of the zooxanthellae to UV-C light. A filamentous VLP, ZFV1, infecting *Symbiodinium* spp. has been isolated and characterised. Molecular characterisation of ZFV1 was attempted to further identify the filamentous VLP. Several genomic libraries prepared from the lysates of UV-induced cultures were sequenced with the ultimate goal of identifying novel genes that could be employed in molecular probes to detect potential latent infections in field samples on coral reefs.

3.2 Results

3.2.1 Evaluation of induction methods

The 16 zooxanthellae cultures (Table 2.1) were exposed to three experimental induction treatments. Haemocytometry was used to make daily cell counts for each strain. Results of elevated temperature of 34°C, direct exposure to UV radiation of 254 nm and exposure to Mitomycin C are shown in Figure 3.1. The haemocytometer counting chamber is subject to a statistical error of +/- 2%. These preliminary data, using single replicates, showed variability between the induction method and zooxanthella strain. Overall the strains showed a greatest sensitivity to UV treatment; heat shock and Mitomycin C treatment showed more variable results over the time course of the experiments. The reduction in cell numbers 96 h after treatment in the UV-treated strains ranged from 33%-85% (average 60%), heat treatment showed reductions from 11%-72% (average 45%), and Mitomycin C treatment showed declines in cells numbers from 15%-67% (average 48%).

The results were compared to look for a pattern in the sensitivity of the clades to the different induction methods (Figure 3.2). UV induction showed the most consistent reduction in zooxanthellae numbers relative to the control, while Mitomycin C treatment showed the most variability over the time course. Heat shock appeared to have an initial beneficial effect on the growth of clade F while the remaining clades showed a decrease in cell numbers relative to the control. The greatest decrease among the clades, 96 h after the experimental treatments occurred in the UV-treated clades (45%-75% -average 58%); heat shock treatment showed the least reduction (5%-45% - average 32%). Clades A, B, and F were most sensitive to UV treatment, while Clades E and C were most sensitive to Mitomycin C treatment (40%-65% -average 50%). As a result of these preliminary induction experiments, it was decided to use UV light for induction in subsequent experiments.

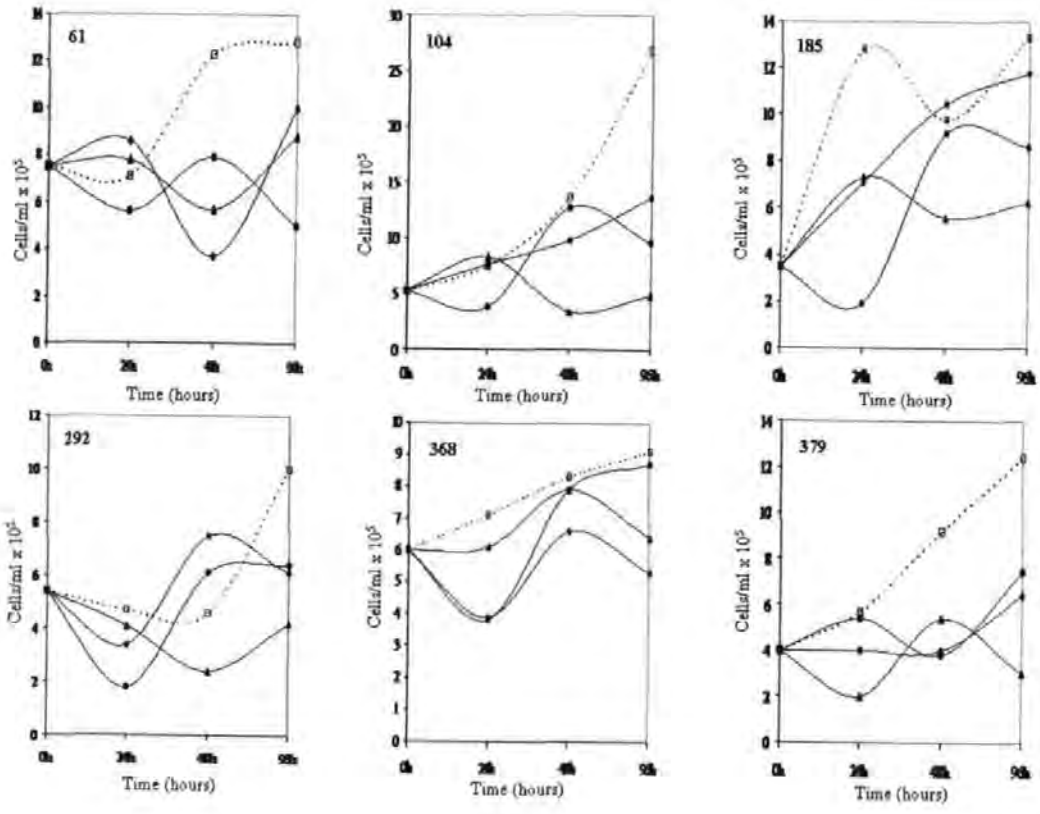

Figure 3.1. Preliminary induction graphs showing the effects of elevated temperature, UV-C light and Mitomycin C on clade A *Symbiodinium* strains, 61; 104; 185; 292; 368 and 379. The control is represented by the □, exposure to elevated temperature (34°C for 24 h) is represented by the ♦, exposure to UV light (2 min) is represented by the ▲ and exposure to Mitomycin C (1 µg/ml) is represented by the ●. Strain designation is shown in the upper left hand corner of the respective graph (n=1). A statistical error of +/- 2% is associated with the counting chamber of the haemocytometer.

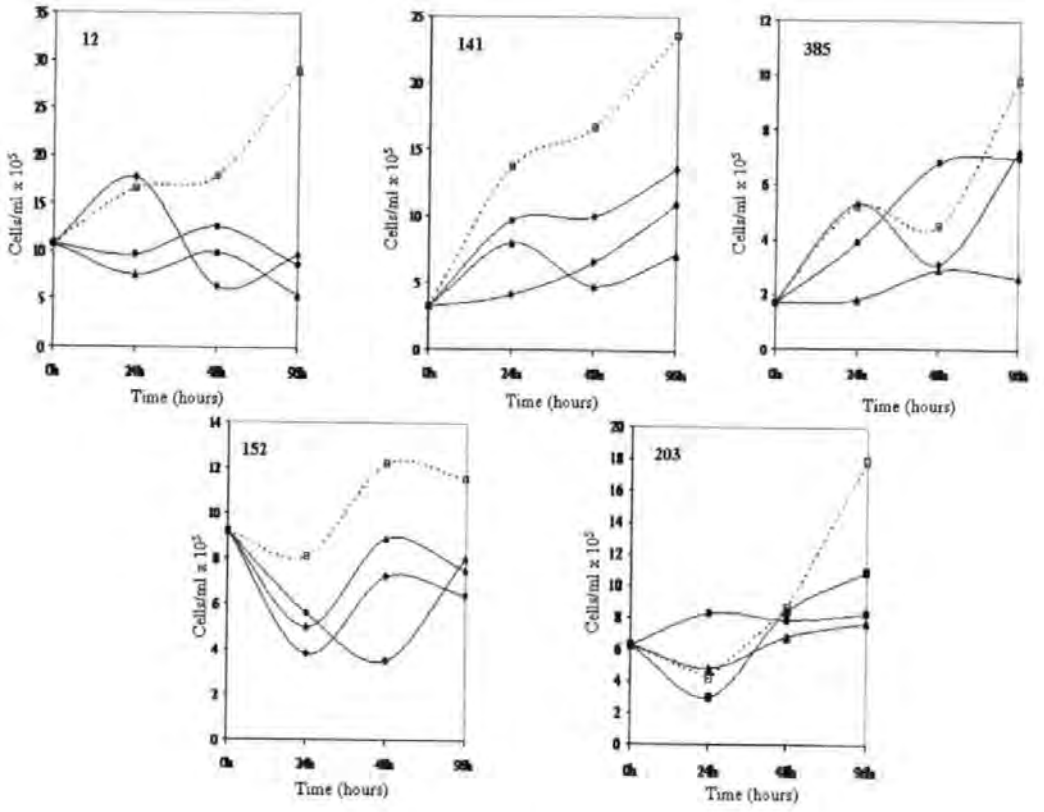

Figure 3.1 (cont.). Preliminary induction graphs showing the effects of elevated temperature, UV light and Mitomycin C on clade B (strain 12, 141 and 385) and clade C (strain 152 and 203) *Symbiodinium* strains. The control is represented by the □, exposure to elevated temperature (34°C for 24 h) is represented by the ♦, exposure to UV-C light for (2 min) is represented by the ▲ and exposure to Mitomycin C (1 µg/ml) is represented by the ●. Strain designation is shown in the upper left hand corner of the respective graph (n=1). A statistical error of +/- 2% is associated with the counting chamber of the haemocytometer.

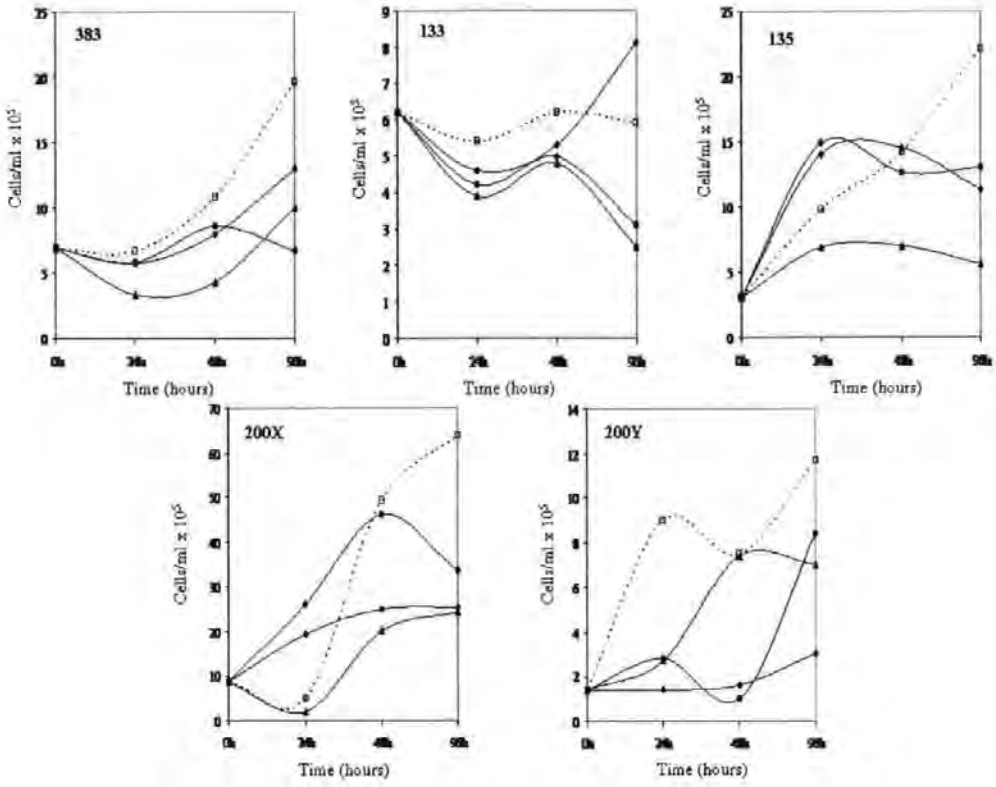

Figure 3.1 (cont.). Preliminary induction graphs showing the effects of elevated temperature, UV light and Mitomycin C on clade E (strain 383), clade F (strain 133 and 135) and the two unknown clades (strain 200X and 200Y) of *Symbiodinium* strains . The control is represented by the □, exposure to elevated temperature (34°C for 24 h) is represented by the ♦, exposure to UV-C light for (2 min) is represented by the ▲ and exposure to Mitomycin C (1 µg/ml) is represented by the ●. Strain designation is shown in the upper left hand corner of the respective graph (n=1). A statistical error of +/- 2% is associated with the counting chamber of the haemocytometer.

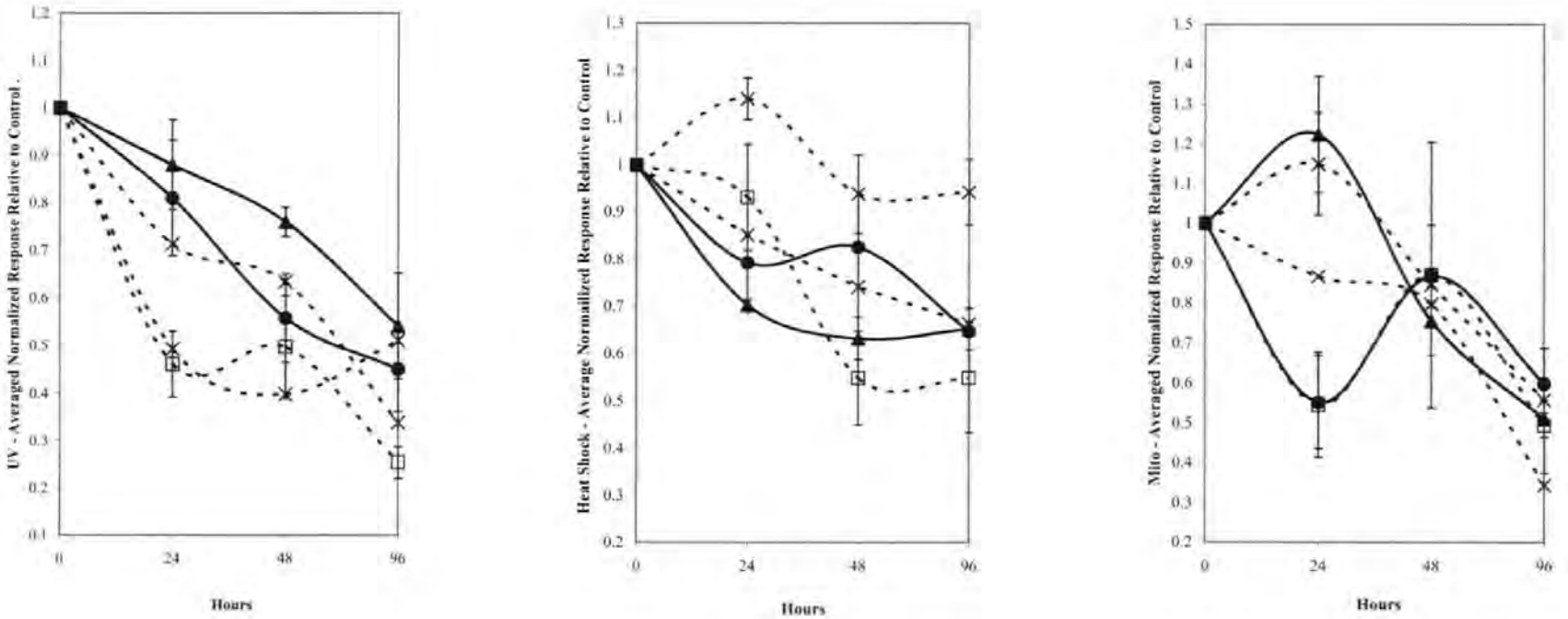

Figure 3.2. Tthe average of normalised response relative to the control during UV-induction, heat-shock and Mitomycin C treatment. The response in the treated cultures for each strain was divided by the respective control to normalise; all strains in individual clades were grouped and the response was then averaged for each clade. The averaged normalised response to UV treatment is shown in panel A, heat-shock treatment is shown in panel B and Mitomycin C treatment is shown in Panel C. Clade A (—●—) (n=6, strain 61, 104, 185, 292, 368, 379), Clade B (--□--)(n=3, strain 12, 141, 385), Clade C (—▲—) (n=2, strain 152, 203), Clade E (--x--) (n=1, strain 383), Clade F (--*--) (n=2, strain 133, 135).

3.2.2 Enumeration of zooxanthellae

After preliminary induction experiments, enumeration of the zooxanthellae was performed with AFC. Representative AFC dot plots are shown in Figure 3.3. Four parameters (side scatter, forward scatter, orange fluorescence and red fluorescence) were used to assess the fluorescence and enumerate the zooxanthellae in control and UV-induced cultures. Panels A and B show the control at 0 h and 96 h, respectively. Increases in the number of events measured with the four sets of parameters indicate an increase in cell numbers. In the UV-treated cultures, a decrease in events and fluorescence was observed, as shown in Figure 3.3 C (0 h) and Figure 3.3 D (96 h). The number of events in the area highlighted (Figure 3.3 A) was analysed daily in triplicate for both the control and UV-treated cultures.

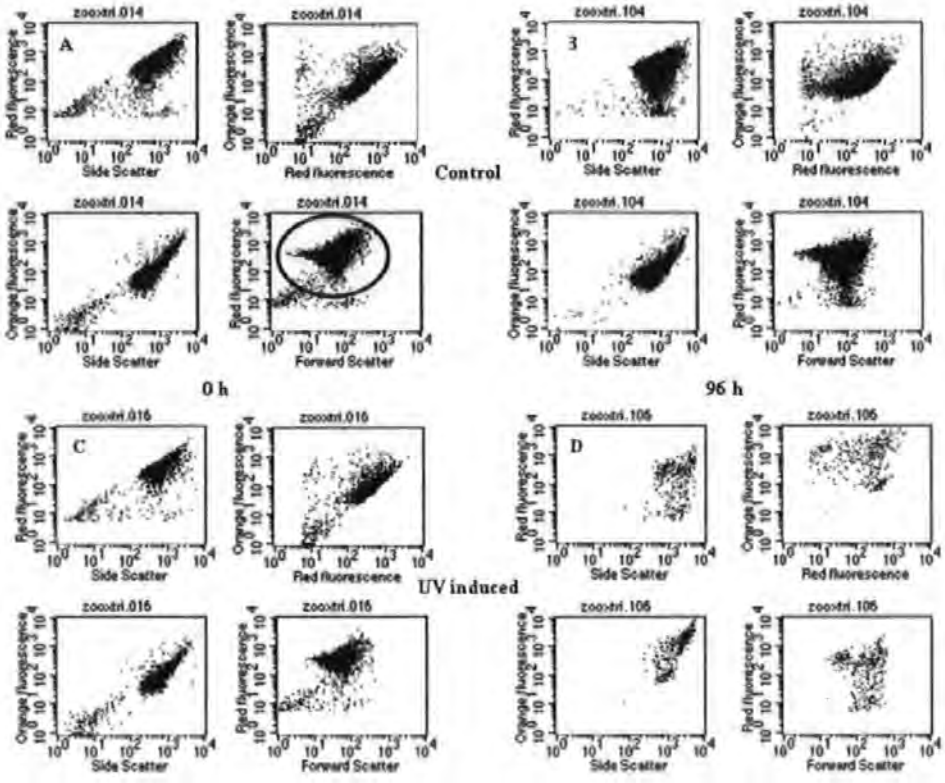

Figure 3.3. Representative AFC dot plots of strain 292, enumerating live zooxanthellae in controls and UV-induced cultures at 0 h and 96 h. Controls are shown in panel A (0 h) and panel B (96 h). The UV-induced zooxanthellae are shown in panel C (0 h) and panel D (96 h). The area highlighted in panel A shows the group analysed for the number of events occurring in each sample.

3.2.3 Enumeration of VLPs

Counts of VLPs and bacteria were made using AFC. Representative dot plots showing the groups of bacteria, bacteriophage and potential VLPs are shown in Figure 3.4. Particles were stained with SYBRgreen I and assessed using side scatter (SSC) and green fluorescence (GFL). Areas typical of bacteria and bacteriophage have been highlighted in panel A. VLPs of algae are usually larger than bacteriophages yet smaller than bacteria, and are generally seen as a cluster of particles with a SSC and GFL between that of bacteria and bacteriophage. Panels A through D show the plots of the control from 0 h to 96 h, and panels E through H show the plots from the UV-treated culture (strain 292). In panels F through H the appearance and increase of a new group of VLPs is indicated by arrows. The number of events in the highlighted areas (Figure 3.4 A and H) was analysed daily in triplicate for both the control and UV-treated cultures.

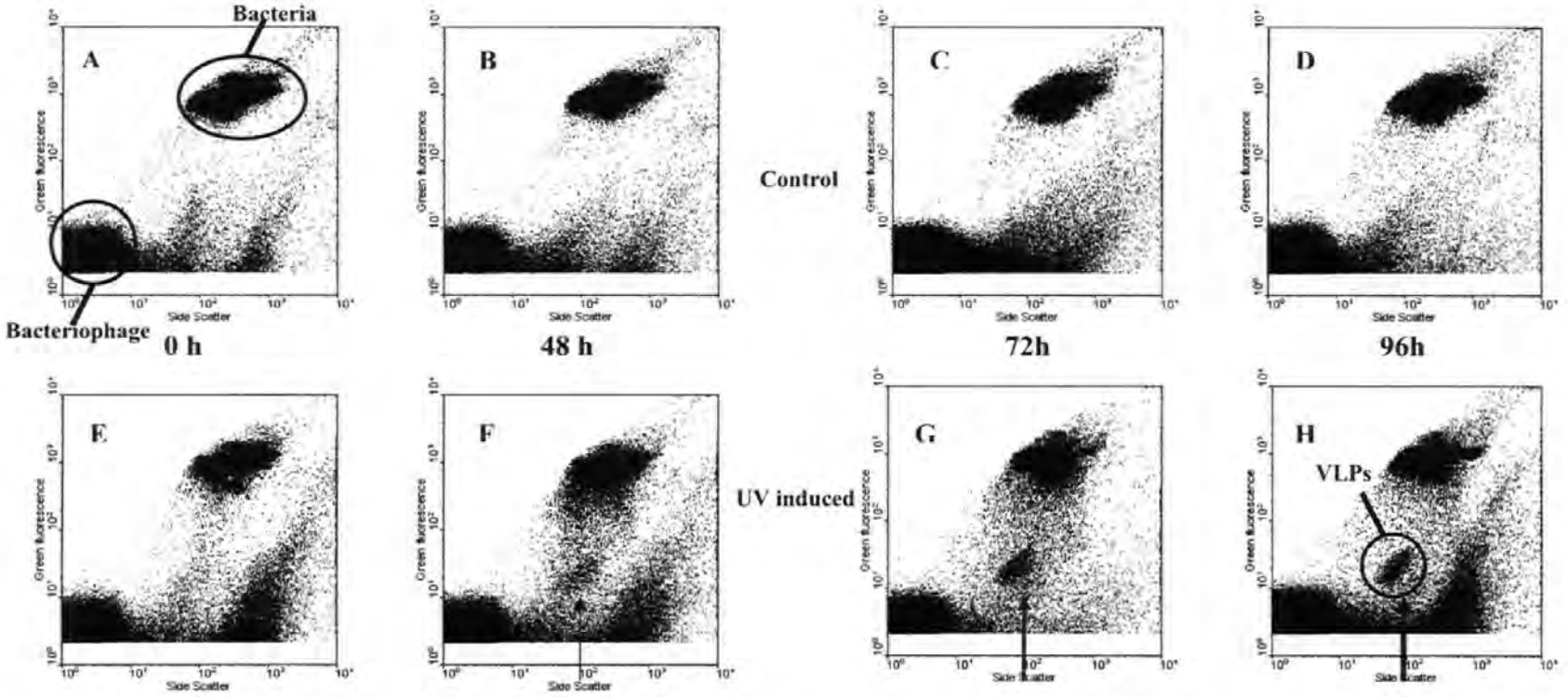

Figure 3.4. Representative AFC dot plots of strain 292, showing SYBRgreen I stained particles in the size range typical of bacteria and VLPs at 0 h and 96 h. Controls are shown in panel A (0 h), B (48 h), C (72 h) and panel D (96 h). The UV-induced zooxanthellae are shown in panel E (0 h), F (48 h), G (72 h) and panel H (96 h). Panel A highlights areas typical of bacteria and bacteriophage and the arrows in panels F, G and H highlight the appearance of a new group of VLPs.

3.2.4 Inducible VLPs

AFC dot plots from the 16 zooxanthellae strains comparing the control and UV-treated cultures at 96 h after UV induction are shown in Figure 3.5. Dot plots of strains 292, 379, 141, 385, 133 and 200Y show that, in each case, a distinct group of VLPs with a high SSC and low GFL present in the UV-treated cultures that was not seen in the controls. Dot plots of strains 61, 104, 12, 203, 383, 135 and 200X show a similar group of high SSC VLPs, but the group is also present in the control and/or the group is not clearly distinguishable. The dots plots show that 37.5% of the strains produced a similar inducible group of VLPs with high SSC and low GFL that is clearly identifiable, while an additional 31.3% of strains showed this similar group in both the control and UV-treated cultures. Table 3.2 summarises the strains that have the cluster of high SSC VLPs. Strains 12 (clade B), 152 (clade C) and 292 (clade A) were selected for further characterisation.

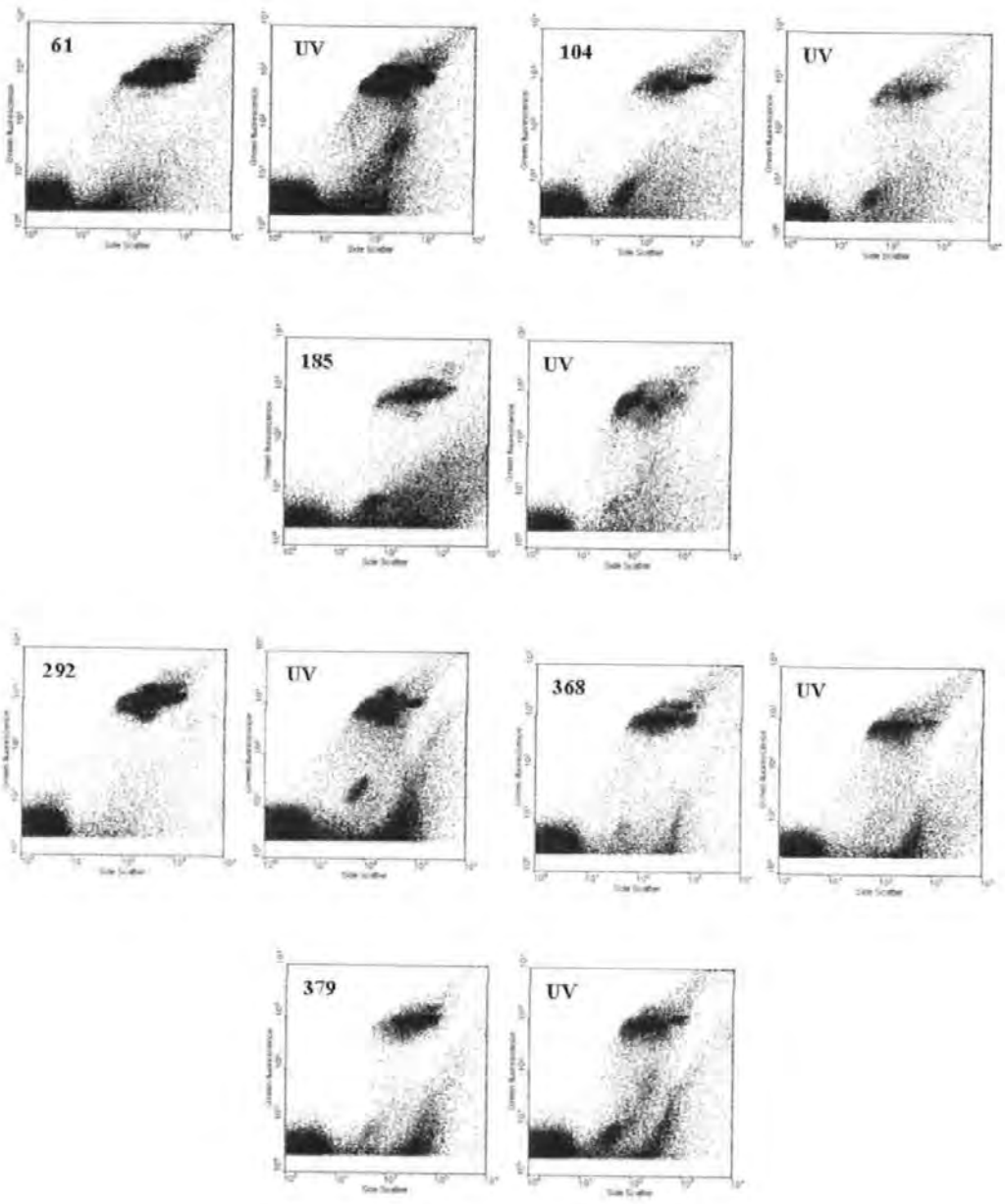

Figure 3.5. UV induction AFC plots showing SYBRgreen I stained particles of clade A strains 96 h after exposure to UV-C light. The left graphs are the controls and the right graph is UV-treated cultures.

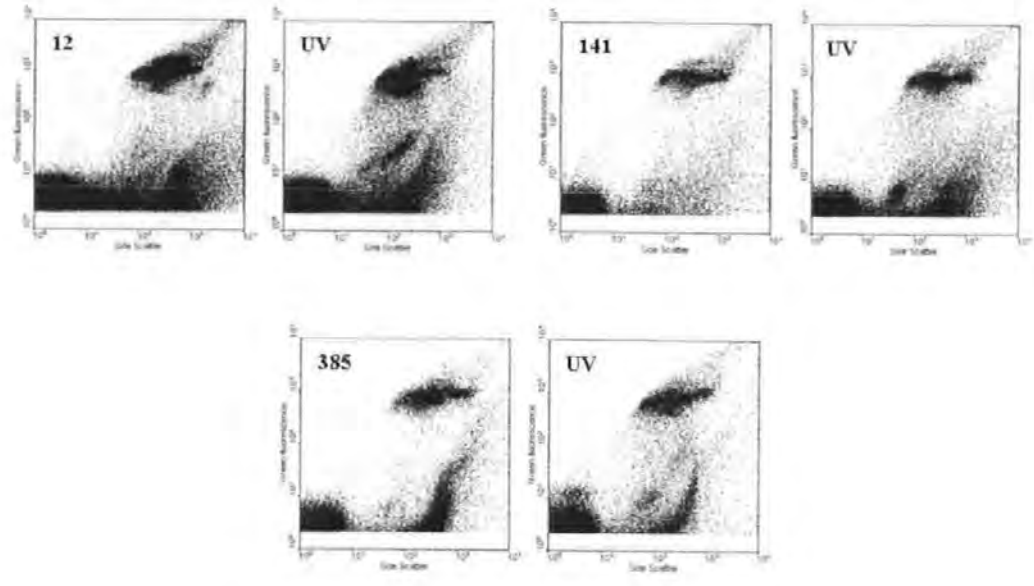

Figure 3.5 (cont.). UV induction AFC plots showing SYBRgreen I stained particles of clade B strains 96 h after exposure to UV-C light. The left graphs are the controls and the right graph is UV-treated cultures.

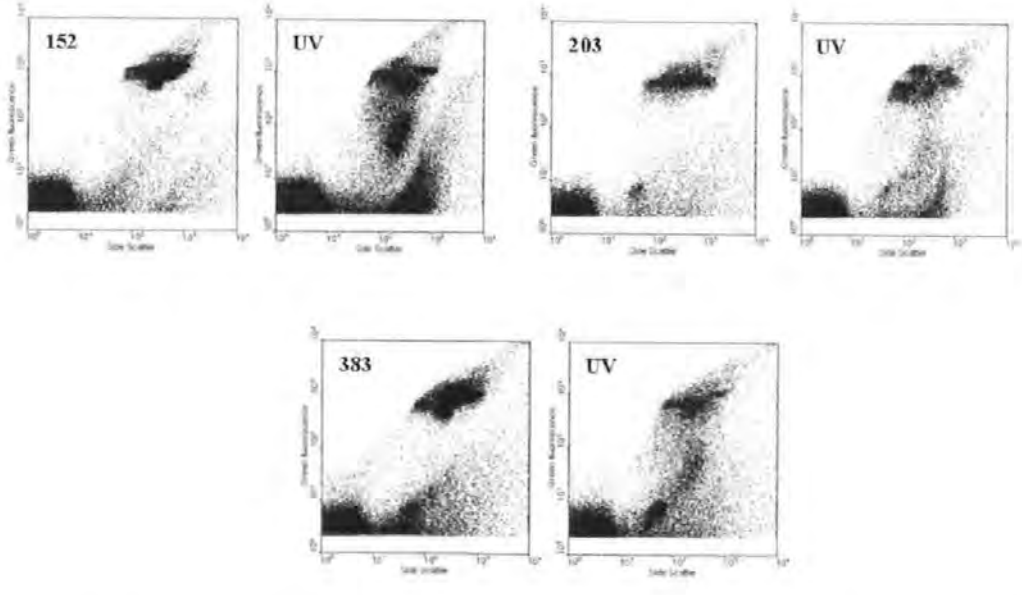

Figure 3.5 (cont.). UV induction AFC plots showing SYBRgreen I stained particles of clade C (strain 152 and 203) and E (strain 383) 96 h after exposure to UV-C light. The left graphs are the controls and the right graph is UV-treated cultures.

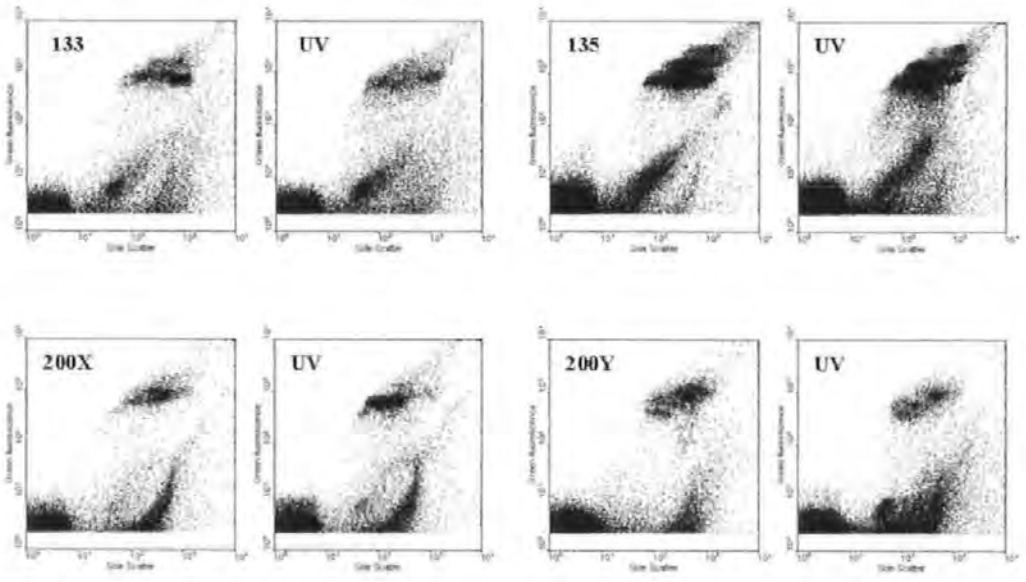

Figure 3.5 (cont.). UV induction AFC plots showing SYBRgreen I stained particles of clade F (strain 133 and 135) and strains 200X and 200Y (clade unknown) 96 h after exposure to UV-C light. The left graphs are the controls and the right graph is UV-treated cultures.

Table 3.2. Table identifying presence of VLP clusters in controls and UV-treated cultures of zooxanthellae strains. n/a, data not available. nc, not consistent.

Zooxanthellae Isolate number	Clade/ITS type	VLP cluster control	VLP cluster UV-treated	Host origin	Symbiont species
61	A1	nc	yes	*Cassiopeia xamachana* (jellyfish)	*Symbiodinium microadriaticum*
104	A2	yes	yes	*Heliopor* species (coral)	n/a
185	A2	nc	no	*Zoanthus sociatus* (sea anemone)	*Symbiodinium pilosum*
292	A3	no	yes	*Tridacna maxima* (giant clam)	*Symbiodinium* species
368	A4	no	no	*Linuche unguiculata* (jellyfish)	*Symbiodinium linucheae*
379	A4	no	yes	*Plexaura homamalla* (sea fan)	*Symbiodinium* species
12	B1	nc	yes	*Aiptasia tagetes* (sea anemone)	*Symbiodinium* species
141	B2.1	no	yes	*Oculina diffusa* (coral)	*Symbiodinium* species
385	B3	no	yes	*Dichotomi* species (jellyfish)	*Symbiodinium* species
152	C1	no	nc	*Discosoma sancti-thomae* (coral)	*Symbiodinium goreaui*
203	C2	yes	yes	*Hippopus hippopus* (giant clam)	*Symbiodinium* species
383	E1	yes	yes	*Anthropleura elegantissima* (sea anemone)	*Symbiodinium californium*
135	F1	yes	yes	*Montipora verrucosa* (coral)	*Symbiodinium kawagutii*
133	F2	yes	yes	*Meandrina meandrites* (coral)	*Symbiodinium* species
200X	n/a	no	yes	*Acropora formosa* (coral)	n/a
200Y	n/a	no	yes	*Acropora formosa* (coral)	n/a

3.2.5 Effect of UV treatment on induction of VLPs over time

AFC dot plot analysis (Sections 3.2.2 and 3.2.3) of zooxanthellae cells, VLPs, bacteria and bacteriophages from strains 12, 152 and 292 are shown in Figures 3.6 a, b and c. Events (particles) occurring in highlighted areas (Figures 3.3 and 3.4) were plotted over the time course of the induction experiments. Panels A, C and E show the host numbers in the control and UV-treated cultures (cells/ml x 10^5) compared to the VLP/ml x 10^5. In all three cultures, a rapid decline in the concentration of zooxanthellae was observed between 24 h and 48 h after UV treatment, which correlated with the appearance and rapid increase in the concentration of the high-SSC VLP group. The concentration of the VLPs continued to increase to ca 2-3 x 10^6 particles ml^{-1} at 96 h after UV treatment, at which point the UV-induced zooxanthellae cultures showed a decline in cell numbers. Panels B, D and F show the numbers of bacteria in the control and UV-treated culture compared to the bacteriophages (cells/ml x 10^6). In all three cultures, the concentration of bacteria decreases within 48 h of UV treatment, while the numbers of the bacteriophages remain relatively stable between the control and the UV-treated cultures.

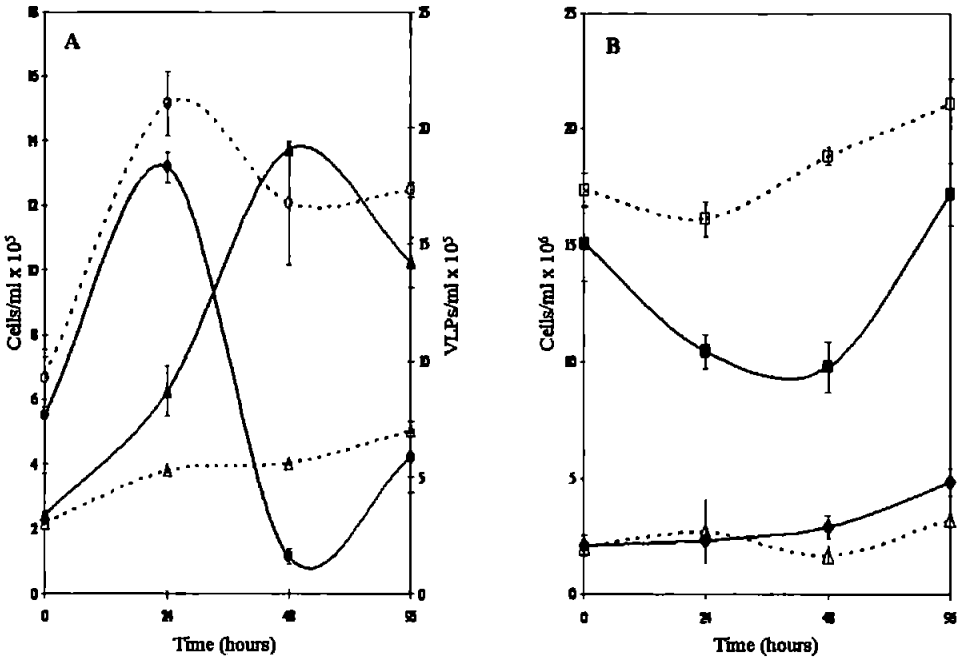

Figure 3.6a. Growth curves showing AFC numbers (cells ml^{-1} x 10^5) of zooxanthellae strain 12 in control (○) and UV-treated cultures (●), together with numbers of the high SSC VLP group (VLPs ml^{-1} x 10^5) in the non-irradiated control cultures (△) and in the UV-treated cultures (▲)(A). Concentrations of bacterial numbers (cells ml^{-1} x 10^6) in the control cultures (□) and in the UV-treated cultures (■) together with the bacteriophage numbers (particles ml^{-1} x 10^6) in the control (◇) and the UV-treated cultures (◆)(B). Error bars represent standard error (SE) of measurements from triplicate cultures, n=3.

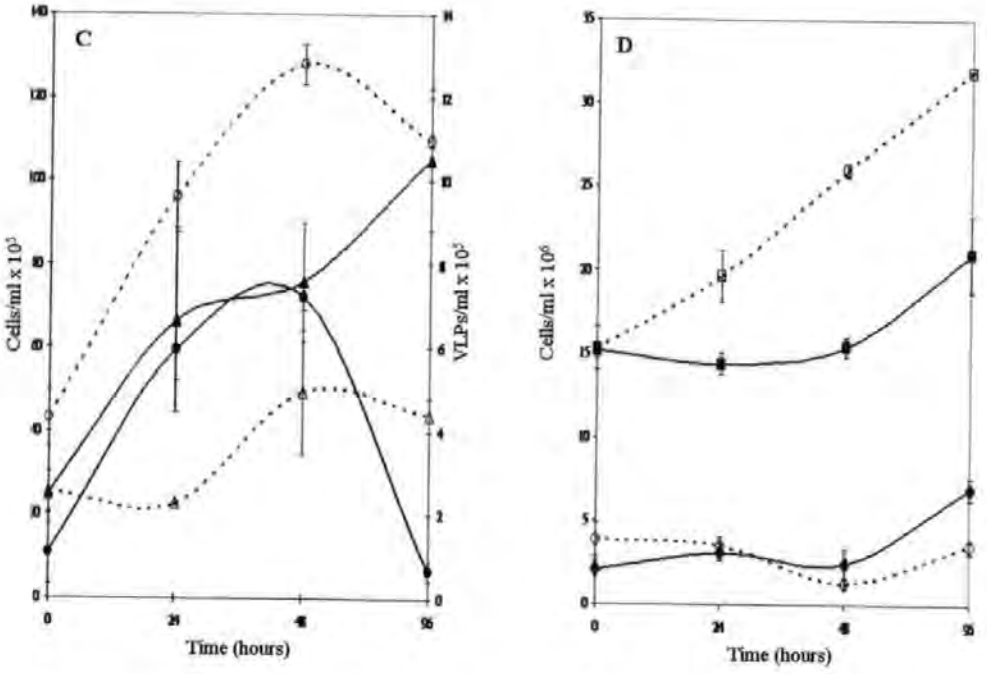

Figure 3.6b. Growth curves showing AFC numbers (cells ml^{-1} x 10^5) of zooxanthellae strain 152 in control (○) and UV-treated cultures (●), together with numbers of the high SSC VLP group (VLPs ml^{-1} x 10^5) in the non-irradiated control cultures (◇) and in the UV-treated cultures (▲)(C). Concentrations of bacterial numbers (cells ml^{-1} x 10^6) in the control cultures (□) and in the UV-treated cultures (■) together with the bacteriophage numbers (particles ml^{-1} x 10^6) in the control (◇) and the UV-treated cultures (♦)(D). Error bars represent standard error (SE) of measurements from triplicate cultures, n=3.

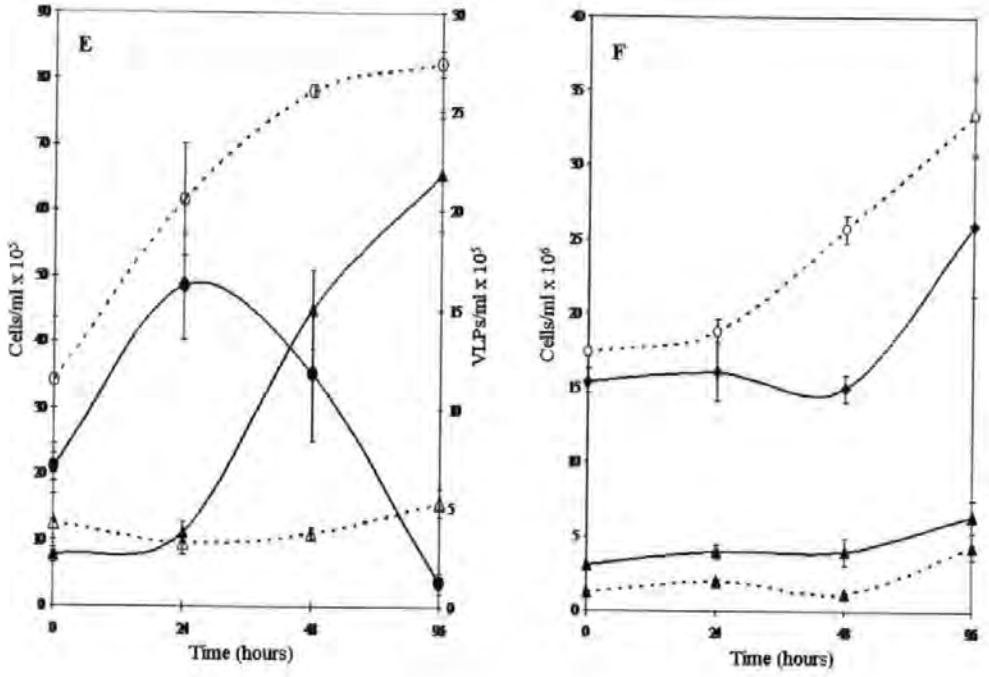

Figure 3.6c. Growth curves showing AFC numbers (cells ml^{-1} x 10^{5}) of zooxanthellae strain 292 in control (○) and UV-treated cultures (●), together with numbers of the high SSC VLP group (VLPs ml^{-1} x 10^{5}) in the non-irradiated control cultures (△) and in the UV-treated cultures (▲)(E). Concentrations of bacterial numbers (cells ml^{-1} x 10^{6}) in the control cultures (□) and in the UV-treated cultures (■) together with the bacteriophage numbers (particles ml^{-1} x 10^{6}) in the control (◇) and the UV-treated cultures (◆)(F). Error bars represent standard error (SE) of measurements from triplicate cultures, n=3.

3.2.6 Isolation and concentration of VLPs

VLPs were isolated from the growth media 96 h after UV exposure. Debris, bacteria and algal cells were removed by centrifugation at 10,000 x *g* for 5 min, followed by 0.45 μm filtration. VLPs were concentrated by tangential flow filtration and ultracentrifugation at 100,000 x *g* for 4 h to a volume of ca. 3 ml.

VLPs were further purified and concentrated on CsCl gradients prepared with CsCl at densities of 1.0, 1.2, 1.4, and 1.6. The concentrated VLPs were added to the 1.0 density aliquot. A translucent white band from strain 292 with a density ca. 1.25 g cm^{-3} is shown in Figure 3.7. Aliquots from the CsCl gradient were analysed by AFC (Figure 3.8). The high SSC VLPs occurred at a much higher density than the sample before concentration (Figure 3.8 panels A and B). The 0.45 μm filtration and CsCl separation removed a majority of the bacteria present in the culture (Figure 3.8 panel B). The concentration of VLPs, 96 h after UV treatment, was ca. 2 x 10^6 particles ml^{-1}, increasing to ca. 3x10^7 VLPs ml^{-1} after CsCl gradient ultracentrifugation.

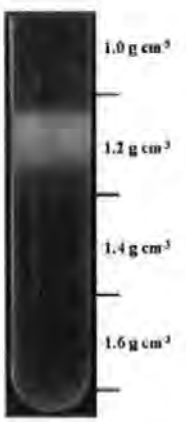

Figure 3.7. CsCl gradient of strain 292, the VLPs with a translucent white band at ca. 1.25 g cm^{-3}.

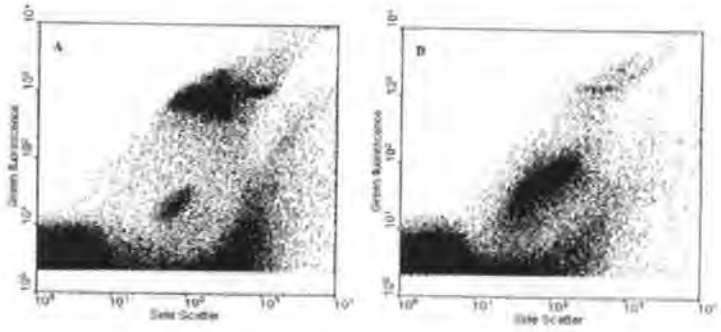

Figure 3.8. AFC analysis of VLPs induced following UV treatment of zooxanthellae culture 292 shows the presence of a new VLP group with high side scatter (A). AFC analysis of concentrated VLPs taken from CsCl gradient shows the presence and increased abundance of the high SSC VLP group as well as a reduction in the bacterial contaminants (B).

3.2.7 Visualisation of VLPs

TEM grids were prepared from fixed lysates of the UV-treated cultures. TEM images of lysates of UV-induced zooxanthellae cultures are shown in Figures 3.9 and 3.10. Figure 3.11 shows images prepared from concentrates of the induced cultures. Flexible filamentous VLPs ca. 2-3 μm in length and ca. 30 nm wide were seen in strains 12, 152 and 292. The morphology of the VLPs present in all three induced strains was similar. Concentrates prepared from strains 152 and 292 show densely concentrated filamentous particles with a similar morphology.

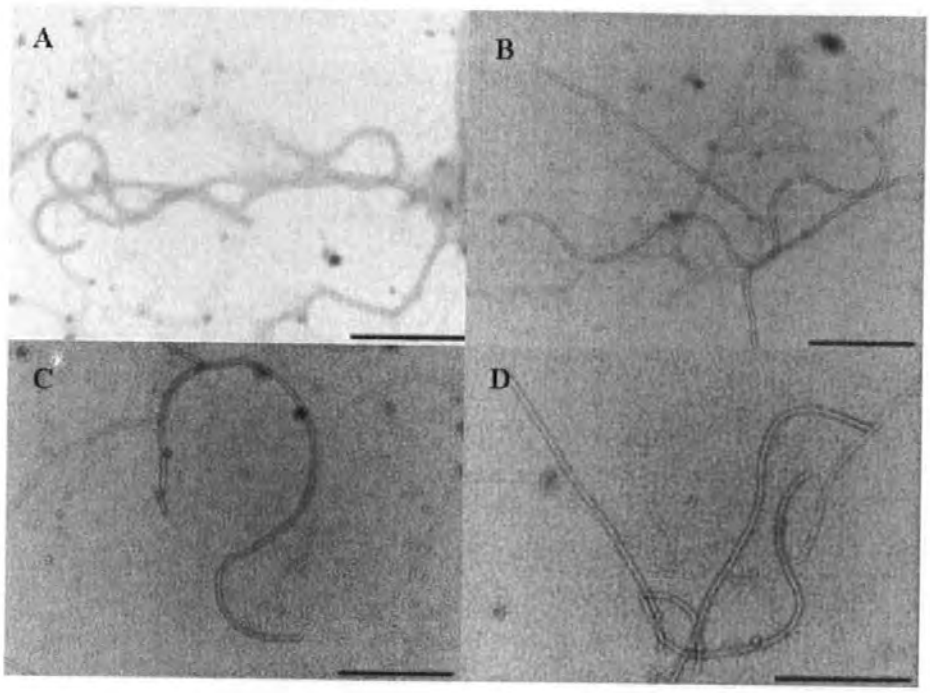

Figure 3.9. TEM images of VLPs from strains 12 (A) and 152 (B, C, D). Scale bars are 500 nm.

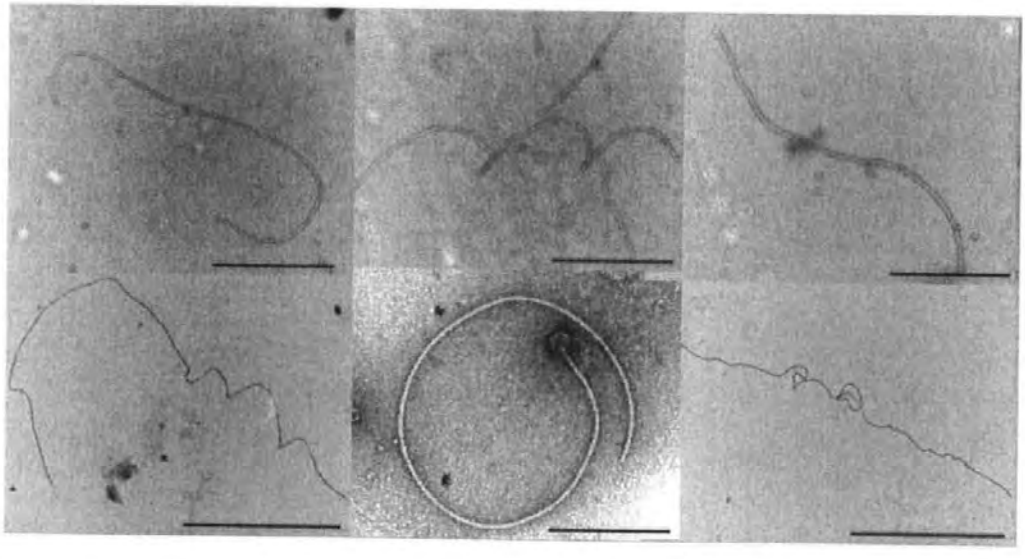

Figure 3.10. TEM images of VLPs from strain 292. Scale bars are 500 nm.

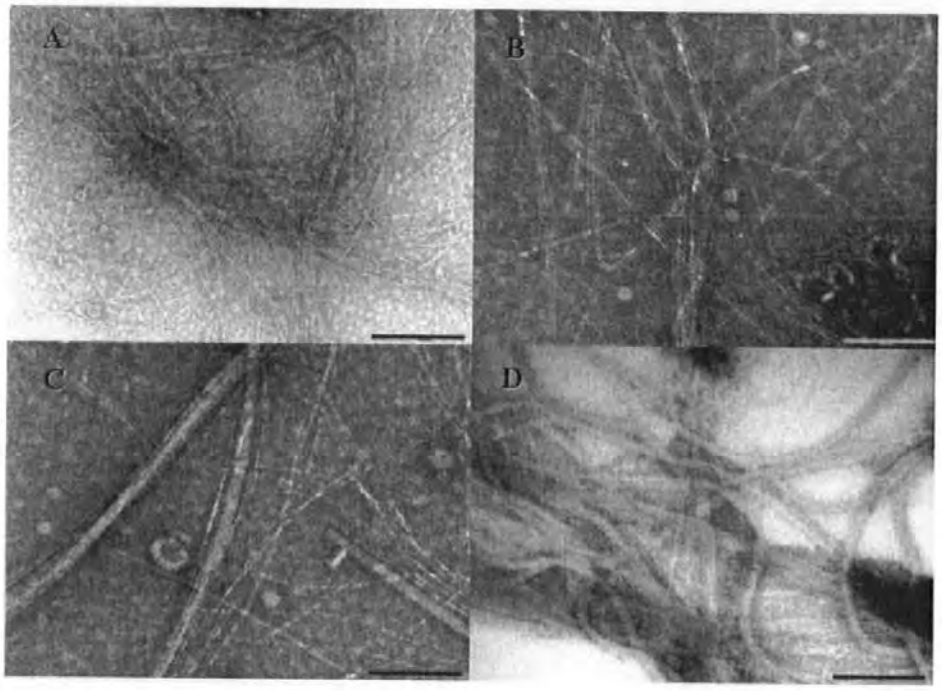

Figure 3.11. TEM images of VLPs from strains 152 (B and C) and 292 (A and D) concentrates. Scale bars are 200 nm in A and D and 100 nm in B and C.

3.2.8 Thin sections

Thin sections prepared after UV induction of strains 152 and 292 are shown in Figure 3.12 and 3.13. Filamentous VLPs were observed in both strains. Organelles have been identified in some of the images. In the thin sections of Figure 3.13 A and C, nucleus, chloroplasts and lipid vacuoles have been labeled. The chloroplasts are seen as dark parallel lines (Figure 3.13 C). The lipid vacuole (Figure 3.13 A) is seen as a large empty ball; this contains a globule of oil.

In panel A and B of Figure 3.12, pinwheel-like VLPs ca. 2-3 μm are present on the outer membrane of the zooxanthella cell. In the cytoplasm of the images in panel C and D (Figure 3.12) filamentous particles ca. 200-600 nm in length are visible. In panel E and F (Figure 3.12) filamentous membrane-like structures are visible, and in panel G and F filamentous particles ca. 2 μm in length are present.

In Figure 3.13, panels A and B, filamentous VLPs ca. 200 nm in length are seen in the periphery of a doublet cell in the mitotic phase of cytokinesis. In panels C and D (Figure 3.13) a pocket of filamentous VLPs ca. 100-200 nm in length can be observed. In panels E and F (Figure 3.13), filamentous VLPs ca. 500 nm in length are visible in the cytoplasm of the zooxanthella cell and in panels G and H filamentous VLPs ca. 200-600 nm are seen in the cytoplasm.

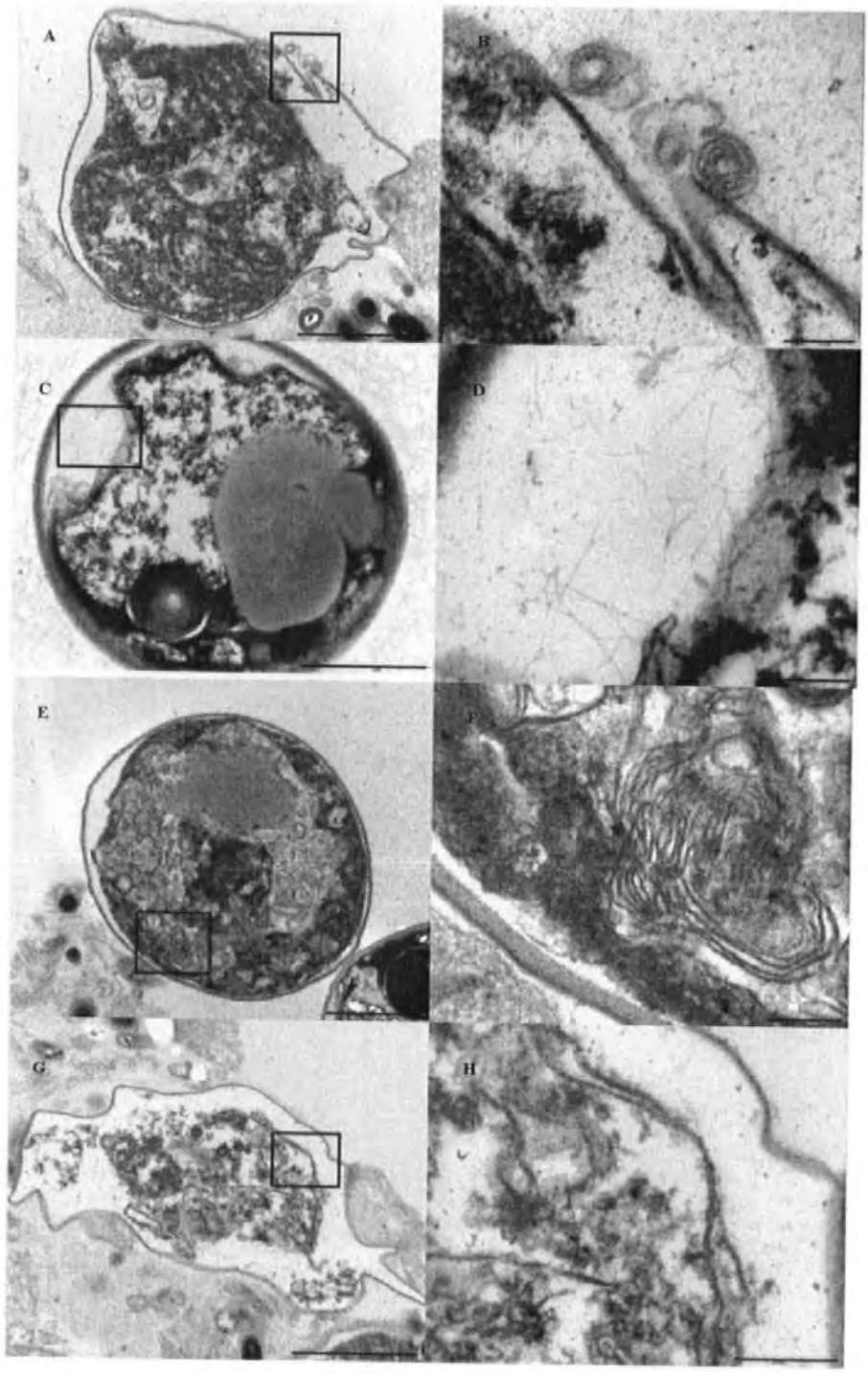

Figure 3.12. TEM images of strain 152 showing the presence of filamentous VLPs within thin sections of zooxanthellae prepared 39 h (C and D, E and F) and 46 h (A and B, G and H) after induction with UV light. The scale bars are 2 μm (A and C, E and G), 500 nm (H) and 200 nm (B, D and F). The black box in (A, C, E and F) highlights the area magnified in (B, D, F and H).

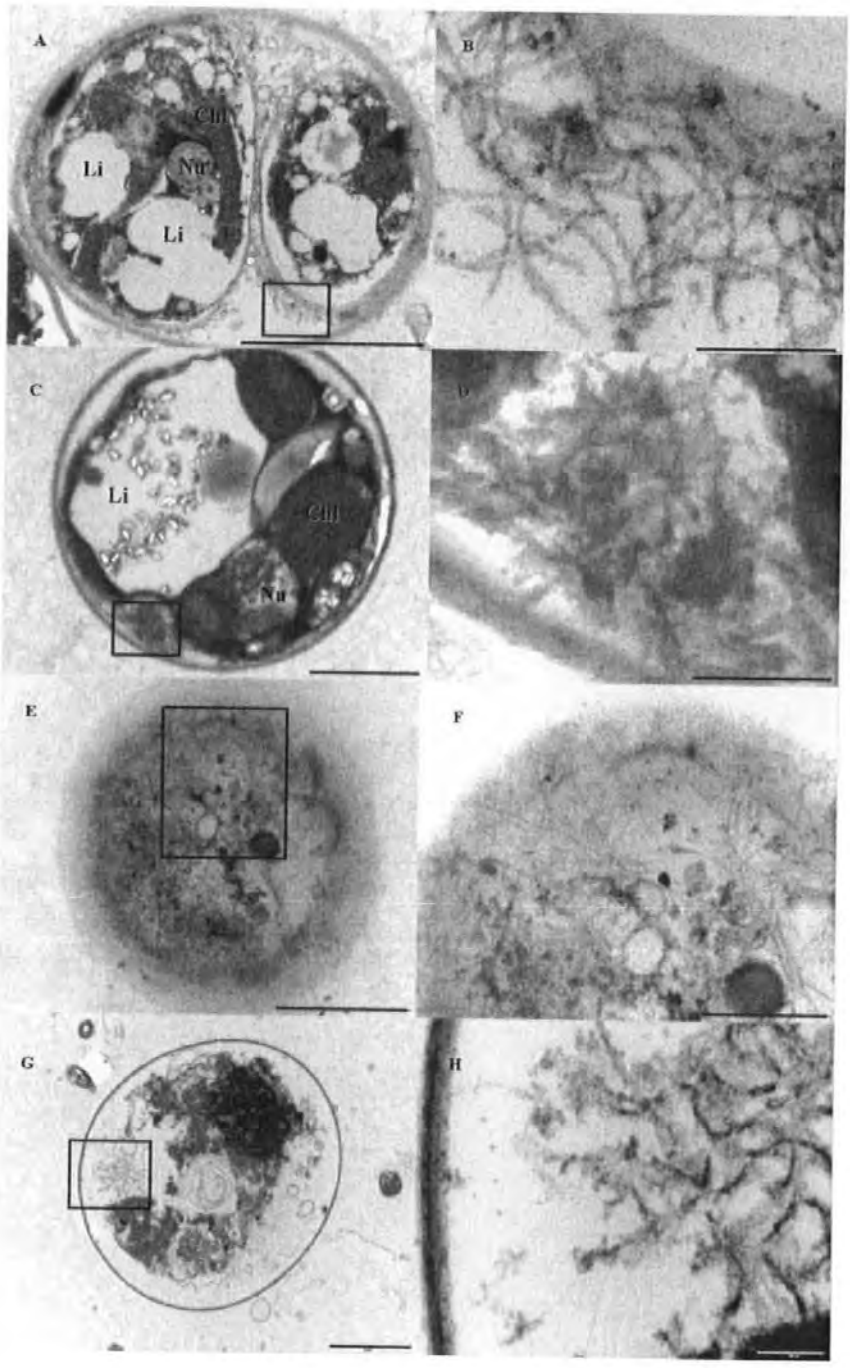

Figure 3.13. TEM images of strain 292 showing the presence of filamentous VLPs within thin sections of zooxanthellae prepared 39 h (A, B, E and F) and 46 h (C, D, G and H) after induction with UV light. The scale bars are 2 μm (A and B), 1 μm (E), 500 nm (F) 200 nm (B, D and F). The black box in (A, C, E and F) highlights the area magnified in (B, D, F and H). Chloroplasts (Chl), nucleus (Nu) and lipid vacuoles (Li) have been labeled.

3.2.9 Molecular characterisation of the filamentous VLPs

3.2.9.1 Preparation of nucleic acid

Nucleic acid preparations (Sections 2.7.2 and 2.7.3) were made from 1-3 l of 0.45 μm filtered lysates of UV-induced cultures, strains 152 and 292. Nucleic acid extracted from the concentrates was treated with both RNase and DNase (Figure 3.14). The size of the untreated nucleic acid relative to a Lambda *Hind*III marker appeared to be ca. 20 kb. Treatment with DNase in both strain 152 (Lane 3) and 292 (Lane 7) removed the band, whereas RNase treatment did not, suggesting the extracted nucleic acid was DNA. Subsequent experiments focused on DNA methodology.

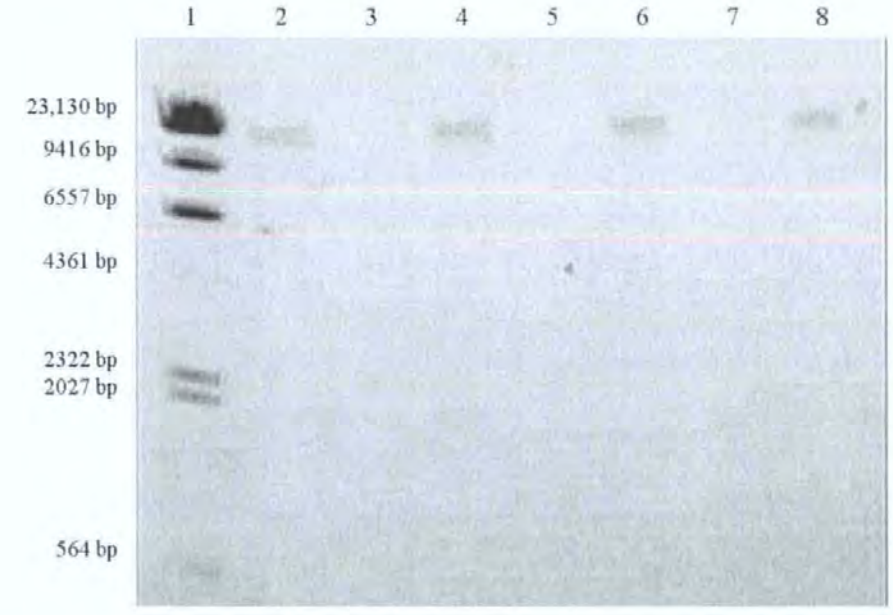

Figure 3.14. Gel image showing nucleic acid extracted from UV-induced strains 152 and 292 treated with RNase and DNase. Lane 2, 3 and 4; strain 152, untreated nucleic acid, nucleic acid treated with DNase and treatment with RNase, respectively. Lane 6, 7 and 8; strain 292, untreated nucleic acid, nucleic acid treated with DNase and treatment with RNase, respectively. Lane 1 Lambda *Hind*III marker and lanes 3, 5 and 7 are empty.

3.2.9.2 PFGE

Concentrates prepared from lysates were digested in agarose plugs (Section 2.8) and examined by PFGE (Figure 3.15). Switch times were run with a pulsed time of 5.5 seconds to 36.5 seconds for 21 h. PFGE analysis revealed a dominant band at ca. 45-65 kb and another faint band ca. 3-5 Mb from strain 152 (lane 7). DNA from strain 292 (lane 6) appeared to be degraded producing a smear.

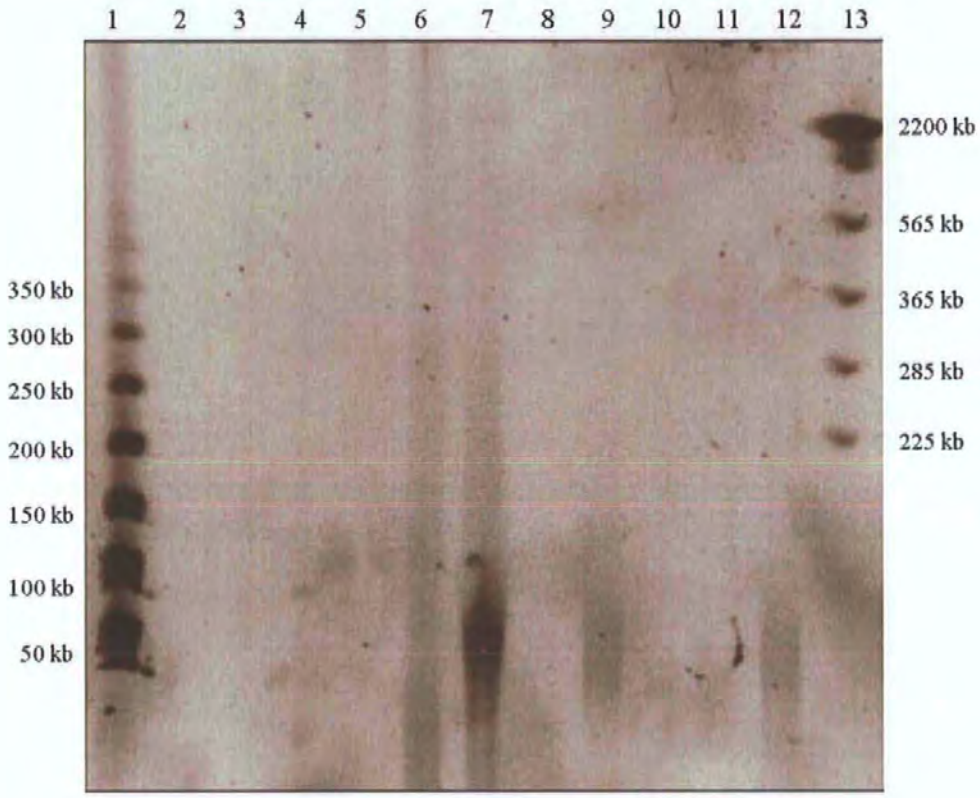

Figure 3.15. PFGE image of concentrates of strains 152 and 292. Lane 6 is the concentrate from strain 292 and lane 7 shows the concentrate from strain 152. Lane 1 shows the lambda molecular weight marker (0.05–1 Mb) and lane 13 shows a 0.2–2.2 Mb *S. cerevisiae* ladder. Lanes 2, 3, 4, 5, 8, 10 and 11 are empty and lanes 9 and 12 do not pertain to this experiment.

3.2.9.3 Clone Libraries

GenomiPhi was used to amplify genomic DNA which was then used to create clone libraries. Figure 3.16 shows the GenomiPhi products from strains 152 and 292. Bands ca. 20 kb were observed from the genome amplification of both strains.

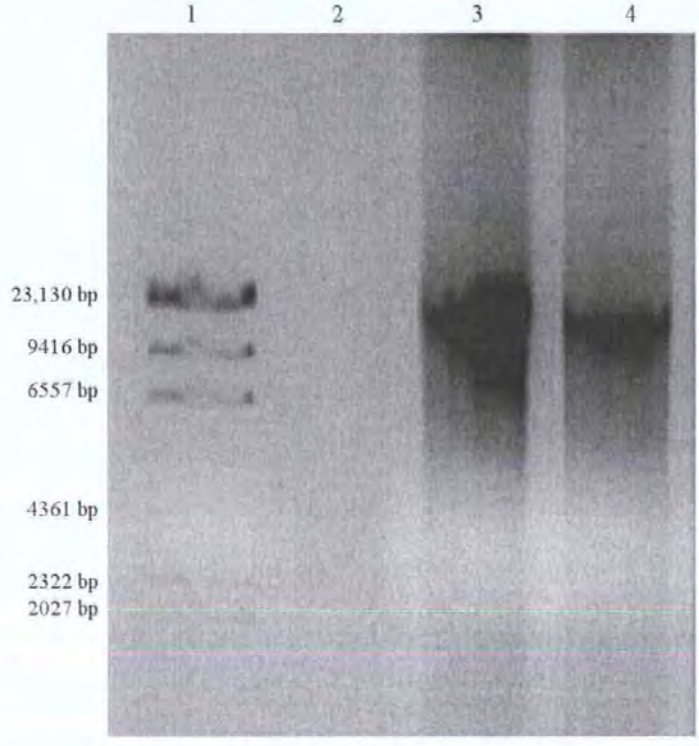

Figure 3.16. Gel image showing GenomiPhi products: lane 3 is strain 152, lane 4 is strain 292 and lane 1 is a Lambda *Hind*III marker. Lane 2 is empty.

Several libraries were prepared from sonicated and restriction enzyme digested DNA. Blunt-ended fragments in the size range of 1-5 kb were excised from agarose gels and used for cloning. Sonicated fragments are shown in the gel image in Figure 3.17. Three conditions of sonication were used to optimise the size range of fragments produced. Restriction digested fragments of strains 152 and 292 are shown in Figure 3.18. Digestion of genomic DNA with the restriction enzymes *Hae*III, *Rsa*I, and *Sma*I, produced smeared bands with similar size ranges in both strains. Fragments in the 1-5 kb sized range were extracted from the gel and cloned.

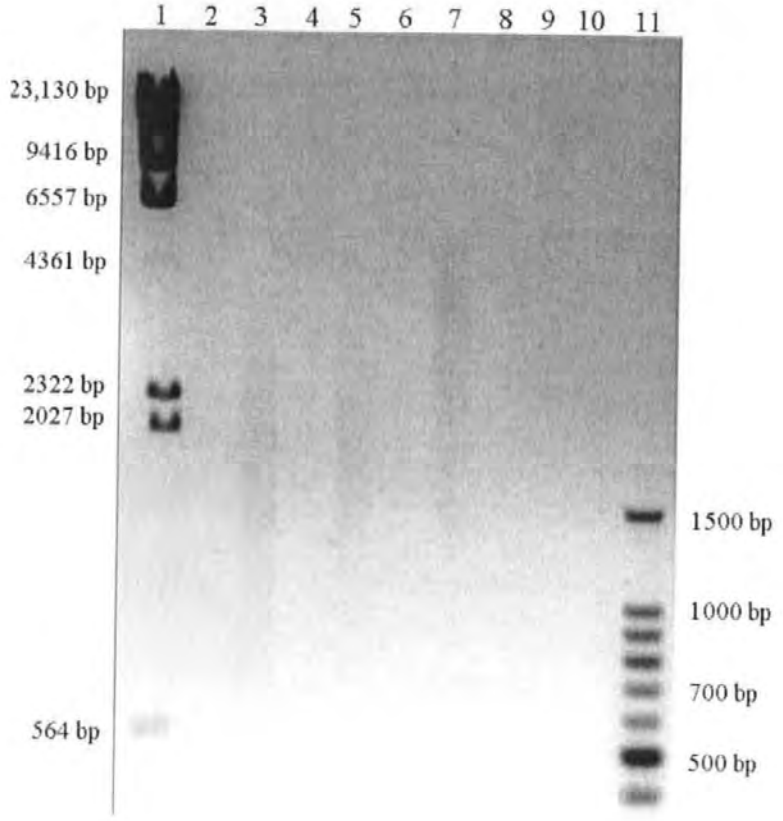

Figure 3.17. Gel image showing sonicated DNA extracted from strain 292. Lanes 3, 5, and 7 are the sonicated DNA with a total energy delivered of 1000 W, 750 W and 500 W, respectively. Lane 1 is a Lambda *Hind*III marker and lane 11 is a 100 bp ladder.

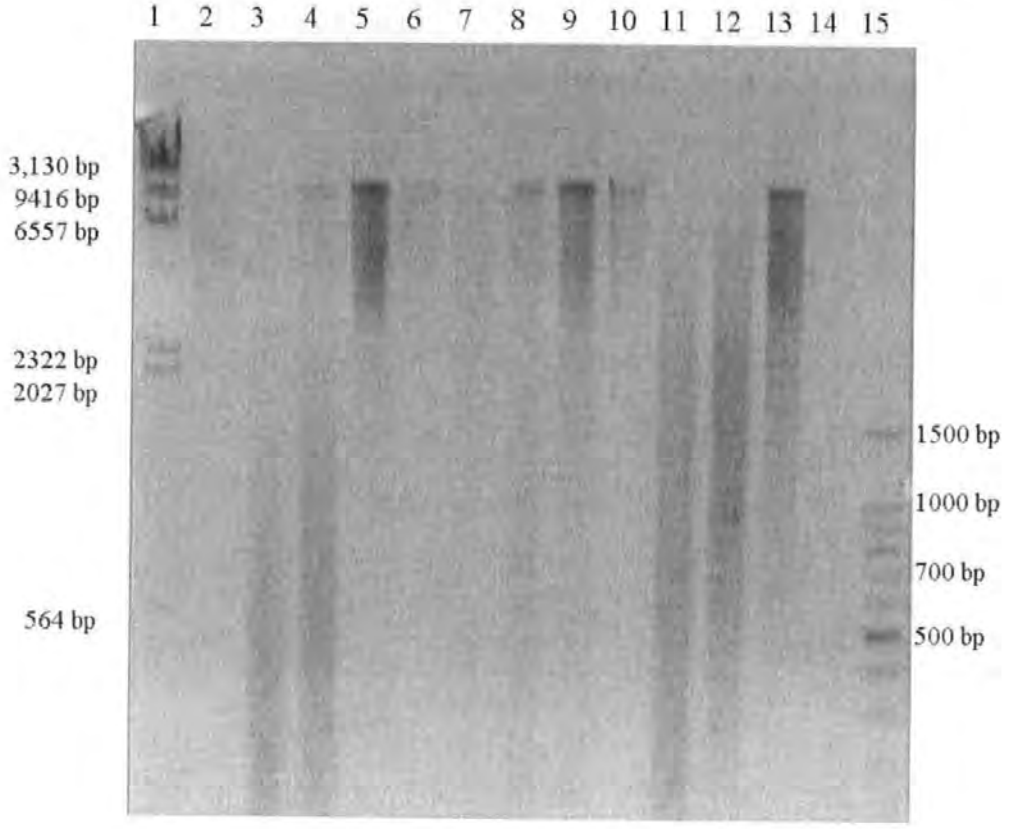

Figure 3.18. Gel image showing restriction digestions. Lanes 2, 3, 4 and 5 are strain 152 digested with no enzyme, *Hae*III, *Rsa*I, and *Sma*I, respectively. Lanes 6, 7, 8 and 9 and again lanes 10, 11, 12 and 13 are strain 292 digested with no enzyme, *Hae*III, *Rsa*I, and *Sma*I, respectively. Lane 1 is a Lambda *Hind*III marker and lane 15 is a 100 bp ladder. Lane 14 is empty.

3.2.9.4 RNA methodology

Nucleic acid treated with RNase and DNase suggested that the nucleic acid obtained from the VLPs was DNA. Despite this, some preliminary RNA work was carried out as the morphology of the filamentous VLP strongly resembled that of ssRNA plant viruses. RNA extractions were used for RT PCR. Random primers were used to generate the first strand. The gel in Figure 3.19 shows the products of the RT PCR which produced smears visible in lane 6 (strain 152) and lane 10 (strain 292). The product observed after the RT PCR was not a product of expected size and RNA work was concluded with no final resolution.

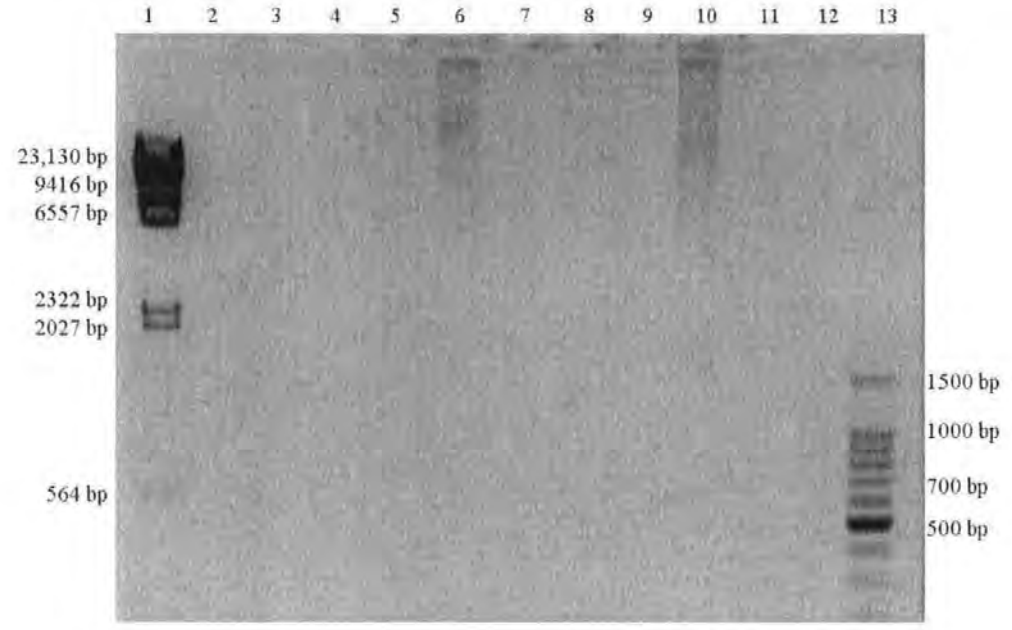

Figure 3.19. Gel image showing RT PCR products from strain 152 in lane 6 and strain 292 in lane 10. Lane 1 is a Lambda *Hind*III marker and lane 13 is a 100 bp ladder.

3.2.9.5 Contigs and sequencing

The clone libraries prepared with RE digestions and sonicated DNA were sequenced. Sequences of several hundred clones were assembled into continuous sequences (contigs) and analysed. A total of 720 clones were sequenced in 96-well plates (forward and reverse sequencing). The sequences assembled into 418 contigs, with a size range ca. 100 bp to 3000 bp (Supplemental Material 1), of which 235 showed sequence similarities to nucleotide sequences of previously described organisms when analysed with BLASTn. A hit was considered significant with E-values below 0.001. Significant nucleotide similarities were found to several bacteria (Appendix 1). Figure 3.20 shows a summary of the organisms that have significant hits to nucleotide sequences of the contigs.

The most frequent sequence similarity was to *Marinobacter aquaeolei* VT8 (149 contigs) which is a Gammaproteobacterium isolated from an oil-producing well of an

offshore platform in southern Vietnam (Huu *et al.*, 1999). It showed nucleotide similarities to 177,804 bp of the 720,000 bp of sequence and 63% of the contigs gave significant hits to this organism.

Figure 3.21 shows the distributions of significant hits to the 418 contigs comparing only nucleotides from viruses available in Genbank. Contigs and their top significant nucleotide similarities to the virus database are listed in Appendix 1. The contigs showed that ca. 89% of the sequence similarities were to bacteria. The sequence similarities are likely to be to prophages in the genomes of these bacteria. The remaining 11% of the significant sequence similarities were to bacteriophage and virus sequences. The most frequent similarity was to the Betaproteobacterium *Azoarcus* spp. BH72. 30 contigs of the 62 contigs with significant sequence to previously described organisms had matches to this bacterium which is involved in nitrogen fixation. Three contigs had sequence similarities to the *Bromoviridae* family of viruses (single-stranded RNA). The top sequence similarity to Contig 305 was to a cucumber mosaic virus segment. The E-value was e-19 which was higher than that of the BLAST results against the entire non-redundant database, which showed sequence similarities to a flowering plant of the class *Liliopsida* (e-18). The two additional contigs (3 and 50) showed sequence similarities to a *Prunus* necrotic ringspot virus (family *Bromoviridae)* which is known to infect plants, in particular prunes and peaches. The BLAST results against the entire non-redunant database showed contigs 3 and 50 to have sequence similarities to organisms in the classes *Chromadorea* and *Oomycete*, respectively.

The 418 contigs were compared to proteins in Genbank using tBLASTx to look for homology with previously described sequences (Appendix 1). The results from this analysis showed 129 of the 367 contigs were homologous to genes involved in metabolism and cellular processes (Figure 3.22). Hypothetical proteins and proteins of unknown function comprised another well-represent portion of the contigs (104

contigs). The remaining 40% of contigs with sequence homology to previously described proteins included replication-associated proteins, transposases, transport and binding proteins, protein involved in secretory pathways, membrane-associated proteins, nucleotide and protein metabolism, and prophage integration.

Figure 3.23 shows the distributions of significant hits to contigs (67 contigs) comparing only proteins from viruses available in Genbank; the full listing of all contigs with significant hits is listed in Appendix 1. The comparison of the contigs with viruses in the protein data base showed sequence similarities to 35 bacteriophage, 19 viruses and 13 bacteria (potential prophage). Assessment of the functions assigned to the previously described protein sequences with homology to the contigs showed the majority of contigs were homologous to replication-associated proteins, proteins involved in metabolism and cellular processes, and several hypothetical proteins and proteins of unknown function. The remaining contigs showed homology to membrane-associated proteins, proteins involved in nucleotide and protein metabolism, and prophage integration and phage assembly.

While many of these contigs have shown significant hits in the nucleotide and protein analysis against the entire non-redundant database of Genbank, several contigs had no significant matches to known nucleotide (183 contigs) or protein (31 contigs) sequences.

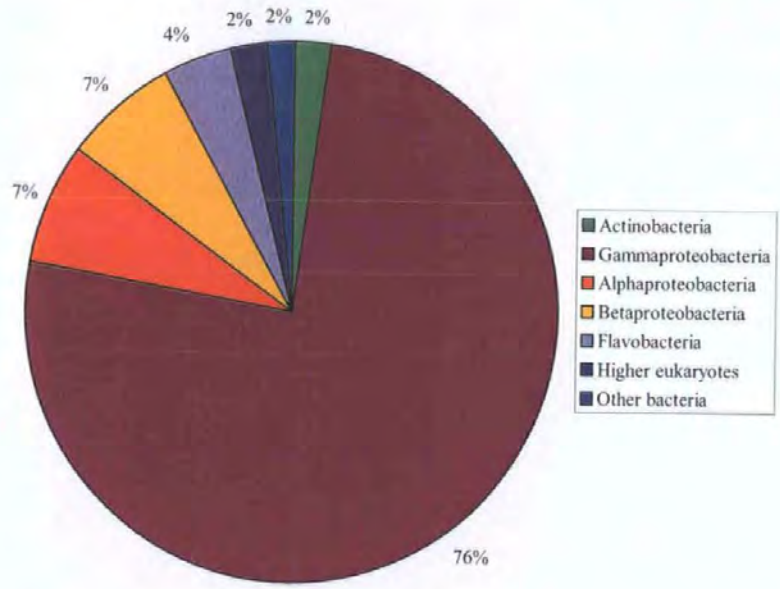

Figure 3.20. The distribution of significant nucleotide hits (BLASTn, non-redundant database) of the contigs assembled from sequencing of strain 292.

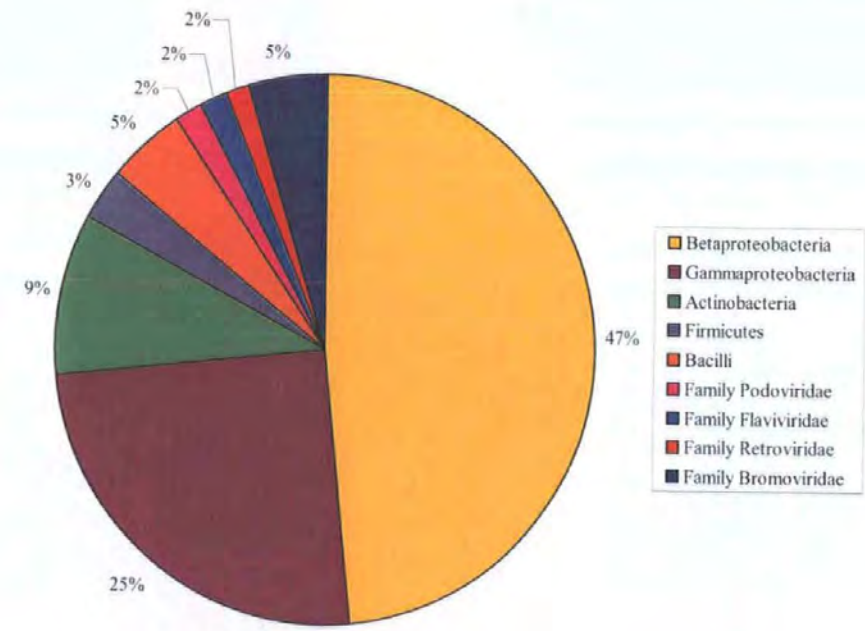

Figure 3.21. The distribution of significant nucleotide hits (BLASTn, non-redundant database restricted to virus sequences) of the contigs assembled from sequencing of strain 292.

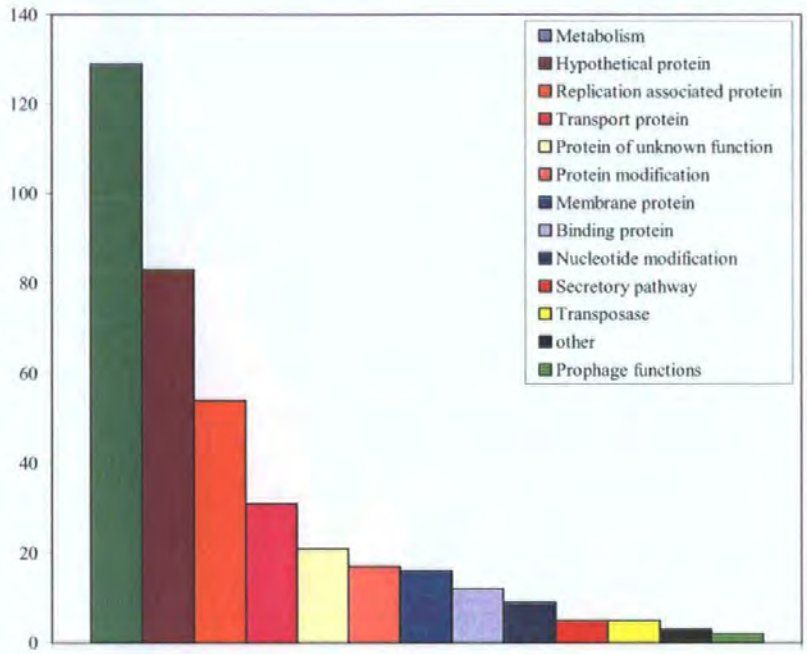

Figure 3.22. The distribution of significant protein hits (tBLASTx) of the contigs assembled from sequencing of strain 292.

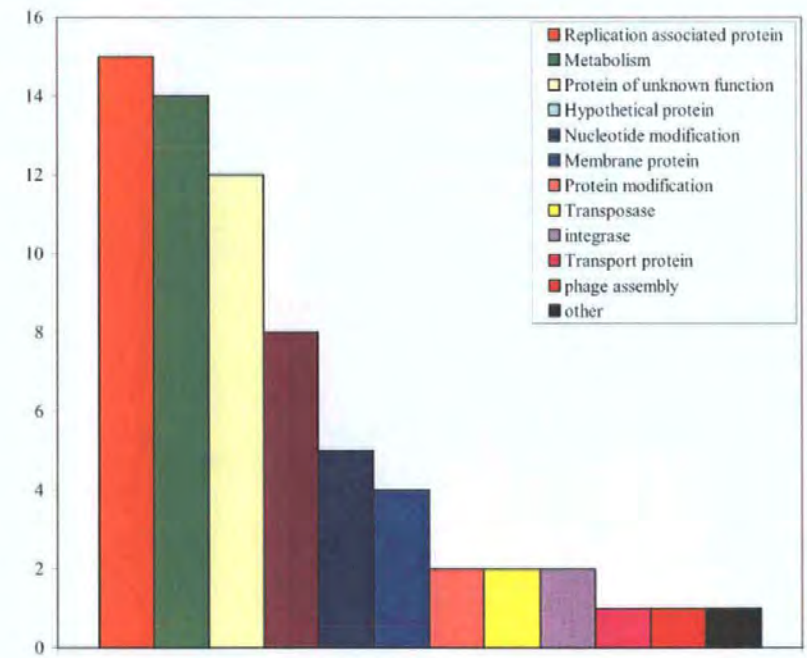

Figure 3.23. The distribution of significant protein hits (tBLASTx restricted to virus sequences) of the contigs assembled from sequencing of strain 292.

3.3 Discussion

Techniques to induce and isolate latent viruses presented here have identified a novel latent host-virus system, potentially of great importance in understanding the mechanisms of coral bleaching. The *Symbiodinium* species examined were isolated from hosts collected from several locations in the world's oceans and they belong to five different clades of the eight known *Symbiodinium* clades. Almost half of the strains screened for inducible VLPs were originally isolated from corals. In small scale screening of inducible latent viruses of zooxanthellae, the filamentous VLPs observed in this study could be easily overlooked. Sixteen strains of zooxanthellae isolated from a variety of cnidarian hosts were used to demonstrate that zooxanthellae harbour inducible filamentous VLPs.

3.3.1 Evaluation of induction methods

The preliminary evaluation of methods of induction by elevated temperature, exposure to UV radiation and exposure to Mitomycin C, was carried out to assess the most appropriate induction method to induce potential latent viruses from the zooxanthellae strains. While induction of lysogenic prokaryotic organisms has been well documented using all three methods, information on virus induction of eukaryotic organisms is limited. All three methods produced declines in zooxanthellae numbers relative to the control. Variability occurred between the induction method and zooxanthellae strain; overall the individual strains and clades showed the greatest sensitivity to UV treatment (Figure 3.1 and 3.2).

Elevated temperature is an environmentally relevant induction method (since it may be linked to coral bleaching) and it has been used in previous coral/zooxanthellae studies to induce VLPs (Davy *et al.*, 2006; Wilson *et al.*, 2001; Wilson *et al.*, 2005). Despite this, it was decided not to pursue induction by elevated temperature in further studies

because of the variability in the tolerance of the different strains, as well as the lack of space and incubators to accommodate induction at increased temperatures.

In the initial inductions, heat shock showed the most variable results of the three induction methods. In some cases, elevated temperature appeared to provide more optimal growth, while in other cases the increased temperature caused substantial decline in zooxanthellae numbers within the first 24 h. The overall sensitivity to heat treatment was the least in the individual strains as well as in the grouping of strains into clades.

Mitomycin C is frequently used for induction of lysogenic bacteria (Jiang & Paul, 1996; Weinbauer & Suttle, 1996). This induction method led to a substantial decline in the zooxanthellae numbers; however the results were sporadic in the first 24 hours. This method was dismissed, mainly due to the health and safety issues associated with the use of Mitomycin C and the fact that UV-induction worked so well.

Increased irradiation from the sun is a likely factor leading to some episodes of coral bleaching, as clear and/or shallow water above reefs allow for more penetration of the sun's rays. Ultraviolet radiation can penetrate several meters of seawater (Calkins & Thordardottir, 1980) with the longer wavelengths penetrating further. Ultraviolet A (UV A, 400–320 nm) rays fall at the longer end of the UV spectrum and contain less energy. The lower wavelengths of the ultraviolet spectrum with higher energy are ultraviolet B (UV B, 320–280 nm) and UV C (< 280 nm) rays. UVA and UV B can penetrate the clouds and the water surface. Although UV C is blocked by clouds and does not penetrate more that a few centimeters of water, making it ecologically irrelevant, it is the most powerful wavelength for induction.

UV B light can cause damaging effects to DNA in natural environments; UV C is a much more intense mutagen. UV B and UV C irradiation disrupts base pairing, and lead to the formation of dimers through photochemical reactions. This damage to the host

cell during exposure to UV light triggers a response mechanism which is known to lead to the excision of prophage from the host chromosome (Jiang & Paul, 1998). Comparison of the susceptibility of different clades to the induction methods tested showed clades A, B and F to be most susceptible to UV light and clades C and E to be most susceptible to Mitomycin C. Clade F was highly resistant to heat shock with less that a 5% decrease in cell numbers relative to the control. Studies of stress tolerance of *Symbiodinium* in the natural environment have mostly focused on the effects of irradiance and temperature on clade distribution. Certain clades, A and B for example, which are generally found at shallower depths are known to produce mycosporine-like amino acids (MAAs), which act like a natural sunscreen helping to protect the host and the zooxanthellae from UV light (Laurion *et al.*, 2004). Several studies have examined the effects of UV light on *Symbiodinium* which show detrimental effect to occur as a result of UV exposure (Lesser & Shick, 1990; Rogers *et al.*, 2001).

3.3.2 Enumeration of zooxanthellae

Symbiodinium species have been previously enumerated using haemocytometry and AFC (Lesser & Shick, 1989; Lesser & Shick, 1990; Wilson *et al.*, 2001). The zooxanthellae strains were difficult to count by haemocytometry due to movement of active cells, clumping of cells and uneven distribution. The high-throughput AFC analysis of autofluorescence of chlorophyll a (red fluorescence) and forward scatter (cell size) were utilised in the subsequent experiments after the initial inductions. AFC eliminated the problems of counting dead or partial husks of cells as the AFC not only made counts of particles passing the laser, but also measured fluorescence.

3.3.3 Identification of VLPs by AFC

AFC was originally designed for the clinical quantification of human cells, such as blood cells. Since then, implementation of AFC for the detection of microorganisms has been routinely employed for quantification of algae and bacteria. The use of AFC for the detection and enumeration of viruses was first optimised for PpV-01, the virus which infects *Phaeocystis pouchetii* and is now a commonly used method in virology (Brussaard *et al.*, 2004b; Jacquet *et al.*, 2002; Marie *et al.*, 1999; Wilson *et al.*, 2002). VLPs are identified on the basis of their staining intensity versus their relative size and/or shape (side scatter). AFC has many advantages over other methods used to enumerate viruses. Epifluorescence counts of viruses, for example, is time consuming; AFC analysis, on the other hand, is fast as each sample can be quantified in less than 5 min. The main drawback to AFC analysis is the detection limit and sensitivity of the instrument as many small viruses are at the limit of detection in the lower left hand corner of the AFC dot plots which merge with the instrument noise.

AFC was utilised to identify potential VLPs induced from the UV-treated zooxanthellae cultures. Quantification of potential VLPs released after UV treatment was achieved by analysis of dot plots of SSC (an indicator of cell size/dimension) versus GFL (DNA content) (Brussaard *et al.*, 2000). AFC analysis of UV-induced zooxanthellae cultures revealed the presence of a separate group of high SSC, low GFL particles which were visible ca. 24 h after UV-induction. By 96 h, this group was clearly distinguishable (Figure 3.4). It was concluded that this group contained VLPs, despite the fact it has a unique SSC versus GFL signal with a higher SSC than previously described bacteriophages and viruses (Brussaard, 2004b). The higher SSC suggested that the particles might be filamentous, since SSC is influenced by internal structure and its refractive index (Brussaard, 2004b). Bacteriophage and isocohedral algal viruses, for example, have much lower SSC signals.

Of the zooxanthellae isolates screened for UV-induction of potential latent viruses, 37.5% of the strains produced a similar inducible group of VLPs with high SSC and low GFL that was clearly identifiable (Table 3.1). Over half of the strains that had the inducible latent VLP were originally isolated from corals.

The 31.3% of the strains that had this similar group of high SSC VLPs in both the control and UV-treated cultures may potentially have a chronic infection. Filamentous viruses of bacteria, such as the *Escherichia coli* phages M13, fd and f1 are known to have chronic cycles in which the phages assemble during their passage through the membrane without killing the host (Hofer & Sommaruga, 2001; Marciano *et al.*, 1999).While chronic infections have not been described in algal systems, the possibility exists as it has been described for prokaryotic system.

3.3.4 Effect of UV treatment on induction of VLPs over time

Analysis of AFC dot plots of zooxanthellae and VLPs was carried out on strains 12 (clade B), 152 (clade C) and 292 (clade A). Characterisation on the effect of UV treatment on the cultures showed a common trend occurring in the three strains. A decline in the zooxanthellae concentration was observed from 24 h after UV induction, which correlated with the appearance and rapid increase in the concentration of the high SSC VLP group (Figure 3.6 A, C and E). The concentration of these VLPs continued to increase to ca. 2-3 x 10^6 particles ml^{-1} at 96 h after UV treatment, at which point the UV-induced zooxanthellae culture had lysed. Since the zooxanthellae cultures were non-axenic, a group with a signal characteristic of bacteria was present in the control as well as in the UV-treated zooxanthellae cultures (Figure 3.4). To rule out lysogenic bacteria being the source of the high SSC VLPs, bacterial concentrations were also monitored throughout the induction experiments. Temporal progression of bacterial concentrations was similar in the control and UV-treated cultures although there was a slight drop in

the UV-treated cultures between 24-48 h, before they regained the same growth rate as the control (Figure 3.6 B, D and F). This initial drop in bacterial concentrations could be caused by several factors, such as lysis of UV-sensitive bacteria and/or induction of lysogenic bacteriophage.

Bacteriophages usually group in the area above the instrument noise (Figure 3.4); this group was analyzed. There was no apparent increase in bacteriophage numbers compared to the control during the induction experiments (Figure 3.6 B, D and F). While the experimental treatment appears to have an effect on the numbers of bacteria present in the non-axenic zooxanthellae culture, the clear correlation between the crash of the zooxanthellae populations and the concurrent increase in VLP concentration suggests that bacterial contaminants are not the source of the new VLP group observed by AFC.

In previous experiments, VLPs have been observed in stressed corals and zooxanthellae. However a clear correlation identifying the host of the VLP group associated with the decline in the zooxanthellae has not been identified. This correlation found in all three strains examined in this study suggests the high SSC group is the causative agent responsible for the demise of the zooxanthellae.

3.3.5 Isolation and concentration of VLPs

Several strains of zooxanthellae were cultured to large volumes to obtain high concentrations of the high SSC VLPs. The culturing of zooxanthellae outside of their host and the volumes of cultures required to isolate inducible latent viruses from these cultures were problematic issues. The zooxanthellae cultures were slow growing and obtaining the large volumes of cultures to prepare CsCl gradient took several months. Technical issues and equipment failure, such as faulty tubing which was compromised during the concentration step slowed the progress in obtaining quantities of the high

SSC VLPs and incubator malfunctions devastated the original set of cultures. Technical issues were overcome and concentrated lysates of strains 152 and 292 were prepared. The high SSC VLPs present in the lysates of the cultures were concentrated an order of magnitude. Filtering of 1-3 l of zooxanthellae cultures 152 and 292, 96 h after UV induction, removed the majority of the contaminating bacteria. The discrete white band at 1.25 g cm^{-3} in the CsCl gradient (Figure 3.7) contained an intense group of the same high SSC group of VLPs observed before concentrating (Figure 3.8).

3.3.6 Visualisation of VLPs

Free VLPs in the UV-treated supernatants and concentrates were observed post induction by TEM as long flexible filaments 2-3 μm in length and approximately 30 nm in width (Figure 3.9 and 3.10). VLPs purified by CsCl gradient centrifugation showed an increased concentration of the filamentous VLPs, $3x10^7$ VLPs ml^{-1} (Figure 3.10). VLPs observed in the three separate lysed cultures, strains 12, 152 and 292 all showed similar morphology. The inductions of morphologically similar VLPs suggest these latent filamentous VLPs are potentially present in many different strains and clades of zooxanthellae.

VLPs observed in the TEM images further support the AFC data which suggests a latent VLP is induced from the zooxanthellae after UV treatment. The high SSC group observed in the AFC would be consistent with a filamentous VLP as most described viruses are isocohedral and have a lower SSC signal. The dimension of a filamentous particle would increase the light scatter and shift the group to the right.

The filamentous particles observed in the TEM images do not appear to be TEM artifacts due to staining as staining artifacts generally have a geometrical shape. In the case of small round or icosahedral VLPs visualised at lower magnification, stain artifact

could potentially be mistaken for VLPs. In the case of the filamentous VLPs observed here this may be ruled out.

TEM images of concentrates further support that the filamentous VLPs visualised by TEM are this same group and the AFC analysis of concentrates shows a substantial increase in the high SSC VLP group. Thin sections of UV-treated zooxanthellae revealed filamentous VLPs of similar morphology within the cytoplasm and around the membranes of zooxanthellae cells exposed to UV light (Figure 3.11- 3.13). In the two strains examined by thin sectioning, strains 152 and 292, filamentous particles were observed in the UV-treated cells, but were not seen in controls. The incidence of VLPs observed in the thin sections increased markedly between 39 and 46 h post induction. The demonstration of intracellular VLPs provides further evidence that the particles observed are actually infecting the zooxanthellae rather than infecting bacteria present in the cultures. This new group of VLPs has been termed "zooxanthellae filamentous virus 1" (ZFV1) (Lohr *et al.*, 2007).

3.3.7 Molecular work

Molecular approaches such as PFGE, digestion with enzymes, phylogenetic markers and genome sequencing are common techniques used to classify and characterise viruses (van Regenmortel *et al.*, 2000). Application of several molecular techniques was used to try to further characterise the filamentous VLP.

The morphological similarities noted between ZFV1 and previously described viruses indicated that this could be a RNA virus. Initially RNA methods were attempted with the filamentous VLP, but this work was excluded as treatment of the nucleic acid with RNase and DNase showed the nucleic acid to be sensitive to DNase, suggesting that the VLP is composed of DNA. All subsequent studies were carried out using DNA methodology.

Sizing of the potential virus genomes was determined by PFGE. Genomic DNA was prepared for PFGE by lysing VLPs that had been encased in agarose blocks; this improves the resolutions of the genomic DNA by minimising shearing. The run conditions of the electrophoresis were selected to resolve fragments in the size range of 50-500 kb. PFGE run conditions differ from conventional agarose electrophoresis in that the orientation of electrical field alternates as opposed to being unidirectional; this variability in the electric field allows PFGE to resolve very large fragments (>600 kb) as smaller fragments reorient quicker and therefore migrate faster through the gel.

PFGE analysis of strain 152 showed one band was ca. 3-5 Mb and another ca. 45-65 kb. Genomic DNA from strain 292 produced a smear; this is likely to be caused by shearing. It was concluded that the band ca. 3-5 MB was bacterial contamination and that the band ca. 45-65 kb is likely to be the filamentous VLP. In a previous study of inducible viruses of corals and freshly isolated zooxanthellae, PFGE analysis showed the most abundant VLP in the samples had a genome size ≤48.5 kb (Davy *et al.*, 2006). In this same study, filamentous particles ca. 3 μm were observed in the heat shock coral/zooxanthellae samples.

The scarcity of genomic DNA from the filamentous VLPs was a limiting factor on the quantity of molecular techniques that could be performed. Whole genome amplification was used to increase the concentrations of DNA. GenomiPhi, which is considered the most accurate amplification method available to generate a higher DNA concentration (Pinard *et al.*, 2006), was used to amplify the genomic DNA obtained from the filamentous VLPs. It must be acknowledged that whole genome amplification can introduce bias in the relative concentrations of different genomes (Angly *et al.*, 2006). The non-axenic zooxanthellae cultures contain several types of bacteria and more than likely, several types of bacteriophages. Although aliquots taken from CsCl gradients appeared to have had a majority of the bacterial contamination removed, bacterial

contamination made the genome sequencing troublesome. Even small amounts of bacterial contamination, whether from the original VLP concentrate or contamination acquired during the genome amplification processes, were problematic in the sequencing process. The sequences assembled into several contigs ranging in size from a few hundred base pairs up to 3kb. BLAST results showed strong similarities to previously described bacterial sequences found in GenBank.

The close association of bacteria with dinoflagellates is well established (Kogure *et al.*, 1982; Silva, 1982). It has been demonstrated in *Pfiesteria*-like dinoflagellate cultures that the elimination of the bacterial contaminants can have adverse effects on the growth of the dinoflagellate cultures. Alavi (2001) proposed that a subset of bacteria physically associated with the dinoflagellate cells may be required for the growth of dinoflagellate populations (Alavi *et al.*, 2001). It has been previously demonstrated that *Pfisteria piscicida* consumes bacteria (Burkholder & Glasgow, 1997). In the *Pfiesteria*-like dinoflagellate cultures, it was shown that one of the dominant members in the bacterial community of the dinoflagellate culture is a marine alpha-proteobacterium (Alavi *et al.*, 2001).

The comparison of contigs sequences obtained from strain 292 to the Genbank database showed that 63% of the contigs were related to the gammaproteobacterium *Marinobacter aquaeolei* VT8. The important number of sequences related to *Marinobacter aquaeolei* VT8 suggests a close association between strain 292 and the gammaproteobacterium *Marinobacter aquaeolei* VT8. This bacterium could be the principal diet element of strain 292 similar to the results reported by Alavi (Alavi *et al.*, 2001). Alternatively, *Marinobacter aquaeolei* VT8 could be a symbiont of strain 292 contributing to the lifestyle of strain 292. The food versus symbiosis type relationship between strain 292 and *Marinobacter aquaeolei* VT8 could be tested by fluorescent in situ hybridisation (FISH) and labeling *Marinobacter aquaeolei* VT8 using a specific

16S rRNA fluorescent probe to determine the location of the gammaproteobacterium. Furthermore, microbial community analysis could be used to determine if *Marinobacter aquaeolei* VT8 is an artifact amplified by the Genomephi process or truly a dominant member of the bacterial community associated with strain 292.

To overcome bacterial contamination in the sequencing step, more thorough separation through tighter CsCl gradients or perhaps the application of several CsCl gradients would achieve a bacteria-free aliquot of VLPs. The method of filtration may not have removed all bacteria as some bacteria can pass through 0.45 μm filters.

The sequencing data did not provide a clear indication of the identity of the filamentous VLPs induced from the zooxanthellae cultures. Molecular characterisation of ZFV1 is essential to confirm this relationship, but initial sequencing attempts were unsuccessful.

3.4 Implications for coral bleaching

Wilson *et al* (Wilson *et al.*, 2001) first suggested that zooxanthellae may harbor a latent infection, after showing that VLPs were present in zooxanthellae of thermally stressed anemones and that isolated VLPs could re-infect zooxanthellae. Further studies have shown the presence of VLPs in three species of tropical coral (Davy *et al.*, 2006). While the hosts of the numerous VLPs remain unknown, their abundance and close association with corals and their symbiotic zooxanthellae are evident. A variety of VLP forms have been observed, and while most of these are hexagonal, it is notable that a filamentous VLP (up to 3 μm in length) of similar morphology to ZFV1 has been observed following exposure of the coral *Acropora formosa* to heat stress (Davy *et al.*, 2006).

The majority of algal viruses described to date are members of *Phycodnaviridae*, which are a family of large dsDNA viruses with an isocohedral shape (van Etten & Meints, 1999; Wommack & Colwell, 2000). More recently, a number of RNA viruses have also been isolated and characterised (Lang *et al.*, 2004; Tai *et al.*, 2003; Tomaru *et al.*,

2004). ZFV1 shows striking morphological similarities to RNA viruses which are known to infect plants, in particular the family *Closteroviridae*. Members of this family are filamentous and flexuous with lengths ranging from 1500-2200 nm (Agranovsky *et al.*, 1995; van Regenmortel *et al.*, 2000). As the morphology of ZFV1 is strikingly similar to RNA viruses further work based on RNA characterisation seems a logical next step in trying to identify the filamentous VLP induced from the zooxanthellae strains.

Although the experiments utilised non-axenic cultures, results clearly indicate that zooxanthellae contain a latent virus that is induced by UV treatment, leading to the lysis of the zooxanthellae. Extrapolation of this virus-host interaction and its effects on zooxanthellae viability provides a novel link to the impact of latent infection on symbiotic dinoflagellates and the subsequent disruption reef ecosystems. If stress-induced viral induction in zooxanthellae occurs within the natural reef environment, the observation of this new group of filamentous VLPs is clearly of importance.

3.5 Conclusions

The inducible filamentous VLP observed in several zooxanthellae strains are highly suggestive that the filamentous VLP, ZFV1, is a latent virus of zooxanthellae. The microbiology and virology of the multiple strains further strengthens this conclusion as these filamentous particles were observed in several strains. It seems unlikely that multiple strains would have the same VLP as an artifact or common contaminant. While AFC or TEM alone cannot be used to claim that the VLPs observed in the UV-treated zooxanthellae are truly viruses, the VLPs observed in AFC, TEM and thin sections strongly support the conclusion that ZFV1 is a latent virus of zooxanthellae.

CHAPTER 4 Inducible VLPs of a freshwater cyanobacterium

4.1 Introduction

The class Cyanophyceae is a incredible group of simple photosynthetic microorganisms. These unique bacteria represent an evolutionary link between prokaryotes and the simplest photosynthesising eukaryotes. The division Cyanophyta belongs to the kingdom Eubacteria with a prokaryotic nature of the cell structure of cyanobacteria and the absence of membrane-bound organelles which is consistent with those of other bacteria. The structure of cyanobacterial thylakoids, which lie free in the cytoplasm, are similar to those found in the chloroplasts of eukaryotic algae and higher photosynthesising organisms.

Cyanobacteria are millions of years old with fossil records dating back to the early Precambrian period (Hall *et al.*, 1974). Evolution of prokaryotes changed the geology of the planet; cyanobacteria are believed to be the first organisms to release elemental oxygen, which allowed the development of aerobic metabolisms and higher plants and animals (Farquhar *et al.*, 2000; Holland, 1994). Eukaryotic cells appears to have evolved from captured and ingested prokaryotic cells (Bhattacharya & Medlin, 1998; Delwiche, 1999; McFadden, 2001; Palmer, 2003; van den Hoek *et al.*, 1995). The chloroplasts are believed to have arisen from endosymbiosis of cyanobacterial cells which were eventually transformed into organelles (van den Hoek *et al.*, 1995). Molecular comparison of ribosomal RNA (rRNA) from cyanobacteria to that of chloroplasts from algae and higher plants implies that photosynthetic capabilities were derived by endosymbiosis of cyanobacteria (Fay, 1983; Margulis, 1993). Evolutionary development of this early symbiosis resulted in three primary lineages; Glaucocystophyta, Chlorophyta and Rhodophyta (Moreira *et al.*, 2000). Other groups of photosynthetic eukaryotic algae arose from secondary and tertiary endosymbiosis events from these lineages (Delwiche, 1999). These events are evident by examining the

number of membranes surrounding the plastid; for example two, three or four membranes indicate primary, secondary and tertiary endosymbiosis respectively. Analysis of nuclear and plastid genomes further support the evolution (Cavalier-Smith, 2002). Structural similarities between chloroplasts and cyanobacteria cells as well as similarities in rRNAs show highly similar composition and functions of the photosynthetic apparatus in chloroplasts and cyanobacteria.

Assessment of phylogenetic relatedness between cyanobacteria and other groups of microorganisms based on 16S rRNA gene phylogeny has been used to discern genealogical relationships. The universal distribution, ease of isolation and the slow rate of change occurring in the nucleotide sequence of the 16S rRNA gene makes it a very good phylogenetic marker to assess the relatedness between bacteria and archaea. Comparative analysis of 16S rRNA gene sequences has been successfully applied to reveal the phylogenetic affinities among cyanobacteria and other major groups of prokaryotes as well as between cyanobacteria and chloroplasts of eukaryotic algae. Based on 16S rDNA phylogeny, cyanobacteria resemble the bacteria more than eukaryotic algae and other plant groups. Cyanobacteria are phylogenetically remote from other bacteria while the chloroplasts of red algae (*Porphyridium*) are more closely related to cyanobacteria.

The prokaryotic cellular structure of cyanobacteria is similar to that of other bacteria, while the photoautotrophic metabolism is similar to that of eukaryotic plants. The thylakoids of cyanobacteria are not closely associated or membrane-bound like those of eukaryotic photosynthetic organisms, as prokaryotes lack membrane-bound organelles. However, the presence of chlorophyll a, thylakoids, and an electron transport system show similarities to those found in plants (Hall *et al.*, 1974).

Cyanobacteria are important in biogeochemical cycles, especially the carbon and nitrogen cycles. A majority of the bioavailable carbon in aquatic environments is

produced from photosynthetic carbon fixation. The marine cyanobacteria *Synechococcus* and *Prochlorococcus*, for example, can account for 25% to 89% of global primary production (Clokie & Mann, 2006; Muhling *et al.*, 2005). Cyanobacteria manufacture organic molecules through the assimilation of CO_2 into ribulose-1, 5-bisphosphate (RuBP). The sunlight required to facilitate this reaction is captured by photosynthetic pigments, phycobiliproteins, in the thylakoids. Light energy is absorbed by the photosynthetic pigments and electron carriers (Photosytems I and II) and releases high energy electrons from photolysis of water. The reaction facilitates the movement of the released electrons through a proton gradient generating ATP in the process of photophosphorylation and releases free O_2. Once the CO_2 is incorporated into a 5-carbon acceptor, RuBP, the reaction is catalyzed by the carboxylating enzyme RuBP carboxylase. The metabolic transformations, through the sugar phosphate intermediates to the final product, glucose, occur during the Calvin cycle (Figure 4.1). The RuBP is then regenerated and is available to accept another CO_2 molecule.

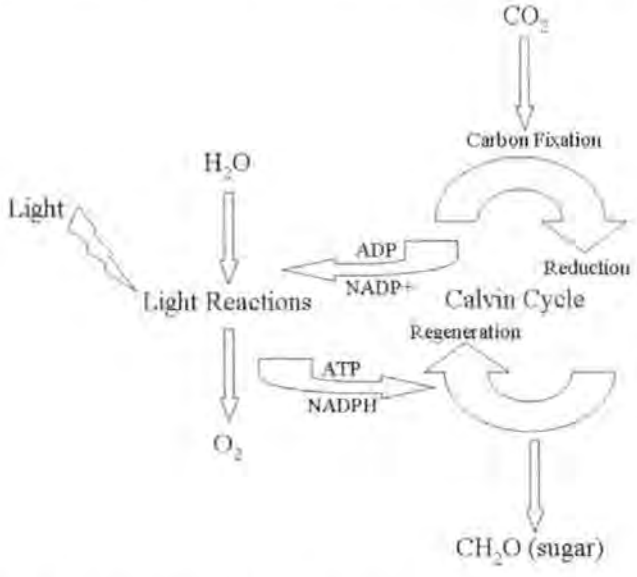

Figure 4.1. Flow chart showing the reactions occurring during photosynthesis.

While cyanobacteria have a major role in primary production, they play an even more important role in biological nitrogen fixation (Capone, 2001). In marine environments, nitrogen is a common limiting nutrient for primary production and cyanobacteria are one of the main organisms responsible for fixing nitrogen (Tyrell, 1999). Cyanobacteria are one of the few groups of organisms that can convert atmospheric nitrogen into an organic form, which is vital to the nitrogen cycle. Annual marine nitrogen fixation is estimated to be up to 190 Tg N y^{-1} and *Trichodesmium* spp. alone is estimated to contribute over 50% of fixed nitrogen, ca. 100 Tg N y^{-1} (Berman-Frank *et al.*, 2003). Beside their contribution to biogeochemical cycles in aquatic environments, cyanobacteria are well known for bloom formations where their abundant growth can be detrimental to local aquatic ecosystems (Fay, 1983). Bloom-forming species, mostly freshwater species, that produce toxic secondary metabolites have been the focus of many studies as the blooms can have both environmental and economic impacts (Wiegand & Pflugmacher, 2005). *Microcystis aeruginosa* which produces microcystins, is one of the more ecologically damaging species; the microcystin-producing blooms affect aquatic and terrestrial organisms as well as humans (Baptista & Vasconcelos, 2006; de Figueiredo *et al.*, 2004). Many studies are underway to assess the various factors responsible for these cyanobacterial blooms (McGillicuddy *et al.*, 2007). Viruses that infect cyanobacteria are ecologically significant factors that have crucial influences on the structure of microbial communities and bloom formations. Freshwater LPP-1 and LPP-2 cyanophages were the first isolated cyanophages. These cyanophages, infecting filamentous forms of cyanobacteria in the genera *Lyngbya*, *Plectonema* and *Phormidium* (Safferman & Morris, 1963; Safferman *et al.*, 1969), have been shown to occur throughout the world (Safferman *et al.*, 1973). The cyanophage SM-1, also discovered in the 1960s (Safferman *et al.*, 1969), was the first cyanophage found to infect a unicellular form of cyanobacteria. It was not until the early 1980's that the first

marine cyanophages were reported (Moisa *et al.*, 1981). Since then, cyanophages have been identified from each of the three well recognised bacteriophage morphological families: *Myoviridae*, *Siphoviridae* and *Podoviridae* (Safferman *et al.*, 1983; Suttle & Chan, 1993) and have been shown to be ubiquitous, diverse and abundant in aquatic environments (Suttle, 1999).

Many investigations have focused on lytic cyanophages (Mann, 2003). Lytic cyanophages are known to be involved in the termination of blooms and it is possible that selective pressure on community composition of cyanobacteria by cyanophages may potentially prevent blooms (Tucker & Pollard, 2005; Weinbauer & Rassoulzadegan, 2004). Prophages are known to confer immunity to similar viruses and it has been proposed that cyanobacterial blooms may also result from a conferred immunity of the host to the prevalent cyanophage (McDaniel *et al.*, 2006).

Temperate cyanophages can have other profound influences on cyanobacterial populations as well. Prophages can influence cyanobacteria by conferring phenotypic traits to the host. Phage conversion by temperate cyanophage, for example, has been proposed as a possible mechanism responsible for toxin production in some strains of cyanobacteria. For example, in a study on a toxin-producing strain of *Microcystis aeruginosa* it was shown that an inducible phage was present, while in the non-toxic strain inducible phages were absent (Vance, 1977). The possibility of temperate cyanophages in toxic strains of other cyanobacteria has been suggested (Orjala *et al.*, 1995), although few have been isolated (Ohki & Fujita, 1996; Ohki, 1999). The implications of temperate cyanophages are poorly comprehended as few temperate systems have been characterised.

The genome sequencing of cyanobacteria and cyanophages has identified possible integrase genes, suggesting that lysogeny in cyanobacteria may be common (Palenik *et al.*, 2003; Sullivan *et al.*, 2005) and it has been proposed that integrases found in the

cyanophage Syn5 genome may be due to a possible temperate life style (Pope *et al.*, 2007). Lysogenic infections in natural populations of marine *Synechococcus* spp. has been demonstrated, with inducible viruses detected in 46% of the strains tested (McDaniel *et al.*, 2002). In filamentous forms of cyanobacteria, prophage induction has been demonstrated as well (Cannon *et al.*, 1971; Ohki & Fujita, 1996; Padan *et al.*, 1972). Recently an inducible temperate cyanophage, AS-1, which infects *Anacystis nidulans* has been isolated and characterized. While lytic phages infecting *Anacystis nidulans* have been previously characterised this is the first report of a temperate phage of *Anacystis nidulans* (Lee *et al.*, 2006). Characterisation of temperate cyanophages is important to reveal knowledge of their prevalence and their potential roles in the environment.

Cyanophages infecting *Pseudanabaena* populations are completely unknown, as is the possibility of lysogeny in this genus. The filamentous cyanobacterial genus *Pseudanabaena* contains morphologically simple members of the order *Oscillatoriales*. They are commonly present in low numbers in lakes on several continents, namely Asia, Africa, Northern Europe and North America (Komárek & Kling, 1991). Studies have shown that *Pseudanabaena* species are most abundant below five meters in the water column and densities reach their peak in late summer (Kling & Watson, 2003). The *Pseudanabaena* cyanobacterium, PPt10905, was isolated from Priest Pot, a pond in the English Lake District, from a water sample collected at a depth of 0.5 m (Baker, 2005). The unusual interaction of this freshwater cyanobacterium and its inducible VLPs are described here.

4.2 Results

4.2.1 Growth curves

The growth assessment of the strain of *Pseudanabaena*, strain PPt10905, was carried out using two methods, haemocytometry and Coulter counter (Figure 4.2). Both methods showed exponential growth of the cultures in the first 10 days. The haemocytometer counts continued to show exponential growth of the culture through day 17. The counts obtained by the Coulter counter showed a plateau and slight decline in cell numbers after day 10.

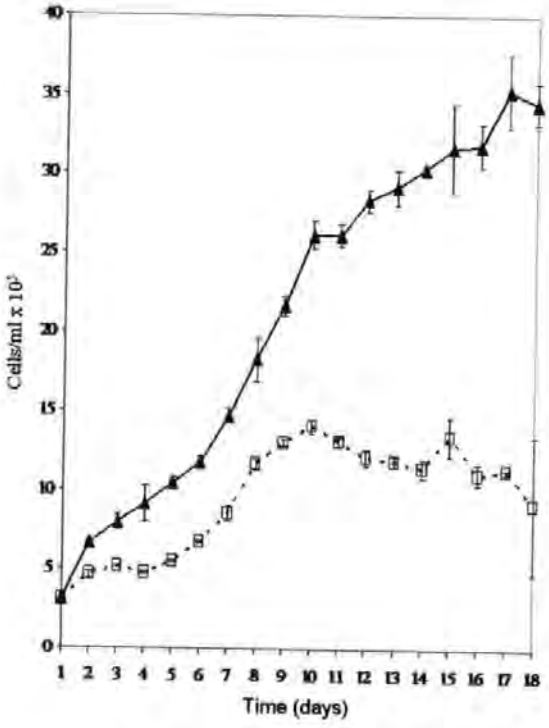

Figure 4.2. Growth curves from cells counts obtained from the Coulter counter are represented by the □ and the cell counts from the haemocytometer are represented by the ▲. Error bars represent standard error (SE) of measurements from replicate cultures, n=3.

4.2.2 Enumeration of VLPs

Exponentially growing cultures were transferred to an incubator at 34°C to heat induce potential VLPs, whilst control cultures were maintained at 26°C; both had similar light regimes (Section 2.1.2). Heat-treated cyanobacterial cultures were screened for the presence of inducible VLPs using AFC. Representative dot plots from the lysates of control and heat-treated lysates are shown in Figure 4.3. The dot plots in panels I through L show the appearance of a new group of VLPs. The abundance of this group of VLPs increased in abundance from 48 h to 144 h after the heat treatment of the cyanobacterial cultures. The areas typical of bacteriophage/noise (Panel A), bacteria (Panel E) and the new group of VLPs (Panel L) are highlighted in Figure 4.3.

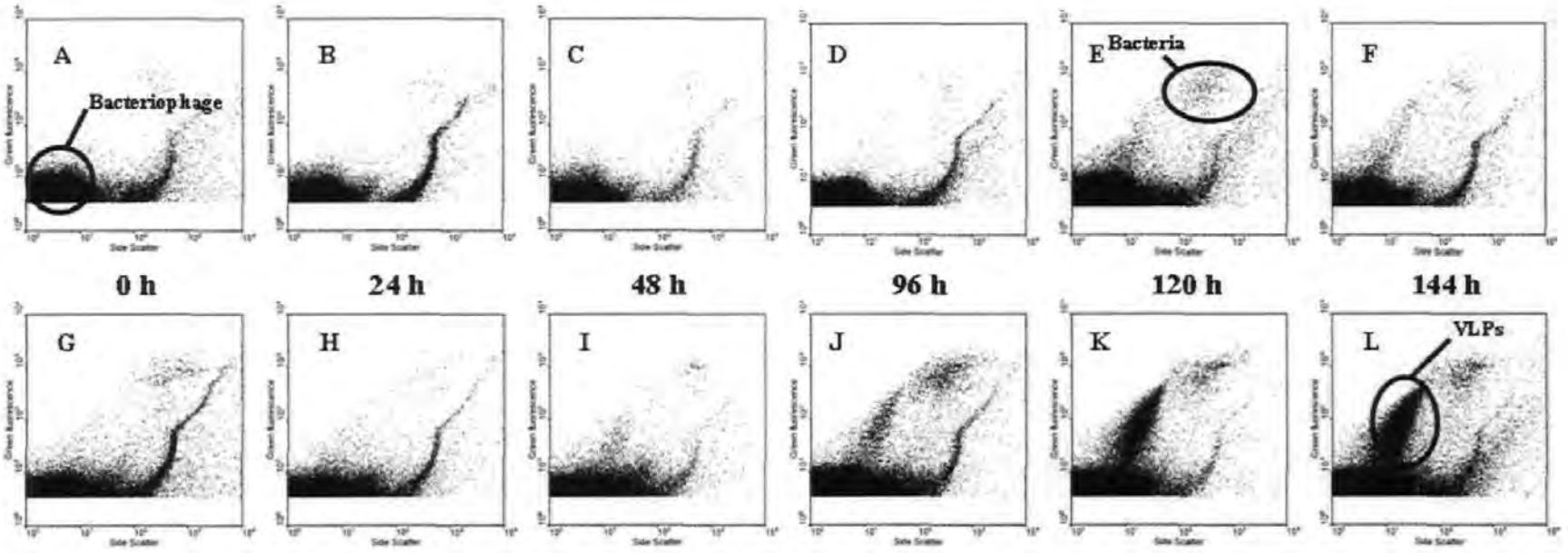

Figure 4.3. Representative AFC dot plots of strain PPt10905, showing SYBRgreen I stained particles in the size range typical of bacteria and VLPs. The controls are shown in panels A through F (0 h to 144 h) and the heat-treated samples are shown in panels G through L (0 h to 144 h). Panel A highlights areas typical of noise and small bacteriophage and the highlighted area in panel E shows the area typical of bacteria. In panels I through L a new group of VLPs increase in abundance over time; the highlighted area in panel L defines this new group of VLPs.

4.2.3 Induction curves

To discern an interaction between the cyanobacterial host and the group of VLPs appearing in the heat-treated cultures, cell counts of the host were plotted against the group of VLPs observed in the AFC analysis (Figure 4.4). A decline in host density was observed in the heat-treated cultures and a substantial increase in VLPs was observed in the heat-treated cultures. A decrease in host abundance was observed within 24 h of heat treatment with a continual decrease up to 120 h. AFC analysis of VLPs induced following heat treatment of the cyanobacterial cultures revealed a group of VLPs increasing in abundance. The appearance of the VLPs began ca. 48 h after introduction of the cultures to increased temperature and continued to increase, with the maximum number of VLPs occurring at 144 h during this time the growth of host cells appeared static.

Groups of particles in the areas representative of bacteriophage/noise (Figure 4.3, panel A), bacteria (Figure 4.3, panel E) were also analyzed. The residual events in the area typical of bacteria remained unchanged between the treated and control cultures over the time course of the experiment. The area typical of noise/bacteriophage showed extreme fluctuations between replicates, with the control appearing to have more events and variations in this area.

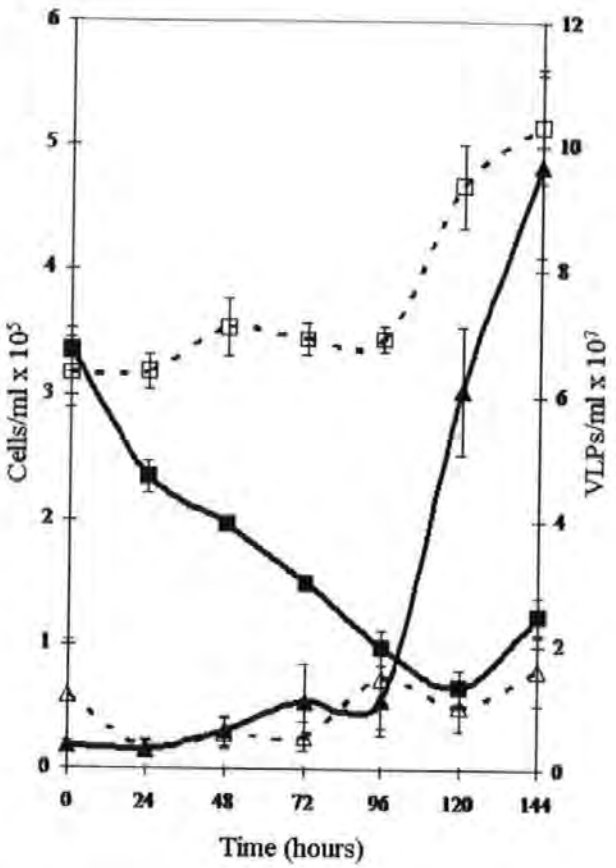

Figure 4.4. The induction curve shows the control (□) and heat-treated (■) cyanobacterium (cells ml^{-1} x 10^{6}) in relation to the VLPs (VLPs ml^{-1} x 10^{7}) present in control (△) and heat- treated cultures (▲). Error bars represent standard error (SE) of measurements from triplicate cultures, n=3.

4.2.4 Visualisation of VLPs

TEM analysis of the lysates from the heat-treated cultures showed an abundance of VLPs ranging in size from 70-100 nm in diameter. The VLPs had a circular shape with a thick capsid surrounding a less electron dense inner core (Figure 4.5).

Thin sections of strain PPt10905, prepared after 96 h of heat treatment, are shown in Figures 4.6 and 4.7. The peripheral regions of the cytoplasm, which contain the photosynthetic apparatus consisting of a few membranes extending in concentric sheets beneath the cell membrane, are defined in panel A of Figures 4.6 and 4.7. Particles of two morphologies were observed in the heat-treated thin sections. The VLPs observed in Figure 4.6 were similar in size and morphology to those observed in the TEM of the lysates. These VLPs ranged in size from 50-100 nm and had a round morphology. In panels A, B, C and D, VLPs similar in size and morphology to those observed in the heat-treated lysates are seen clustered (30-50 VLPs) at the periphery of the host cell. In Figure 4.7, particles ca. 200 nm in diameter with a distinctive isocohedral shape shaped were observed. The larger icosahedral particles, presumed to be carboxysomes, were observed in the controls but at a much lower frequency (1-2 per cell). In the heat-treated cells the larger icosahedral particles were ca. 10 x more abundant than in the controls (10-15 per cell).

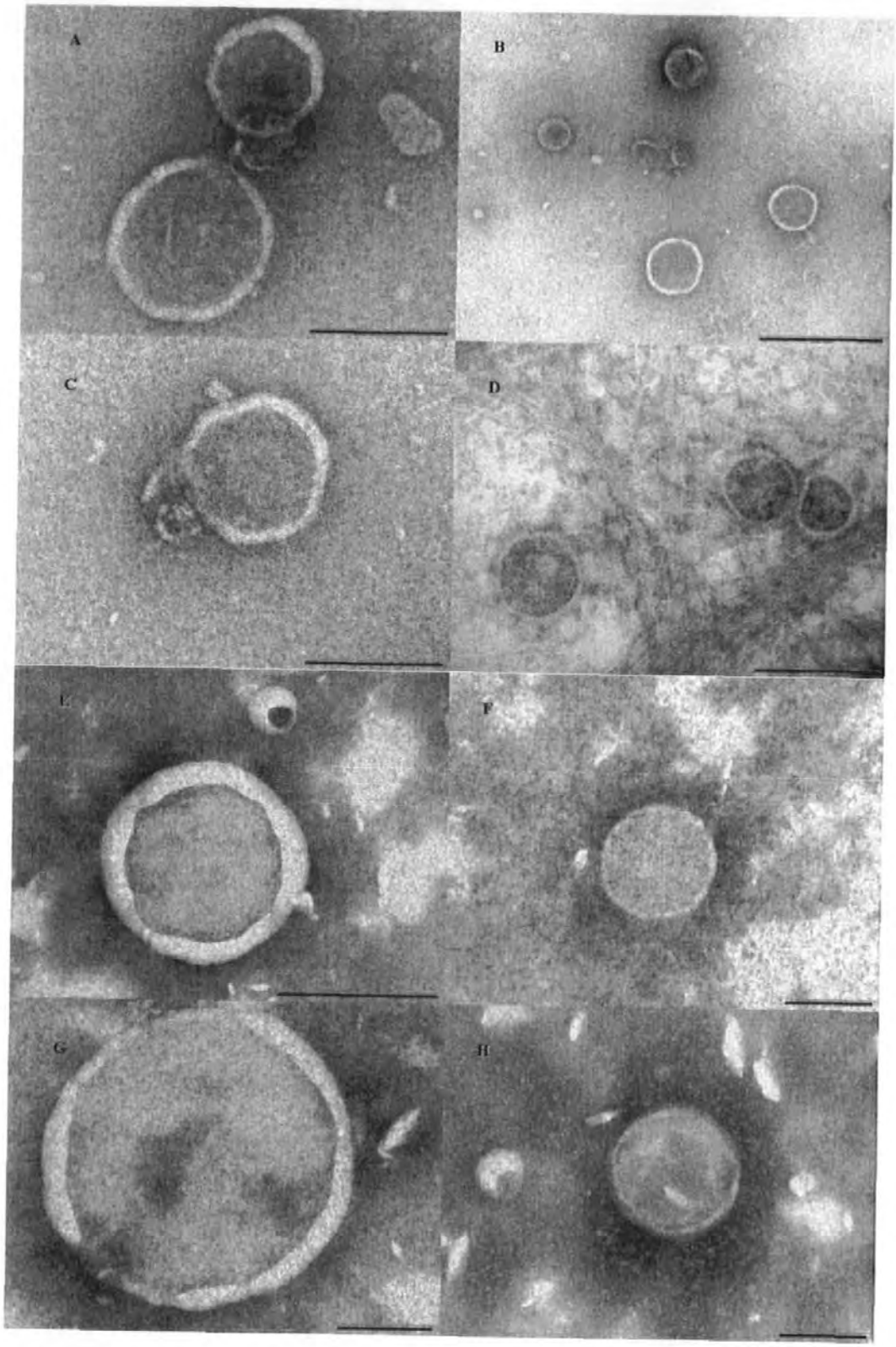

Figure 4.5. TEM images of VLPs from heat-induced strain PPt10905. Scale bars are 200 nm (A and C), 500 nm (B), 300 nm (D), 200 nm (E) and 100 nm (F, G and H).

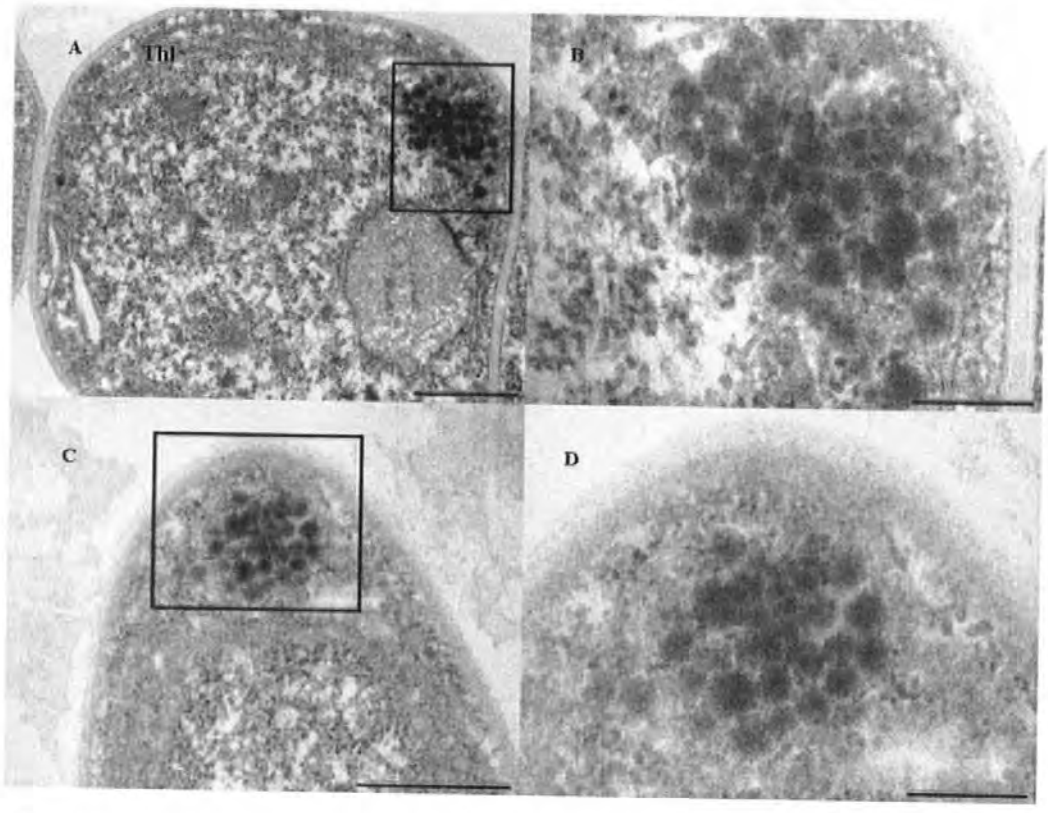

Figure 4.6. TEM images of strain PPt10905 showing the presence of VLPs within thin sections prepared 96 h after heat treatment. The scale bars are 500 nm (A and C), 300 nm (B) and 200 nm (D). The boxed area in A and C highlights the area magnified in B and D, respectively. Thl, thylakoid.

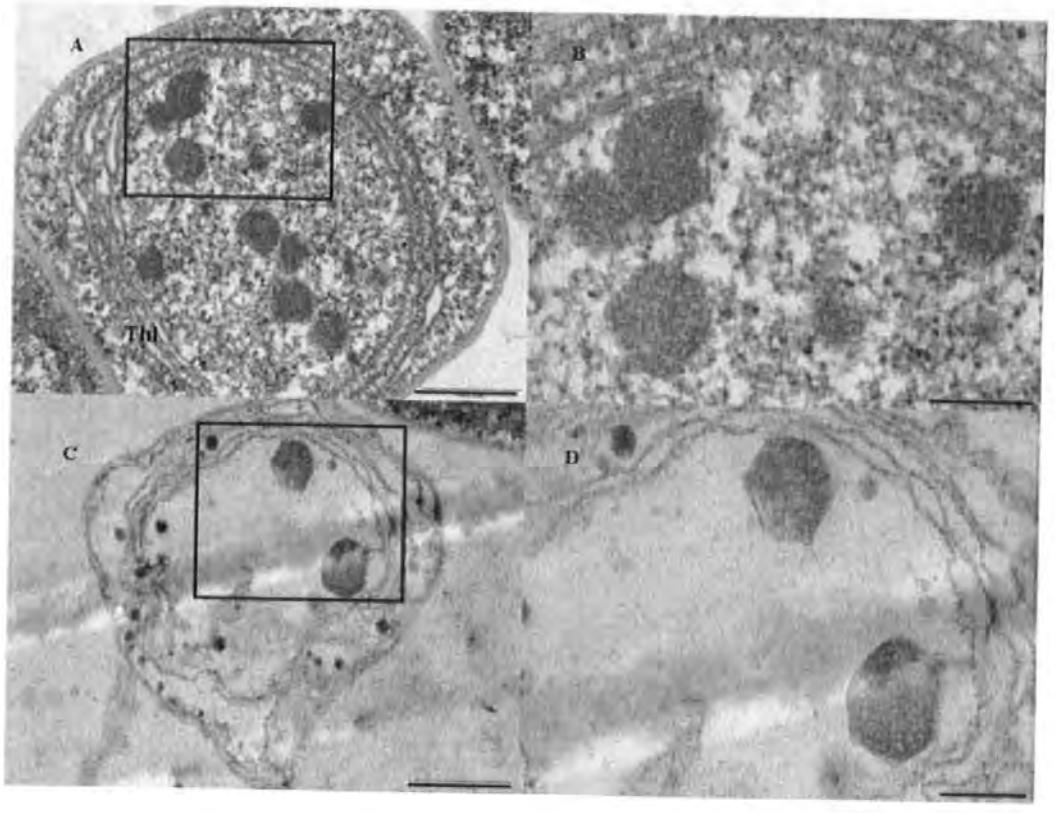

Figure 4.7. TEM images of strain PPt10905 showing the presence of icosahedral particles within thin sections prepared 96 h after heat treatment. The scale bars are 500 nm (A and C) and 200 nm (B and D). The boxed area in A and C highlights the areas magnified in E and F. Thl, thylakoid.

4.2.5 Molecular studies

4.2.5.1 Preparation of nucleic acid

To further characterise the VLPs present in the heat-treated cultures, lysates (1-3 l) were 0.2 µm filtered and concentrated (Section 2.5.2). Nucleic acid extracted from heat-treated culture was separated by conventional gel electrophoresis revealing a discrete band (Figure 4.8, lane 5). Treatment with RNase and DNase showed the nucleic acid to be sensitive to DNase.

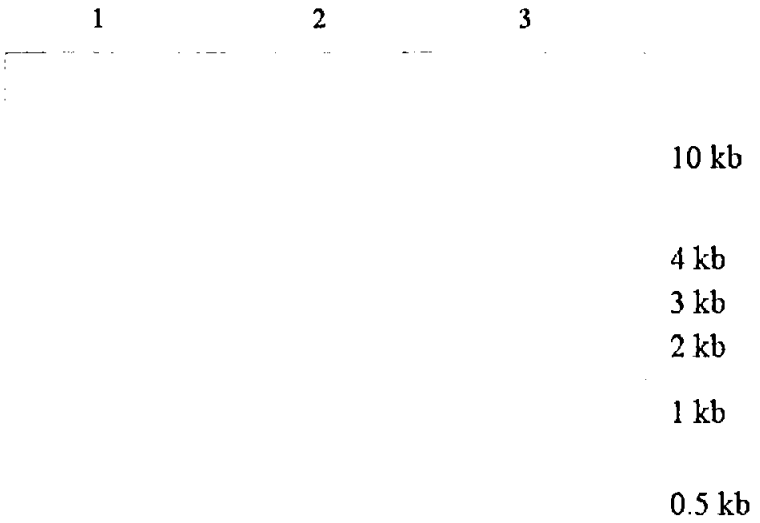

Figure 4.8. Gel image showing nucleic acid extracted from the virus fraction of the heat-treated strain PPt10905. Lane 1 shows the discrete band of nucleic acid. Lane 3 shows the 1 kb molecular weight marker. Lane 2 is empty.

4.2.5.2 PFGE

Concentrates prepared from lysates were digested in agarose plugs (Section 2.8) and examined by PFGE (Figure 4.9 and 4.10); liquid loading of nucleic acid extracted from concentrates was also examined by PFGE (Figure 4.11). Figure 4.9 and 4.10 show gels run with a pulsed time of 5.5 sec to 36.5 sec for 21 h; the gel in Figure 4.11 was run with switch times of 1 sec to 15 sec for 22 h. PFGE analysis revealed one slightly degraded band ca. 45- 50 kb in lane 4 of the gel in Figure 4.8 and lanes 2 and 5 in Figure 4.10. Lane 2, in Figure 4.11, shows the result of the loading of a liquid sample (nucleic acid extraction) which revealed a degraded band < 20 kb.

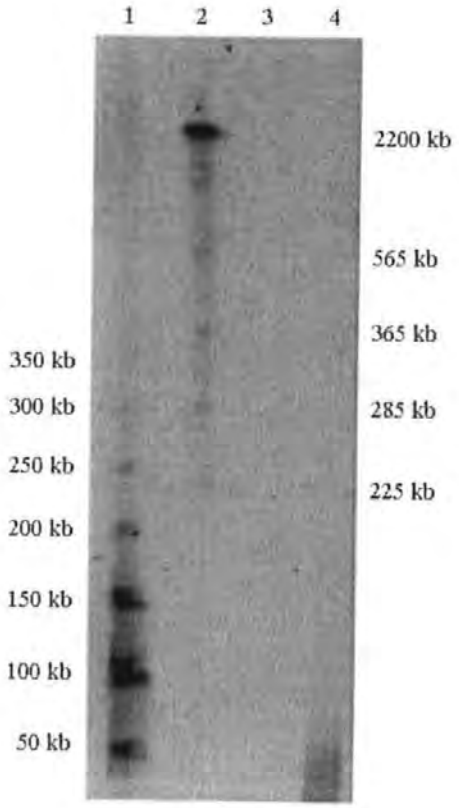

Figure 4.9. PFGE image of concentrated lysate from heat-induced strain PPt10905. Lane 4 is the concentrated lysate digested in an agarose plug. The switch time of 5.5 sec to 36.5 sec was run for 21 h. Lanes 1 shows the lambda molecular weight marker (0.05–1 Mb) and lane 2 shows a 0.2–2.2 Mb *S. cerevisiae* ladder. Lane 3 is empty.

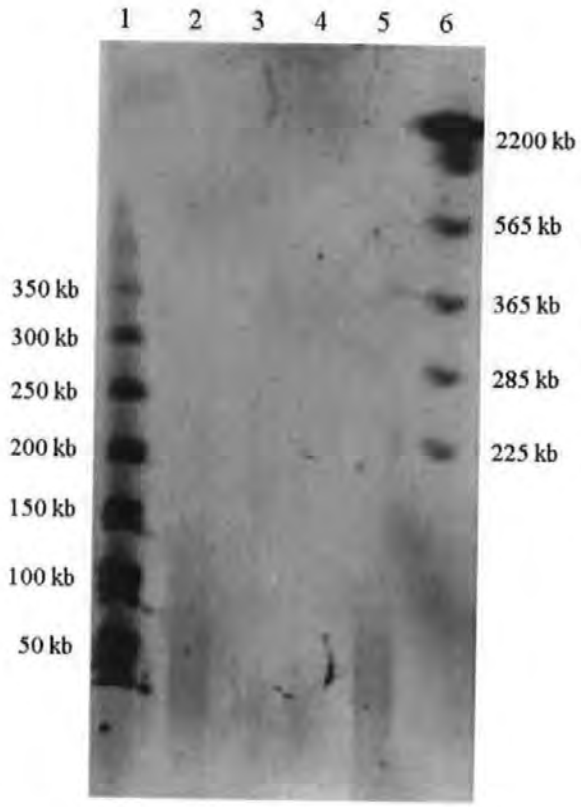

Figure 4.10. PFGE image of concentrated lysate from heat-induced strain PPt10905. Lanes 2 and 5 show the concentrated lysates digested in an agarose plug. The switch time of 5.5 sec to 36.5 sec was run for 21 h. Lanes 1 shows the lambda molecular weight marker (0.05–1 Mb) and lane 6 shows a 0.2–2.2 Mb *S. cerevisiae* ladder. Lanes 3 and 4 are empty.

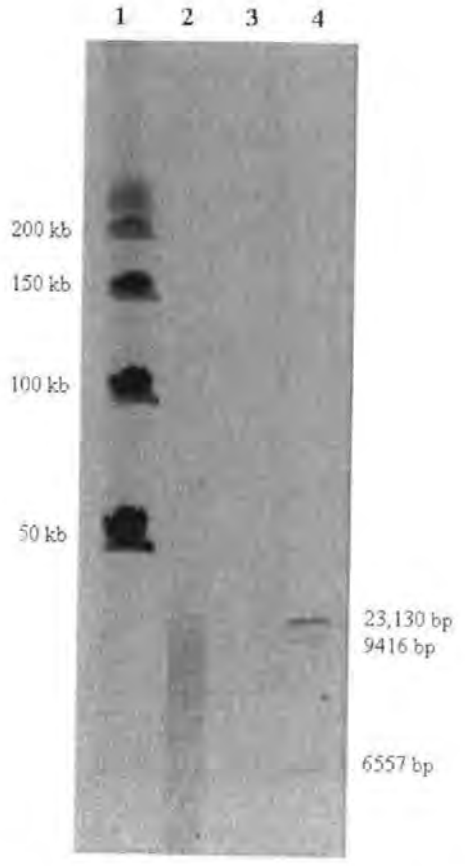

Figure 4.11. PFGE image of nucleic acid extracted from strain PPt10905. Lane 2 shows result of the loading of a liquid sample of nucleic acid. The switch time of 1 sec to 15 sec was run for 22 h. Lane 1 shows the lambda molecular weight marker (0.05–1 Mb) and lane 4 shows a lambda *Hind*III ladder. Lane 3 is empty.

4.2.5.3 Clone libraries

Clone libraries were prepared from DNA extracted from concentrates of the heat-treated lysates (Section 2.7.3). Various sonication times (30 sec to 2 min) were tested in order to yield a DNA size appropriate for cloning. Sonicated fragments are shown in the gel image in Figure 4.12. The sample in lane 2 was sonicated 30 sec and the sample in lane 3 was sonicated for 1 min. The blunt-ended fragments in the size range of 1-5 kb were excised from agarose gels and used for cloning.

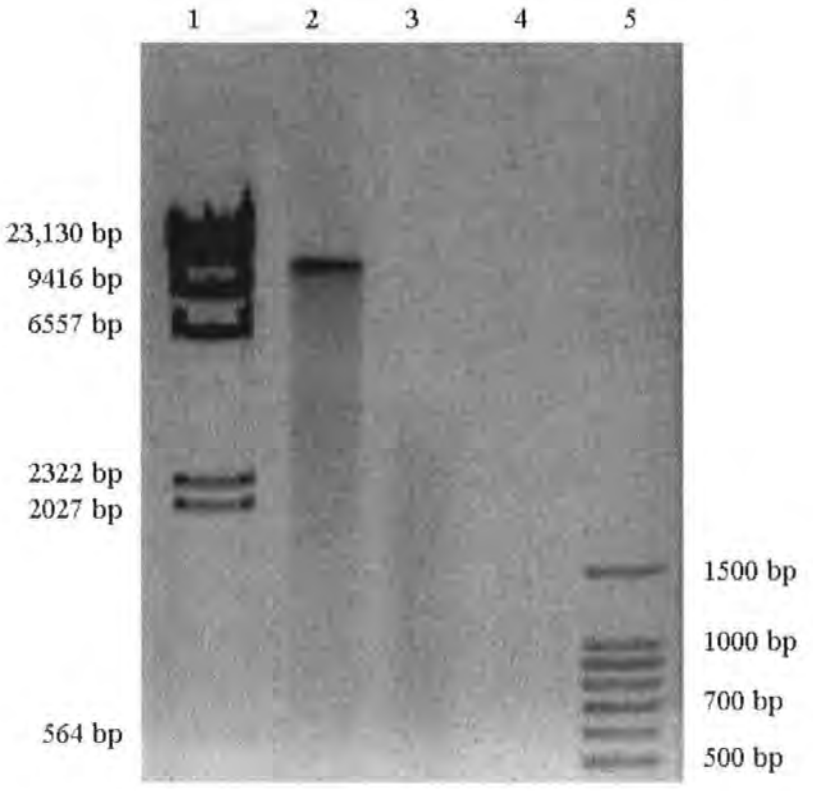

Figure 4.12. Gel image showing sonicated DNA extracted from PPt10905 lysate. The sonicated DNA is shown in lane 2 (30 sec) and lane 3 (1 min). Lane 1 is a Lambda *Hind*III marker and lane 5 is a 100 bp ladder. Lane 4 is empty.

4.2.5.4 Contigs and sequencing

Several clone libraries were prepared from the sonicated DNA and larger inserts in the size range of 1-5 kb were sequenced. A total of 24 clones were sequenced with forward and reverse primers. Sequences of clones were assembled into continuous sequences (contigs) using PhredPhrap. The sequences assembled into 18 contigs and/or clone sequences ranging in size from 246 bp to 1482 bp (Supplemental Material 2). Contigs were compared to Genbank database using BLASTn, 14 of the contigs showed similarities to previously described organisms. A hit was considered significant with E-values below 0.001. The distribution of BLAST hits showed 79% of the contigs showed significant nucleotide similarities to heterotrophic bacteria, 14% showed sequence similarities to cyanobacteria and the remaining 7% showed similarities to previously

described bacteriophages (Table 4.1). Although not the top BLAST hit, two contigs, contig 2 and contig 4 showed sequence similarities to cyanophage AS-1 contigs 5, 14 and 16 (Accession numbers; DQ115812, DQ115821, DQ115823) using BLASTn restricted to virus sequences present in the GenBank database. While the sequence similarity was significant (3e-06) no putative function has been assigned to the cyanophage AS-1 contigs.

Table 4.1. BLAST results.

Contig	Length	BLASTn results	E-value	Accession #
1	496	*Acidovorax* spp. JS42, complete genome	1.00E-102	CP000539
2	1035	*Pseudomonas mendocina* ymp, complete genome	0.00E+00	CP000680
4	1031	*Pseudomonas mendocina* ymp, complete genome	0.00E+00	CP000680
5	940	*Verminephrobacter eiseniae* EF01-2, complete genome	0.00E+00	CP000542
6	649	*Xanthomonas axonopodis* pv. citri str. 306, complete genome	2.00E-119	AE011733
7	1044	*Pseudomonas mendocina* ymp, complete genome	0.00E+00	CP000680
8	1343	*Acidovorax* spp. JS42, complete genome	4.00E-114	CP000539
11	469	*Sinorhizobium meliloti* 1021 plasmid pSymA complete plasmid sequence	1.00E-140	AE007214
12	1190	*Anabaena variabilis* ATCC 29413 chromosome, complete sequence	5.00E-10	CP000117
13	340	*Pseudomonas fluorescens* Pf-5, complete genome	7.00E-27	CP000076
14	246	*Burkholderia cenocepacia* phage BcepB1A, complete genome	2.00E-06	AY616033
15	1011	*Sinorhizobium meliloti* 1021 complete chromosome	8.00E-172	AL591793
16	1482	*Pseudanabaena* spp. cpeBA	9.00E-15	X63073
18	913	*Bradyrhizobium* spp. BTAi1, complete genome	3.00E-11	CP000494

Contig	Length	BLASTn results virus database	E-value	Accession #
2	1035	*Salmonella enterica* subsp. *enterica* serovar Choleraesuis str. SC-B67, complete genome	2.00E-28	AE017220
4	1031	*Saccharopolyspora erythraea* NRRL2338 complete genome	8.00E-14	AM420293
14	246	*Burkholderia cenocepacia* phage BcepB1A, complete genome	6.00E-08	AY616034
15	1011	*Saccharopolyspora erythraea* NRRL2338 complete genome	5.00E-16	AM420293
18	913	Mycobacteriophage Omega, complete sequence	4.00E-10	AY129338

Table 4.1 (cont.). BLAST results.

Contig	Length	BLASTx results	E-value	Accession #
1	496	aminomethyl transferase [*Delftia acidovorans* SPH-1]	7.00E-76	EAV72887
2	1035	nuclease [*Pseudomonas mendocina* ymp]	1.00E-105	YP_001186040
4	1031	diguanylate cyclase/phosphodiesterase [*Pseudomonas mendocina* ymp]	2.00E-113	YP_001186260
5	940	D-alanine--D-alanine ligase [*Comamonas testosteroni* KF-1]	7.00E-73	ZP_01517992
6	649	phosphoesterase [*Stenotrophomonas maltophilia*]	6.00E-33	ZP_01643009
7	1044	flagellar hook-associated 2 domain protein [*Pseudomonas mendocina*]	7.00E-83	YP_001188320
8	1343	putative transcriptional regulator [*Acidovorax avenae* subsp. *citrulli* AAC00-1]	6.00E-53	YP_972751
11	469	histidinol dehydrogenase [*Sinorhizobium medicae* WSM419]	1.00E-74	ZP_01412085
12	1190	uncharacterised conserved protein [*Nostoc punctiforme*]	1.00E-38	ZP_00111140
13	340	methyltransferase type 12 [*Pseudomonas putida* GB-1]	1.00E-26	ZP_01716206
14	246	gp37 [*Burkholderia* phage phiE255]	6.00E-17	YP_001111237
15	1011	putative DNA polymerase III alpha protein [*Sinorhizobium meliloti* 1021]	5.00E-133	NP_387277
16	1482	hypothetical protein L8106_11892 [*Lyngbya* spp. PCC 8106]	1.00E-70	ZP_01621542
18	913	site-specific DNA-methyltransferase [*Bradyrhizobium* spp.]	1.00E-43	YP_001242420

Contig	Length	BLASTx results virus database	E-value	Accession #
2	1035	putative DNase/RNase endonuclease [Bacteriophage SPBc2]	3.00E-10	NP_046558
14	246	gp37 [*Burkholderia* phage phiE255]	4.00E-18	YP_001111237
15	1011	DNA polymerase III alpha subunit [*Saccharomonospora* phage PIS]	1.00E-29	AAL66178
18	913	gp155 [Mycobacterium phage Omega]	4.00E-39	NP_818455

4.3 Discussion

4.3.1 Growth curves

Assessing the growth of filamentous cyanobacteria in liquid culture can be challenging due to their filamentous nature which renders difficult the growth monitoring with common methods such as O.D. Alternative methods to monitor the growth of the cyanobacterium PPt10905 were investigated and compared for efficiency (Figure 4.2), as previous growth curves using optical density proved to be an unreliable method (Baker, 2005). Filamentous morphologies are the most troublesome to quantify as broken and dividing filaments have a tendency to clump, making the use of optical density readings inaccurate. The results of the comparison between haemocytometry and the Coulter counter to monitor the growth of strain PPt10905 showed that both methods generated growth curves in accordance with the classical bacteria growth model; lag, log and stationary phases.

During the division, the cyanobacterium reproduces by trichome formation and the fragments of the filaments detach and break away. The Coulter counter measures the electrolyte displacement produced by particles, which is proportional to the volume of the particle, as they are drawn through an aperture. The output shows the size distribution of particles, particle diameter (μm), within the selected range, but omits small fragments of the dividing cells as they lie outside of the range and within the background noise. The fragmentation of the actively reproducing cells interfered with Coulter counter measurements. The dividing fragments noticeably lowered the counts of the exponentially growing cultures ca. day 10 during mid-late exponential growth of the culture, at which time the Coulter counter measurements showed the culture to be in stationary phase. Unlike Coulter counter the haemocytometer is not biased against small dividing fragments and gave a better assessment of the exponential growth. The haemocytometer showed exponential growth of the culture through to day 17. The

dividing strategy found in this strain of filamentous cyanobacteria is best compensated for with direct counts and overall haemocytometry counts generated more accurate growth curves.

4.3.2 Identification and enumeration of VLPs by AFC

Identification and quantification of inducible VLPs released after heat treatment of strain PPt10905 was achieved by analysis of dot plots of SSC versus GFL. AFC analysis revealed the presence of a group of particles which started appearing ca. 48 h after heat treatment. The group of particles continued to increase in abundance and was clearly distinguishable 144 h after treatment (Figure 4.3). It was concluded that this group contained inducible VLPs of strain PPt10905, although the SSC and GFL signal was outside of the size range typical of known lytic cyanophages (Brussaard *et al.*, 2000; Chen *et al.*, 2001). The size discrepency observed in the AFC analysis may be due to the VLPs sticking together making the group of VLPs in the dot plots appear larger.

Haemocytometer counts of the cyanobacterium were plotted against the analysis of the AFC dot plots of the VLPs to discern a relationship. A decline in the concentration of cyanobacteria was observed within 24 h after heat treatment; the appearance of the VLP group began ca. 48 h and a rapid increase in the concentration of VLPs occurred after ca. 72 h (Figure 4.4). The concentration of these VLPs continued to increase to ca. 9.7 x 10^7 particles ml^{-1} at 144 h after heat treatment, at which point the heat-treated cyanobacterial cultures had substantially declined and had become static. A direct correlation seen in a typical host-virus interaction was not observed; the increase in VLPs occurred later than those seen in other virus-induced culture crashes, such as that observed in the *Symbiodinium* spp. (Section 3.2.5). This observation is most likely due to absorption of the released VLPs to the actively dividing cells as this would account

for the drop in host numbers and the lag in the appearance of VLPs. As the samples were analysed a couple hours after the artifical light cycle was initiated the peak of the observed VLPs may represent viral release from the second round of infected host cells consecutive to the initial induction of the prophage. It has been proposed that phage infection reaches a maximum during daylight hours of the diel cycle which would be consistant with the observed results (Clokie *et al.*, 2006).

4.3.3 Visualisation of VLPs

The VLPs observed in the supernatants of the heat-treated cultures had a round morphology with no discernable tail and a diameter ca. 70-100 nm. Particles with a similar morphology were observed in the thin sections of the heat-treated cultures. VLPs with this morphology are typical of podoviruses (Safferman *et al.*, 1983). In the thin sections of the heat-treated cultures, clusters of the VLPs were observed in the periphery of the cells at 96 hours after heat treatment (Figure 4.6). The increase in abundance of VLPs observed in AFC occurred during this time, further supporting the evidence that the VLPs observed in AFC are an inducible phage of strain PPt10905. In thin sections of the heat-treated cultures, several larger isocohedral particles with a diameter ca. 200 nm were observed. These larger particles were observed in thin sections of the controls, but they were ca. 10 times more prevalent in the thin sections heat-treated cultures. These larger icosahedral particles had morphology similar to carboxysomes, which are commonly found in cyanobacteria (Fay, 1983; Tanaka *et al.*, 2008). Carboxysomes are structures 200-300 nm in diameter that contain a metabolically active form of the primary photosynthetic enzyme ribulose-1, 5 bisphosphate carboxylase/oxygenase (RuBisCO) which catalyses CO_2 fixation into ribulose 1, 5 bisphosphate (RuBP), the primary step in the dark reactions of photosynthesis.

Carboxysomes were first observed in *Nostoc pruniforme* (Jensen & Bowen, 1961) and are commonly mistaken for viruses due to their morphology (Bobik, 2007). The increase in abundance in carboxysomes in the heat-treated cultures was unexpected. Investigations have shown many cyanophage, up to 88% (Hill, 2006), may carry photosystem II genes that benefit both the phage and the host (Mann, 2003; Mann *et al.*, 2005; Sullivan *et al.*, 2006).

4.3.4 Molecular studies

Nine cyanophage genomes have been fully sequenced (Genbank, March, 2008). The characterised cyanophage genomes consist of 4 podoviruses and 5 myoviruses with genome sizes ranging from 40,938 nt (Cyanophage Pf-WMP4) (Liu *et al.*, 2007) to 196,280 nt (Cyanophage S-PM2) (Mann *et al.*, 2005). The cyanopodovirus genomes; Syn5 (Pope *et al.*, 2007), Pf-WMP4 (Liu *et al.*, 2007), P-SSP7 (Sullivan *et al.*, 2005) P60 (Chen & Lu, 2002), have genome sizes between 40-48 kb. PFGE showed a genome size of the VLPs of strain PPt10905 to be ca. 45-50 kb (Figure 4.9 and 4.10). This genome size estimation of the putative cyanopodovirus of strain PPt10905 is in agreement with that of other cyanopodovirus genomes and tends to point toward an average cyanopodovirus size of ca. 45 kb.

The size difference of the VLPs of strain PPt10905 observed in Figure 4.11 may be due to shearing caused by the loading of a liquid sample when pipetting or it may be due to the run conditions of the PFGE as pulse times can dramatically affect the way a product may migrate. Over half of the cyanophage genomes available in Genbank are circularly permuted. With a shorter pulse time, similar to the running conditions of the gel in Figure 4.11, a circular genome would migrate faster relative to the linear lambda ladder. A linear genome should migrate to the same position relative to the linear marker regardless of the running conditions; the changes in migration relative to the linear

lambda concatamers suggest the putative cyanophage genome of strain PPt10905 might be circularly permuted.

4.3.5 Contigs and sequencing

Several cloning methods were attempted to produce a clone library. Variations in blunt ending methods, cloning vector and transformation procedures were tried to produce a library. Sonicated fragments were blunt ended with three different methods; the sonicated fragments were filled in with the enzyme Pfu, or ends of the fragments were cut back with the Mung bean enzyme and lastly a commercial blunt ending kit from Lucigen was employed. In all three cases, ligation controls were as expected, but clones containing inserts in the desired size range were low. As the cloning difficulties may have been due to incompatibility between the phage DNA and the vector, three cloning vectors were used; Invitrogen Zero blunt, Lucigen HC Kan and Lucigen pJAZZ. The Invitrogen vector yielded clones with the fragments of the desired size, but the efficiency was very low as <30% of the clones had inserts and many of these were small fragments. The Lucigen kits were employed to eliminate issues due to highly modified phage DNA, toxic genes, AT rich areas and/or repeats, which are often a problem with phage cloning. The Lucigen HC Kan kit yielded many clones, ca. 85% with large inserts. The vector primers did not work in the sequencing reactions. After many trouble-shooting steps, it was concluded the vector was compromised and this library was dismissed. The final attempt to clone the VLPs of strain PPt10905 employed a Lucigen pJAZZ vector. Both electrocompetent and chemically competent cells were used, yet none of them gave satisfactory transformation. Cloning of phage and viruses can be tricky as there are frequently modified nucleotides, toxic genes and/or repeat regions. Selecting cloning vectors which are more compatible can overcome some of the difficulties with cloning viruses. Other methods, such as pyrosequencing bypass

cloning altogether. While pyrosequencing has its own drawbacks such as short reads, more complex assembly processing and problems assembling repeat regions it could circumvent problems associated with cloning the phage genome (Wommack *et al.*, 2008).

Clones obtained from the Invitrogen zero blunt cloning were screened for larger inserts and sequenced. This provided ca. 15 kb of sequence which assembled into 18 contigs. Contigs obtained from the preliminary sequencing showed several sequence similarities to cyanophage genomes, cyanobacteria genomes, bacterial genomes as well as some of a T7-like phage. Cyanophage Pf-WMP4, which infects the freshwater cyanobacterium (*Phormidium foveolarum*) (Liu *et al.*, 2007) and other cyanophages have sequence similarities to T7-like phages (Liu *et al.*, 2007). Some of the hits from the 18 contigs of the PPt10905 cyanophage were to T7 phages and possibly prophages associated with their hosts. Two contigs showed sequence similarities to undescribed contigs from the cyanobacteria phage AS-1. Interestingly, Xinyao *et al.*, 2007 recently showed AS-1 to have a lysogenic life cycle, supporting the hypothesis that the VLP induced from PPt10905 could be a lysogenic cyanophage.

The complete sequence analysis of this freshwater temperate cyanophage will be of great interest, as the comparison of this genome with the previously described cyanophage genomes will provide an insight into the differences and similarities found in freshwater and marine cyanophages. Furthermore, as there are no unambiguously temperate cyanophage genomes currently sequenced, it would be most interesting to see how this one compares to the genomes of lytic cyanophages. This could potentially explain some of the mechanisms behind the temperate lifestyles of cyanophages and their host interaction.

4.4 Conclusions

The inducible VLPs observed in the cyanobacterial strain, PPt10905, are highly suggestive that cyanobacterium PPt10905 harbours an inducible temperate phage. The results showing the group of VLPs appearing in the AFC of the heat-treated cultures, the podovirus morphology of the particles observed in the TEM and the clusters of VLPs observed in the thin sectioning of the heat-treated cultures all strongly support the hypothesis that the cyanobacterium PPt10905 harbours a prophage which appears to be lysogenic. The significance of lysogenic cyanophages in freshwater cyanobacteria is not well understood and the isolation and characterisation will provide valuable information about aquatic temperate cyanophages.

CHAPTER 5 Latency in algal culture collections

5.1 Introduction

Marine algae have a central role in the marine environment. Their numbers and ubiquity make them essential contributors in a variety of major biogeochemical cycles as well as key members of the marine food web (Rao, 2006). The different algal studies have shed light on the complex and numerous roles that algae play in the environment from primary production (Marra, 2002) to CO_2 sinks (Buitenhuis, 2001). Completion of several algal genomes (*Dunalellia salina*, *Chlorella vulgaris* and *Micromonas pusilla*; DOE Joint Genome Institute), will provide much information that will increase our knowledge of these organisms and help grasp the full extent of their capabilities.

The economy of marine algae has developed following the growth of aquaculture industries which use algae as a source of live and preserved feeds. In 1993, 90% of the 14.5 million metric tons of aquaculture-produced animals utilised phytoplankton during at least one of their developmental stages (Duerr *et al.*, 1998). With the aquaculture industry growing at a rate of 8% per year (Pulz & Gross, 2004), there is a need for more intense alga production. The average estimated production cost of one kg of dry algae is $50-$150 (Pulz & Gross, 2004) and can be as much as $600 in smaller hatcheries (Borowitzka, 1997); these high prices have prompted significant research on algal production and algal physiology in order to provide a better knowledge of the strains used and eventually reduce the price of alga feeds.

In marine environments, phytoplankton growth is influenced by numerous factors and seasonal increases in phytoplankton density (blooms) can have great ecological importance in marine food webs (Munn, 2004). While not all blooms are toxic, the term harmful algal bloom (HAB) is used to describe algal blooms which have ecological and economical impacts. Toxic HABs are caused mainly by cyanobacteria, dinoflagellates, and diatoms which produce toxins that can be harmful to fish, shellfish and humans. For

example, a HAB that is common to the eastern Gulf of Mexico, is caused by the dinoflagellate *Karenia brevis* that produces brevetoxin, and HABs that occur in the gulf of Maine are a result of the dinoflagellate *Alexandrium fundyense* which produces saxitoxin. A study in the United States reported that HABs over a period of 15 years (estimates based on costs from 1987-1992) cost about $450 million and impacted sectors such as public health, commercial fishery and tourism (www.whoi.edu/redtide/pertinentinfo/Economics_report.pdf). The mechanisms by which algal blooms form and dissipate remain unclear and much research has been devoted to explaining the different factors that can affect these blooms (McGillicuddy *et al.*, 2007).

Strains in algal culture collections are used as model organisms to provide a better understanding of the multiple contributions of algae. At the ecological level, research involving species found in culture collections has provided evidence of their role in nutrient cycles, food web dynamics and algal bloom formations. At the economic level, culture collection specimens have provided for improvements of algae production for aquaculture purposes (Borowitzka, 1997; Day *et al.*, 1999).

Marine algae collected from the planet's various water bodies are preserved in different culture collections around the world, where they are maintained and made available to researchers and industry. Algae culture collections, which contain thousands of strains, represent a vast and relatively untapped resource for the study of algae (Table 5.1). The Plymouth Culture Collection (PCC) of Marine Algae (Plymouth, UK, http://www.mba.ac.uk/education/education_outreach.php?culturecollection), for example, which was established in 1910, was originally created for the provision of algae as food organisms and for taxonomic research. Since the establishment of the Plymouth algal collection, which currently contains 285 different strains of algae, its focus has extended to other fields of study such as carbon acquisition in various species

and calcification in coccolithophorids. As described below, algal cultures are utilised to understand algal life cycles, their roles in species succession and phytoplankton dynamics. The use of culture collection algae strains under laboratory conditions to replicate environmentally occurring blooms has shown to be an adequate model system that has provided insights into the bloom cycles (Pettersson *et al.*, 2000; Solé *et al.*, 2006). The mathematical modeling of algal blooms has been a challenging task due to the multiplicity of factors involved under environmental conditions. By incorporating the effect of viral lysis, these mathematical models have proven to be a better fit in predicting the abundance of phytoplankton during the various stages of bloom events at magnitudes similar to those observed *in situ* (Beltrami & Carroll, 1994).

Table 5.1. List of the main algal culture collection throughout the world.

Country	Algal Culture Collection
Australia	CSIRO Microalgae Research Centre
Canada	University of Toronto Culture Collection of Algae and Cyanobacteria Canadian Center for the Culture of Microorganisms
Czech Republic	Culture Collection of Algae of Charles University Prague Culture Collection of Algal Laboratory, Trebon
France	Microalgal Culture Collection of the University of Caen Basse-Normandie Roscoff Culture Collection Pasteur Culture Collection of Cyanobacteria
Germany	Culture Collection of Algae at the University of Cologne Culture Collection of Algae at the University of Götting Department of Cell Biology and Applied Botany, Philipps-University The Friedrich Hustedt Diatom Collection
Japan	National Institute of Environmental Studies Marine Biotechnology Institute Culture Collection IAM Culture Collection WFCC-MIRCEN World Data Centre for Microorganisms Marine Biotechnology Institute Culture collection
Mexico	CIBNOR Microalgae Culture Collection, La Paz
United Kingdom	Culture Collection of Algae and Protozoa The Plymouth Culture Collection of Marine Algae
United States	University of Texas Culture Collection of Algae American Type Culture Collection Provasoli-Guillard Culture Collection of Marine Phytoplankton Antarctic Protist Culture Collection at Woods Hole. MA Loras College Diatom Culture Collection Culture Collection of Microorganisms from Extreme Environments The Diatom Collection of the California Academy of Sciences

The work on *Emiliania huxleyi* best exemplifies the successful use of a strain from a culture collection that provided much information into the role of algae in the microbial loop as well as bloom formation. *E. huxleyi* is one of the ca. 300 known bloom-forming marine microalgae. *E. huxleyi* is a very cosmopolitan microalga that is found in all but polar oceans (Le Vu *et al.*, 2003). It forms blooms in various regions, from the Bering Sea (Stockwell *et al.*, 2001) to the English Channel (Wilson *et al.*, 2002) and these blooms can be large enough that they can be monitored from space by satellite remote sensing (Smyth *et al.*, 2004). Studies of *E. huxleyi* blooms have shown that they can have a major environmental impact through water albedo and dimethyl sulfide production (Levasseur *et al.*, 1996). Furthermore, it has been shown that *E. huxleyi* blooms are sinks of atmospheric carbon dioxide through calcification and photosynthesis (Buitenhuis, 2001).

Most of our knowledge about the genetic diversity of algal viruses comes from studies of viruses which have been isolated and purified in the laboratory. Algal viruses of major marine bloom-forming algal species such as *E. huxleyi*, *Phaeocystis* spp. and *Micromonas pusilla* have provided most of the studied algal viruses (Baudoux & Brussaard, 2005; Brussaard *et al.*, 2004b; Schroeder *et al.*, 2002).

The study of viral latency in microalgae has not been the subject of much attention, unlike the viruses of the macroalgae *Ectocarpus siliculosus* and *Feldmannia* species (Delaroque *et al.*, 2001; Müller & Frenzer, 1993). Latency in aquatic algae has been for the most part overlooked. Research, as part of this thesis, used algal strains belonging to five of the nine recognised algal divisions: namely, *Chlorophyta*, *Heterokontophyta*, *Cryptophyta*, *Haptophyta*, *Rhodophyta*; each was examined for potential latent viruses. To evaluate the potential contribution of latency found in the Plymouth algal culture collections the percentage of latent viruses in algae and/or the frequency of potential latent viruses was determined. A total of 49 strains of pico and nano algae from the

Plymouth Culture Collection of Marine Algae (Table 2.4) were screened for latent viruses using PCR, AFC, TEM, thin sectioning, gel electrophoresis, PFGE and genomic sequencing.

5.2 Results

5.2.1 Amplification of algal culture with virus specific primers

DNA extracts prepared from the 49 strains from the PCC algal culture collection (Table 2.4) were tested for the presence of a latent virus using primers designed to amplify an algal virus-specific DNA polymerase gene (AVS1 and POL primers) (Section 2.9.1). PCR conditions were optimised to minimise non-specific amplification. Figure 5.1 shows a representative gel with PCR products produced from several of the algal strains with an annealing temperature of 50°C. Amplification of DNA extracted from the algal cultures showed much non-specific amplification. As a reduction of the non-specific amplification was not achieved with variations in PCR conditions alternative methods to screen the algal cultures for potential latent viruses were explored.

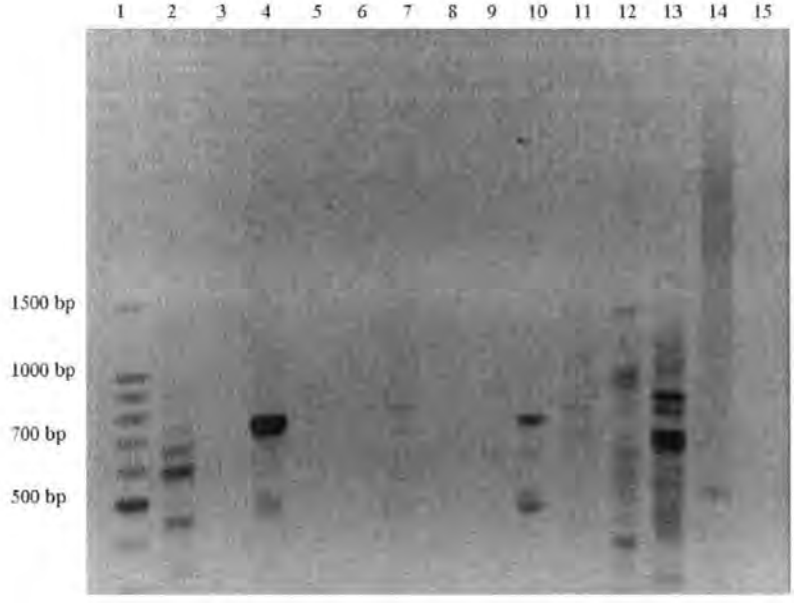

Figure 5.1. Gel image showing PCR products produced using the primer set AVS1 and POL. Lane 2, 3, 4, 5, 6, 9, 10, 12 as follows: phytoplankton strains 272, 570, 305, 512, 511A, 513, 443 and 491 respectively (Table 2.4). Lane 7, 8, 11, 13 are zooxanthellae strains 2455, 2465, 2466, 2459, respectively (Table 2.1). Lane 14 is the positive control (EhV V2), lane 15 is the negative control and lane 1 is the 100 bp marker.

5.2.2 Inducible VLPs

AFC dot plots (using parameters to detect viruses) from lysates of 30 algal strains comparing the control and UV-treated cultures at 96 h after UV induction are shown in Figure 5.2. Dot plots of strains 85, 430, 491, 315, 570, 93, 156, 240, 351, 536 and 564 showed a group of VLPs in the UV-treated cultures that were not seen in the controls. Dot plots of strains 83, 430, 491, 315, 377, 378(1), 506(A), 564 and 565 showed increases in potential VLP groups that had a higher GFL signal, between 50-300 AU (arbitrary units). In the dot plots of strains 85, 272, 299, 663, 8, 133, 240, 508 and 515, a decrease in the group of particles with a high GFL signal relative to the control was observed. Table 5.2 summarises the differences observed in the control and the UV-treated lysates for each culture.

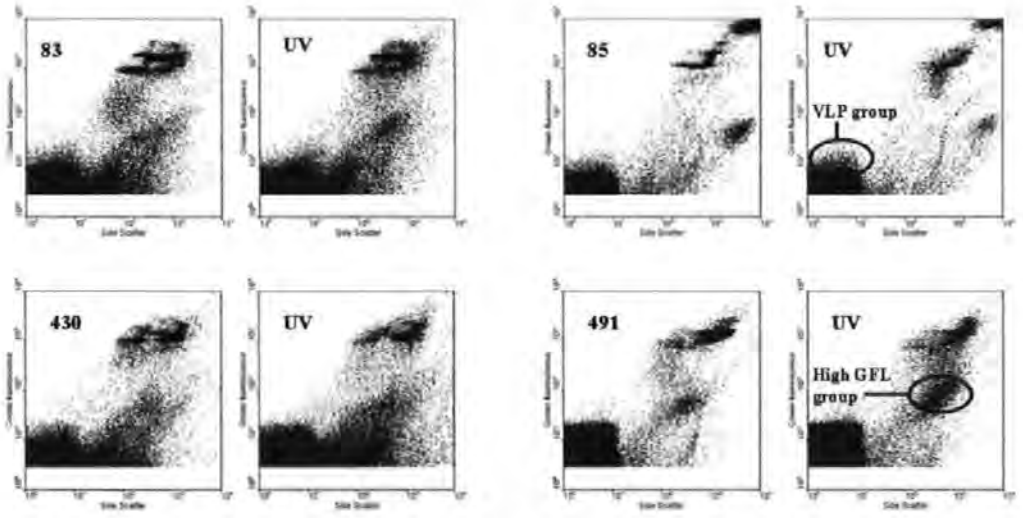

Figure 5.2a. AFC showing SYBRgreen I stained particles of UV-induced cultures (96 h-post induction) (using settings to detect viruses (Section 2.3)) in strains 83, 85, 430, 491 division Chlorophyta, class Chlorophyceae. The control is shown on the left and the UV-induced lysate is shown on the right. Areas representative of VLP groups and high GFL groups are circled.

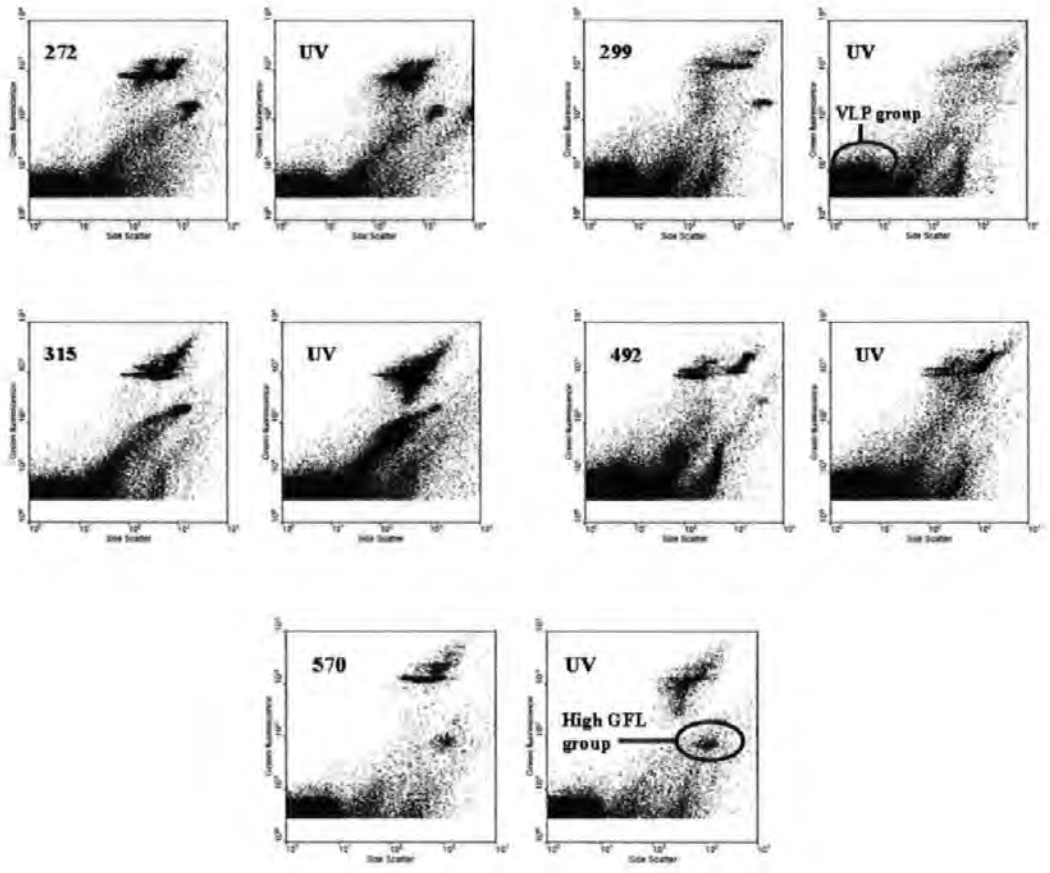

Figure 5.2b. AFC showing SYBRgreen I stained particles of UV-induced cultures (96 h-post induction) (using settings to detect viruses (Section 2.3)) in strains 272, 299, 315, 492, 570 division Chlorophyta, class Prasinophyceae. The control is shown on the left and the UV-induced lysate is shown on the right. Areas representative of VLP groups and high GFL groups are circled.

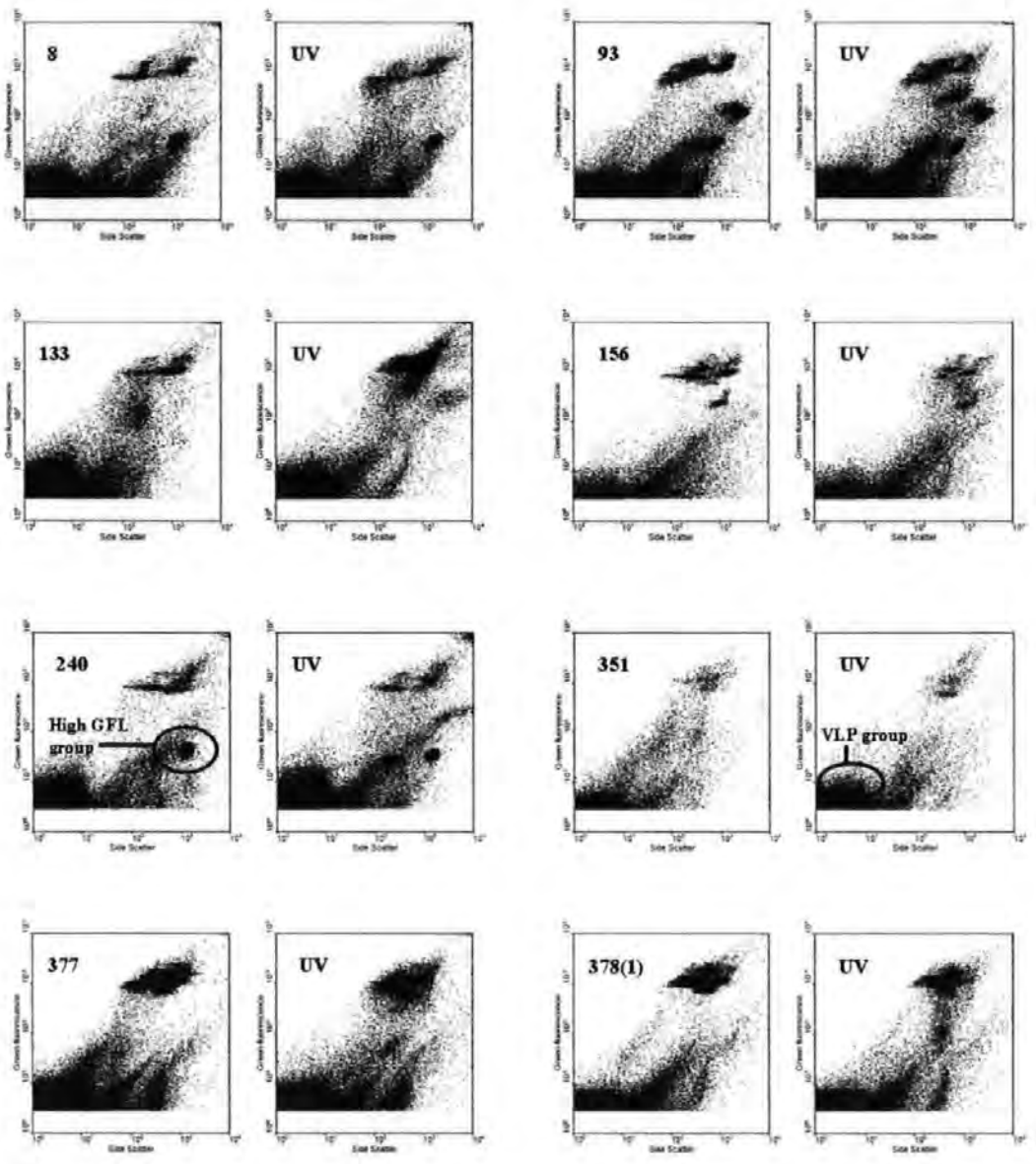

Figure 5.2c. AFC showing SYBRgreen I stained particles of UV-induced cultures (96 h-post induction) (using settings to detect viruses (Section 2.3)) in strains 8, 93, 133, 156, 240, 351, 377 and 378(1) (division Haptophyta). The control is shown on the left and the UV-induced lysate is shown on the right. Areas representative of VLP groups and high GFL groups are circled.

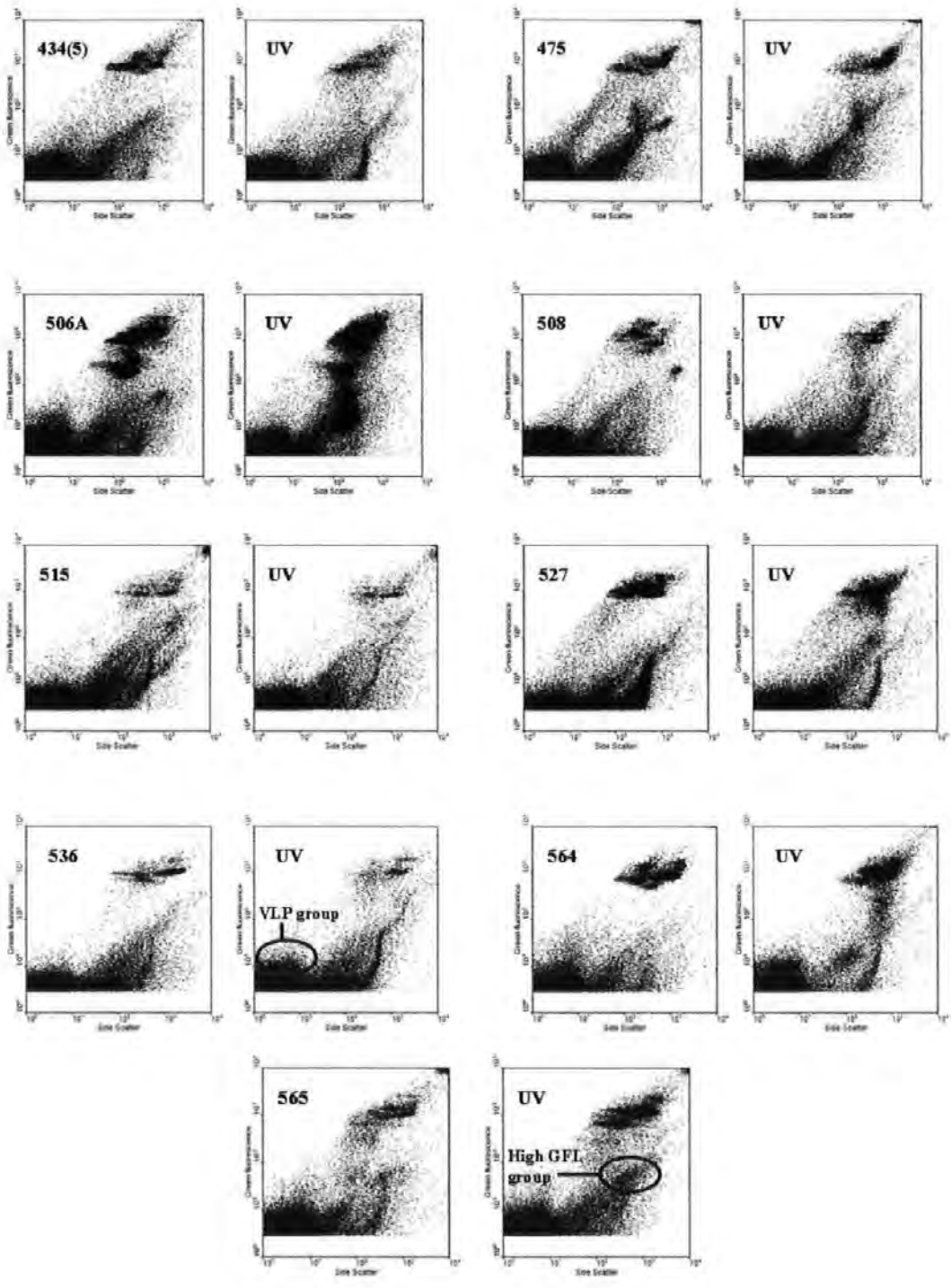

Figure 5.2d. AFC showing SYBRgreen I stained particles of UV-induced cultures (96 h-post induction) (using settings to detect viruses (Section 2.3)) in strains 434(5), 475, 506A, 508, 515, 527, 536, 564 and 565 (division Haptophyta). The control is shown on the left and the UV-induced lysate is shown on the right. Areas representative of VLP groups and high GFL groups are circled.

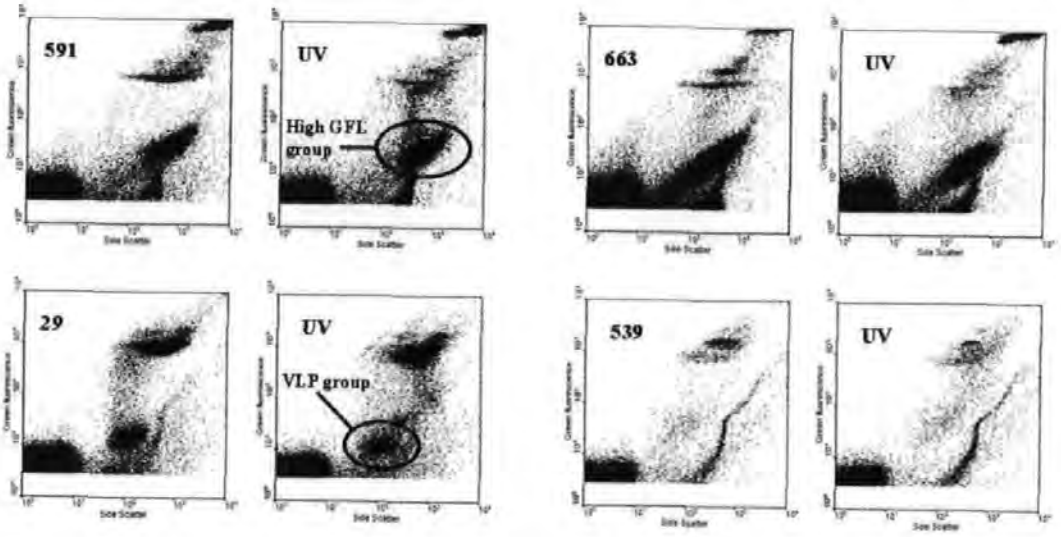

Figure 5.2e. AFC showing SYBRgreen I stained particles of UV-induced cultures (96 h-post induction) (using settings to detect viruses (Section 2.3)) in the division Heterkontophyta,; strains 591 and 663, strain 29 (division Cryptophyta) and strain 539 (division Rhodophyta). The control is shown on the left and the UV-induced lysate is shown on the right. Areas representative of VLP groups and high GFL groups are circled.

Table 5.2. Summary table of changes in UV-induced algal cultures. No change (0), absent (-), present (+) and increase (++). GFL – Green fluorescence.

Division (Class)	PCC Designation	Species	VLPs	High GFL Group Control	High GFL Group UV
Chlorophyta (Chlorophyceae)	83	*Dunaliella tertiolecta*	0	+	++
	85	*Chlorella stigmatophora*	+	++	+
	430	*Dunaliella minuta*	+	+	++
	491	*Chlamydomona concordia*	+	+	++
Chlorophyta (Prasinophyceae)	272	*Tetraselmis tetrathele*	0	++	+
	299	*Pyraminonas urceolata*	0	+	-
	315	*Tetraselmis* spp.	+	+	++
	492	*Pyraminonas panceae*	0	-	-
	570	*Tetraselmis marina ?*	+	+	+
Heterokontophyta (Eustigmatophyceae)	591	*Nannochloropsis salina*	0	+	+
	663	*Nannochloropsis oculata*	0	++	+
Cryptophyta (Cryptophyceae)	29	*Cryptomonas maculata*	0	-	-
Rhodophyta (Rhodophyceae)	539	*Porphridium purpureum*	0	-	-

Table 5.2 (cont.). Summary table of changes in UV-induced algal cultures. No change (0), absent (-), present (+) and increase (++).

GFL – Green fluorescence.

Division (Class)	PCC Designation	Species	VLPs	High GFL Group Control	High GFL Group UV
Haptophyta (Prymnesiophyceae)	8	*Isochrysis aff. galbana*	0	++	+
	93	*Pavlova gyrans*	+	+	+
	133	*Imantonia rotunda*	-	+	-
	156	*Pleurochrysis carterae*	+	+	+
	240	*Isochrysis* spp.	+	++	+
	351	*Cricosphaera ?*	+	-	-
	377	*Chrysotila stipitata*	-	-	+
	378 (1)	*Pleurochrysis carterae*	0	-	+
	434 (5)	*Ochisphaera ?*	0	-	-
	475	*Chrysotila lamellosa*	-	+	+
	506A	*Isochrysis* spp.	-	+	++
	508	*Apistonema* spp.	0	+	-
	515	*Pavlova virescens*	0	+	-
	527	*Prymnesium patelliferum*	0	-	+
	536	*Hymenosa globosa*	+	-	-
	564	*Dicrateria inornata*	+	-	+
	565	*Isochrysis galbana*	0	+	++

5.2.3 Effect of UV treatment on induction of VLPs over time

From the thirty strains examined (Section 5.2.2), 15 strains were further characterised by AFC. AFC dot plot analyses of algal cells compared to potential VLPs are shown in Figure 5.3. Triplicate cultures of each strain were exposed to UV irradiation. Algal cells in the control and the UV-treated cultures were enumerated by AFC and the lysates of each strain were analysed using AFC to detect potential VLPs. The images in the upper left hand corner of each figure shows the control and UV-induced cultures 96 h after UV treatment and the dot plots in the lower left hand corner show the potential VLPs in the control and UV-treated lysates 96 h after UV treatment. Events occurring in the region between 0.5 to 5 AU (GFL) and 0 to 1 AU (SSC) were analysed for potential VLPs. The potential VLPs (VLPs/ml x 10^6) were plotted against the number of algal cells (cells/ml x 10^5) over the time course of the induction experiments.

Seven of the strains (430, 491, 156, 240, 475, 508 and 536) showed a static or reduced growth after UV treatment and had an increase in the VLP groups (Figure 5.2 a and c). Five of the strains (85, 29, 133, 564 and 565) showed a decline in growth 24-48 h after UV treatment and had increases in the VLP groups (Figure 5.2 a, c and d). Three strains (515, 663 and 83) had unclear interactions occurring (Figure 5.2 a, c and d). From the six strains (430, 85, 491, 29, 156, 240 and 491) that had VLPs that were easy to distinguish, four strains were selected for further characterisation (strains 29, 85, 156 and 430) (Figure 5.2 a, c and d).

AFC dot plots of the bacteria, noise and the high GFL groups were analysed; no striking differences were noted between the controls and UV-treated cultures. The bacterial groups in most cases had a slight decrease in numbers following UV treatment and then resumed a similar growth rate to that of the controls. The high GFL group noted in Table 5.2 did not appear consistently in the triplicates of the cultures; despite this the group was analysed for each culture. While most strains did not have this group

appearing, the ones that did, showed no significant variation between controls and UV-treated cultures. Strains 515 and 240 were an exception and showed slight decreases in this group in the UV-treated cultures (Figure 5.2 c).

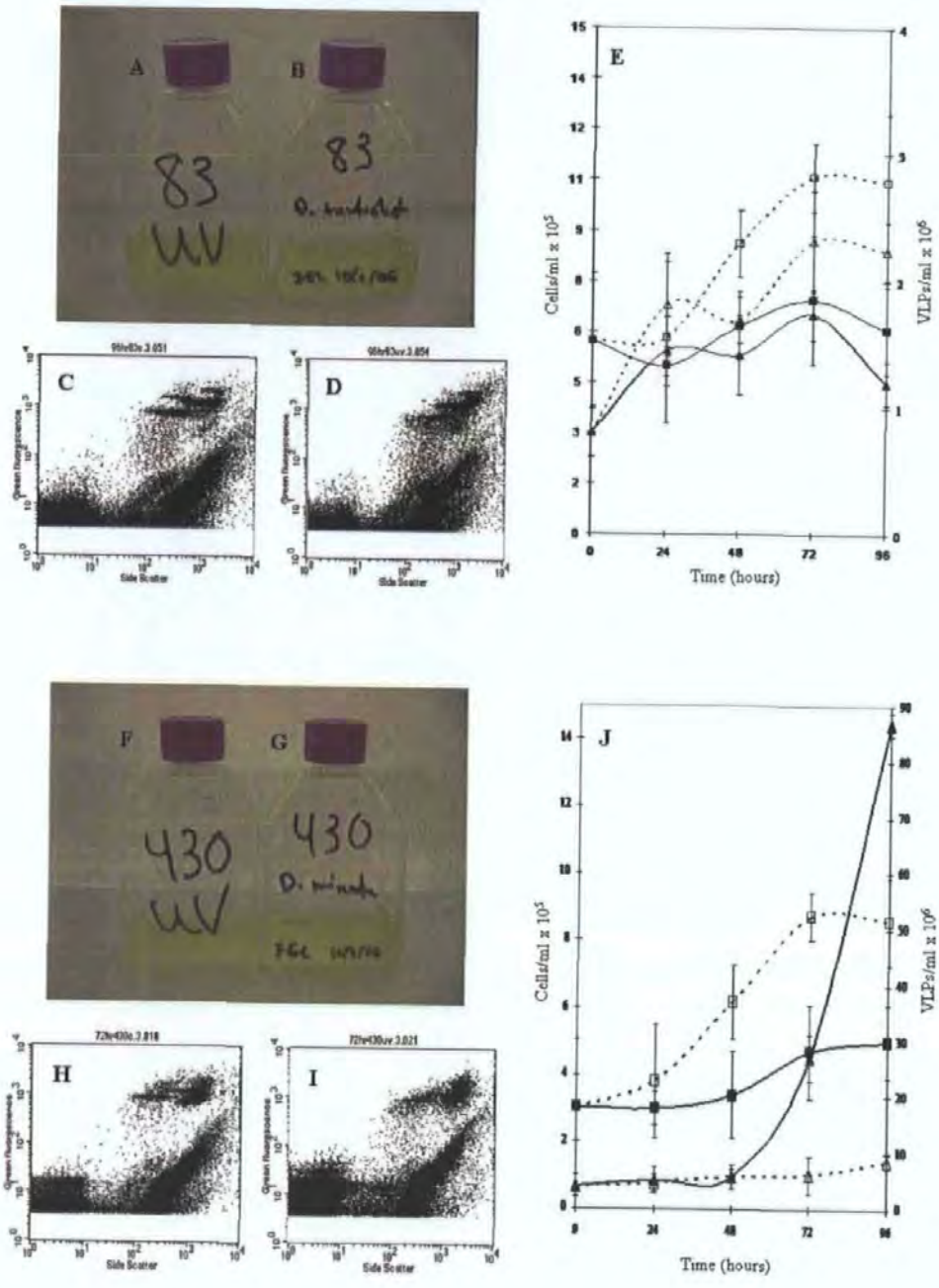

Figure 5.3a. Induction data for phytoplankton culture strains 83 (A-E) and 430 (F-J) at 96 h. Culture images of controls (A, F) and UV-induced (B, G); virus dot plots of controls (C, H) and UV-induced (D, I); graphs of algal cell numbers (cells/ml x 10^5), control (□) and UV-induced (■), plotted against the VLP numbers (VLPs/ml x 10^6), control (△) and UV-induced (▲), over the time course of the experiment (E, J). Error bars represent standard error (SE) of measurements from triplicate cultures, n=3.

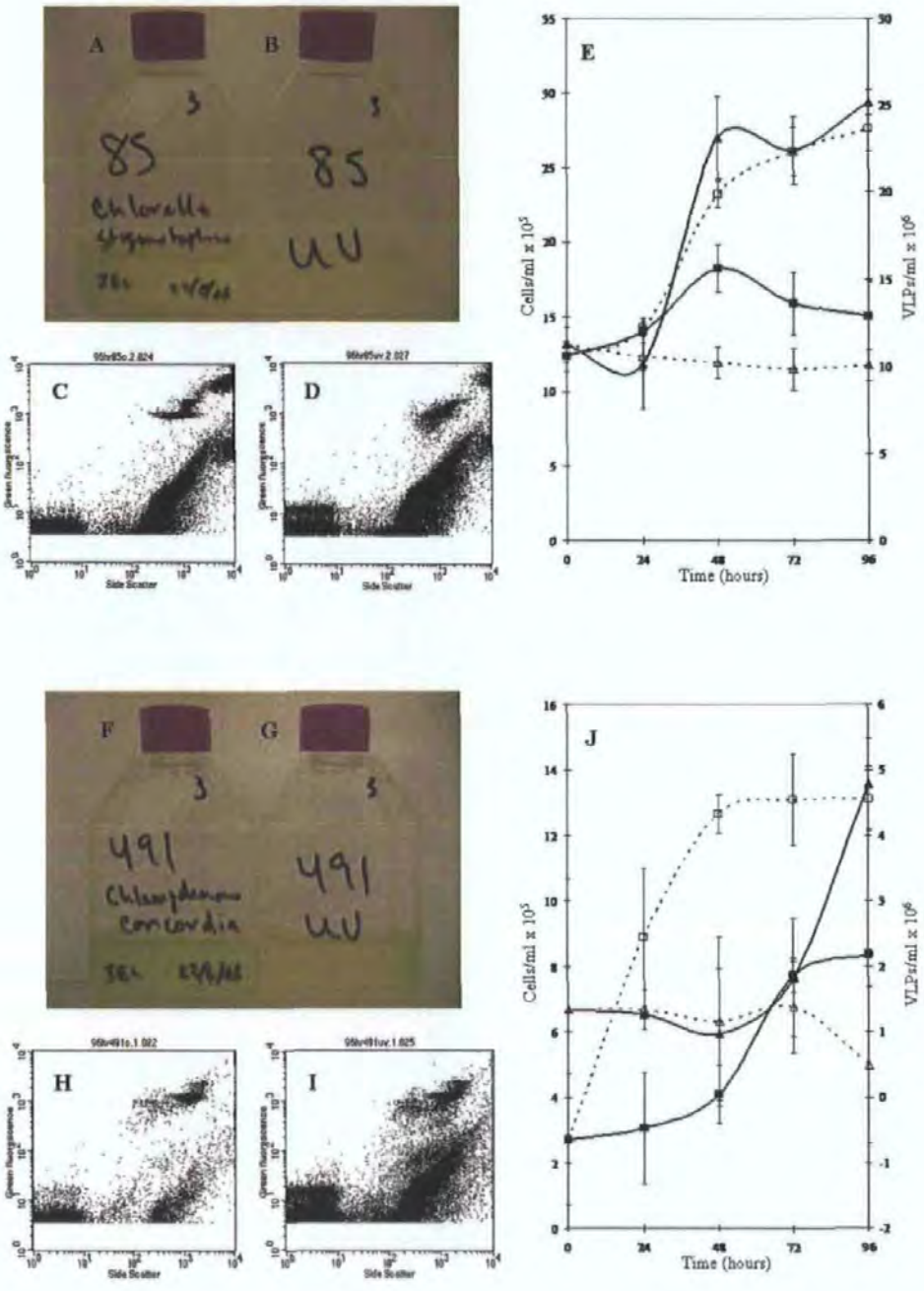

Figure 5.3b. Induction data for phytoplankton culture strains 85 (A-E) and 491 (F-J) at 96 h. Culture images of controls (A, F) and UV-induced (B, G); virus dot plots of controls (C, H) and UV-induced (D, I); graphs of algal cell numbers (cells/ml x 10^5), control (□) and UV-induced (■), plotted against the VLP numbers (VLPs/ml x 10^6), control (△) and UV-induced (▲), over the time course of the experiment (E, J). Error bars represent standard error (SE) of measurements from triplicate cultures, n=3.

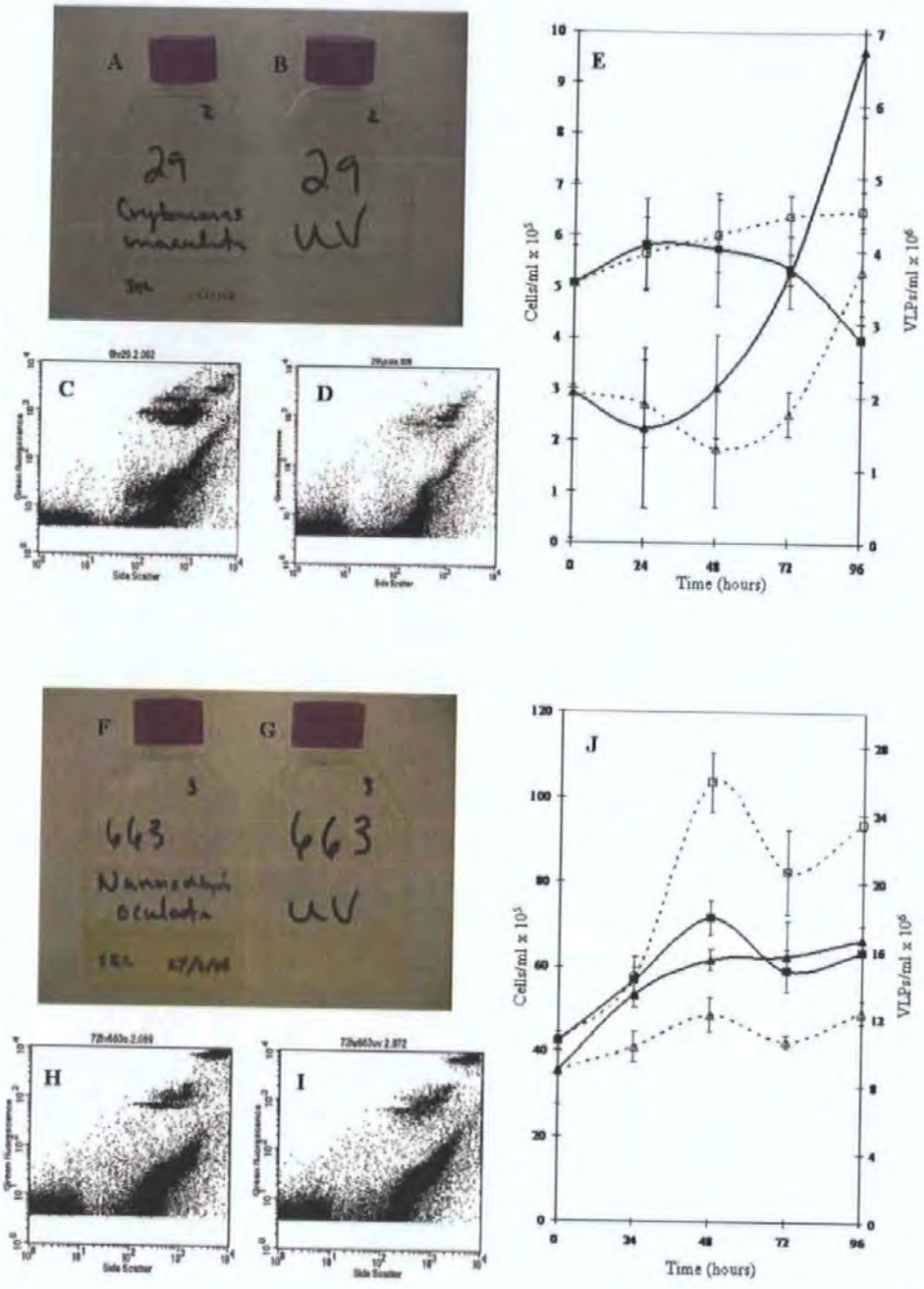

Figure 5.3c. Induction data for phytoplankton culture strains 29 (A-E) and 663 (F-J) at 96 h. Culture images of controls (A, F) and UV-induced (B, G); virus dot plots of controls (C, H) and UV-induced (D, I); graphs of algal cell numbers (cells/ml x 10^5), control (□) and UV-induced (■), plotted against the VLP numbers (VLPs/ml x 10^6), control (△) and UV-induced (▲), over the time course of the experiment (E, J). Error bars represent standard error (SE) of measurements from triplicate cultures, n=3.

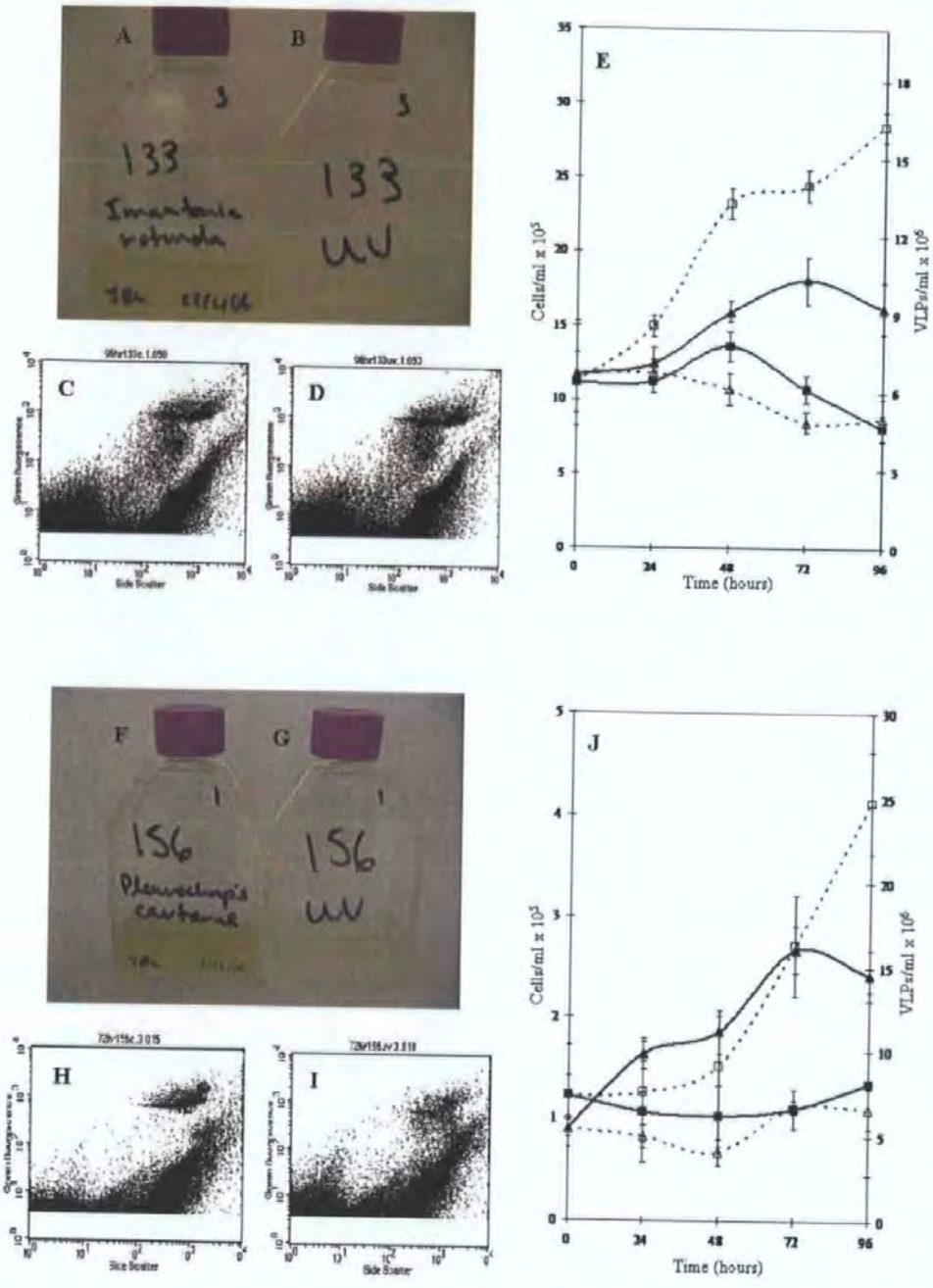

Figure 5.3d. Induction data for phytoplankton culture strains 133 (A-E) and 156 (F-J) at 96 h. Culture images of controls (A, F) and UV-induced (B, G); virus dot plots of controls (C, H) and UV-induced (D, I); graphs of algal cell numbers (cells/ml x 10^5), control (□) and UV-induced (■), plotted against the VLP numbers (VLPs/ml x 10^6), control (△) and UV-induced (▲), over the time course of the experiment (E, J). Error bars represent standard error (SE) of measurements from triplicate cultures, n=3.

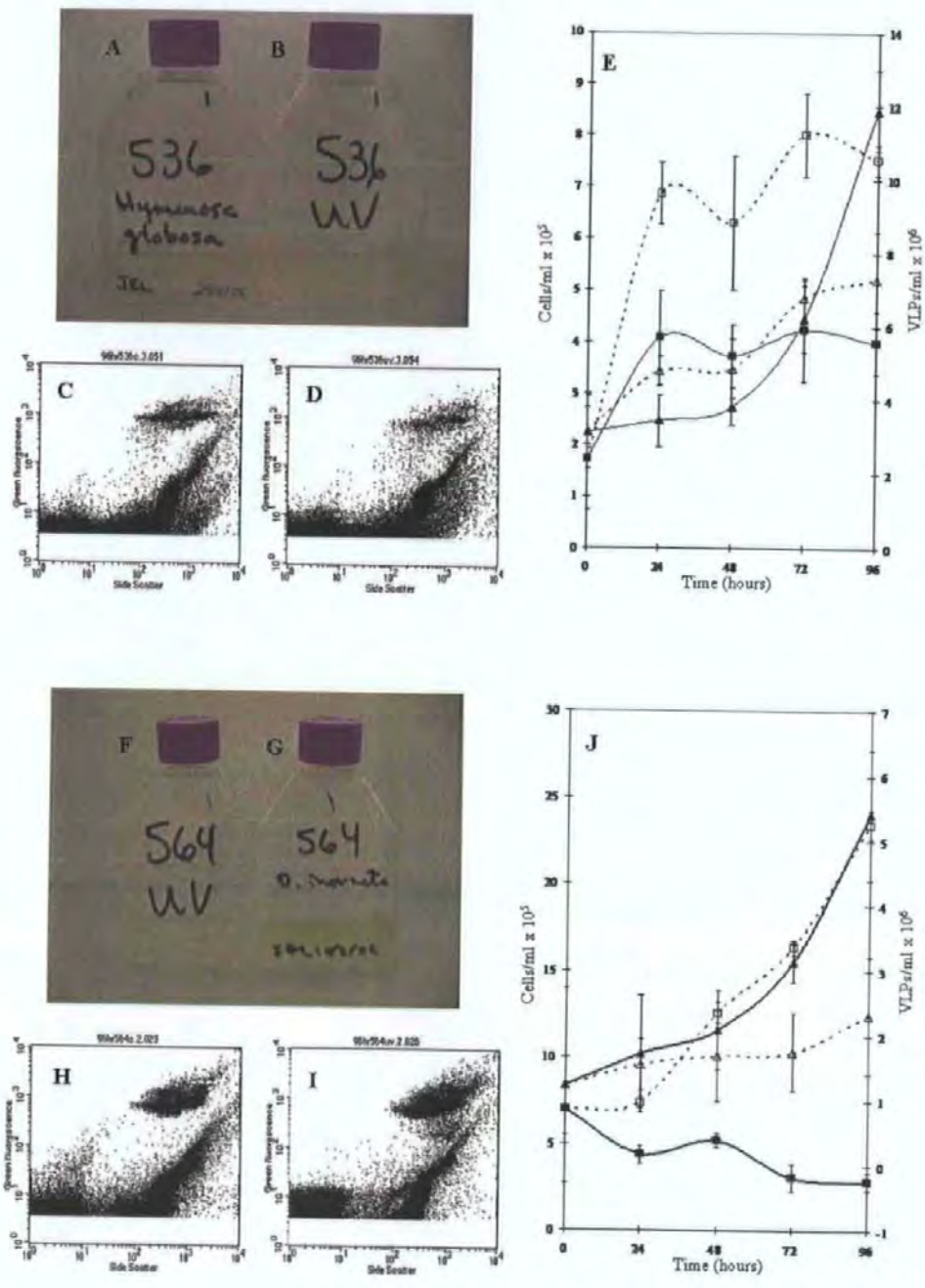

Figure 5.3e. Induction data for phytoplankton culture strains 536 (A-E) and 564 (F-J) at 96 h. Culture images of controls (A, F) and UV-induced (B, G); virus dot plots of controls (C, H) and UV-induced (D, I); graphs of algal cell numbers (cells/ml x 10^5), control (□) and UV-induced (■), plotted against the VLP numbers (VLPs/ml x 10^6), control (△) and UV-induced (▲), over the time course of the experiment (E, J). Error bars represent standard error (SE) of measurements from triplicate cultures, n=3.

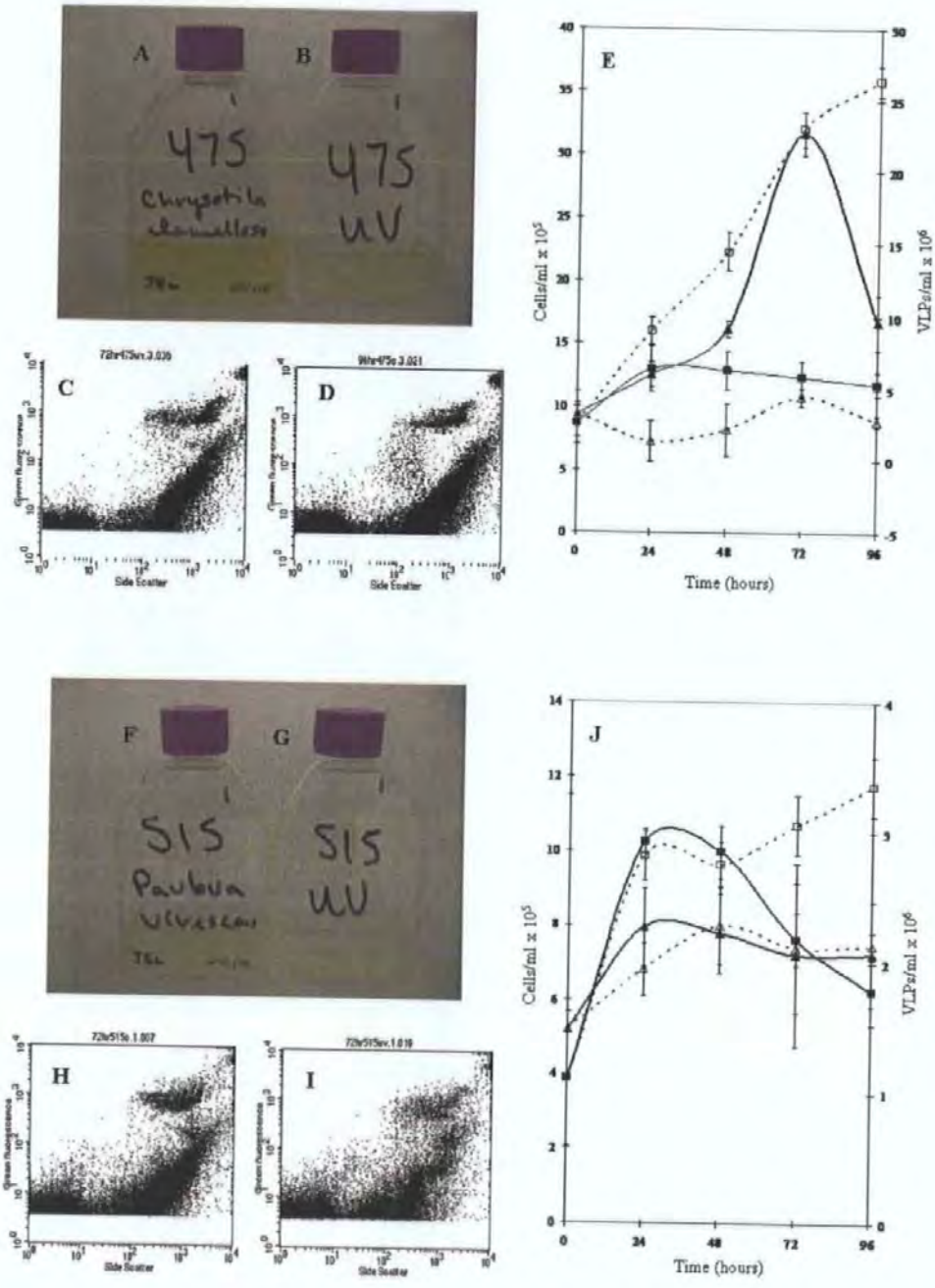

Figure 5.3f. Induction data for phytoplankton culture strains 475 (A-E) and 515 (F-J) at 96 h. Culture images of controls (A, F) and UV-induced (B, G); virus dot plots of controls (C, H) and UV-induced (D, I); graphs of algal cell numbers (cells/ml x 10^5), control (□) and UV-induced (■), plotted against the VLP numbers (VLPs/ml x 10^6), control (△) and UV-induced (▲), over the time course of the experiment (E, J). Error bars represent standard error (SE) of measurements from triplicate cultures, n=3.

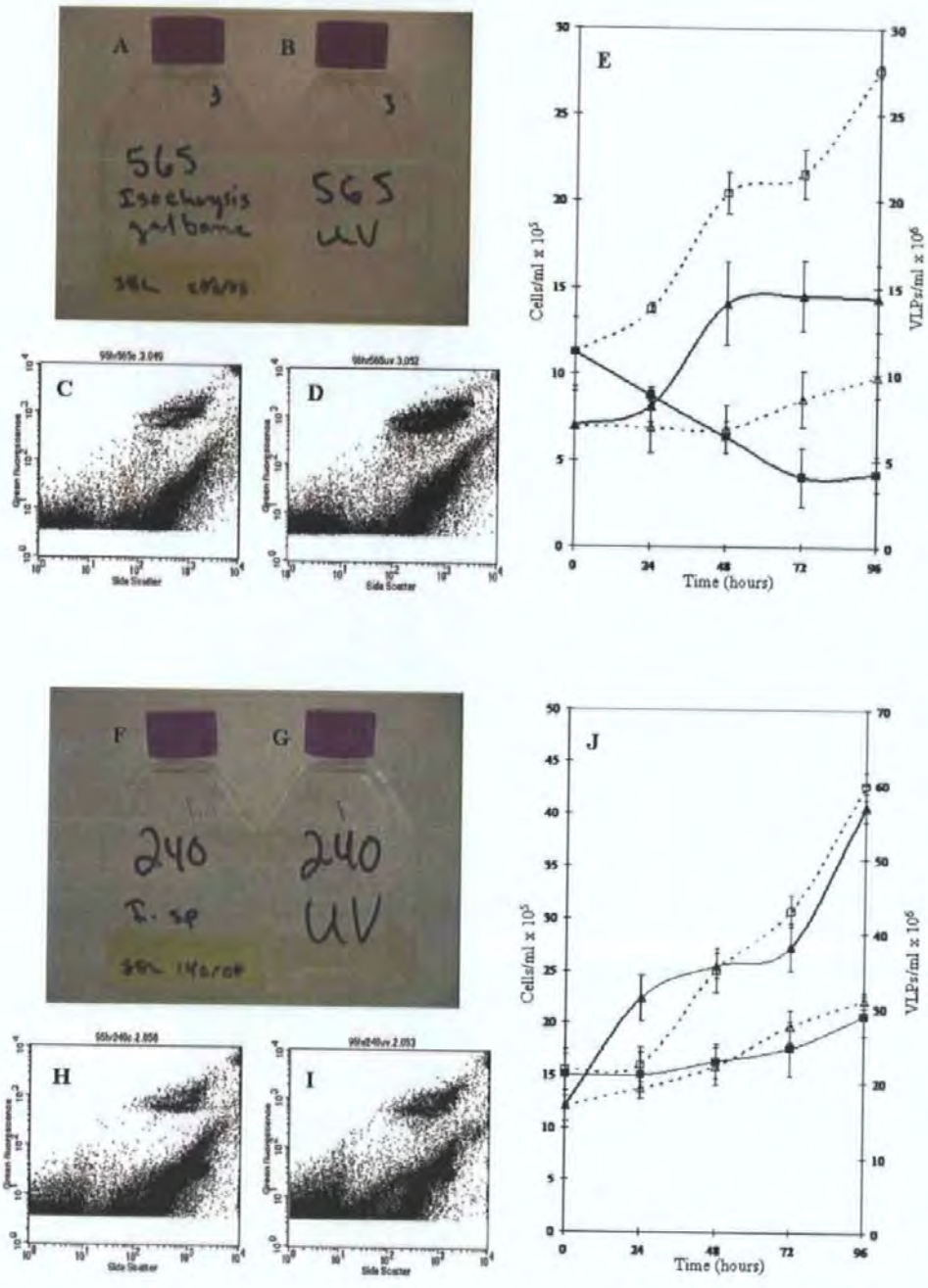

Figure 5.3g. Induction data for phytoplankton culture strains 565 (A-E) and 240 (F-J) at 96 h. Culture images of controls (A, F) and UV-induced (B, G); virus dot plots of controls (C, H) and UV-induced (D, I); graphs of algal cell numbers (cells/ml x 10^5), control (□) and UV-induced (■), plotted against the VLP numbers (VLPs/ml x 10^6), control (△) and UV-induced (▲), over the time course of the experiment (E, J). Error bars represent standard error (SE) of measurements from triplicate cultures, n=3.

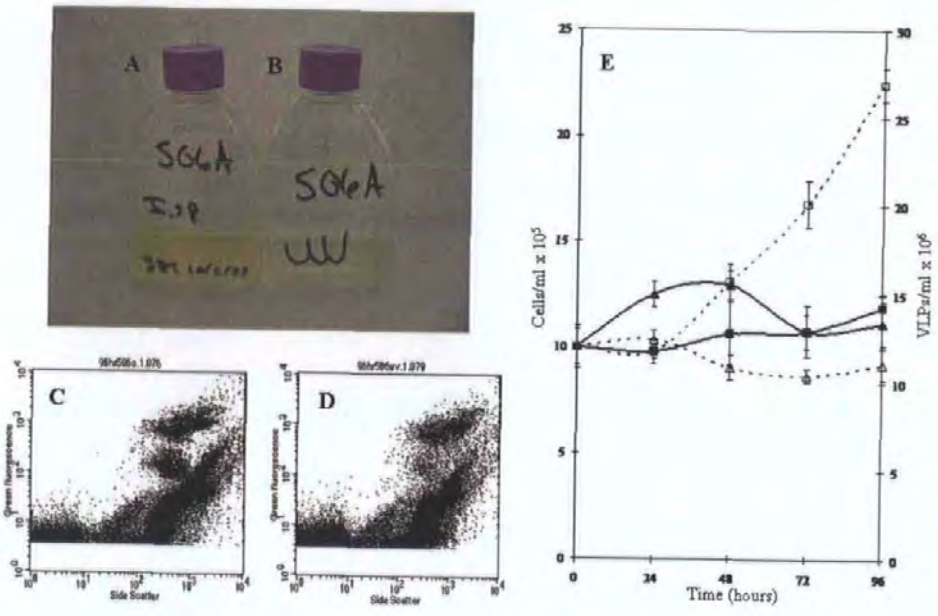

Figure 5.3h. Induction data for phytoplankton culture strain 506A (A-E) at 96 h. Culture images of controls (A) and UV-induced (B); virus dot plots of controls (C) and UV-induced (D); graphs of algal cell numbers (cells/ml x 10^5), control (□) and UV-induced (■), plotted against the VLP numbers (VLPs/ml x 10^6), control (△) and UV-induced (▲), over the time course of the experiment (E). Error bars represent standard error (SE) of measurements from triplicate cultures, n=3.

5.2.4 Visualisation of VLPs

TEM grids were prepared from fixed lysates of several UV-treated strains. TEM images of lysates from UV-induced strains 83, 430, 85, 491 and 29 are shown in Figures 5.4 and 5.5. Figure 5.4 shows images from the lysates of the induced *Dunaliella* strains, 83 and 430. Round, slightly icosahedral particles ca. 75 nm were observed in both strains. In strain 430, clusters of the VLPs were observed.

TEM images from *Chlorella stigmatophora*, strain 85, are shown in Figure 5.5 (Panels A-D). The diameter of the particles observed are ca. 175 nm in diameter and spikes protruding from the central core of the particles are ca. 300-400 nm in length. Panel E shows the lysate from *Pleurochrysis carterae*, strain 156. The VLP shown in this image has a diameter ca. 175 nm. Panel F shows a particle observed in the lysate of *Cryptomonas maculata*, strain 29, the icosahedral particle is ca. 200 nm in diameter.

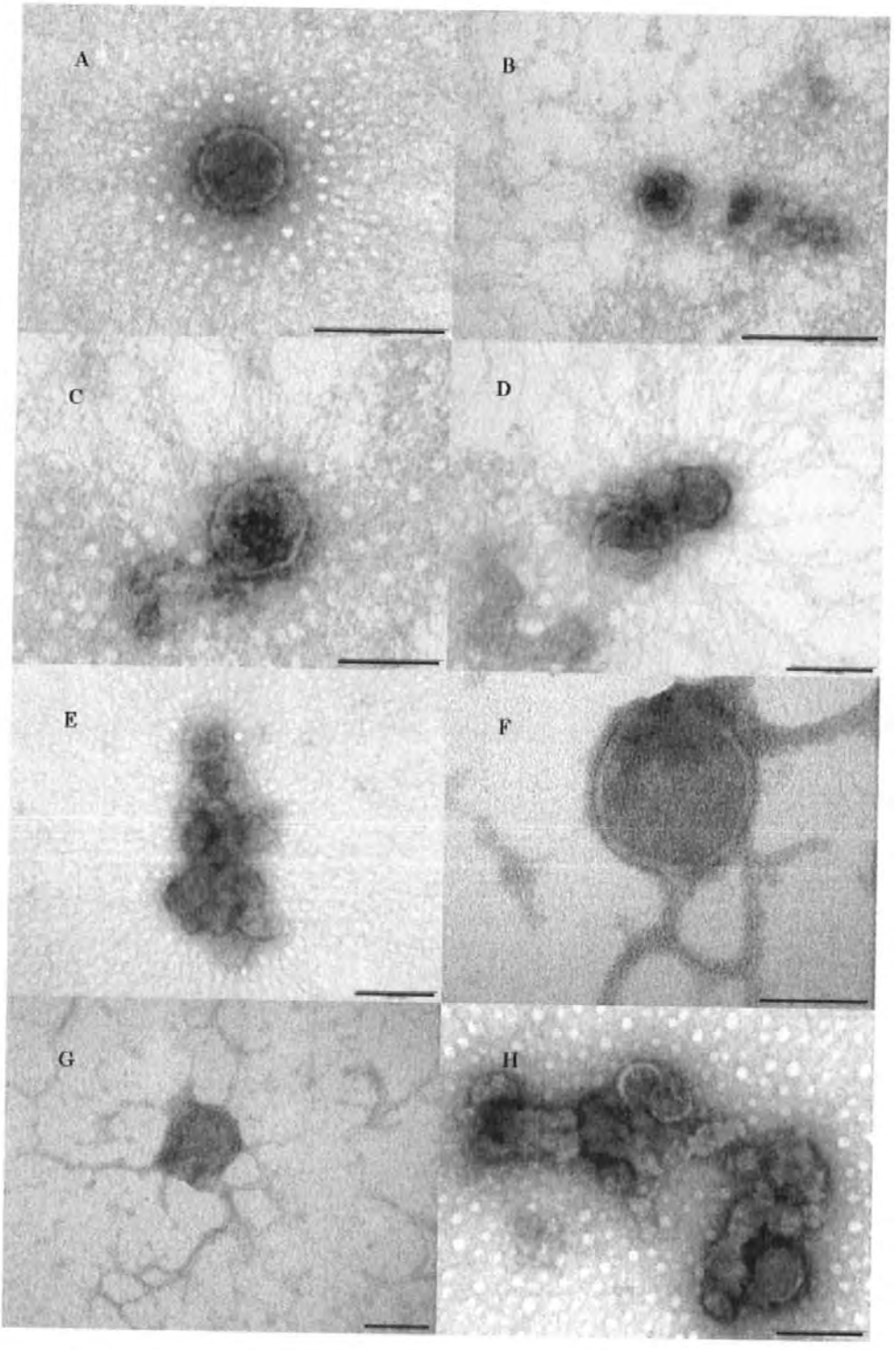

Figure 5.4. TEM images of the UV-induced cultures *Dunaliella tertiolecta*, strain 83 (A-D), and *Dunaliella minuta*, strain 430 (E-H). Scale bars are 200 nm (B, E and H), 100 nm (A, C, D and G) and 50 nm (F).

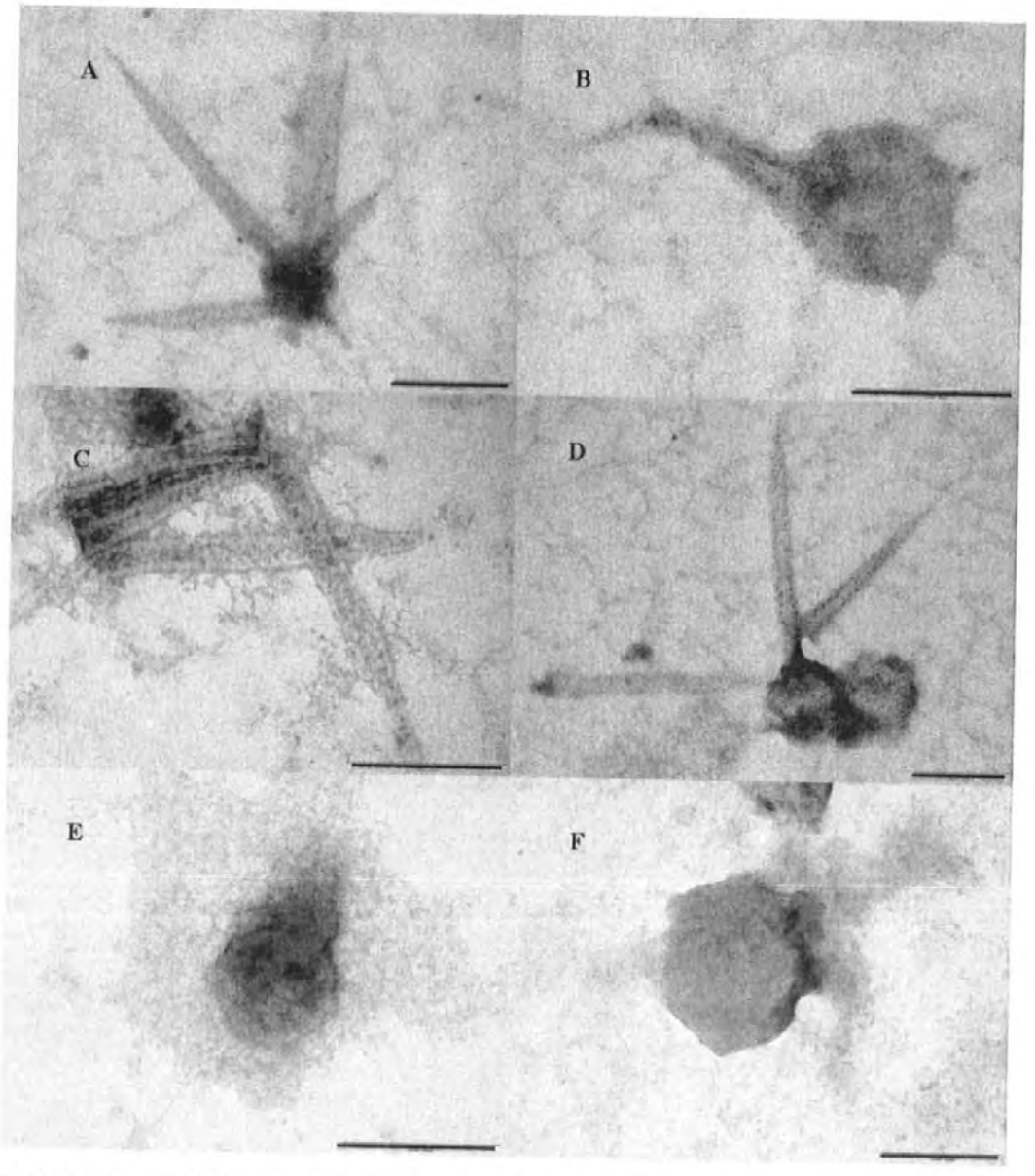

Figure 5.5. TEM images of the UV-induced cultures *Chlorella stigmatophora*, strain 85 (A-D), *Pleurochrysis carterae*, strain 156 (E) and *Cryptomonas maculata*, strain 29 (F). Scale bars are 200 nm (A-F).

5.2.5 Thin sections

Thin sections prepared 43 h after UV induction of strains 85, 156 and 430 are shown in Figures 5.6, 5.7 and 5.8, respectively. In Figure 5.6 (strain 85), VLPs ca. 100 nm in diameter are shown in panels A-H. In Figure 5.6a, panels A and B, VLPs are visible outside of the nuclear envelope. VLPs with an electron dense core and several VLPs which look like empty shells are seen in the chloroplast area. In panels C and D, many VLPs are visible in the pyrenoid. In panels E-H, VLPs ca. 100 nm in diameter are visible in the region between the nuclear envelope and the chloroplasts. In Figure 5.6b, panels A and B show a cell undergoing mitosis, in interphase. VLPs are visible migrating to the periphery of the cells and electron dense particles are visible on the periphery of the cells. Panels C through F show the electron dense particles which appear to be integrated into the outer membrane of the algal cell (Panels C, F, G and H) and the VLPs appear to be migrating toward these particles (Panel A and F).

In Figure 5.7a, strain 156, VLPs ca. 100 nm in diameter are visible around the edges of a vacuole in panels A and B. In panels C and D, a VLP ca. 100 nm in diameter can be observed under the edge of a coccolith. In panels E through H (Figure 5.7a) and panels A-H (Figure 5.7b), several VLPs are seen on the periphery and inside of the cells.

In Figure 5.8a, strain 430, (panels A through H) and 5.8b (A through F), VLPs ca. 150-200 nm are visible within the cells.

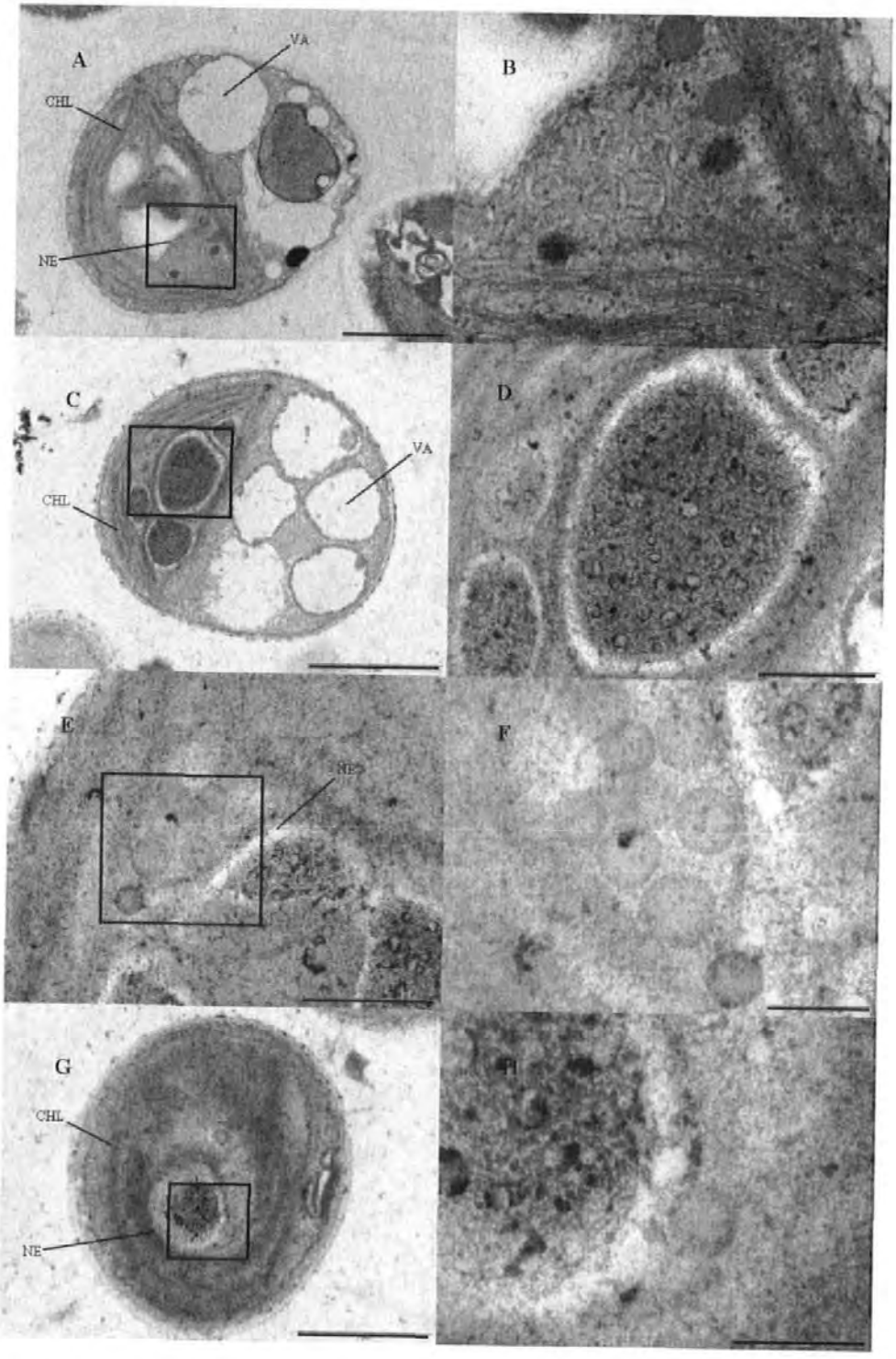

Figure 5.6a. TEM images of *Chlorella stigmatophora* (PCC 85) showing the presence of VLPs within thin sections prepared 43 h after induction with UV light. The scale bars are 2 μm (C), 1 μm (A and G), 500 nm (D and E), 200 nm and (B, F and H). The black box in (A, C, E and G) highlights the area magnified in (B, D, F and H). CHL-Chloroplast, NE-Nuclear envelope and VA-Vacuole.

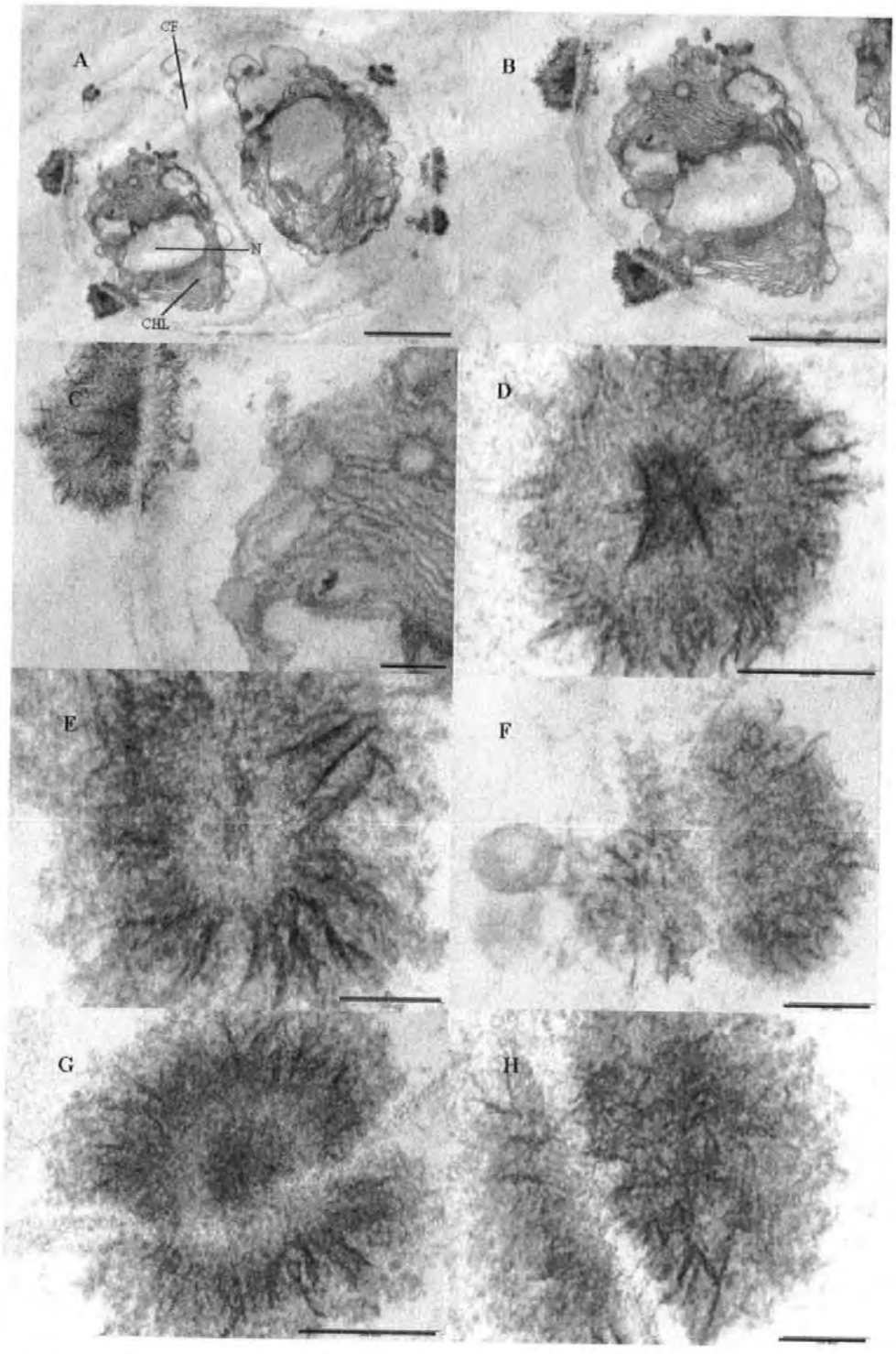

Figure 5.6b. TEM images of *Chlorella stigmatophora* (PCC 85) showing the presence of VLPs within thin sections prepared 43 h after induction with UV light. The scale bars are 1 μm (A and C), 200 nm (B, D and G) and 100 nm (E, F and H). The black box in (A and C) highlights the area magnified in (B and D). CHL-Chloroplast, N-Nucleus and CF-Cleavage furrow.

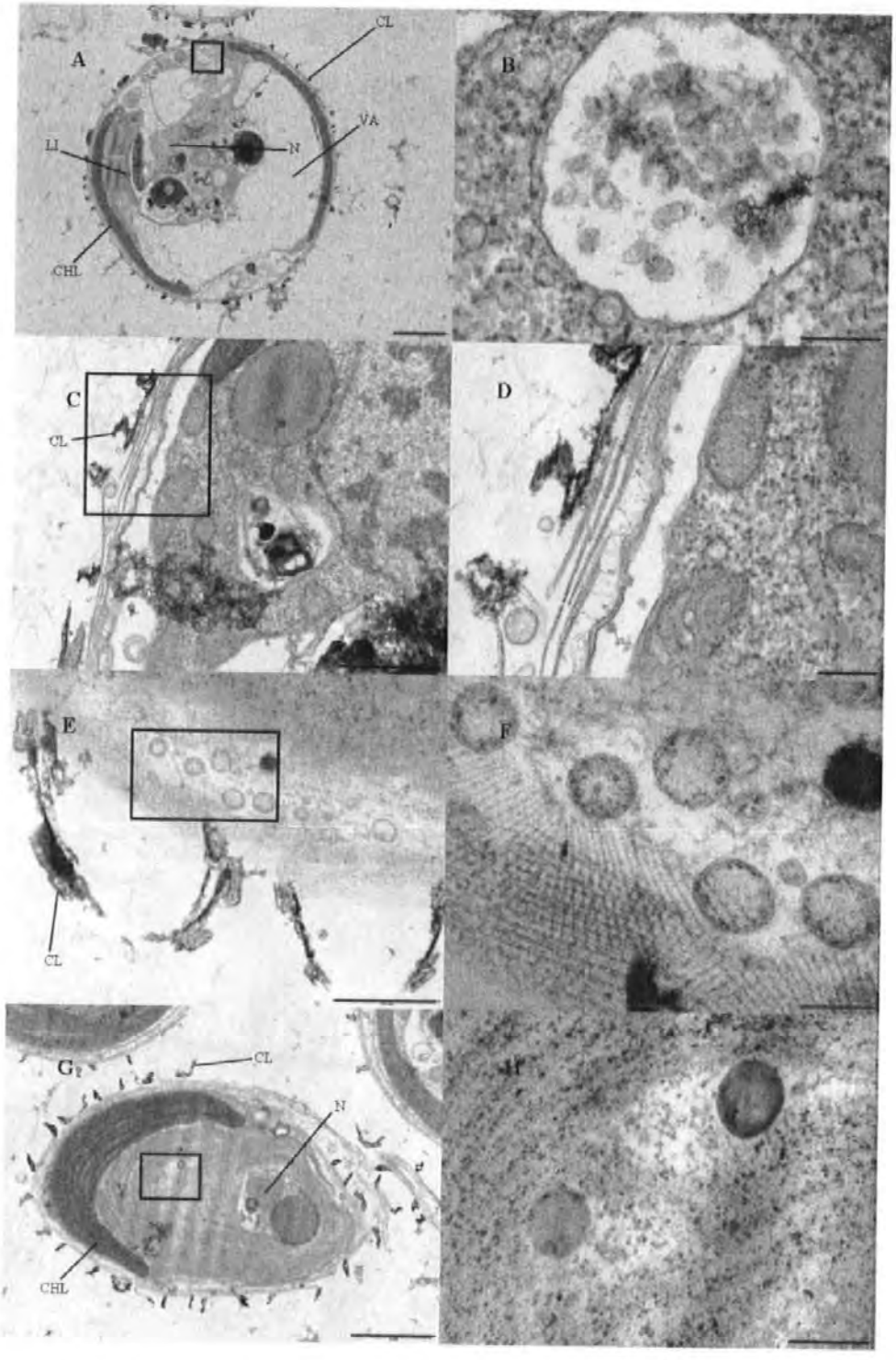

Figure 5.7a. TEM images of *Pleurochrysis carterae* (PCC 156) showing the presence of VLPs within thin sections prepared 43 h after induction with UV light. The scale bars are 2 μm (A and G), 1 μm (C), 500 nm (E), 200 nm (B, D and H) and 100 nm (F). The black box in (A, C, E and G) highlights the area magnified in (B, D, F and H). CHL-Chloroplast, N-Nucleus, VA-Vacuole, LI-Lipid and CL-Coccolith.

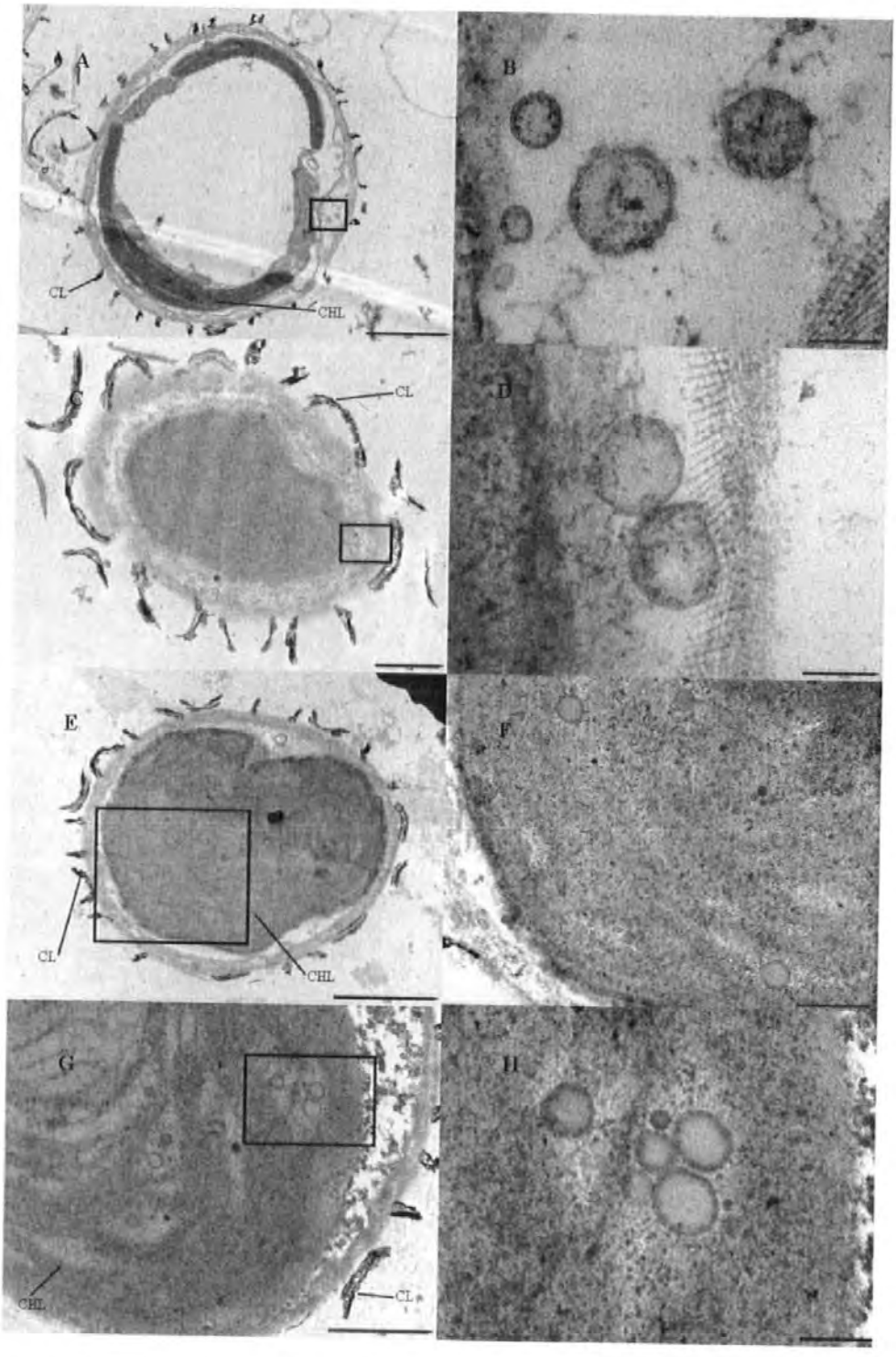

Figure 5.7b. TEM images of *Pleurochrysis carterae* (PCC 156) showing the presence of VLPs within thin sections prepared 43 h after induction with UV light. The scale bars are 2 μm (A and E), 1 μm (B), 500 nm (F), 200 nm (H) and 100 nm (B and D). The black box in (A, C, E and G) highlights the area magnified in (B, D, F and H). CHL-Chloroplast and CL-Coccolith.

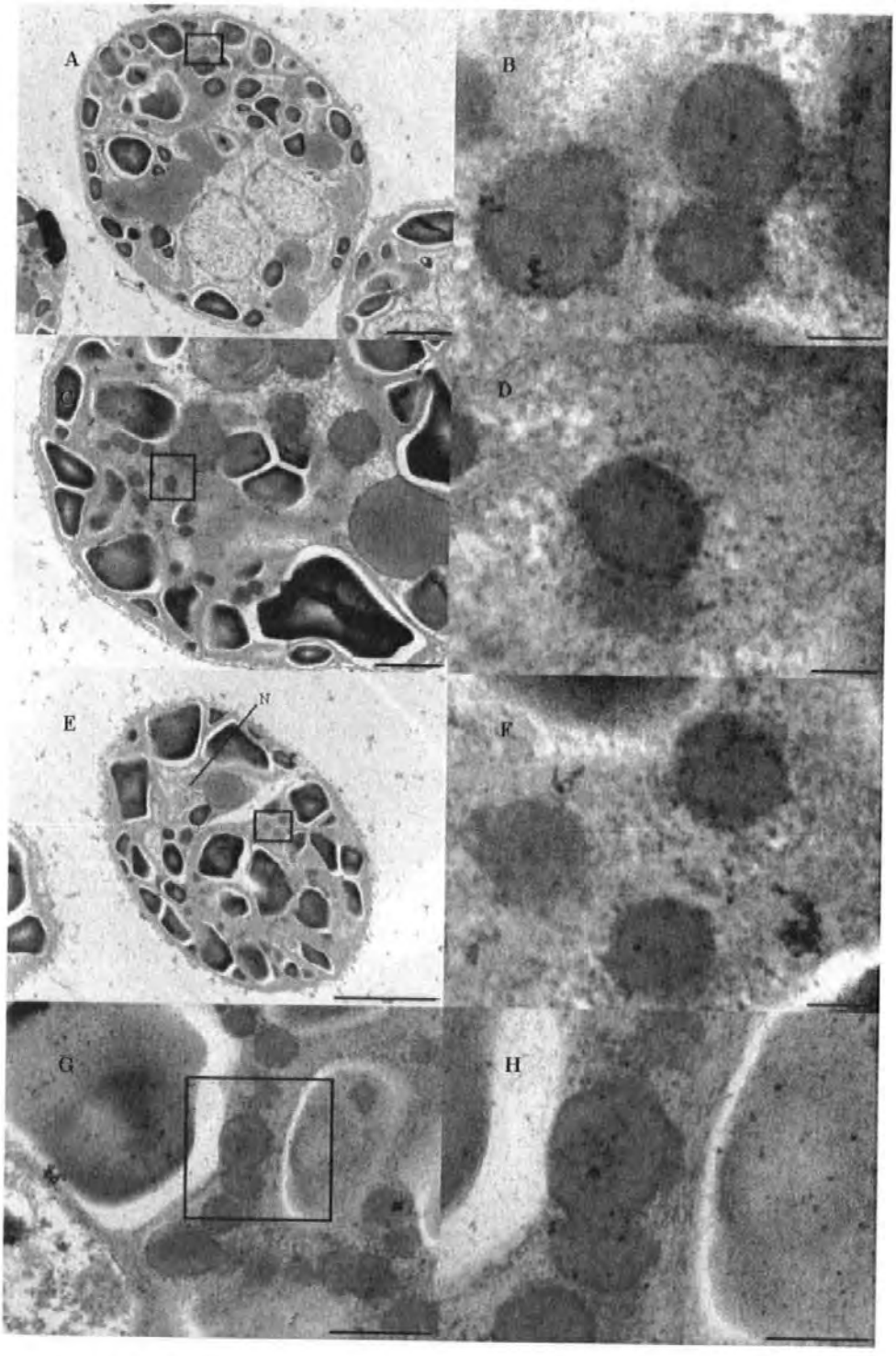

Figure 5.8a. TEM images of *Dunaliella minuta* (PCC 430) showing the presence of VLPs within thin sections prepared 43 h after induction with UV light. The scale bars are 2 μm (A and E), 1 μm (C), 500 nm (G), 200 nm (H) and 100 nm (B, D and F). The black box in (A, C, E and G) highlights the area magnified in (B, D, F and H). N-Nucleus.

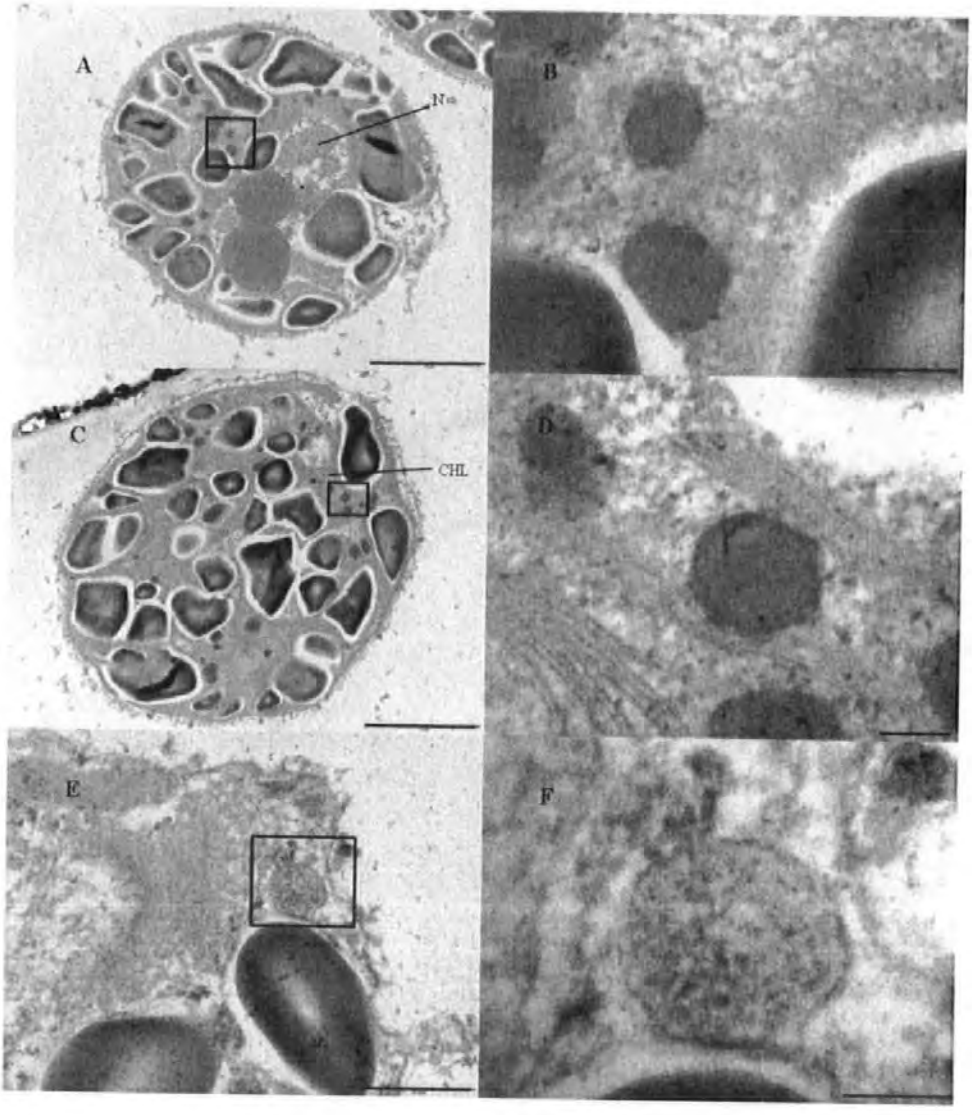

Figure 5.8b. TEM images of *Dunaliella minuta* (PCC 430) showing the presence of VLPs within thin sections prepared 43 h after induction with UV light. The scale bars are 2 µm (A and C), 500 nm (E), 200 nm (B) and 100 nm (D and F). The black box in (A, C, E and G) highlights the area magnified in (B, D, F and H). CHL-Chloroplast and N-Nucleus.

5.2.6 Molecular studies

5.2.6.1 Preparation of nucleic acid

To further characterise the VLPs present in the UV-treated cultures, lysates (1-3 l) were 0.2 μm filtered, and concentrated from strains 29, 85, 156 and 430. Nucleic acid extracted from the UV-treated cultures was separated by conventional gel electrophoresis revealing a discrete band in strains 29 and 430; treatment with RNase and DNase showed the nucleic acid to be sensitive to DNase (Data not shown). Figure 5.9 shows the discrete band from PCC 430. Figure 5.10 shows the result of running nucleic acid extract from strain 85; the extract of strain 85 consistently degraded the gel, note degradation of agarose in lane 3.

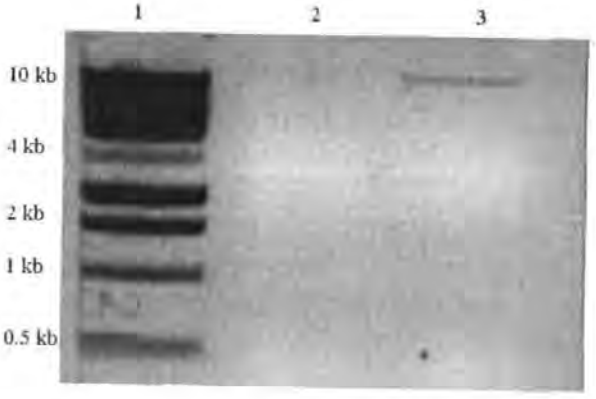

Figure 5.9. Gel image showing nucleic acid extracted from UV-treated strain 430. Lane 3 shows the discrete band of nucleic acid. Lane 1 shows the 1 kb molecular weight marker. Lane 2 is empty.

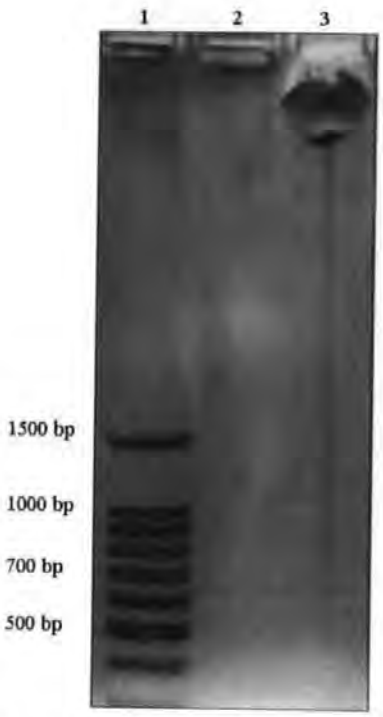

Figure 5.10. Gel image showing nucleic acid extracted from UV-treated strain 85. Lane 3 shows degraded agarose from running the nucleic acid. Lane 1 shows the 100 bp molecular weight marker. Lane 2 is empty.

5.2.6.2 PFGE

Concentrates prepared from lysates were digested in agarose plugs and examined by PFGE. PFGE of strain 430 revealed one discrete band ca. 75 kb (Figure 5.11) and strain 29 revealed two discrete bands of ca. 60 and 70 kb (Figure 5.12). The gel in Figure 5.11 was run with switch times of 1 sec to 15 sec for 22 h and the gel in Figure 5.12 was run with a pulsed time of 5.5 sec to 36.5 sec for 21 h.

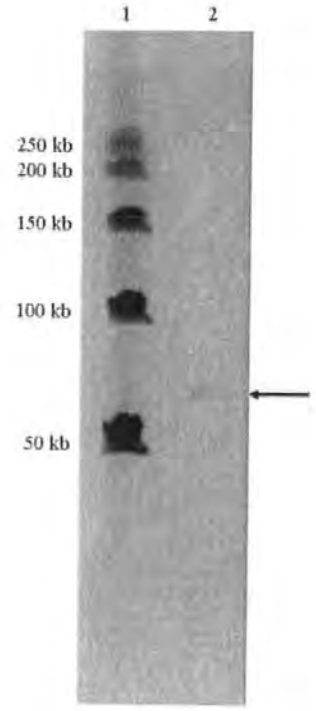

Figure 5.11. PFGE image showing the DNA extracted from strain 430 (lane 2). Lane 1, Lambda ladder.

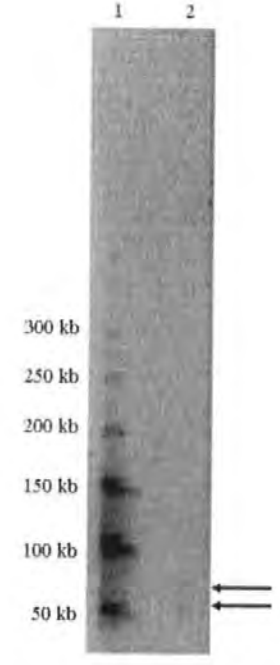

Figure 5.12. PFGE image showing the DNA extracted from strain 29 (lane 2). Lane 1, Lambda ladder.

5.2.6.3 Amplification of DNA polymerase gene

DNA extracted from the lysates of strains 29, 85, 156 and 430 was amplified with the algal virus-specific DNA polymerase primers AVS1 and POL. Figure 5.13 shows the PCR products from dilutions (10^{0} to 10^{-3}) of extracts of strains 29, 85, 156 and 430 (annealing temperature 50°C). Figure 5.14 shows the PCR products produced with optimised concentration of DNA with an annealing temperature of 50°C. Figure 4.16 shows the PCR products produced with an increased annealing temperature of 55°C. Potential latent viruses from strain 430 (Figure 5.15) was directly sequenced from PCR product. PCR products from strains 29, 156 and 430 were all cloned into TopoTA kit. Strains 29 and 156 both produced a PCR product ca. 900 bp and strain 430 produced a PCR product ca. 500 bp; these products were cloned and sequenced. PCR from strain 85 was unsuccessful. The resulting sequences show no significant nucleotide similarities to previously described sequences.

Figure 5.13. DNA polymerase PCR, 50°C annealing. Lanes 6-9, lanes 11-14, lanes 16-19 and lanes 21-25 are as follows: strain 29, 85, 156, 430. Lane 1 and 27, 100 bp marker. Lane 3 is the negative control and lane 4 is the positive control (EhV V2). Lanes 2, 5, 10, 15, 20 and 26 are empty.

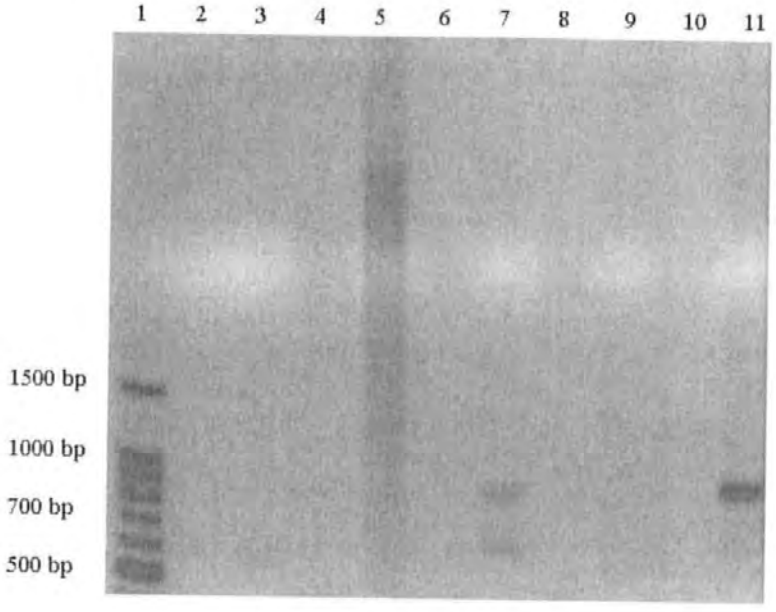

Figure 5.14. DNA polymerase PCR, 50°C annealing. Lane Lane 5, 7, 9, 11 are as follows: strain 29, 85, 156, 430. 1 100 bp marker. Lane 2 negative control, lane 3 positive control. Lanes 4, 6, 8 and 10 are empty.

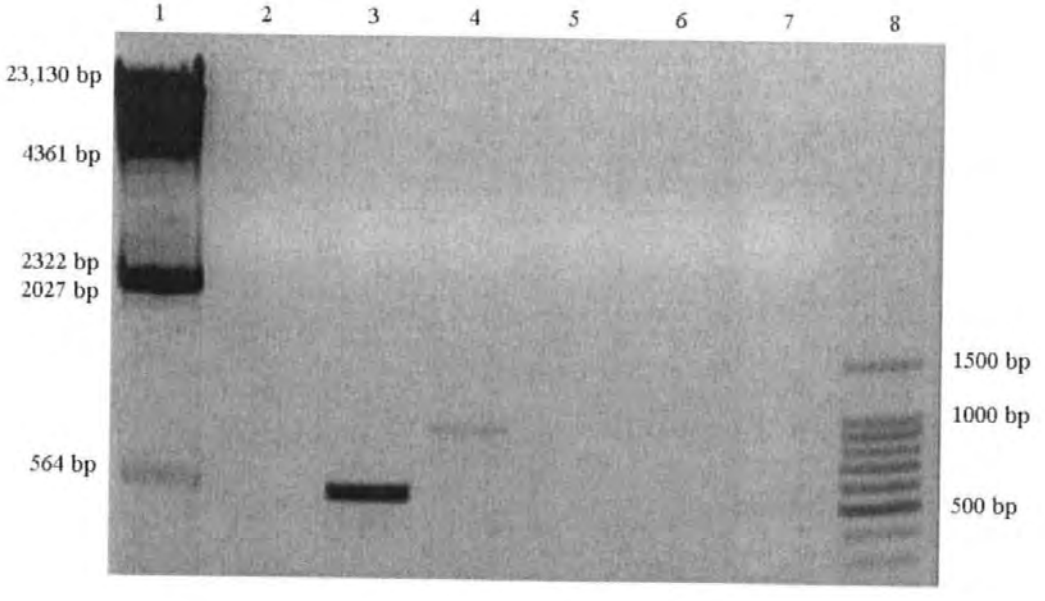

Figure 5.15. DNA polymerase PCR, 55°C annealing. Lane 4, 5, 6 and 7 are as follows: 29, 85, 156 and 430. Lane 1 shows a *Hind*III ladder and lane 8 shows a 100 bp marker. Lane 2 negative control, lane 3 positive control (EhV V2).

5.2.6.4 Clone libraries

Clone libraries were prepared from sonicated genomic DNA and genomic DNA from VLPs digested with restriction enzyme (*Bam*HI, *Hind*III, and *Hha*I) from lysates of UV-treated *Dunaliella minuta*, strain 430. An example of restriction digested fragments of strain 430 is shown in Figure 5.15. Blunt-ended fragments in the size range of 1-5 kb were excised from agarose gels and used for cloning. Several clone libraries were produced from restriction enzyme digested fragments as well as sonicated fragments.

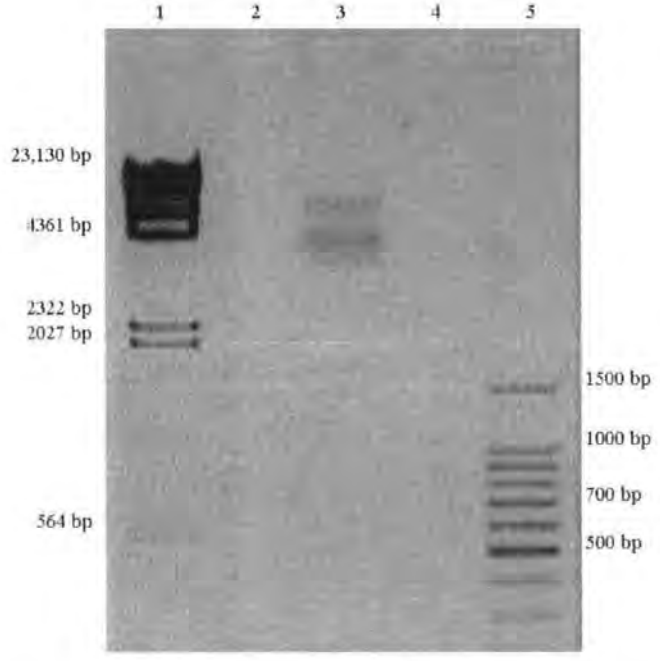

Figure 5.16. Restriction digestion of strain 430 with *Bam*HI, lane 3. Lane 1 is a Lambda *Hind* III marker and lane 5 is a 100 bp marker. Lanes 2 and 4 are empty.

5.2.6.5 Contigs and sequencing

The clone libraries prepared from the sonicated DNA and restriction enzyme digested DNA were sequenced. A total of 48 clones from strain 430 were sequenced with forward and reverse primers. Sequences of clones were assembled into continuous sequences (contigs) using PhredPhrap. The sequences assembled into 25 contigs

ranging in size from 310 bp to 2673 bp (Supplemental Material 3). Contigs were compared to Genbank database using BLASTn; 14 of the contigs showed similarities to previously described organisms. Figure 5.17 shows a summary of the organisms that have significant hits to nucleotides of the contigs. A hit was considered significant with E-values below 0.001. The distribution of BLAST hits showed 79% of the contigs showed significant nucleotide similarities to heterotrophic bacteria and 14% showed sequence similarities to previously described bacteriophages (Table 5.3).

Figure 5.18 shows the distributions of significant hits to 7 of the 25 contigs restricted to nucleotides from viruses available in Genbank. Contigs and their top significant nucleotide similarities to the virus database are listed in Table 5.3. The contigs showed about 43% sequence similarities to bacteria. The remaining 57% of the significant sequence similarities were to bacteriophage sequences.

The 25 contigs were compared to proteins in Genbank using tBLASTx to look for homology with previously described sequences (Table 5.3). The results from this analysis showed that 20 of the 25 contigs were homologous to previously described proteins. Hypothetical proteins and proteins of unknown function comprised 60% of the homologies. The remaining 40% of contigs had sequence homology to previously described proteins involved in protein and nucleotide modification and metabolism. The distributions of significant hits to contigs comparing only proteins from viruses available in Genbank (Table 5.3) showed sequence similarities to hypothetical proteins (74%) of bacteriophage and viruses. Assessment of the functions assigned to the previously described protein sequences with homology to the contigs showed homology to proteins involved in nucleotide modification and phage assembly.

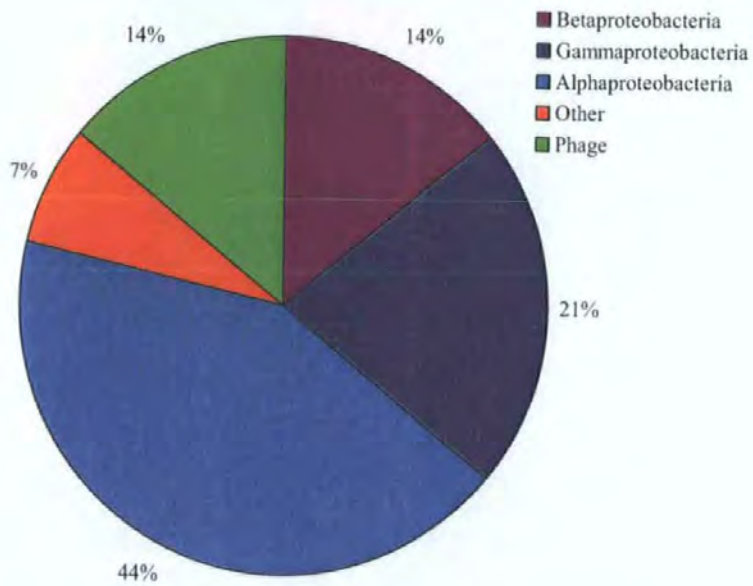

Figure 5.17. The distribution of significant nucleotide hits (BLASTn, non-redundant database) of the contigs assembled from the sequencing of viruses induced from strain 430.

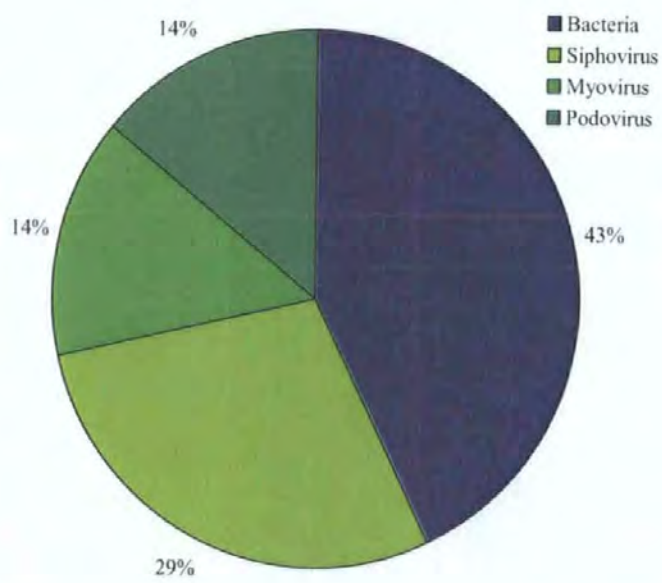

Figure 5.18. The distribution of significant nucleotide hits (BLASTn, non-redundant database restricted to viruses) of the contigs assembled from the sequence analysis of strain 430.

Table 5.3. BLAST results.

Contig	Length	BLASTn results	E-value	Accession #
2	473	*Homo sapiens* chromosome 17, complete sequence	9.00E-09	AC015724
5	589	*Xanthomonas campestris* pv. *campestris* str. ATCC 33913, section	3.00E-60	AE012194
6	757	*Ralstonia metallidurans* CH34 megaplasmid, complete sequence	3.00E-86	CP000353
8	1195	*Pseudomonas fragi* gene for D(-)-3-hydroxybutyrate dehydrogenase, complete cds	1.00E-177	AB183516
9	1106	Bacteriophage 16-3, central region	5.00E-10	AJ131679
11	550	*Acidovorax avenae* subsp. *citrulli* AAC00-1, complete genome	3.00E-09	CP000512
12	675	*Burkholderia cenocepacia* phage BcepB1A, complete genome	7.00E-06	AY616033
13	1081	*Paracoccus denitrificans* PD1222 chromosome 2, complete genome	6.00E-85	CP000490
14	1386	*Silicibacter* spp. TM1040 mega plasmid, complete sequence	5.00E-11	CP000376
15	1132	*Sinorhizobium medicae* WSM419, complete genome	4.00E-24	CP000738
16	762	*Pseudomonas putida* KT2440 complete genome	2.00E-25	AE015451
25	2272	*Bradyrhizobium* spp. BTAi1, complete genome	9.00E-11	CP000494
Contig	**Length**	**BLASTn results virus database**	**E-value**	**Accession #**
6	757	*Saccharopolyspora erythraea* NRRL2338 complete genome	6.00E-08	AM420293
8	1195	*Saccharopolyspora erythraea* NRRL2338 complete genome	3.00E-08	AM420293
9	1106	Bacteriophage 16-3, central region	1.00E-11	AJ131679
12	675	*Burkholderia cenocepacia* phage BcepB1A, complete genome	2.00E-07	AY616033
14	1386	*Salmonella enterica* subsp. *enterica serovar Choleraesuis* str. SC-B67, complete genome	6.00E-04	AE017220
16	762	*Burkholderia cepacia* phage Bcep22, complete genome	4.00E-16	AY349011
25	2272	Mycobacteriophage Omega, complete sequence	1.00E-09	AY129338

Table 5.3 (cont.). BLAST results.

Contig	Length	BLASTx results	E-value	Accession #
4	1379	hypothetical protein BACCAC_00738 [*Bacteroides caccae* ATCC 43185]	5.00E-26	EDM22357
5	589	UDP-2,3-diacylglucosamine hydrolase [*Stenotrophomonas maltophilia* R551-3]	4.00E-31	ZP_01643008
6	757	beta-ketoacyl synthase [*Stenotrophomonas maltophilia* R551-3]	2.00E-58	ZP_01642905
7	345	hypothetical protein B3ORF52 [*Pseudomonas* phage B3]	2.00E-18	YP_164089
8	1195	3-hydroxybutyrate dehydrogenase [*Stenotrophomonas maltophilia* R551-3]	2.00E-141	ZP_01642828
9	1106	RB16 HNH(AP2) 3 [Enterobacteria phage RB16]	9.00E-20	AAY44388
10	790	hypothetical protein Smed_1641 [*Sinorhizobium medicae* WSM419]	2.00E-15	YP_001327313
11	550	protease Do [*Delftia acidovorans* SPH-1]	2.00E-19	ZP_01578888
12	675	gp37 [*Burkholderia* phage phiE255]	2.00E-16	YP_001111237
13	1081	hypothetical protein Pden_0135 [*Paracoccus denitrificans* PD1222]	9.00E-44	ZP_00629337
14	1386	hypothetical protein Bcep1808_1162 [*Burkholderia vietnamiensis* G4]	1.00E-06	YP_001119008
15	1132	peptidoglycan-binding domain 1 protein [*Sinorhizobium medicae* WSM419]	2.00E-29	YP_001326997
16	762	site-specific DNA methylase [*Magnetospirillum magneticum* AMB-1]	5.00E-52	YP_419725
18	1136	protein of unknown function DUF1250 [*Geobacter metallireducens* GS-15]	7.00E-08	YP_385991
19	1257	hypothetical protein SSE37_25418 [*Sagittula stellata* E-37]	8.00E-60	ZP_01748454
20	418	hypothetical protein Oant_0250 [*Ochrobactrum anthropi* ATCC 49188]	5.00E-11	ABS12981
21	2673	hypothetical protein SPSV3_gp49 [*Salmonella* phage SETP3]	2.00E-65	YP_001110849
22	1605	hypothetical protein ISM_08110 [*Roseovarius nubinhibens* ISM]	2.00E-39	ZP_00959783
24	1896	hypothetical protein amb0352 [*Magnetospirillum magneticum* AMB-1]	4.00E-46	YP_419715
25	2272	site-specific DNA-methyltransferase (adenine-specific) [*Bradyrhizobium* spp. BTAi1]	5.00E-73	ABQ38514

Table 5.3 (cont.). BLAST results.

Contig	Length	BLASTx results virus database	E-value	Accession #
4	1379	portal protein [*Pseudomonas* phage D3112]	6.00E-08	NP_938234
7	345	hypothetical protein B3ORF52 [*Pseudomonas* phage B3]	1.00E-19	YP_164089
8	1195	hypothetical protein [*Trichoplusia ni* ascovirus 2c]	2.00E-15	YP_803294
9	1106	RB16 HNH(AP2) 3 [Enterobacteria phage RB16]	6.00E-21	AAY44388
10	790	hypothetical protein Era103g26 [*Erwinia amylovora* phage Era103]	6.00E-11	YP_001039657
12	675	gp37 [*Burkholderia* phage phiE255]	1.00E-17	YP_001111237
14	1386	gp90 [Mycobacteriophage Llij]	4.00E-04	YP_655086
15	1132	gp27 [Mycobacteriophage Halo]	5.00E-04	YP_655544
16	762	DNA methyltransferase [Enterobacteria phage P1]	2.00E-23	AAQ14149
17	548	hypothetical protein Era103g26 [*Erwinia amylovora* phage Era103]	5.00E-04	YP_001039657
18	1136	hypothetical protein Mx8p19 [Bacteriophage Mx8]	2.00E-05	NP_203433
19	1257	putative tail fiber protein H [Bacteriophage 16-3]	2.00E-07	CAD98810
21	2673	hypothetical protein SPSV3_gp49 [*Salmonella* phage SETP3]	1.00E-66	YP_001110849
24	1896	hypothetical protein BCBBV1cgp14 [*Bacillus clarkii* bacteriophage BCJA1c]	2.00E-27	YP_164392
25	2272	gp155 [Mycobacterium phage Omega]	2.00E-61	NP_818455

5.3 Discussion

5.3.1 Amplification of with algal virus specific primers

Algal DNA extractions were amplified with primers specifically designed to amplify the algal virus DNA polymerase gene. The possibility of being able to screen algal cultures using a molecular approach offers an attractive, simple and quick method for the detection of latent viruses in these organisms. The specificity of the DNA primers was tested and refined on the 49 algal strains (Section 5.2.1). The detection of latent viruses using the specific algal virus DNA polymerase primer set AVS1 and POL, did not appear to amplify the latent VLPs of the algal strains tested (Section 5.2.1). To reduce the background "contamination", algal DNA extraction methodology was optimised to obtain cleaner DNA preparations. Various PCR conditions and concentrations of PCR reactions mixtures were tried to minimise the background amplification.

These PCR primers labeled 'Algal Virus Specific' (AVS), have a misleading designation as the primer set only amplifies some double stranded DNA algal viruses (Willie Wilson, personal communication). The highly conserved DNA polymerase sequence found in lytic phycodnaviruses has been shown in a previous study using latent macroalgae viruses (*Ectocarpus* and *Feldmannia* viruses), not to amplify the expected conserved DNA polymerase (Chen & Suttle, 1996).

Inducible VLPs from three out of four of the algal strains tested and amplified with AVS1 and POL yielded products with sizes ranging from ca. 500bp to 900bp compared with an expected product size of 550bp (Section 5.2.5.3). The quality of the DNA proved to be critical in order to obtain a PCR product; furthermore, a high concentration of primers was found to be required to yield a product. This high primer concentration helps when using degenerated primers to compensate for the unspecific priming that may occur and improves the likelihood of obtaining a PCR product (Chen & Suttle, 1996; Short & Suttle, 2002).

The sequences obtained from the PCR product did not have significant sequence similarities to previously characterised lytic phycodnaviruses sequences deposited in Genbank. The difficult amplification of the DNA polymerase using primers targeting the conserved region of this gene and the fact that the sequence showed only weak similarities to other latent viruses seem to point toward a higher variability of DNA polymerases throughout latent virus polymerases. Interestingly, the sequences from the PCR products from three of the VLPs from algal strains did have similarities, at the nucleotide level, to short fragments (20-30 bp) of DNA polymerase sequences of the latent herpesviruses. The availability of latent virus DNA polymerase sequences are limited to mostly clinical latent viruses, such as herpes, and latent viruses of macro algae (*Ectocarpus* and *Feldmannia* viruses). Herpesviruses appear to share an ancestor with the *Feldmania* DNA Pol (Villarreal & DeFilippis, 2000) and it has been demonstrated that DNA polymerase sequences of phycodnaviruses are more closely related to those of herpes viruses that any other family of viruses (Chen & Suttle, 1996). The design of new primers based on DNA polymerase or other genes common from latent algal viruses would likely lead to a better amplification therefore providing a reliable method of detection of latent algal viruses. In order to create suitable sets of primers, a few latent algal viruses will need to be sequenced to provide a representative and diverse sample of genes on which the primers would be based.

5.3.2 Inducible VLPs detected by AFC

AFC dot plots of SSC versus GFL were analysed to identify potential groups of VLPs released after UV treatment of the algal cultures. AFC analysis of UV-induced algal cultures revealed the presence of two grouping of potential VLPs (Section 5.2.2). Several cultures had an increase in particles with a low SSC and low GFL in the range typical of viruses and bacteriophage particles (Brussaard, 2004a). Of the 30 algal strains

screened, 37% showed an increase of particles with AFC signals typical of VLPs in the UV-treated cultures that were not seen in the controls. Of these, five Chlorophyta strains (85, 430, 492, 315 and 570) and six Haptophyta strains (93, 156, 240, 351, 536 and 564) had increases in the group of VLPs (Table 5.2).

Another group of particles were observed in the AFC analysis. This group had a higher GFL signal than that typical of viruses and bacteriophages, yet lower than that typical of bacteria at ca. 50-300 AU (arbitrary units); the SSC signals of these group were also higher than those typical of viruses and bacteriophages ($>10^3$). Dot plots of Chlorophyta strains 83, 430, 491, 315 and Haptophyta strains 377, 378(1), 506(A), 564 and 565 showed increases in these groups of unascribed particles (33%) (Table 5.2). A decrease in these unascribed groups of particles compared to the control was observed in the dot plots of Chlorophyta strains 85, 272, 299, Heterkontophyta strain 663 and Haptophyta strains 8, 133, 240, 508 and 515 (30%) (Figure 5.2).

The screening of lysates of UV-induced cultures with AFC revealed an intriguing result. AFC has been conducted on many viruses and bacteriophage which has defined AFC signatures for many types of viruses (Brussaard, 2004a; Brussaard *et al.*, 2000; Marie *et al.*, 1999). Some strains (37%) had obvious VLP groups appearing in AFC in UV-induced cultures while, unexpectedly, many of the control cultures contained the unascribed group of particles with the higher GFL and SSC signals. The unascribed group was not consistent throughout the experiments carried out and their AFC signal did not match any other known AFC signal (Corina Brussaard, personal communication). A further study of these particles would allow for their identification and determine if they are a novel group. After establishing conditions that would consistently assert the presence of this group, it would be possible to use flow cytometric cell sorting to isolate these particles that could subsequently undergo molecular analysis and microscopic characterisation.

5.3.3 Effect of UV treatment on induction of VLPs over time

The 15 strains examined here were selected from the original 30 strains screened to try to discern a host-virus interaction. Typical virus-induced crashes in the host cell population, such as that observed in the *Symbiodinium* spp. (Section 3.2.5), were not observed. A total of 67% of the strains examined showed a reduced growth or static growth in UV-treated algae cultures and had an increase in the VLP groups (Figure 5.3). The rest of the strains showed a decline in the UV-treated algal cultures 24-48 h after induction and had increases in the VLP groups (Figure 5.3). Many of the cultures had static or reduced growth rates; this suggests that potential latent viruses of the algae tested did not efficiently infect the host. This may be due to mispackaging of the virus DNA or a small burst size. Other factors that could result in this effect are a lack of efficient reintegration of the virus and/or a mixture of sensitive and resistant hosts.

5.3.4 Visualisation of VLPs

VLPs were observed in the UV-treated supernatants of strains 29, 83, 85, 156 and 430 (Figures 5.4 and 5.5). Thin sections of the UV-treated strains 85, 156 and 430 (Figures 5.6, 5.7 and 5.8) revealed the presence of VLPs within the UV-treated host cells. The morphology of the VLPs were similar to that of previously described phycodnaviruses having a round and/or icosahedral shape.

A reduction in the growth rate of the algal cells was observed immediately after UV induction in the *Dunaliella* strains 83 and 430 (Figure 5.3a). While the reduced growth rate may have been due to the UV treatment, a distinct group of VLPs became apparent in the AFC dot plots of the UV-treated cultures of strain 430, ca. 48 h after UV induction and increased in abundance to ca. 8.7×10^7 VLPs/ml (Figure 5.3a). Strain 83 also showed a decrease in the rate of growth in the algal culture after UV induction and while an increase in VLPs in the UV-treated cultures relative to the controls was not

observed there appeared to be more VLPs in the AFC dot plots of the UV-treated cultures (Figure 5.3a).

TEM images of lysates from the UV-treated strains 83 and 430 revealed the presence of VLPs with similar morphology in both lysates. The round slightly icosahedral particles ca. 75 nm in diameter were observed in the strains (Figure 5.4). Thin sectioning of strain 430, 43 h after UV induction revealed VLPs within the host cells. The appearance of VLPs in the AFC occurred shortly after this time frame suggesting that the VLPs observed in the thin sections are the group of VLPs appearing in the AFC dot plots. The shape of the particles observed in the thin sections was similar to those seen in the lysates. A size discrepancy observed between the VLPs in the lysates and the VLPs in the thin sections is likely due to sample preparation. The morphological similarities of the VLPs in the lysates of strains 83 and 430, the presence of VLPs of a similar shape present in the thin sections of strain 430 and the correlation of a decline in host cell abundance to the increase in VLPs in the UV-treated strain 430 suggest the *Dunaliella* strains have a high likelihood of possessing a latent virus.

The *Chlorella stigmatophora*, strain 85 showed a reduction in host cell numbers ca. 48 h after UV induction and ca. 48 h a group of VLPs became appearant and increased in abundance to ca. 2.5 x 10^7 VLPs/ml (Figure 5.3b). TEM images from the lysate of the UV-treated strain 85 showed VLPs with a unique morphology. The particles present in the lysate of the UV-treated culture had a round central core ca. 200 nm in diameter with spikes ca. 200-300 nm in length protruding from the central core (Figure 5.5). While several of the particles observed had multiple spikes, some of the particles had only one; these particles with only one spike share morphological similarities to the PBCV-1 viruses (Yamada *et al.*, 2006). These spikes may function as receptor binding sites or they may be involved in cell wall degradation. The cell-wall-degrading activity is suspected to be located in the spike structure of the PBCV-1 virus (van Etten *et al.*,

1991). Another similarity to the PBCV-1 virus was also observed in the thin sections of strain 85. After attachment and entry of the PBCV-1 virus an empty capsid remains on the host surface (Meints *et al.*, 1984). The thin section images of the UV-treated strain 85 showed several electron dense particles present around the periphery of the cells which might be capsids (Figure 5.6b). It is possible that these particles are capsids resulting from infection of the cells by the virus.

The AFC analysis of strain 29 showed an interaction in which the appearance and increase of the VLP group (6.7×10^6 VLPs/ml) correlated with a decline in the cell numbers of the UV-treated culture (Figure 5.3 c). In strain 156, the algal numbers in the UV-treated culture remained static while the VLP numbers continually increased in the UV-treated cultures to 2.2×10^7 VLPs/ml (Figure 5.3 d). The lysate from the UV-treated cultures of strains 29 and 156 revealed VLPs (Figure 5.5) with morphologies similar to that of phycodnaviruses. Thin section images from UV-treated host cells of strain 156 showed VLPs within the cells and near the periphery of the cells.

VLPs observed in the TEM images and in the thin sections of the UV-treated host cells of the algal strains examined support the AFC data which indicate that latent VLPs are induced from these algal culture after UV treatment. The implication for this finding could potentially explain the variations observed in culture based studies which implement algal strains that may harbour a latent virus. For example, in a previous study utilising *Dunaliella minuta*, strain 430, the reduction in algal growth rate was attributed to binding of heavy metal to sulfhydryl groups inhibiting normal cell division (Visviki & Rachlin, 1991). While this may be a factor that can result in inhibition of cell division, the addition of heavy metals to an algal culture could act as a stimulant to induce a latent virus. Although heavy metal induction of latent viruses of algae has not been demonstrated, a study on the cyanobacterium *Anacystis nidulans* showed that the presence of copper (concentrations from 3.1×10^{-6} M to 3.1×10^{-4} M) resulted in the

induction of the lysogenic phage AS-1 (Lee *et al.*, 2006). Another example of a potential latent virus affecting results in a previous study is shown for *Chlorella stigmatophora* (Kalinkina & Yasyukova, 2001). The data demonstrated that under chemical stress, increased concentrations of NaCl, the glycolate pathway is inhibited leading to oxidative stress and the destructive after effect to the algal cells (Kalinkina & Yasyukova, 2001). Again under stressful condition, the induction of a potential latent virus would be favored which in many cases would appear to be due to the effect of the chemical stress on the cell. The effect of the chemical stress could in actuality be the effect of the propagation of an induced latent virus.

The TEM data is highly suggestive of latent viruses being present in the algal culture collection. The thin sections of the UV-treated strains of algae show the presence of VLPs which until this study on latent infections in culture collections were unknown. The AFC data presented here shows that ca. 40% of the strains tested have what appear to be inducible latent viruses. While other studies using these culture collection strains have not taken into account the possibility that the strains might harbour latent viruses this data shows latent viruses are present in a substantial number of the algal strains in the culture collection. While the full implication for the impact on studies utilising a culture collection strain harbouring a latent virus is unknown, it could alter results. These results provide additional data for further documentation of the role of viruses in culture collections. These results should be taken into account when considering the viability of strains originating from culture collections. It is to be acknowledged that suboptimal conditions could trigger lysis events leading to the crash of the culture.

5.3.5 Molecular analysis

Five algal virus genomes have been fully sequenced, three dsDNA phycodnaviruses and two RNA algal viruses. The dsDNA viruses are EsV-1, which infects a marine

filamentous brown alga, *Ectocarpus siliculosus* (335,593 bp) (Delaroque *et al.*, 2001), PBCV-1, which infects a chlorella-like green algal symbiont of the freshwater protozoa *Paramecium bursaria* (330,744 bp) and EhV-86 which infects the bloom-forming coccolithophore *Emiliania huxleyi* (407,339 bp) (Wilson, 2005). Viruses of eukaryotic algae tend to have large genomes; from the few marine algal viruses examined by PFGE, genome sizes from 126 to 400 kb are typical (Reisser, 1993; Steward *et al.*, 2000). From the examination of PFGE fingerprints of natural virus assemblages from seawater samples, it has been proposed that viral genomes in the size range of 76–100 kb are likely to be cyanophages while other bacteriophages are generally less than 65 kb (Steward *et al.*, 2000). Although lytic algal virus genome sizes are generally bigger than that seen in the PFGE of this study, the possibility of a smaller latent algal virus genome can not be ruled out. Sizes of the latent algal viruses of macro algae *Feldmannia* spp. and *Ectocarpus* spp. are larger, ca. 150-350 kb, (Delaroque *et al.*, 2003; Ivey *et al.*, 1996) whilst latent viruses of microalgae have not previously been examined. The 70-75 kb genome sizes observed in the PFGE for strains 29 (Figure 5.12) and 430 (Figure 5.11) could nevertheless be within the genome size range of a latent virus as latent viruses of microalgae have not been investigated.

Amplification of DNA extracts from UV-treated lysates of strains 29, 85, 156 and 430 (Figures 5.13, 5.14 and 5.15) with algal virus-specific DNA polymerase primers did not show significant sequence similarities to previously described algal virus sequences. However, an interesting trend among the products sequenced occurred; several small stretches (20-40 bp) of the sequences obtained had high sequence similarity (>95% identity) to herpesviruses. This is an interesting result as the herpesviruses are also latent. The genomes of latent viruses of the macroalgal viruses (phaeoviruses) have also shown numerous repeat sequences similar to those in baculoviruses and herpesviruses (Lee *et al.*, 1995; van Etten *et al.*, 2002). The phaeoviruses and herpesviruses integrate

within the host cell and require an excision event prior to viral replication. It has been suggested that the common repeat elements may be involved in the excision process (Lee *et al.*, 1995).

Sequencing of strain 430 was carried out concurrently with strain PPt10905 and several cloning and sequencing issues were encountered and are described in section 4.3.4. Clones obtained from the Invitrogen zero blunt cloning were screened for larger inserts and sequenced, providing ca. 26 kb of Sanger sequence. Comparison of the 25 assembled contigs to sequences present in Genbank did not reveal strong identities to other algal viruses (Table 5.3). This result was expected as there are only a few algal virus genomes for comparison in databases and these viruses are mostly lytic viruses of unrelated species of algae. As the predominant sequence similarities were to that of bacteria and bacteriophage sequences present in Genbank, the potential that the cloned sequence was that of contaminating bacteria and/or bacteriophage can not be ruled out. Future work on latent VLPs from the algal strains of this study or similar systems could implement additional clean up steps, such as CsCl gradients, to minimise the possibility of contamination in the DNA preparations. It is possible that single cell sequencing could limit the problem of non-algal DNA contamination. Using micromanipulation, it is possible to isolate a cell through single cell capillary transfer and replicate its DNA using phi 29 DNA polymerase based rolling circle amplification (Oldrach *et al.*, 2000; Edvardsen *et al.*, 2003). The use of single cell sequencing may improve greatly the quality of the algal DNA preparation however, symbiotic algae-associated bacteria, either extracellular attached directly to the membrane or intracellular will likely remain an obstacle in obtaining a pure algal DNA preparation. The sequence obtained from the PCR products amplified from the lysates suggest that the VLPs may be latent viruses based on the short stretches of high DNA similarity to known latent viruses. To overcome the issues of successfully cloning the VLPs present in the UV-induced lysates

alternative sequencing procedures, such as 454 pyrosequencing which bypasses the need for cloning, may be suited to obtain the genomes of these potential latent viruses. The knowledge that will be gained from the completion of a latent microalgal virus, will provide much information about characteristics of latent viruses, host virus interaction and the mechanisms by which latent infection exist.

5.4 Conclusions

The isolation and characterisation of latent viruses from a variety of pico and nano algae in the Plymouth Culture Collection presented here provides a base line of data for the potential influence and prevalence of latent viruses found in algal collections. Induction with UV-C has been used to screen 30 algal species for potential latent viruses. Thousands of species are maintained in algal collections around the world and the presence of latent infections within these collections has not been addressed to date. From the 30 algal species examined in this study over 35% appear to contain an inducible agent.

Induction curves have been used to characterise 15 species of algae which are susceptible to UV light induction. AFC and TEM images have confirmed the presence of VLPs, and thin sections of UV-induced cultures further support the presence of inducible VLPs in the algal cultures. Molecular characterisation of the VLPs, using algal virus-specific primers has been attempted and the widely used algal specific DNA polymerase primers do not appear to amplify the highly conserved DNA polymerase gene found in lytic algal viruses. The data presented here reveal that a significant proportion of the algae in this culture collection contain putative latent viruses. This emphasises the fragile environmental equilibrium in which algae harbouring latent viruses are living. Changes in environmental conditions can trigger a lytic event which can lead to the crash of the algal community. On the beneficial side, viruses are well

known vectors of horizontal gene transfer and the widespread presence of latent viruses within algal genomes opens the possibility of a significant contribution to their host genetic diversity, likely improving environmental fitness. Additional studies to examine the genetic contribution of the latent viruses through genomic analysis would be able to identify which genes have been acquired via viral horizontal gene transfer. Through the analysis of multiple algal genomes it may be possible to identify where a gene transferred and whether its maintenance within the host is random or if some sort of selection occurred, making it possible, by comparing genomes, to identify "favored transfered genes" that would likely shed light on the genetic evolution of algae.

CHAPTER 6 Conclusions and Suggestions for Future Work

6.1 General overview

Studies of temperate and latent viruses are underrepresented. Latent viruses can influence the genetic diversity of the host organisms and/or confer immunity or toxin production to increase the fitness of the host populations. Latent viruses may also be the factors causing unexplained variations or declines in host populations that have only considered lytic viruses in ecological studies. This work presents specific aspects of unique and important temperate and latent viruses of aquatic photosynthetic microorganisms. Three types of aquatic photosynthetic microorganisms were examined and new methodology was established, using a variety of techniques such as AFC, electron microscopy, and molecular tools. The aim of the first study was to investigate the possibility of zooxanthellae harbouring latent viruses and to subsequently isolate and characterise these viruses. The goal of the second study was to isolate and characterise VLPs of a freshwater cyanobacterium. Finally, the third study assessed the presence of latent viruses in the PCC algal collection.

6.2 Latent viruses of *Symbiodinium* spp.

The study of *Symbiodinium* spp. showed that ca. 37% of the strains tested had an group of filamentous VLPs which was designated as zooxanthellae filamentous virus 1 (ZFV1) that is inducible by UV-c treatment. This is the first study that conclusively shows that latent viruses are present in *Symbiodinium* spp. Extrapolation of this virus-host interaction and its effects on zooxanthellae viability is a milestone in the understanding of the complex chain of events that may yield to coral bleaching. The coral reef ecosystem is a finely tuned ecosystem for which environmental changes such as water temperature elevation or increase in nutrient concentration can result in dramatic changes. This research shows how stressful conditions represented by an

increase of UV exposure can affect the most intimately associated coral relationship, that of the symbiotic dinoflagellate. As viral induction *in vitro* is stimulated by exposure to UV light in cultures of *Symbiodinium* spp., it is possible that in shallow coral reefs, natural UV irradiation (UV-A and UV-B) could stimulate induction of latent viruses, illustrating the importance of the observation of this new group of filamentous VLPs. In the last few decades there has been an increased frequency of severe bleaching events which coincides with times of climatic events such as severe El Nino events and global warming. In the coral *Acropora formosa*, exposure to heat stress has been shown to lead to an increase in VLPs in the coral and in the zooxanthella (Davy *et al.*, 2006; Wilson *et al.*, 2001). Modeling of seawater temperatures predicts increases between 1°C to 2°C per century; as healthy coral reefs are at the upper thermal limit, even slight increases in temperature may trigger temperature-induced viral propagation (Jones *et al.*, 2000; Pockley, 2000). In addition to these climatic stresses, other stresses such as chemical pollutants or host disease agents could also be involved in degrading the coral reef ecosystem. All these stresses could individually or collectively be responsible for the induction of latent viruses of zooxanthellae which in turn would lead to the demise of symbiotic relationships of zooxanthellae with coral and other cnidarians, likely contributing to coral bleaching.

A complete genome sequence of the inducible filamentous VLP would provide much information, especially on the interaction of the latent virus and the host zooxanthellae. The coexistence of the zooxanthellae with an integrated latent virus under stable environmental conditions may offer protection from highly virulent lytic viruses. Genome data might reveal mechanisms involved in the infection process such as "sensor" genes involved in triggering the lytic life cycle. Identification of molecular probes that can amplify a conserved gene (DNA polymerase or structural proteins) could be tested on strains identified in this study as candidates for harbouring latent

viruses. The application of a molecular probe that could detect latent viruses in cultures of *Symbiodinium* spp. could then be applied to whole animal systems, such as corals and sea anemones and would allow for the detection of zooxanthellae harbouring latent viruses. The assessment of the world's reefs using this type of a molecular approach coupled with the monitoring of stress factors leading to lytic cycle induction might provide a way to predict bleaching events.

6.3 Freshwater temperate cyanophages

The work carried out on the cyanobacterium PPt10905 suggests that this freshwater cyanobacterium harbours a prophage. The group of VLPs appearing in the AFC of the heat-treated cultures correlate with the podovirus morphology of the particles observed in the TEM and the clusters of VLPs observed in the thin sectioning of the heat-treated cultures.

The significance of lysogenic cyanophages in freshwater cyanobacteria is not well understood and the isolation and characterisation of this temperate virus will help determine the potential functions and interactions of aquatic temperate cyanophages. The complete sequence analysis of this temperate cyanophage will provide information on the mechanisms involved in the infection and integration processes and the maintenance of the phage in the host genome. While the majority of cyanophages investigated to date are lytic, comparison of this temperate cyanophage genome with the previously described lytic cyanophage genomes will provide a genomic comparative base. Comparison of this freshwater temperature cyanophage genome to the only sequenced freshwater cyanophage, Pf-WMP4 (Liu *et al.*, 2007), will provide information on genomic differences and similarities found in freshwater and marine cyanophages that could explain physiological and biological interactions, such as selective adaptations to local conditions (Noble & Fuhrman, 1997). Furthermore, the

lytic cyanophages of the genomes of eight cyanophages have provided much information on novel characteristics, such as the presence of photosynthesis genes. Cyanophage genomes have been shown to contain genes encoding for the Photosystem II core proteins PsbA and PsbD, which help to maintain and enhance photosynthesis during viral infection, optimising propagation of new viral particles (Hill, 2006; Mann *et al.*, 2005; Sullivan *et al.*, 2006). Cyanophages of *Prochlorococcus* spp. and *Synechococcus* spp. have been examined for the presence of the Photosystem II core proteins, PsbA and PsbD, and these genes have been found in all the different cyanophage families: cyanomyoviruses, cyanosiphoviruses and cyanopodoviruses (Sullivan *et al.*, 2006). While not all cyanophages carry these genes, investigations into the prevalence of the photosynthesis genes has shown that 88% of the cyanophages examined contain PsbA and 50% contain PsbD (Sullivan *et al.*, 2006).

The cyanobacterium PPt10905, its inducible VLPs and the co-occurring increase in carboxysomes could be a new mechanism in which lysogeny benefits freshwater cyanobacteria, possibly increasing the host's photosynthetic efficiency. The unusual interaction observed in this freshwater cyanobacterium, where the abundance of carboxysome-like particles increased 10 times in heat-treated cultures, might be due to the presence of photosynthesis genes similar to those seen in other cyanophages. As carboxysomes are reserves for photosynthetic enzyme that catalyse CO_2 fixation in the primary step in the dark reactions of photosynthesis, the mechanism behind this increase of carboxysomes could provide useful insight into the interaction which occurs in the host cyanobacterium during viral infection encouraging an increased rate of carboxysome production. It will be of interest to see if Photosystem II core proteins are present in this temperate cyanophage.

6.4 Latent viruses in algal culture collections

From the 30 algal species examined in this study, over 35% appear to contain an inducible infectious agent. AFC and TEM images have confirmed the presence of VLPs, and thin sections of UV-induced cultures further support the presence of VLPs in the UV-induced cultures. Algal culture studies have been beneficial to the aquaculture industries and have brought much insight into how algal species can influence natural environments. Thousands of species are maintained in algal collections around the world and this is the first study to examine the presence of latent infections within one of these collections.

Molecular characterisation of the inducible VLPs, using algal virus-specific primers has been attempted. Algal virus specific DNA polymerase primers amplified a product in the inducible VLPs of the algal strains tested. In previous studies, it was concluded that the highly conserved DNA polymerase sequence found in lytic phycodnaviruses could not be amplified in the latent macroalgae viruses of *Ectocarpus* spp. and *Feldmannia* spp. (Chen & Suttle, 1996; Short & Suttle, 2002). The products amplified from the UV-induced VLPs of the algal strains 156 and 85 were bigger than the expected size and the product from strain 430 was smaller than the expected size using the algal virus-specific DNA polymerase primers. This variation observed in the amplified product could be due insertions or deletions in the DNA polymerase gene.

The sequences obtained from the PCR product did not yield significant sequence similarities to previously characterised lytic phycodnaviruses. However, the products sequenced from the induced VLPs showed an unexpected similarity to herpes viruses. While significant sequence similarities were not seen; short fragments (20-30 bp) of sequence had high levels of similarities (>90%) to that of herpes virus DNA polymerase sequences. The sequence similarity to the short fragments of a latent virus suggests that latent viruses contain a variation in the DNA polymerase. It is possible that the

variability in the latent viruses enhance the fitness of the virus by disguising it and preventing recognition by the host, improving the chances of survival. Future work to design a primer set which would amplify a conserved gene of latent algal viruses would provided a tool to assess algal cultures which are commonly used from culture collections for latent viruses.

The knowledge of strains that harbour latent viruses could prove useful in aquaculture industries that depend on algal cultures as a key component in sustaining successful harvest. In addition, results of modeling studies that only factor in lytic viruses may experience unexpected variations due to latent viruses not taken into account. The isolation and characterised of latent viruses from pico and nano algae presented here provides a base line of data for the potential influence and prevalence of latent viruses found in algal collections.

6.5 Future directions

This work showed that viable latent viruses are widespread across a variety of algal species and that under certain conditions, they can be induced. This extends the knowledge on latent viruses was until now mostly speculative. Because of the economical use of algae as well as their ecological roles further research on latent algal viruses is warranted.

The affordability of DNA sequencing has made large scale genomic sequencing accessible. Genomic sequencing of latent algal virus systems will provide much information regarding the insertion sites in the host as well as a detailed sequence of the latent virus that can be use for comparison with other viruses closely related by their host, habitat or lifestyle. A proteomic study of these systems, similar to the work on the *Emiliania huxleyi* virus, EhV86 (Allen *et al.*, 2006b; Wilson *et al.*, 2005), would complement the DNA sequencing by providing information on the various viral and

host proteins that may be involved in the regulation of the latent stages. These proteomic results could also be used to answer the question as to how viruses are "sensing" changes in their environment.

A detailed study of the various conditions triggering the lytic cycle should be conducted under conditions reproducing those experienced in aquaculture facilities, in case of algae farming and the broader more complex environmental conditions that can be experienced in open water bodies. In the case of algae farming, the results of such research would provide guidelines as to how to optimally grow algae in order to avoid crashes of whole culture batches ultimately resulting in higher yield and reduced cost of production which would be of much interest to the aquaculture industry.

The study of environmental algae and their latent viruses would be a more delicate endeavor due to the complexity of their environment and the multiplicity of factors susceptible to influence the latent host-virus association. Nonetheless, a model study should be devised that would replicate as closely as possible natural conditions. Similar to the studies carried out on the *Symbiodinium* spp., this model could follow the effect of a variety of natural conditions that, for example, could mimic more or less extreme global warming climatic consequences such as increase/decrease in water temperature, change in salinity or variation in the microbial composition of the water bodies. By testing these different factors, it will be possible to gather information as to what may trigger a change in the virus latent stage. In this report, it was established that latent viruses of coral-associated *Symbiodinium* spp. can be triggered into a lytic cycle by exposure to UV. The extrapolation of this result provides a new level of events that may play a role in coral bleaching.

The findings of this work show that latent viruses are present in a large proportion of the algae examined. It is most likely that latent viruses are ubiquitously present in other algae and that the algae of this report not showing traces of latent viruses might not

have been virus-free, but rather the methods employed were unable to detect these viruses. The impact and role of these latent viruses on their hosts and more importantly on the whole ecosystem remains unclear. However, it is easy to imagine that because of the abundance of algae and their implication in the planetary biochemical cycles, any effect of these latent viruses on their host could disturb these cycles possibly having climatic consequences.

Appendix 1

Contig	Length	BLASTn results	E-value	Accession #
1	1150	*Alcanivorax borkumensis* SK2, complete genome	6.58E-27	AM286690
3	881	*Bursaphelenchus conicaudatus* cytochrome oxidase subunit 1, partial cds	9.80E-44	AB083736
5	815	*Marinobacter aquaeolei* VT8, complete genome	4.00E-52	CP000514
8	740	*Drosophila hydei* AMYREL (Amyrel) gene, complete cds	2.15E-10	AY733042
9	637	*Marinobacter aquaeolei* VT8, complete genome	1.66E-75	CP000514
10	1751	*Pseudomonas* spp. CF600 phenol/3,4-dimethylphenol catabolic enzymes (plasmid encoded)	2.06E-83	X60835
11	1281	*Marinobacter aquaeolei* VT8, complete genome	2.23E-05	CP000514
13	706	*Marinobacter aquaeolei* VT8, complete genome	4.80E-05	CP000514
16	731	*Marinobacter aquaeolei* VT8, complete genome	6.97E-32	CP000514
18	1371	*Marinobacter aquaeolei* VT8 plasmid pMAQU01, complete sequence	2.58E-11	CP000515
19	694	*Marinobacter aquaeolei* VT8, complete genome	2.11E-124	CP000514
20	1230	*Silicibacter* spp. TM1040, complete genome	5.45E-43	CP000377
21	985	*Marinobacter aquaeolei* VT8, complete genome	2.15E-97	CP000514
28	1080	*Marinobacter aquaeolei* VT8, complete genome	4.29E-108	CP000514
29	688	*Marinobacter aquaeolei* VT8, complete genome	0.00E+00	CP000514
31	1304	*Erythrobacter litoralis* HTCC2594, complete genome	0.00E+00	CP000157
36	1026	*Alcanivorax borkumensis* SK2, complete genome	1.49E-101	AM286690
37	549	*Marinobacter aquaeolei* VT8, complete genome	6.22E-10	CP000514
38	560	*Rhodobacter sphaeroides* 2.4.1 plasmid B, complete sequence	9.56E-06	CP000145
39	1127	*Shewanella amazonensis* SB2B, complete genome	9.70E-23	CP000507
40	496	*Marinobacter aquaeolei* VT8, complete genome	5.81E-13	CP000514
41	455	*Marinobacter aquaeolei* VT8, complete genome	2.26E-18	CP000514

42	1167	*Marinobacter aquaeolei* VT8, complete genome	3.31E-44	CP000514
43	953	*Marinobacter aquaeolei* VT8, complete genome	3.35E-25	CP000514
44	815	*Arthrobacter* spp. FB24, complete genome	6.23E-14	CP000454
45	548	*Marinobacter aquaeolei* VT8, complete genome	1.69E-16	CP000514
46	805	*Marinobacter aquaeolei* VT8, complete genome	4.26E-58	CP000514
48	650	*Marinobacter aquaeolei* VT8, complete genome	4.12E-73	CP000514
49	650	*Magnetospirillum magneticum* AMB-1 DNA, complete genome	2.82E-06	AP007255
50	549	*Saprolegnia ferax* strain ATCC 36051 mitochondion, complete genome	5.01E-66	AY534144
51	560	*Marinobacter aquaeolei* VT8, complete genome	4.23E-14	CP000514
53	1235	*Marinobacter aquaeolei* VT8, complete genome	2.32E-11	CP000514
56	1400	*Erythrobacter litoralis* HTCC2594, complete genome	9.00E-36	CP000157
56	1400	*Pseudomonas syringae* pv. tomato str. DC3000 complete genome	3.82E-04	AE016853
57	1121	*Erythrobacter litoralis* HTCC2594, complete genome	8.34E-48	CP000157
58	993	*Pseudomonas aeruginosa* UCBPP-PA14, complete genome	3.24E-19	CP000438
59	1287	*Alkalilimnicola ehrlichei* MLHE-1, complete genome	1.55E-12	CP000453
61	534	*Marinobacter aquaeolei* VT8, complete genome	5.05E-69	CP000514
62	1105	*Marinobacter aquaeolei* VT8, complete genome	5.46E-52	CP000514
63	1231	*Gramella forsetii* KT0803 complete genome	1.37E-06	CU207366
64	706	*Marinobacter aquaeolei* VT8 plasmid pMAQU01, complete sequence	7.01E-72	CP000515
65	742	*Vogesella indigofera* indigoidine biosynthesis locus, complete sequence	9.52E-19	AF088856
66	949	*Marinobacter aquaeolei* VT8, complete genome	1.85E-88	CP000514
67	567	*Marinobacter aquaeolei* VT8, complete genome	1.90E-59	CP000514
67	567	*Marinobacter aquaeolei* VT8, complete genome	1.57E-07	CP000514
68	578	*Marinobacter aquaeolei* VT8, complete genome	6.09E-04	CP000514

69	1373	*Mycobacterium* spp. JLS, complete genome	2.68E-14	CP000580
73	1262	*Rhodoferax ferrireducens* DSM 15236, complete genome	1.58E-15	CP000267
74	727	*Polaromonas* spp. JS666, complete genome	4.95E-05	CP000316
76	762	*Marinobacter aquaeolei* VT8, complete genome	4.86E-73	CP000514
79	700	*Paracoccus denitrificans* PD1222 chromosome 2, complete genome	2.27E-19	CP000490
82	1677	*Azoarcus* spp. EbN1 complete genome	4.76E-07	CR555306
86	1505	*Gramella forsetii* KT0803 complete genome	4.27E-07	CU207366
87	1294	*Marinobacter aquaeolei* VT8, complete genome	9.26E-08	CP000514
89	1553	*Marinobacter aquaeolei* VT8, complete genome	5.77E-102	CP000514
90	1533	*Marinobacter aquaeolei* VT8, complete genome	3.90E-35	CP000514
92	994	*Marinobacter aquaeolei* VT8, complete genome	0.00E+00	CP000514
93	632	*Marinobacter aquaeolei* VT8, complete genome	4.14E-39	CP000514
94	1329	*Shewanella amazonensis* SB2B, complete genome	9.17E-05	CP000507
95	1511	*Marinobacter aquaeolei* VT8, complete genome	0.00E+00	CP000514
96	1744	*Marinobacter aquaeolei* VT8, complete genome	1.63E-28	CP000514
99	1508	*Marinobacter aquaeolei* VT8, complete genome	6.75E-117	CP000514
102	1611	*Marinobacter aquaeolei* VT8, complete genome	1.88E-46	CP000514
103	1255	*Marinobacter aquaeolei* VT8, complete genome	1.23E-179	CP000514
105	636	*Marinobacter aquaeolei* VT8, complete genome	3.87E-33	CP000514
106	912	*Marinobacter aquaeolei* VT8, complete genome	0.00E+00	CP000514
107	1214	*Marinobacter aquaeolei* VT8, complete genome	1.53E-89	CP000514
110	516	*Marinobacter aquaeolei* VT8, complete genome	8.84E-80	CP000514
112	1050	*Marinobacter aquaeolei* VT8, complete genome	5.57E-21	CP000514
115	556	*Marinobacter aquaeolei* VT8, complete genome	1.03E-48	CP000514

116	1586	*Marinobacter aquaeolei* VT8, complete genome	2.40E-30	CP000514
117	1331	*Polaromonas* spp. JS666 plasmid 2, complete sequence	7.96E-67	CP000318
118	1791	*Marinobacter aquaeolei* VT8, complete genome	0.00E+00	CP000514
120	1467	*Marinobacter aquaeolei* VT8 plasmid pMAQU02, complete sequence	6.49E-06	CP000516
122	1222	*Marinobacter aquaeolei* VT8, complete genome	4.16E-22	CP000514
123	1047	*Marinobacter aquaeolei* VT8 plasmid pMAQU01, complete sequence	2.19E-20	CP000515
124	1280	*Acidothermus cellulolyticus* 11B, complete genome	2.32E-08	CP000481
126	434	*Marinobacter aquaeolei* VT8, complete genome	1.34E-90	CP000514
127	673	*Marinobacter aquaeolei* VT8, complete genome	1.95E-47	CP000514
128	709	*Marinobacter aquaeolei* VT8, complete genome	5.82E-20	CP000514
129	1581	*Marinobacter aquaeolei* VT8, complete genome	1.43E-62	CP000514
130	1311	*Gramella forsetii* KT0803 complete genome	1.42E-40	CU207366
131	1194	*Marinobacter aquaeolei* VT8, complete genome	1.67E-24	CP000514
133	727	*Marinobacter aquaeolei* VT8, complete genome	4.97E-42	CP000514
134	1377	*Marinobacter aquaeolei* VT8, complete genome	1.54E-06	CP000514
136	1454	*Marinobacter aquaeolei* VT8, complete genome	4.61E-16	CP000514
137	1613	*Marinobacter aquaeolei* VT8, complete genome	2.44E-30	CP000514
139	1490	*Marinobacter aquaeolei* VT8, complete genome	3.40E-63	CP000514
142	1239	*Marinobacter aquaeolei* VT8, complete genome	1.73E-24	CP000514
143	612	*Marinobacter aquaeolei* VT8, complete genome	6.02E-35	CP000514
144	1149	*Cellulophaga lytica* ATP-synthetase beta-subunit gene, complete cds	8.02E-153	M22535
146	716	*Burkholderia xenovorans* LB400 chromosome 1, complete sequence	7.35E-38	CP000270
147	1068	*Marinobacter aquaeolei* VT8, complete genome	2.24E-20	CP000514
150	573	*Marinobacter aquaeolei* VT8, complete genome	8.15E-28	CP000514

151	725	*Marinobacter aquaeolei* VT8, complete genome	1.82E-72	CP000514
153	1054	*Marinobacter aquaeolei* VT8, complete genome	4.63E-06	CP000514
154	698	*Rhodopseudomonas palustris* CGA009 complete genome; segment 4/16	3.05E-43	BX572596
155	1191	*Marinobacter aquaeolei* VT8, complete genome	1.07E-25	CP000514
157	1225	*Marinobacter aquaeolei* VT8, complete genome	2.14E-42	CP000514
158	508	*Marinobacter aquaeolei* VT8, complete genome	8.96E-09	CP000514
159	1480	*Ralstonia eutropha* JMP134 chromosome 2, complete sequence	7.90E-21	CP000091
160	1561	*Mesorhizobium loti* MAFF303099 DNA, complete genome	4.26E-04	BA000012
162	1091	*Marinobacter aquaeolei* VT8, complete genome	1.21E-06	CP000514
163	1496	*Marinobacter aquaeolei* VT8, complete genome	4.74E-16	CP000514
164	1290	*Marinobacter aquaeolei* VT8, complete genome	5.13E-71	CP000514
165	1515	*Marinobacter aquaeolei* VT8, complete genome	8.15E-95	CP000514
166	1077	*Marinobacter aquaeolei* VT8, complete genome	2.03E-85	CP000514
170	688	*Cytophaga hutchinsonii* ATCC 33406, complete genome	1.85E-04	CP000383
173	1359	*Haemophilus somnus* 129PT, complete genome	6.00E-06	CP000436
186	739	*Marinobacter aquaeolei* VT8, complete genome	9.48E-19	CP000514
188	364	*Marinobacter aquaeolei* VT8 plasmid pMAQU02, complete sequence	5.25E-31	CP000516
189	987	*Marinobacter aquaeolei* VT8, complete genome	2.99E-13	CP000514
192	856	*Sphingopyxis alaskensis* RB2256, complete genome	1.10E-18	CP000356
194	1396	*Ralstonia solanacearum* GMI1000 chromosome complete sequence	4.95E-25	AL646052
197	1116	*Marinobacter aquaeolei* VT8, complete genome	0.00E+00	CP000514
198	1850	*Marinobacter aquaeolei* VT8, complete genome	1.50E-90	CP000514
200	1527	*Marinobacter aquaeolei* VT8, complete genome	2.77E-08	CP000514
201	1521	*Marinobacter aquaeolei* VT8, complete genome	7.07E-120	CP000514

205	922	*Marinobacter aquaeolei* VT8, complete genome	3.02E-56	CP000514
206	1189	*Marinobacter aquaeolei* VT8, complete genome	2.24E-48	CP000514
207	1627	*Gramella forsetii* KT0803 complete genome	2.04E-15	CU207366
208	1249	*Marinobacter aquaeolei* VT8, complete genome	1.51E-49	CP000514
209	528	*Paracoccus denitrificans* PD1222 chromosome 2, complete genome	5.55E-04	CP000490
211	781	*Marinobacter aquaeolei* VT8, complete genome	7.83E-146	CP000514
213	1595	*Bacteroides fragilis* NCTC 9343, complete genome	1.93E-12	CR626927
214	1440	*Marinobacter aquaeolei* VT8, complete genome	0.00E+00	CP000514
215	1069	*Roseobacter denitrificans* OCh 114, complete genome	1.86E-05	CP000362
216	1075	*Marinobacter aquaeolei* VT8, complete genome	0.00E+00	CP000514
217	1088	*Marinobacter aquaeolei* VT8, complete genome	1.05E-31	CP000514
218	1143	*Gramella forsetii* KT0803 complete genome	8.47E-11	CU207366
223	801	*Xanthomonas oryzae* pv. *oryzae* MAFF 311018 DNA, complete genome	2.52E-53	AP008229
224	1192	*Marinobacter aquaeolei* VT8, complete genome	6.58E-24	CP000514
227	1238	*Marinobacter aquaeolei* VT8, complete genome	2.51E-17	CP000514
231	1340	*Paracoccus versutus*, plasmid partitioning protein and replication protein genes, complete cds	1.25E-28	AF390867
234	1315	*Marinobacter aquaeolei* VT8, complete genome	9.13E-79	CP000514
235	1299	*Burkholderia xenovorans* LB400 chromosome 1, complete sequence	1.82E-24	CP000270
243	1334	*Bordetella parapertussis* strain Bpp5 subtractive hybridisation product 6727 genomic sequence	6.87E-55	DQ518927
244	1455	*Chlorobium chlorochromatii* CaD3, complete genome	1.04E-07	CP000108
248	423	*Xanthomonas campestris* pv. vesicatoria complete genome	1.08E-38	AM039952
250	818	*Gramella forsetii* KT0803 complete genome	4.00E-15	CU207366
251	1379	*Pseudomonas syringae* pv. *phaseolicola* 1448A, complete genome	9.52E-05	CP000058
252	891	*Marinobacter aquaeolei* VT8, complete genome	0.00E+00	CP000514

257	1365	*Erythrobacter litoralis* HTCC2594, complete genome	9.42E-05	CP000157
258	1482	*Chromohalobacter salexigens* DSM 3043, complete genome	4.53E-13	CP000285
261	1389	*Marinobacter aquaeolei* VT8, complete genome	0.00E+00	CP000514
261	1389	*Pseudomonas viridiflava* isolate LH215.1b DNA gyrase subunit B (gyrB) gene, partial cds	3.40E-32	AY606739
262	1339	*Pseudomonas aeruginosa* UCBPP-PA14, complete genome	4.74E-25	CP000438
264	1450	*Marinobacter aquaeolei* VT8, complete genome	2.63E-08	CP000514
265	1309	*Gramella forsetii* KT0803 complete genome	2.65E-17	CU207366
267	1722	*Marinobacter aquaeolei* VT8, complete genome	4.71E-04	CP000514
268	1420	*Marinobacter aquaeolei* VT8, complete genome	3.92E-115	CP000514
270	1308	*Marinobacter aquaeolei* VT8, complete genome	4.03E-124	CP000514
271	1180	*Acidovorax* spp. JS42, complete genome	1.86E-144	CP000539
272	1488	*Alkalilimnicola ehrlichei* MLHE-1, complete genome	1.07E-07	CP000453
273	834	*Marinobacter aquaeolei* VT8, complete genome	3.65E-06	CP000514
275	1481	*Marinobacter aquaeolei* VT8 plasmid pMAQU02, complete sequence	3.39E-100	CP000516
276	1241	*Alcanivorax borkumensis* SK2, complete genome	2.01E-36	AM286690
277	1367	*Marinobacter aquaeolei* VT8, complete genome	2.33E-113	CP000514
278	252	*Xanthomonas oryzae* pv. *oryzae* MAFF 311018 DNA, complete genome	2.35E-35	AP008229
280	87	*Xanthomonas campestris* pv. *campestris* str. ATCC 33913, section 70 of 460 of the complete genome	7.80E-11	AE012162
281	175	*Xanthomonas axonopodis* pv. *citri* str. 306, section 183 of 469 of the complete genome	2.96E-49	AE011805
282	98	*Xanthomonas campestris* pv. *campestris* str. ATCC 33913, section 51 of 460 of the complete genome	4.02E-19	AE012143
283	1391	*Marinobacter aquaeolei* VT8, complete genome	3.79E-04	CP000514
284	1401	*Marinobacter aquaeolei* VT8, complete genome	1.30E-28	CP000514
285	1408	*Sinorhizobium meliloti* 1021, complete chromosome	6.25E-43	AL591791
289	1420	*Marinobacter aquaeolei* VT8, complete genome	3.62E-72	CP000514

290	1304	*Maricaulis maris* MCS10, complete genome	1.58E-49	CP000449
292	257	*Polaromonas* spp. JS666, complete genome	7.57E-17	CP000316
294	929	*Marinobacter aquaeolei* VT8, complete genome	1.24E-21	CP000514
297	911	*Marinobacter aquaeolei* VT8, complete genome	9.41E-38	CP000514
299	793	*Marinobacter aquaeolei* VT8, complete genome	4.07E-129	CP000514
300	783	*Marinobacter aquaeolei* VT8, complete genome	8.72E-81	CP000514
301	942	*Marinobacter aquaeolei* VT8, complete genome	2.75E-10	CP000514
302	1284	*Marinobacter aquaeolei* VT8, complete genome	3.63E-07	CP000514
304	717	*Marinobacter aquaeolei* VT8, complete genome	4.38E-33	CP000514
305	1293	*Triticum aestivum* clone wlsu2.pk0001.h3:fis, full insert mRNA sequence	1.68E-18	BT009458
307	1586	*Arthrobacter aurescens* TC1, complete genome	1.14E-07	CP000474
310	2568	*Marinobacter aquaeolei* VT8, complete genome	1.34E-91	CP000514
312	1467	*Marinobacter aquaeolei* VT8, complete genome	5.03E-59	CP000514
313	1905	*Marinobacter aquaeolei* VT8, complete genome	2.69E-61	CP000514
317	1239	*Marinobacter aquaeolei* VT8, complete genome	5.47E-06	CP000514
319	656	*Marinobacter aquaeolei* VT8, complete genome	7.54E-84	CP000514
321	541	*Marinobacter aquaeolei* VT8, complete genome	9.57E-09	CP000514
322	487	*Marinobacter aquaeolei* VT8, complete genome	3.26E-05	CP000514
325	1921	*Marinobacter aquaeolei* VT8, complete genome	1.49E-13	CP000514
326	1446	*Alcanivorax borkumensis* SK2, complete genome	7.16E-15	AM286690
327	1299	*Marinobacter aquaeolei* VT8, complete genome	5.74E-06	CP000514
329	1317	*Tetraodon nigroviridis* full-length cDNA	1.02E-13	CR655357
332	1379	*Marinobacter aquaeolei* VT8, complete genome	7.11E-55	CP000514
336	373	*Marinobacter aquaeolei* VT8, complete genome	1.77E-15	CP000514

337	521	*Xanthomonas campestris* pv. *vesicatoria* complete genome	5.98E-158	AM039952
338	1235	*Marinobacter aquaeolei* VT8, complete genome	1.60E-18	CP000514
340	1599	*Marinobacter aquaeolei* VT8, complete genome	1.61E-34	CP000514
342	1772	*Marinobacter aquaeolei* VT8, complete genome	2.68E-30	CP000514
344	1153	*Pseudomonas syringae* pv. *tomato* str. DC3000 complete genome	2.01E-05	AE016853
345	980	*Marinobacter aquaeolei* VT8, complete genome	9.10E-66	CP000514
347	1637	*Marinobacter aquaeolei* VT8, complete genome	1.27E-13	CP000514
348	1134	*Marinobacter aquaeolei* VT8, complete genome	8.09E-08	CP000514
349	1329	*Marinobacter aquaeolei* VT8, complete genome	3.95E-121	CP000514
350	1108	*Marinobacter aquaeolei* VT8, complete genome	6.63E-104	CP000514
352	2739	*Alcanivorax borkumensis* SK2, complete genome	4.08E-175	AM286690
354	1142	*Marinobacter aquaeolei* VT8, complete genome	5.07E-80	CP000514
355	1798	*Marinobacter aquaeolei* VT8, complete genome	3.80E-20	CP000514
357	1553	*Marinobacter aquaeolei* VT8, complete genome	1.88E-12	CP000514
358	1998	*Pelobacter propionicus* DSM 2379 plasmid pPRO1, complete sequence	3.51E-05	CP000483
359	990	*Gramella forsetii* KT0803 complete genome	5.65E-27	CU207366
360	267	*Azoarcus* spp. EbN1 complete genome	2.89E-10	CR555306
364	2104	*Marinobacter aquaeolei* VT8, complete genome	6.22E-10	CP000514
369	2065	*Marinobacter aquaeolei* VT8, complete genome	3.92E-48	CP000514
373	1535	*Marinobacter aquaeolei* VT8, complete genome	2.15E-24	CP000514
376	1371	*Ralstonia eutropha* H16 chromosome 2	7.87E-27	AM260480
377	1353	*Marinobacter aquaeolei* VT8, complete genome	6.94E-18	CP000514
378	1110	*Marinobacter aquaeolei* VT8, complete genome	5.29E-49	CP000514
379	2359	*Marinobacter aquaeolei* VT8, complete genome	1.10E-119	CP000514

380	1061	*Gramella forsetii* KT0803 complete genome	1.65E-33	CU207366
381	1973	*Marinobacter aquaeolei* VT8, complete genome	0.00E+00	CP000514
384	1066	*Marinobacter aquaeolei* VT8, complete genome	1.49E-24	CP000514
385	1109	*Alcanivorax borkumensis* SK2, complete genome	0.00E+00	AM286690
385	1109	*Alcanivorax borkumensis* SK2, complete genome	2.00E-08	AM286690
386	1824	*Marinobacter aquaeolei* VT8, complete genome	1.02E-60	CP000514
388	1402	*Marinobacter aquaeolei* VT8, complete genome	6.22E-43	CP000514
390	2402	*Roseobacter denitrificans* OCh 114 plasmid pTB4, complete sequence	1.16E-85	CP000467
391	1208	*Marinobacter aquaeolei* VT8, complete genome	3.07E-72	CP000514
396	1967	*Marinobacter aquaeolei* VT8, complete genome	1.42E-07	CP000514
397	1724	*Marinobacter aquaeolei* VT8, complete genome	5.52E-90	CP000514
398	1695	*Marinobacter aquaeolei* VT8, complete genome	0.00E+00	CP000514
399	2068	*Saccharopolyspora erythraea* NRRL2338 complete genome	5.67E-04	AM420293
400	1912	*Marinobacter aquaeolei* VT8, complete genome	1.56E-164	CP000514
402	706	*Xanthomonas axonopodis* pv. *citri* str. 306, section 130 of 469 of the complete genome	1.01E-27	AE011752
403	801	*Dechloromonas aromatica* RCB, complete genome	1.49E-11	CP000089
405	2776	*Marinobacter aquaeolei* VT8, complete genome	0.00E+00	CP000514
407	1562	*Marinobacter aquaeolei* VT8, complete genome	8.79E-172	CP000514
410	2103	*Marinobacter aquaeolei* VT8, complete genome	1.90E-25	CP000514
411	2907	*Dechloromonas aromatica* RCB, complete genome	5.12E-05	CP000089
413	1196	*Marinobacter aquaeolei* VT8, complete genome	9.56E-17	CP000514
Contig	**Length**	**BLASTn results virus database**	**E-value**	**Accession #**
1	1150	Enterobacteria phage Sf6, complete genome	1.00E-04	AF547987
3	881	*Prunus* necrotic ringspot virus mRNA for coat protein (CP gene) from Kullu, India	2.00E-25	AM408910

9	637	*Salmonella enterica* subsp. *enterica* serovar Choleraesuis str. SC-B67, complete genome	8.00E-14	AE017220
10	1751	*Azoarcus* spp. BH72, complete genome	3.00E-06	AM406670
19	694	*Azoarcus* spp. BH72, complete genome	5.00E-09	AM406670
21	985	*Azoarcus* spp. BH72, complete genome	8.00E-18	AM406670
36	1026	*Salmonella enterica* subsp. *enterica* serovar Choleraesuis str. SC-B67, complete genome	2.00E-25	AE017220
43	953	*Azoarcus* spp. BH72, complete genome	2.00E-09	AM406670
50	549	*Prunus* necrotic ringspot virus mRNA for coat protein (CP gene) from Kullu, India	2.00E-26	AM408910
56	1400	*Salmonella enterica* subsp. *enterica* serovar Choleraesuis str. SC-B67, complete genome	6.00E-04	AE017220
58	993	*Saccharopolyspora erythraea* NRRL2338 complete genome	2.00E-06	AM420293
62	1105	*Azoarcus* spp. BH72, complete genome	2.00E-15	AM406670
66	949	*Azoarcus* spp. BH72, complete genome	1.00E-25	AM406670
69	1373	*Azoarcus* spp. BH72, complete genome	1.00E-05	AM406670
73	1262	*Azoarcus* spp. BH72, complete genome	9.00E-09	AM406670
99	1508	*Azoarcus* spp. BH72, complete genome	3.00E-09	AM406670
102	1611	*Salmonella enterica* subsp. *enterica* serovar Choleraesuis str. SC-B67, complete genome	2.00E-04	AE017220
106	912	Hepatitis C virus (isolate D54) polyprotein gene, partial cds	4.00E-04	DQ155561
107	1214	*Azoarcus* spp. BH72, complete genome	2.00E-09	AM406670
110	516	*Azoarcus* spp. BH72, complete genome	9.00E-04	AM406670
126	434	*Azoarcus* spp. BH72, complete genome	2.00E-10	AM406670
127	673	*Salmonella enterica* subsp. *enterica* serovar Choleraesuis str. SC-B67, complete genome	2.00E-14	AE017220
131	1194	*Salmonella enterica* subsp. *enterica* serovar Choleraesuis str. SC-B67, complete genome	9.00E-12	AE017220
144	1149	*Bacillus cereus* ATCC 14579, complete genome	2.00E-22	AE016877
150	573	Porcine endogenous retrovirus PERV-B6 env gene for envelope protein, genomic RNA	6.00E-05	AJ288591
154	698	*Azoarcus* spp. BH72, complete genome	1.00E-12	AM406670

164	1290	*Salmonella enterica* subsp. *enterica* serovar Choleraesuis str. SC-B67, complete genome	6.00E-10	AE017220
166	1077	*Azoarcus* spp. BH72, complete genome	5.00E-07	AM406670
194	1396	*Azoarcus* spp. BH72, complete genome	1.00E-17	AM406670
198	1850	*Saccharopolyspora erythraea* NRRL2338 complete genome	4.00E-09	AM420293
201	1521	*Azoarcus* spp. BH72, complete genome	2.00E-04	AM406670
207	1627	*Streptococcus pyogenes* MGAS6180, complete genome	5.00E-08	CP000056
214	1440	*Salmonella enterica* subsp. *enterica* serovar Choleraesuis str. SC-B67, complete genome	1.00E-14	AE017220
216	1075	*Salmonella enterica* subsp. *enterica* serovar Choleraesuis str. SC-B67, complete genome	4.00E-54	AE017220
234	1315	*Azoarcus* spp. BH72, complete genome	6.00E-07	AM406670
252	891	*Azoarcus* spp. BH72, complete genome	8.00E-24	AM406670
261	1389	*Salmonella enterica* subsp. *enterica* serovar Choleraesuis str. SC-B67, complete genome	6.00E-32	AE017220
276	1241	*Azoarcus* spp. BH72, complete genome	7.00E-25	AM406670
277	1367	*Azoarcus* spp. BH72, complete genome	4.00E-05	AM406670
281	175	*Azoarcus* spp. BH72, complete genome	8.00E-11	AM406670
290	1304	*Azoarcus* spp. BH72, complete genome	1.00E-04	AM406670
294	929	*Azoarcus* spp. BH72, complete genome	1.00E-04	AM406670
305	1293	Cucumber mosaic virus segment RNA 1 complete sequence	1.77E-19	AJ879490
313	1905	*Azoarcus* spp. BH72, complete genome	6.62E-20	AM406670
326	1446	*Salmonella enterica* subsp. *enterica* serovar Choleraesuis str. SC-B67, complete genome	4.15E-05	AE017220
336	1446	*Saccharopolyspora erythraea* NRRL2338 complete genome	1.61E-04	AM420293
337	521	*Saccharopolyspora erythraea* NRRL2338 complete genome	1.58E-11	AM420293
340	1599	*Salmonella enterica* subsp. *enterica* serovar Choleraesuis str. SC-B67, complete genome	8.03E-13	AE017220
350	1108	*Azoarcus* spp. BH72, complete genome	2.19E-12	AM406670
352	2739	*Azoarcus* spp. BH72, complete genome	3.51E-50	AM406670

354	1142	*Salmonella enterica* subsp. *enterica* serovar Choleraesuis str. SC-B67, complete genome	5.31E-44	AE017220
359	990	*Streptococcus pyogenes* M1 GAS, complete genome	1.25E-13	AE004092
360	267	*Azoarcus* spp. BH72, complete genome	2.86E-05	AM406670
379	2359	*Azoarcus* spp. BH72, complete genome	4.69E-12	AM406670
380	1061	*Salmonella enterica* subsp. *enterica* serovar Choleraesuis str. SC-B67, complete genome	4.91E-07	AE017220
381	1973	*Saccharopolyspora erythraea* NRRL2338 complete genome	3.64E-06	AM420293
386	1824	*Salmonella enterica* subsp. *enterica* serovar Choleraesuis str. SC-B67, complete genome	1.38E-08	AE017220
391	1208	*Azoarcus* spp. BH72, complete genome	3.46E-05	AM406670
397	1724	*Salmonella enterica* subsp. *enterica* serovar Choleraesuis str. SC-B67, complete genome	1.26E-05	AE017220
399	2068	*Saccharopolyspora erythraea* NRRL2338 complete genome	1.51E-05	AM420293
400	1912	*Azoarcus* spp. BH72, complete genome	4.94E-33	AM406670
407	1562	*Azoarcus* spp. BH72, complete genome	2.99E-09	AM406670

Contig	**Length**	**BLASTx results**	**E-value**	**Accession #**
12	727	Replication protein C [*Roseovarius* spp. 217]	2.92E-77	ZP_01038470
17	836	putative acyl-CoA dehydrogenase [*Pseudomonas stutzeri* A1501]	1.82E-79	ABP77808
19	694	exporters of the RND superfamily [*Marinobacter aquaeolei* VT8]	2.74E-98	YP_959332
21	985	RNA polymerase, sigma 32 subunit, RpoH [*Marinobacter aquaeolei* VT8]	6.68E-74	YP_960999
28	1080	HflK protein [*Marinobacter aquaeolei* VT8]	4.89E-145	YP_960029
37	549	signal transduction histidine kinase [*Marinobacter aquaeolei* VT8]	1.65E-47	YP_960159
56	1400	ribosomal protein S6 modification protein [*Stappia aggregata* IAM 12614]	2.14E-109	ZP_01546195
61	534	sodium:neurotransmitter symporter [*Marinobacter aquaeolei* VT8]	4.61E-60	YP_957556
62	1105	triosephosphate isomerase [*Marinobacter* spp. ELB17]	4.02E-41	ZP_01735869
67	567	MATE efflux family protein [*Marinobacter aquaeolei* VT8]	1.74E-82	YP_957355
70	716	Ornithine cyclodeaminase [*Sphingomonas wittichii* RW1]	7.10E-28	ZP_01606249

73	1262	probable iron-sulphur protein [*Pseudomonas stutzeri* A1501]	7.34E-90	ABP80967
78	1370	transglutaminase domain protein [*Marinobacter aquaeolei* VT8]	1.16E-59	YP_958846
82	1677	siderophor receptor, TonB-dependent [*Marinobacter* spp. ELB17]	5.04E-165	ZP_01739345
87	1294	OmpA/MotB domain protein [*Marinobacter aquaeolei* VT8]	8.03E-140	YP_960912
89	1553	37kDa nucleoid-associated protein [*Marinobacter aquaeolei* VT8]	6.23E-159	YP_959998
93	632	HesB/YadR/YfhF-family protein [*Marinobacter aquaeolei* VT8]	2.00E-54	YP_958796
106	912	anti-ECFsigma factor, ChrR [*Marinobacter aquaeolei* VT8]	1.46E-93	YP_957712
110	516	type IV-A pilus assembly ATPase PilB [*Marinobacter aquaeolei* VT8]	3.45E-83	YP_959943
116	1586	putative silver efflux pump [*Hahella chejuensis* KCTC 2396]	0.00E+00	YP_434212
122	1222	protein containing tetratricopeptide repeat [*Marinobacter aquaeolei* VT8]	3.21E-79	YP_959307
129	1581	type III restriction enzyme, res subunit [*Marinobacter aquaeolei* VT8]	1.07E-104	YP_960220
146	716	RNA-directed DNA polymerase [*Burkholderia xenovorans* LB400]	6.55E-103	YP_559418
147	1068	pilus (MSHA type) biogenesis protein MshL [*Marinobacter aquaeolei* VT8]	2.50E-126	YP_958037
148	487	Protein IpsA [*Dichelobacter nodosus*]	3.15E-50	P39907
157	1225	sodium/hydrogen exchanger [*Marinobacter aquaeolei* VT8]	1.54E-81	YP_957416
183	1193	putative competence-damage inducible [*Flavobacteriales bacterium* HTCC2170]	1.93E-89	ZP_01108150
214	1440	preprotein translocase, SecY subunit [*Marinobacter aquaeolei* VT8]	2.51E-73	YP_958023
217	1088	F0F1 ATP synthase subunit B [*Marinobacter* spp. ELB17]	4.08E-61	ZP_01738573
221	1060	thiamine pyrophosphate-requiring enzyme [*Hahella chejuensis* KCTC 2396]	2.26E-99	YP_433790
222	1061	Maltoporin precursor (Maltose-inducible porin) [*Aeromonas salmonicida*]	1.83E-24	Q44287
231	1340	plasmid partitioning ATPase [*Paracoccus versutus*]	7.79E-85	AAL56549
235	1299	putative 2-nitropropane dioxygenase [*Ralstonia eutropha* H16]	2.91E-113	NP_943030
247	1339	PA14 domain protein [*Marinobacter aquaeolei* VT8]	1.14E-24	YP_958892
266	512	trehalose-6-phosphate synthase [Flavobacteriales bacterium HTCC2170]	2.44E-49	ZP_01106094

269	1140	Bap-like [*Trichomonas vaginalis* G3]	1.33E-07	XP_001328612
274	1424	TraB [*Photobacterium damselae* subsp. *piscicida*]	8.48E-74	YP_908651
276	1241	Ribonuclease H [*Marinobacter aquaeolei* VT8]	1.62E-94	YP_959796
285	1408	translocation protein TolB precursor [*Stappia aggregata* IAM 12614]	2.02E-89	ZP_01545734
289	1420	DNA mismatch repair protein MutS [*Marinobacter aquaeolei* VT8]	7.62E-91	YP_959354
292	257	40-residue YVTN family beta-propeller repeat protein [*Delftia acidovorans* SPH-1]	3.62E-43	ZP_01577728
296	942	putative Mannose-sensitive agglutinin biogenesis protein MshQ [*Alteromonas macleodii*]	8.97E-17	ZP_01108616
298	1036	sensor histidine kinase [*Oceanospirillum* spp. MED92]	8.00E-17	ZP_01165811
299	793	CTP synthase [*Marinobacter aquaeolei* VT8]	1.27E-105	YP_958202
301	942	putative signal transduction protein [*Marinobacter aquaeolei* VT8]	1.27E-87	YP_959499
305	1293	PREDICTED: similar to retinoid X receptor alpha isoform 4 [*Bos taurus*]	7.56E-18	XP_887036
306	1403	putative protein with predicted kinase domain [*Alteromonadales bacterium* TW-7]	1.17E-75	ZP_01611785
312	1467	wax ester synthase [*Marinobacter hydrocarbonoclasticus*]	0.00E+00	ABO21021
313	1905	Multimeric flavodoxin WrbA [*Marinobacter* spp. ELB17]	1.32E-67	ZP_01738839
315	747	sensory box histidine kinase/response regulator [*Marinobacter* spp. ELB17]	1.39E-70	ZP_01737019
323	893	TPP-dependent acetoin dehydrogenase complex [*Colwellia psychrerythraea* 34H]	7.55E-63	YP_269750
329	1317	PREDICTED: similar to CG6439-PA [*Tribolium castaneum*]	2.48E-48	XP_973953
338	1235	riboflavin biosynthesis protein RibF [*Marinobacter aquaeolei* VT8]	8.22E-107	YP_958144
343	1985	multicopper oxidase family protein [*Marinobacter* spp. ELB17]	2.72E-156	ZP_01735813
345	980	UDP-glucose 4-epimerase [*Marinobacter aquaeolei* VT8]	1.48E-102	YP_958982
349	1329	Succinylglutamate desuccinylase/aspartoacylase [*Marinobacter aquaeolei* VT8]	6.92E-115	YP_959615
350	1108	oxygen-independent coproporphyrinogen III oxidase [*Marinobacter aquaeolei* VT8]	1.11E-136	YP_960361
351	1889	integrase/recombinase XerC [*Listeria welshimeri* serovar 6b str. SLCC5334]	2.35E-08	YP_849491
355	1798	putative RNA methylase [*Marinobacter aquaeolei* VT8]	0.00E+00	YP_958318

376	1371	D-amino acid dehydrogenase small subunit [*Marinobacter* spp. ELB17]	2.00E-35	ZP_01737201
378	1110	Secreted/periplasmic Zn-dependent peptidase, insulinase-like protein [*Marinobacter* spp. ELB17]	3.83E-108	ZP_01736964
388	1402	dihydroorotase, multifunctional complex type [*Marinobacter aquaeolei* VT8]	7.41E-86	YP_961016
389	755	putative porin protein [*Methylibium petroleiphilum* PM1]	2.52E-26	YP_001019556
390	2402	RepA [*Roseobacter denitrificans* OCh 114]	2.15E-121	YP_771892
391	1208	Ribosomal protein S7 [*Marinobacter* spp. ELB17]	1.25E-131	ZP_01738518
393	1408	transfer system protein TraE [*Salmonella enterica* subsp. *enterica* serovar Newport str. SL254]	5.08E-42	YP_001101953
397	1724	FeS assembly protein SufD [*Marinobacter aquaeolei* VT8]	4.70E-145	YP_960414
401	1003	Sigma-70, region 4 type 2 [*Shewanella denitrificans* OS217]	1.92E-36	YP_561581
405	2776	flagellar motor switch protein FliG [*Marinobacter aquaeolei* VT8]	4.03E-156	YP_959264
Contig	**Length**	**BLASTx results virus database**	**E-value**	**Accession #**
1	1150	gene 56 protein [Enterobacteria phage Sf6]	3.00E-24	AAQ12256
15	754	Fusion protein, Feo [Hepatitis C virus]	4.00E-09	BAD00047
18	1371	similar to DNA helicase [Bacteriophage RM 378]	6.00E-50	NP_835691
20	1230	putative ATP-binding cassette transporter [*Amsacta moorei* entomopoxvirus]	3.00E-04	AAG02836
35	1185	NADH dehydrogenase subunit B [*Echinochloa crus-galli*]	4.00E-25	CAD58586
36	1026	DNA polymerase III alpha subunit [*Saccharomonospora* phage PIS 136]	3.00E-77	AAL66178
38	560	putative ATP-binding cassette transporter [*Amsacta moorei* entomopoxvirus]	2.00E-04	AAG02836
50	560	cytochrome oxidase subunit I [*Aedes w-albus*]	4.00E-35	AAQ01584
52	1100	gp2 [Equid herpesvirus 1]	4.00E-04	AAU09476
54	1003	putative non-heme haloperoxidase [Mycobacteriophage D29]	3.00E-04	AAC18502
57	1121	Crip-31 [*Clerodendrum inerme*]	9.00E-07	AAN07178
64	706	pseudomonas resinovorans ORF80-like [*Ralstonia solanacearum* phage RSA1]	4.00E-19	BAF52423
64	706	hypothetical protein HK022p32 [Enterobacteria phage HK022]	5.00E-17	NP_597891

66	949	Zn-dependent alcohol dehydrogenase [*Acanthamoeba polyphaga mimivirus*]	3.00E-11	AAV50763
71	1313	DUF955 [*Clostridium* phage phiC2]	2.00E-06	YP_001110758
75	703	Orf-87 [*Salmonella typhimurium* bacteriophage ST64T]	1.00E-07	NP_720284
79	700	gp3 [Mycobacteriophage Qyrzula]	7.00E-18	YP_655683
80	1354	Hypothetical protein BHLF1 early reading frame [Human herpesvirus 4 type 1]	9.00E-04	P03181
84	1160	hypothetical protein ORF012L [Singapore grouper iridovirus]	5.00E-04	YP_164107
85	1557	methyltransferase [*Clostridium difficile* bacteriophage phi CD119]	6.00E-04	YP_529621
89	1553	nucleoid-associated protein [*Pseudomonas aeruginosa* phage F116]	2.00E-14	AAT45874
99	1508	glutamine:fructose-6-phosphate amidotransferase GFAT [*Chlorella* virus]	4.00E-96	BAD15299
115	556	Stage 0 sporulation protein J [*Bacillus* spp. B14905]	7.00E-11	ZP_01724179
123	1047	type II DNA-methyltransferase [Bacteriophage phi-3T]	2.00E-06	CAA56493
129	673	putative helicase [*Listonella pelagia* phage phiHSIC]	5.00E-30	YP_224270
131	1194	integrase [bacteriophage bIL310]	2.00E-10	AAK08405
140	1626	putative triacylglycerol lipase [*Acanthamoeba polyphaga mimivirus*]	7.00E-08	AAV50790
144	1149	putative type III secretion system ATP synthase [*Candidatus* Hamiltonella defensa]	3.00E-15	ABA29443
145	1229	putative DNA methylase [*Sinorhizobium meliloti* phage PBC5]	4.00E-08	NP_542283
146	716	reverse transcriptase [*Bordetella* phage BPP-1]	9.00E-05	NP_958675
147	1068	unnamed protein product [Enterobacteria phage Ike]	2.00E-05	CAA26076
151	725	putative transposase [*Staphylococcus* phage phiPVL108]	3.00E-04	BAF41205
154	698	phospholipase D/Transphosphatidylase [*Anaeromyxobacter* spp. Fw109-5]	2.00E-06	ZP_01667863
161	1317	head-tail preconnector protein gp5 of bacteriophage [*Escherichia coli* UTI89]	1.00E-16	AAA32343
163	1496	Hypothetical protein BHLF1 early reading frame [Human herpesvirus 4]	8.00E-04	P03181
165	1515	voltage-dependent calcium channel [*Loligo bleekeri*]	3.00E-15	BAA13136
172	702	LYCV glycosyl hydrolase [*Clostridium acetobutylicum* ATCC 824]	4.00E-04	AAK76896

191	892	putative ATP-binding cassette transporter [*Amsacta moorei* entomopoxvirus]	1.00E-12	AAG02836
207	1627	unknown [*Diachasmimorpha longicaudata* entomopoxvirus]	2.00E-04	AAT99858
234	1315	T7 Dna Polymerase Ternary Complex With 8 Oxo Guanosine And Ddctp At The Insertion Site	9.00E-38	1TK0_B
234	1315	thioredoxin, putative [*Aspergillus fumigatus* Af293]	8.00E-04	EAL91252
244	1455	putative transglycosylase [Bacteriophage SPBc2]	3.00E-08	AAC13005
250	818	thioredoxine reductase [*Streptococcus pneumoniae*]	3.00E-08	CAB96624
257	1365	Replication factor C [*Staphylothermus marinus* F1]	7.00E-09	YP_001041227
261	1389	putative DNA gyrase B subunit [*Clostridium* phage c-st]	8.00E-16	BAE47797
276	1241	putative ribonuclease [*Emiliania huxleyi* virus 86]	9.00E-29	CAI65828
278	252	Aspartyl-tRNA synthetase bacterial/mitochondrial type [*Ralstonia eutropha* JMP134]	9.00E-10	AAZ59821
303	1202	Polyphosphate kinase [*Azotobacter vinelandii* AvOP]	3.00E-06	EAM06691
313	1905	gp117 [Mycobacteriophage CJW1]	2.00E-08	NP_817564
326	1446	gene 56 protein [Enterobacteria phage Sf6]	2.00E-23	AAQ12256
336	373	UL36 [*Cercopithecine* herpesvirus 16]	1.00E-03	ABA29290
340	1599	Chlorella virus CVK2 translation elongation factor homolog [*Paramecium bursaria Chlorella* virus 1]	1.00E-27	NP_049022
342	1772	response regulator protein [*Bacillus thuringiensis* phage MZTP02]	1.00E-08	AAX62130
345	980	nucleotide-sugar epimerase [Cyanophage P-SSM2]	2.00E-14	AAX44647
346	840	EBNA-1 [Human herpesvirus 4 type 2]	7.00E-05	YP_001129471
351	1889	phage-related integrase [Cyanophage P-SSP7]	3.00E-04	AAX44192
356	1442	DNA primase bacterial DnaG type [*Thermus thermophilus* phage YS40]	1.00E-11	YP_874036
360	267	orf229 gp [*Streptococcus thermophilus* bacteriophage Sfi19]	5.00E-08	AAD44067
378	1110	putative Zn-dependent peptidase [*Acanthamoeba polyphaga mimivirus*]	2.00E-13	AAV50506
391	1208	hypothetical protein PSSM2_176 [Cyanophage P-SSM2]	1.00E-55	AAX44554
394	977	putative DNA polymerase [*Staphylococcus* phage K]	3.00E-30	YP_024516

397	1724	aminotransferase [Environmental halophage 1 AAJ-2005]	1.00E-38	ABB77916
398	1695	putative monoglyceride lipase [Cowpox virus]	9.00E-04	ABD97390
405	2776	transposase [*Sodalis* phage phiSG1]	2.00E-04	BAE80487
410	2103	gp32 [Mycobacteriophage Halo]	4.00E-10	YP_655549
411	2907	FirrV-1-B9 [*Feldmannia irregularis* virus a]	2.00E-10	AAR26884

REFERENCES

Ackermann, H. W. (1987). Bacteriophage taxonomy in 1987. *Microbiological Sciences* **4**, 214-218.

Ackermann, H. W. & DuBow, M. S. (1987). *Viruses of Prokaryotes*. Boca Raton, Florida: CRC Press.

Ackermann, H. W., Berthiaume, B. L. & Tremblay, M. (1998). *Virus Life in Diagrams* Boca Raton, Florida: CRC Press LLC.

Ackermann, H. W. (2001). Frequency of morphological phage descriptions in the year 2000. Brief review. *Archives of Virology* **146**, 843-857.

Ackermann, H. W. (2007). 5500 Phages examined in the electron microscope. *Archives of Virology* **152**, 227-243.

Agranovsky, A. A., Lesemann, D. E., Maiss, E., Hull, R. & Atabekov, J. G. (1995). "Rattlesnake" structure of a filamentous plant RNA virus built of two capsid proteins. *Proceedings of the National Academy of Sciences* **92**, 2470-2473.

Alavi, M., Miller, T., Erlandson, K., Schneider, R. & Belas, R. (2001). Bacterial community associated with *Pfiesteria*-like dinoflagellate cultures. *Environmental Microbiology* **3**, 380-396.

Alberts, B., Bray, D., Lewis, J., Raff, M., Roberts, K. & Watson, J. D. (1994). *Molecular Biology of The Cell.* New York, New York: Garland Publishing.

Allen, M. J., Schroeder, D. C., Holden, M. T. & Wilson, W. H. (2006a). Evolutionary history of the Coccolithoviridae. *Molecular Biology and Evolution* **23**, 86-92.

Allen, M. J., Forster, T., Schroeder, D. C., Hall, M., Roy, D., Ghazal, P. & Wilson, W. H. (2006b). Locus-specific gene expression pattern suggests a unique propagation strategy for a giant algal virus. *Journal of Virology* **80**, 7699-7705.

Altschul, S. F., Madden, T. L., Schaffer, A. A., Zhang, J., Zhang, Z., Miller, W. & Lipman, D. J. (1997). Gapped BLAST and PSI-BLAST: a new generation of protein database search programs. *Nucleic Acids Research* **25**, 3389-3402.

Angly, F. E., Felts, B., Breitbart, M. & other authors (2006). The marine viromes of four oceanic regions. *PLoS Biology* **4**, e368.

Attoui, H., Jaafar, F. M., Belhouchet, M., de Micco, P., de Lamballerie, X. & Brussaard, C. P. (2006). *Micromonas pusilla* reovirus: a new member of the family Reoviridae assigned to a novel proposed genus (Mimoreovirus). *Journal of General Virology* **87**, 1375-1383.

Bailey, S., Clokie, M. R., Millard, A. & Mann, N. H. (2004). Cyanophage infection and photoinhibition in marine cyanobacteria. *Research in Microbiology* **155**, 720-725.

Baker, A. (2005). Ph.D. thesis. Molecular Investigations of Freshwater Cyanophages: University of Leeds. Leeds, United Kingdom.

Baker, A. C. (2001). Reef corals bleach to survive change. *Nature* **411**, 765-766.

Baker, A. C. (2003). Flexibility and specificity in coral-algal symbiosis: diversity, ecology, and biogeography of *Symbiodinium. Annual Review of Ecology, Evolution and Systematics* **34**, 661-689.

Baker, A. C. & Rowan, R. (1997). Diversity of symbiotic dinoflagellates (zooxanthellae) in scleractinian corals of the Caribbean and eastern Pacific. *Proceeding of the 8th International Coral Reef Symposium* **2**, 1301-1306.

Baker, A. C., Starger, C. J., McClanahan, T. R. & Glynn, P. W. (2004). Corals' adaptive response to climate change. *Nature* **430**, 741.

Baker, A. C., Goddard, V. J., Davy, J., Schroeder, D. C., Adams, D. G. & Wilson, W. H. (2006). Identification of a diagnostic marker to detect freshwater cyanophages of filamentous cyanobacteria. *Applied and Environmental Microbiology* **72**, 5713-5719.

Baltimore, D. (1971). Expression of animal virus genomes. *Bacteriological Reviews* **35**, 235-241.

Banin, E., Ben-Haim, Y., Israely, T., Loya, Y. and Rosenberg, E. (2000). Effect of the environment on the bacterial bleaching of corals. *Water, Air and Soil Pollution* **123**, 337-352.

Baptista, M. S. & Vasconcelos, M. T. (2006). Cyanobacteria metal interactions: requirements, toxicity, and ecological implications. *Critical Reviews in Microbiology* **32**, 127-137.

Baudoux, A. C. & Brussaard, C. P. (2005). Characterization of different viruses infecting the marine harmful algal bloom species *Phaeocystis globosa*. *Virology* **341**, 80-90.

Beltrami, E. & Carroll, T. O. (1994). Modeling the role of viral disease in recurrent phytoplankton blooms. *Journal of Mathematical Biology* **32**, 857-863.

Ben-Haim, Y., Zicherman-Keren, M. & Rosenberg, E. (2003). Temperature-regulated bleaching and lysis of the coral *Pocillopora damicornis* by the novel pathogen *Vibrio coralliilyticus*. *Applied and Environmental Microbiology* **69**, 4236-4242.

Bergh, Ø., Børsheim, K. Y., Bratbak, G. & Heldal, M. (1989). High abundance of viruses found in aquatic environments. *Nature* **340**, 467-468.

Berman-Frank, I., Lundgren, P. & Falkowski, P. (2003). Nitrogen fixation and photosynthetic oxygen evolution in cyanobacteria. *Research in Microbiology* **154**, 157-164.

Besemer, J. & Borodovsky, M. (1999). Heuristic approach to deriving models for gene finding. *Nucleic Acids Research* **27**, 3911-3920.

Bhattacharya, D. & Medlin, L. (1998). Algal phylogeny and the origin of land plants. *Plant Physiology* **116**, 9-15.

Bisen, P. S., Audholia, S., Bhatnagar, A. K. & Bagchi, S. N. (1986). Evidence for lysogeny and viral resistance in the cyanobacterium *Phormidium uncinatum*. *Current Microbiology* **13**, 1-6.

Bobik, T. A. (2007). Bacterial Microcompartments. *Microbe* **2**, 25-31.

Borowitzka, M. (1997). Microalgae for aquaculture: Opportunities and constraints. *Journal of Applied Phycology* **9**, 393-401.

Breitbart, M., Salamon, P., Andresen, B., Mahaffy, J. M., Segall, A. M., Mead, D., Azam, F. & Rohwer, F. (2002). Genomic analysis of uncultured marine viral communities. *Proceedings of the National Academy of Sciences of the United States of America* **99**, 14250-14255.

Breitbart, M. & Rohwer, F. (2005). Here a virus, there a virus, everywhere the same virus? *Trends Microbiol* **13**, 278-284.

Brown, B. E. (1997). Coral bleaching: causes and consequences. *Coral Reefs* **16**, 129-138.

Brussaard, C. (2004a). Viral control of phytoplankton populations - a review. *The Journal of Eukaryotic Microbiology* **51**, 125-138.

Brussaard, C. P., Marie, D. & Bratbak, G. (2000). Flow cytometric detection of viruses. *Journal of Virological Methods* **85**, 175-182.

Brussaard, C. P., Noordeloos, A. A., Sandaa, R. A., Heldal, M. & Bratbak, G. (2004a). Discovery of a dsRNA virus infecting the marine photosynthetic protist *Micromonas pusilla*. *Virology* **319**, 280-291.

Brussaard, C. P., Short, S. M., Frederickson, C. M. & Suttle, C. A. (2004b). Isolation and phylogenetic analysis of novel viruses infecting the phytoplankton *Phaeocystis globosa* (Prymnesiophyceae). *Applied and Environmental Microbiology* **70**, 3700-3705.

Brussaard, C. P. D. (2004b). Optimization of procedures for counting viruses by flow cytometry. *Applied and Environmental Microbiology* **70**, 1506-1513.

Bubeck, J. A. & Pfitzner, A. J. (2005). Isolation and characterization of a new type of chlorovirus that infects an endosymbiotic Chlorella strain of the heliozoon *Acanthocystis turfacea*. *Journal of General Virology* **86**, 2871-2877.

Buddemeier, R. W. & Fautin, D. G. (1993). Coral bleaching as an adaptive mechanism—a testable hypothesis. *BioScience* **43**, 320–326.

Buitenhuis, E. T., van der Wal, P. & de Baar, H. J. W. (2001). Blooms of *Emiliania huxleyi* are sinks of atmospheric carbon dioxide: A field and mesocosm study derived simulation. *Global Biogeochemical Cycles* **15**, 577-587.

Burkholder, J. M. & Glasgow, H. B., Jr. (1997). Trophic controls on stage transformations of a toxic ambush-predator dinoflagellate. *The Journal of Eukaryotic Microbiology* **44**, 200-205.

Calendar, R. (2006). *The Bacteriophages*, Second edn. New York, New York: Oxford University Press, Inc.

Calkins, J. & Thordardottir, T. (1980). The ecological significance of solar UV radiation on aquatic organisms. *Nature* **283**, 563-566.

Cann, A. J. (2001). *Principles of Molecular Virology* Third edn. London: Academic Press.

Cannon, R. E., Shane, M. S. & Bush, V. N. (1971). Lysogeny of a blue-green alga, *Plectonema boryanum*. *Virology* **45**, 149-153.

Capone, D. G. (2001). Marine nitrogen fixation: what's the fuss? *Current Opinion in Microbiology* **4**, 341-348.

Carlos, A. A., Baillie, B. K., Kawachi, M. & Maruyama, T. (1999). Phylogenetic position of *Symbiodinium* (Dinophyceae) isolates from Tridacnids (Bivalvia), Cardiids (Bivalvia), a sponge (Porifera), a soft coral (Anthozoa), and a free-living strain. *Journal of Phycology* **35**, 1054-1062.

Cavalier-Smith, T. (2002). The phagotrophic origin of eukaryotes and phylogenetic classification of Protozoa. *International Journal of Systematic and Evolutionary Microbiology* **52**, 297-354.

Chen, F. & Suttle, C. A. (1996). Evolutionary relationships among large double-stranded DNA viruses that infect microalgae and other organisms as inferred from DNA polymerase genes. *Virology* **219**, 170-178.

Chen, F. & Lu, J. (2002). Genomic sequence and evolution of marine cyanophage P60: a new insight on lytic and lysogenic phages. *Applied and Environmental Microbiology* **68**, 2589-2594.

Chen, F., Lu, J. R., Binder, B. J., Liu, Y. C. & Hodson, R. E. (2001). Application of digital image analysis and flow cytometry to enumerate marine viruses stained with SYBR gold. *Applied and Environmental Microbiology* **67**, 539-545.

Cho, H. H., Park, H. H., Kim, J. O. & Choi, T. J. (2002). Isolation and characterization of Chlorella viruses from freshwater sources in Korea. *Molecules and Cells* **14**, 168-176.

Clokie, M. R. & Mann, N. H. (2006). Marine cyanophages and light. *Environmental Microbiology* **8**, 2074-2082.

Clokie, M. R. J., Millard, A. D., Mehta, J. Y. & Mann, N. H. (2006). Virus isolation studies suggest short-term variations in abundance in natural cyanophage populations of the Indian Ocean. *Journal of the Marine Biological Association of the United Kingdom* **86**, 499-505.

Cochran, P. K. & Paul, J. H. (1998). Seasonal abundance of lysogenic bacteria in a subtropical estuary. *Applied and Environmental Microbiology* **64**, 2308-2312.

Coffroth, M. A. & Santos, S. R. (2005). Genetic diversity of symbiotic dinoflagellates in the genus Symbiodinium. *Protist* **156** 19-34.

Culley, A. I., Lang, A. S. & Suttle, C. A. (2003). High diversity of unknown picorna-like viruses in the sea. *Nature* **424**, 1054-1057.

Davy, S. K., Lucas, I. A. N. & Turner, J. R. (1996). Carbon budgets in temperate anthozoan-dinoflagellate symbioses. *Marine Biology* **126**, 773-783.

Davy, S. K., Burchett, S. G., Dale, A. L., Davies, P., Davy , J. E., Muncke, C., Hoegh-Guldberg, O. & Wilson, W. H. (2006). Viruses: Agents of coral disease? *Diseases of Aquatic Organisms* **69**, 101-110.

Day, J., Benson, E. & Fleck, R. (1999). In vitro culture and conservation of microalgae: Applications for aquaculture, biotechnology and environmental research. *In Vitro Cellular & Developmental Biology - Plant* **35**, 127-136.

de Figueiredo, D. R., Azeiteiro, U. M., Esteves, S. M., Goncalves, F. J. & Pereira, M. J. (2004). Microcystin-producing blooms--a serious global public health issue. *Ecotoxicology and Environmental Safety* **59**, 151-163.

Dekker, M. (1978). *Molecular Biology of Animal Viruses*. New York, New York: Dekker Press.

Delaroque, N., Boland, W., Muller, D. G. & Knippers, R. (2003). Comparisons of two large phaeoviral genomes and evolutionary implications. *Journal of Molecular Evolution* **57**, 613-622.

Delaroque, N., Maier, I., Knippers, R. & Muller, D. G. (1999). Persistent virus integration into the genome of its algal host, *Ectocarpus siliculosus* (Phaeophyceae). *Journal of General Virology* **80** (Pt 6), 1367-1370.

Delaroque, N., Muller, D. G., Bothe, G., Pohl, T., Knippers, R. & Boland, W. (2001). The complete DNA sequence of the *Ectocarpus siliculosus* Virus EsV-1 genome. *Virology* **287**, 112-132.

Delwiche, C. F. (1999). Tracing the thread of plastid diversity through the tapestry of life. *American Naturalist* **154**, S164-S177.

Desnues, C., Rodriguez-Brito, B., Rayhawk, S. & other authors (2008). Biodiversity and biogeography of phages in modern stromatolites and thrombolites. *Nature* **452**, 340-343.

Dimmock, N. J., Easton, A. J. & Leppard, K. N. (2001). *Introduction to Modern Virology*, Fifth edn. Osney Mead, Oxford: Blackwell Science Ltd.

Dorigo, U., Jacquet, S. & Humbert, J. F. (2004). Cyanophage diversity, inferred from g20 gene analyses, in the largest natural lake in France, Lake Bourget. *Applied and Environmental Microbiology* **70**, 1017-1022.

Duerr, E. O., Molnar, A. & Sato, V. (1998). Cultured microalgae as aquaculture feeds. *Journal of Marine Biotechnology* **6**, 65-70.

Edvardsen, B., Shalchian-Tabrizi, K., Jakobsen, K. S., Medlin, L. K., Dahl, E., Brubak, S. & Paasche, E. (2003). Genetic variability and molecular phylogeny of *Dinophysis* species (Dinophyceae) from Norwegian waters inferred from single cell analyses of rDNA1. *Journal of Phycology* **39**, 395-408.

Edwards, R. A. & Rohwer, F. (2005). Viral metagenomics. *Nature Reviews Microbiology* **3**, 504-510.

Ewing, B. & Green, P. (1998). Base-calling of automated sequencer traces using phred. II. Error probabilities. *Genome Research* **8**, 186-194.

Fabricius, K. E., Mieog, J. C., Colin, P. L., Idip, D. & van Oppen, M. J. H. (2004). Identity and diversity of coral endosymbionts (zooxanthellae) from three Palauan reefs with contrasting bleaching, temperature and shading histories. *Molecular Ecology* **13**, 2445-2458.

Farquhar, J., Bao, H. & Thiemens, M. (2000). Atmospheric influence of Earth's earliest sulfur cycle. *Science* **289**, 756-758.

Fay, P. (1983). *The Blue-Greens*. Bedford Square, London: Edward Arnold Publishers Ltd.

Filippini, M., Buesing, N., Bettarel, Y., Sime-Ngando, T. & Gessner, M. O. (2006). Infection paradox: high abundance but low impact of freshwater benthic viruses. *Applied and Environmental Microbiology* **72**, 4893-4898.

Fitt, W. K., Brown, B. E., Warner, M. E. & Dunne, R. P. (2001). Coral bleaching: interpretation of thermal tolerance limits and thermal thresholds in tropical corals. *Coral Reefs* **20**, 51-65.

Franca, S. (1976). On the presence of virus-like particles in the dinoflagellate *Gyrodinium resplendens* (Hulburt). *Protistologica* **12**, 425–430.

Fuhrman, J. A. (1999). Marine viruses and their biogeochemical and ecological effects. *Nature* **399**, 541-548.

Fuhrman, J. A. & Suttle, C. A. (1993). Viruses in marine planktonic systems. *Oceanography* **6**, 50-62.

Glasheen, B. M., Polashock, J. J., Lawrence, D. M., Gillett, J. M., Ramsdell, D. C., Vorsa, N. & Hillman, B. I. (2002). Cloning, sequencing, and promoter identification of Blueberry red ringspot virus, a member of the family Caulimoviridae with similarities to the "Soybean chlorotic mottle-like" genus. *Archives of Virology* **147**, 2169-2186.

Glynn, P. W., Maté, J. L., Baker, A. C. & Calderón, M. O. (2001). Coral bleaching and mortality in Panama and Ecuador during the 1997-1998 El Niño-Southern Oscillation event: spatial/temporal patterns and comparisons with the 1982-1983 event. *Bulletin of Marine Science* **69**, 79-109.

Glynn, P. W., Gassman, N. J., Eakin, C. M., Cortes J., Smith, D. B. & M., G. H. (1991). Reef coral reproduction in the eastern Pacific: Costa Rica, Panama, and Galapagos Islands (Ecuador). *I. Pocilloporidae. Marine Biology* **109**, 355-368.

Graves, M. V. & Meints, R. H. (1992). Characterization of the major capsid protein and cloning of its gene from algal virus PBCV-1. *Virology* **188**, 198-207.

Hall, J. B., Licari, G. R. & Adolph, K. W. (1974). *Blue-Green Algae, IV: Current Research.* New York, New York: MSS Information Corporation.

Hayes, R. L. & Bush, P. G. (1990). Microscopic observations of recovery in the reef building scleratinian coral, *Montastrea annularis*, after bleaching on a Cayman reef. *Coral Reefs* **8**, 203-209.

Hennes, K. P., Suttle, C. A. & Chan, A. M. (1995). Fluorescently labeled virus probes show that natural virus populations can control the structure of marine microbial communities. *Applied and Environmental Microbiology* **61**, 3623-3627.

Henry, E. C. & Meints, R. H. (1992). A persistent virus infection in *Feldmannia* (Phaeophyceae). *Journal of Phycology* **28**, 517-526.

Hill, E. (2006). The cyanophage molecular mixing bowl of photosynthesis genes. *PLoS Biology* **4**, e264.

Hofer, J. S. & Sommaruga, R. (2001). Seasonal dynamics of viruses in an alpine lake: importance of filamentous forms. *Aquatic Microbial Ecology* **26**, 1-11.

Holland, H. D. (1994). *Early life on Earth.* New York, New York: Columbia University Press.

Hunter, C. L., Morden, C. W. & Smith, C. M. (1997). The utility of ITS sequences in assessing relationships among zooxanthellae and corals. *Proceeding of the 8th International Coral Reef Symposium* **2**, 1599-1602.

Hurst, C. J. (2000). *Viral Ecology.* Cincinnati, Ohio: Academic Press.

Huu, N. B., Denner, E. B., Ha, D. T., Wanner, G. & Stan-Lotter, H. (1999). *Marinobacter aquaeolei* sp. nov., a halophilic bacterium isolated from a Vietnamese oil-producing well. *International Journal of Systematic Bacteriology* **49** Pt 2, 367-375.

Ivey, R. G., Henry, E. C., Lee, A. M., Klepper, L., Krueger, S. K. & Meints, R. H. (1996). A Feldmannia algal virus has two genome size-classes. *Virology* **220**, 267-273.

Jacobsen, A., Bratbak, G. & Heldal, M. (1996). Isolation and characterisation of a virus infecting *Phaeocystis pouchetii* (Prymnesiophyceae). *Journal of Phycology* **32**, 23-927.

Jacquet, S., Heldal, M., Iglesias-Rodriguez, D., Larsen, A., Wilson, W. H. & Bratbak, G. (2002). Flow cytometric analysis of an *Emiliania huxleyi* bloom terminated by viral infection. *Aquatic Microbial Ecology* **27**, 111-124.

Jensen, T. E. & Bowen, C. C. (1961). Organization of the centroplasm in *Nostoc pruniforme*. *Proceedings of the Iowa Academy of Science* **68**, 89-96.

Jiang, S. C. & Paul, J. H. (1994). Seasonal and diel abundance of viruses and occurrence of lysogeny/bacteriocinogeny in the marine environment. *Marine Ecology Progress Series* **104**, 163-172.

Jiang, S. C. & Paul, J. H. (1996). Occurrence of lysogenic bacteria in marine microbial communities as determined by prophage induction. *Marine Ecology Progress Series* **142**, 27-38.

Jiang, S. C. & Paul, J. H. (1998). Significance of lysogeny in the marine environment: Studies with isolates and an ecosystem model. *Microbial Ecology* **35**, 235-243.

Jokiel, P. L., and Coles, S.L. (1990). Response of Hawaiian and other Indo Pacific reef corals to elevated temperatures. *Coral Reefs* **8**, 155–162.

Jones, R. J. (1997). Changes in zooxanthellar densities and chlorophyll concentrations in corals during and after a bleaching event. *Marine Ecology Progress Series* **158**, 51-59.

Jones, R. J., Ward, S., Amri, A. Y. & Hoegh-Guldberg, O. (2000). Changes in quantum efficiency of Photosystem II of symbiotic dinoflagellates of corals after heat stress, and of bleached corals sampled after the 1998 Great Barrier Reef mass bleaching event. *Marine and Freshwater Research* **51**, 63-71.

Kalinkina, L. G. & Yasyukova, T. B. (2001). Development of oxidative stress in the cells of *Chlorella stigmatophora* and their bleaching by the glycolate pathway inhibition under salinization conditions. *Russian Journal of Plant Physiology* **48**, 645-650.

Kapp, M. (1998). Viruses infecting marine brown algae. *Virus Genes* **16**, 111-117.

Khemayan, K., Pasharawipas, T., Puiprom, O., Sriurairatana, S., Suthienkul, O. & Flegel, T. W. (2006). Unstable lysogeny and pseudolysogeny in *Vibrio harveyi* siphovirus-like phage 1. *Applied and Environmental Microbiology* **72**, 1355-1363.

Kling, H. J. & Watson, S. (2003). A new planktic species of *Pseudanabaena* (Cyanoprokaryota, Oscillatoriales) from North American large lakes. *Hydrobiologia* **503**, 383–388.

Knipe, D. K. & Howley, P. M. (2001). *Fields Virology*, Fourth edn. Philadelphia, Pennsylvania: Lippincott Williams and Wilkins.

Kogure, K., Simidu, U. & Taga, N. (1982). Bacterial attachment to phytoplankton in sea water. *Journal of Experimental Biology and Ecology* **56**, 197-204.

Kokjohn, T. A. (1989). *Transduction: mechanism and potential for gene transfer in the environment*. New York, New York: MacGraw-Hill.

Komárek, J. & Kling, H. (1991). Variation in six planktonic cyanophyte genera in Lake Victoria (East Africa). *Archiv für Hydrobiologie–Algological Studies* **61**, 21-45.

Kushmaro, A., Rosenberg, E., Fine, M. & Loya, Y. (1997). Bleaching of the coral *Oculina patagonica* by Vibrio AK-1. *Marine Ecology Progress Series* **147**, 159-165.

LaJeunesse, T. (2001). Investigating the biodiversity, ecology, and phylogeny of endosymbiotic dinoflagellates in the genus *Symbiodinium* using the ITS region: In search of a "species" level marker. *Journal of Phycology* **37**, 866-880.

LaJeunesse, T. C., Loh, W. K. W., van Woesik, R., Hoegh-Guldberg, O., Schmidt, G. W. & Fitt, W. K. (2003). Low symbiont diversity in southern Great Barrier Reef corals relative to those of the Caribbean. *Limnology and Oceanography* **48**, 2046-2054.

Lang, A. S., Culley, A. I. & Suttle, C. A. (2004). Genome sequence and characterization of a virus (HaRNAV) related to picoma-like viruses that infects the marine toxic bloom-forming alga *Heterosigma akashiwo*. *Virology* **320**, 206-217.

Larsen, A., Castberg, T., Sandaa, R. A. & other authors (2001). Population dynamics and diversity of phytoplankton, bacteria and viruses in a seawater enclosure. *Marine Ecology Progress Series* **221**, 47-57.

Laurion, I., Blouin, F. & Roy, S. (2004). Packaging of mycosporine-like amino acids in dinoflagellates. *Marine Ecology Progress Series* **279**, 297-303.

Le Vu, B., Ruiz-Pino, D. & De Baar, H. J. W. (2003). From a data synthesis to the ecological niche of *Emiliania huxleyi*. *Geophysical Research Abstracts* **5**, 13614.

Lee, A. M., Ivey, R. G., Henry, E. C. & Meints, R. H. (1995). Characterization of a repetitive DNA element in a brown algal virus. *Virology* **212**, 474-480.

Lee, L. H., Lui, D., Platner, P. J., Hsu, S. F., Chu, T. C., Gaynor, J. J., Vega, Q. C. & Lustigman, B. K. (2006). Induction of temperate cyanophage AS-1 by heavy metal--copper. *BMC Microbiology* **6**, 17.

Leiman, P. G., Kanamaru, S., Mesyanzhinov, V. V., Arisaka, F. & Rossmann, M. G. (2004). Structure and morphogenesis of bacteriophage T4. *Celluar and Molecular Life Sciences* **60**, 2356-2370.

Lesser, M. P. & Shick, J. M. (1989). Effects of irradiance and ultraviolet radiation on photoadaptation in the zooxanthellae of *Aipasia pallida*: Primary production, photoinhibition, and enzymic defenses against oxygen toxicity *Marine Biology* **102**, 243-255.

Lesser, M. P. & Shick, J. M. (1990). Effects of visible and ultraviolet radiation on the ultrastructure of zooxanthellae (*Symbiodinium* sp.) in culture and *in situ*. *Cell and Tissue Research* **261**, 501-508.

Levasseur, M., Michaud, S., Egge, J. & other authors (1996). Production of DMSP and DMS during a mesocosm study of an *Emiliania huxleyi* bloom: influence of bacteria and *Calanus finmarchicus* grazing. *Marine Biology* **126**, 609-618.

Lindauer, A., Fraser, D., Bruderlein, M. & Schmitt, R. (1993). Reverse transcriptase families and a copia-like retrotransposon, Osser, in the green alga *Volvox carteri*. *FEBS Letters* **319**, 261-266.

Lindell, D., Jaffe, J. D., Johnson, Z. I., Church, G. M. & Chisholm, S. W. (2005). Photosynthesis genes in marine viruses yield proteins during host infection. *Nature* **438**, 86-89.

Liu, X., Shi, M., Kong, S., Gao, Y. & An, C. (2007). Cyanophage Pf-WMP4, a T7-like phage infecting the freshwater cyanobacterium *Phormidium foveolarum*: complete genome sequence and DNA translocation. *Virology* **366**, 28-39.

Lohr, J., Munn, C. B. & Wilson, W. H. (2007). Characterization of a latent virus-like infection of symbiotic zooxanthellae. *Applied and Environmental Microbiology* **73**, 2976-2981.

Lohr, J. E., Chen, F. & Hill, R. T. (2005). Genomic analysis of bacteriophage PhiJL001: insights into its interaction with a sponge-associated alpha-proteobacterium. *Applied and Environmental Microbiology* **71**, 1598-1609.

Mann, N. H. (2003). Phages of the marine cyanobacterial picophytoplankton. *FEMS Microbiology Reviews* **27**, 17-34.

Mann, N. H., Clokie, M. R., Millard, A., Cook, A., Wilson, W. H., Wheatley, P. J., Letarov, A. & Krisch, H. M. (2005). The genome of S-PM2, a "photosynthetic" T4-type bacteriophage that infects marine *Synechococcus* strains. *Journal of Bacteriology* **187**, 3188-3200.

Marciano, D. K., Russel, M. & Simon, S. M. (1999). An aqueous channel for filamentous phage export. *Science* **284**, 1516-1519.

Margulis, L. (1993). *Symbiosis in Cell Evolution*, Second edn. New York, New York: Freeman & Co.

Marie, D., Brussaard, C. P. D., Thyrhaug, R., Bratbak, G. & Vaulot, D. (1999). Enumeration of marine viruses in culture and natural samples by flow cytometry. *Applied and Environmental Microbiology* **65**, 45–52.

Marra, J. (2002). *Phytoplankton Productivity:Carbon Assimilation in Marine and Freshwater Ecosystems*. Oxford, UK Wiley-Blackwell.

McDaniel, L., Houchin, L. A., Williamson, S. J. & Paul, J. H. (2002). Lysogeny in marine *Synechococcus*. *Nature* **415**, 496.

McDaniel, L. D., delaRosa, M. & Paul, J. H. (2006). Temperate and lytic cyanophages from the Gulf of Mexico. *Journal of the Marine Biological Association of the UK* **86**, 517-527.

McFadden, G. I. (2001). Primary and secondary endosymbiosis and the origin of plastids. *Journal of Phycology* **37**, 951-959.

McGillicuddy, D. J., Jr., Anderson, L. A., Bates, N. R. & other authors (2007). Eddy/wind interactions stimulate extraordinary mid-ocean plankton blooms. *Science* **316**, 1021-1026.

Meints, R. H., Lee, K., Burbank, D. E. & van Etten, J. L. (1984). Infection of a Chlorella-like alga with the virus, PBCV-1: ultrastructural studies. *Virology* **138**, 341-346.

Millard, A., Clokie, M. R., Shub, D. A. & Mann, N. H. (2004). Genetic organization of the psbAD region in phages infecting marine *Synechococcus* strains. *Proceedings of the National Academy of Sciences of the United States of America* **101**, 11007-11012.

Miller, R. V. (2001). Environmental bacteriophage-host interactions: factors contribution to natural transduction. *Antonie van Leeuwenhoek* **79**, 121-147.

Miller, T. R. & Belas, R. (2003). *Pfiesteria piscicida*, *P. shumwayae*, and other *Pfiesteria*-like dinoflagellates. *Research in Microbiology* **154**, 85-90.

Milligan, K. L. & Cosper, E. M. (1994). Isolation of Virus Capable of Lysing the Brown Tide Microalga, *Aureococcus anophagefferens*. *Science* **266**, 805-807.

Moisa, I., Sotropa, E. & Velehorschi, V. (1981). Investigations on the presence of cyanophages in fresh and sea waters of Romania. *Virologie* **32**, 127-132.

Morden, C. W. & Sherwood, A. R. (2002). Continued evolutionary surprises among dinoflagellates. *Proceedings of the National Academy of Sciences of the United States of America* **99**, 11558-11560.

Moreira, D., Le Guyader, H. & Philippe, H. (2000). The origin of red algae and the evolution of chloroplasts. *Nature* **405**, 69-72.

Mu, J., Yao, X., Chen, Q., Geng, Y. & Qiao, W. (2007). MicroRNAs and their role in viral infection. *Frontiers of Biology in China* **2**, 15-20.

Muhling, M., Fuller, N. J., Millard, A. & other authors (2005). Genetic diversity of marine *Synechococcus* and co-occurring cyanophage communities: evidence for viral control of phytoplankton. *Environmental Microbiology* **7**, 499-508.

Müller, D. G. & Frenzer, K. (1993). Virus infections in three marine brown algae: *Feldmannia irregularis*, *F. simplex*, and *Ectocarpus siliculosus*. *Hydrobiologia* **260-261**, 37-44.

Müller, D. G., Sengco, M., Wolf, S., Brautigam, M., Schmid, C. E., Kapp, M. & Knippers, R. (1996). Comparison of two DNA viruses infecting the marine brown algae *Ectocarpus siliculosus* and *E. fasciculatus*. *Journal of General Virology* **77**, 2329-2333.

Munn, C. B. (2004). *Marine Microbiology - Ecology and Applications*. New York, New York: Bios-Garland Scientific Publishers.

Murphy, F. A., Fauquet, C. M., Bishop, D. H. L., Ghabrial, S. A., Jarvis, A. W., Martelli, G. P., Mayo, M. A. & Summers, M. D. (1995). *Sixth Report of the International Committee on Taxonomy of Viruses*. Wien New York: Springer Verlag.

Muscatine, L. (1990). *The role of symbiotic algae in carbon and energy flux in reef corals: in Ecosystems of the World: Coral Reefs (ed. Z. Dubinsky).* Amsterdam: Elsevier.

Nagasaki, K., Tarutani, K. & Yamaguchi, M. (1999). Growth characteristics of *Heterosigma akashiwo* virus and its possible use as a microbiological agent for red tide control. *Applied and Environmental Microbiology* **65**, 898-902.

Nagasaki, K., Tomaru, Y., Tarutani, K., Katanozaka, N., Yamanaka, S., Tanabe, H. & Yamaguchi, M. (2003). Growth characteristics and intraspecies host specificity of a large virus infecting the dinoflagellate *Heterocapsa circularisquama. Applied and Environmental Microbiology* **69**, 2580-2586.

Nagasaki, K., Tomaru, Y., Katanozaka, N., Shirai, Y., Nishida, K., Itakura, S. & Yamaguchi, M. (2004). Isolation and characterization of a novel single-stranded RNA virus infecting the bloom-forming diatom *Rhizosolenia setigera. Applied and Environmental Microbiology* **70**, 704-711.

Nagasaki, K., Tomaru, Y., Takao, Y., Nishida, K., Shirai, Y., Suzuki, H. & Nagumo, T. (2005). Previously unknown virus infects marine diatom. *Applied and Environmental Microbiology* **71**, 3528-3535.

Noble, R. T. & Fuhrman, J. A. (1997). Virus decay and its causes in coastal waters. *Applied and Environmental Microbiology* **63**, 77-83.

Noble, R. T. & Fuhrman, J. A. (1998). Use of SYBR Green I for rapid epifluorescence counts of marine viruses and bacteria. *Aquatic Microbial Ecology* **14**, 113-118.

O'Kelly, C. J., Sieracki, M. E., Thier, E. & Hobson, I. C. (2003). A transient bloom of *Ostreococcus* (Chlorophyta, Prasinophyceae) in West Neck Bay, Long Island, New York. *Journal of Phycology* **39**, 850-854.

Oakey, H. J. & Owens, L. (2000). A new bacteriophage, VHML, isolated from a toxin-producing strain of *Vibrio harveyi* in tropical Australia. *Journal of Applied Microbiology* **89**, 702-709.

Ohki, K. (1999). A possible role of temperate phage in the regulation of *Trichodesmium* biomass. *Bulletin de l'Institut Oceanographique, Monaco* **19**, 287-291.

Ohki, K. & Fujita, Y. (1996). Occurrence of a temperate cyanophage lysogenizing the marine cyanophyte *Phormidium persicinum. Journal of Phycology* **32**, 365-370.

Oldach, D. W., Delwiche, C. F., Jakobsen, K. S. & other authors (2000). Heteroduplex mobility assay-guided sequence discovery: elucidation of the small subunit (18S) rDNA sequences of *Pfiesteria piscicida* and related dinoflagellates from complex algal culture and environmental sample DNA pools. *Proceedings of the National Academy of Sciences of the United States of America* **97**, 4303-4308.

Onji, M., Nakano, S. & Suzuki, S. (2003). Virus-like particles suppress growth of the red-tide-forming marine dinoflagellate *Gymnodinium mikimotoi. Marine Biotechnology* **5**, 435-442.

Orjala, J., Nagle, D. G., Hsu, V. L. & Gerwick, W. H. (1995). Antillatoxin: an exceptionally ichthyotoxic cyclic lipopeptide from the tropical cyanobacterium *Lyngbya majuscula*. *Journal of the American Chemical Society* **117**, 8281-8282.

Padan, E., Shilo, M. & Oppenheim, A. B. (1972). Lysogeny of the blue-green alga *Plectonema boryanum* by LPP2-SPI cyanophage. *Virology* **47**, 525-526.

Palenik, B., Brahamsha, B., Larimer, F. W. & other authors (2003). The genome of a motile marine *Synechococcus*. *Nature* **424**, 1037-1042.

Palmer, J. D. (2003). The Symbiotic Birth and Spread of Plastids: How Many Times and Whodunit? *Journal of Phycology* **39**, 4-11.

Paul, J. H. & Jiang, S. C. (2001). *Marine Microbiology*. San Diego, California: Academic Press.

Paul, J. H., Sullivan, M. B., Segall, A. M. & Rohwer, F. (2002). Marine phage genomics. *Comparative biochemistry and physiology Part B, Biochemistry & molecular biology* **133**, 463-476.

Pearson, B. R. & Norris, R. E. (1974). Intranuclear virus-like particles in the marine alga *Platymonas* sp. (Chlorophyta, Prasinophyceae). *Phycologia* **13**, 5-9.

Peters, K. E., Walters, C. C. & Moldowan, J. M. (2005). *The Biomarker Guide*. New York, New York: Cambridge University Press.

Pettersson, L. H., Dominique, D. D., Svendsen, E., Noji, T., Soiland, H., Groom, S. B. & Lavender, S. (2000). DeciDe for near real-time use of ocean colour data in management of toxic algae blooms - Specification, definition and design document: NERSC Technical Report ESA under contract no. 13662/99/I-DC, (186-A).

Pienaar, R. N. (1976). Virus-like particles in three species of phytoplankton from San Juan Island, Washington. *Phycologia* **15**, 185-190.

Pinard, R., de Winter, A., Sarkis, G. J., Gerstein, M. B., Tartaro, K. R., Plant, R. N., Egholm, M., Rothberg, J. M. & Leamon, J. H. (2006). Assessment of whole genome amplification-induced bias through high-throughput, massively parallel whole genome sequencing. *BMC Genomics* **7**, 216.

Pockley, P. (2000). Global warming identified as main threat to coral reefs. *Nature* **407**, 932.

Pope, W. H., Weigele, P. R., Chang, J. & other authors (2007). Genome sequence, structural proteins, and capsid organization of the cyanophage Syn5: a "horned" bacteriophage of marine *synechococcus*. *Journal of Molecular Biology* **368**, 966-981.

Proctor, L. M. (1997). Advances in the study of marine viruses. *Microscopy Research and Technique* **37**, 136-161.

Pulz, O. & Gross, W. (2004). Valuable products from biotechnology of microalgae. *Applied Microbiology and Biotechnology* **65**, 635-648.

Rao, S. D. V. (2006). *Why study algae in culture?* New Hampshire, USA: Science Publishers.

Reisser, W. (1993). Viruses and virus-like particles of freshwater and marine eucaryotic algae -a review. *Archiv fuer Protistenkunde* **143**, 257-265.

Ripp, S. & Miller, R. (1997). The role of pseudolysogeny in bacteriophage host interactions in a natural freshwater environment. *Microbiology* **143**, 2065-2070.

Rogers, J. E., Oliver, L. M. & Hansen, L. J. (2001). *Symbiodinium* spp. isolates from stony coral: Isolation, growth characteristics and effects of UV irradiation. *Journal of Phycology* **37**, 43.

Rohwer, F. & Edwards, R. (2002). The phage proteomic tree: a genome-based taxonomy for phage. *Journal of Bacteriology* **184**, 4529-4535.

Rohwer, F., Seguritan, V., Azam, F. & Knowlton, N. (2002). Diversity and distribution of coral-associated bacteria. *Marine Ecology Progress Series* **243**, 1-10.

Rosenberg, E. & Ben-Haim, Y. (2002). Microbial diseases of corals and global warming. *Enviromental Micrbiology* **4**, 318-326.

Rowan, R. (1998). Diversity and ecology of zooxanthellae on coral reefs. *Journal of Phycology* **34**, 407-417.

Rowan, R. & Powers, D. A. (1991). Molecular genetic identification of symbiotic dinoflagellates (zooxanthellae). *Marine Ecology Progress Series* **71**, 65-73.

Rowan, R. & Knowlton, N. (1995). Intraspecific diversity and ecological zonation in coral-algal symbiosis. *Proceedings of the National Academy of Sciences of the United States of America* **92**, 2850-2853.

Rowan, R., Knowlton, N., Baker, A. & Jara, J. (1997). Landscape ecology of algal symbionts creates variation in episodes of coral bleaching. *Nature* **388**, 265-269.

Safferman, R. S. & Morris, M. E. (1963). Algal virus: isolation. *Science* **140**, 679-680.

Safferman, R. S., Morris, M. E., Sherman, L. A. & Haselkorn, R. (1969). Serological and electron microscopic characterization of a new group of blue-green algal viruses (LPP-2). *Virology* **39**, 775-780.

Safferman, R. S., Carr, N. G. & Whitton, B. A. (1973). *The Biology of Blue-Green Algae.* Berkeley, California: University of California Press.

Safferman, R. S., Diener, T. O., Desjardins, P. R. & Morris, M. E. (1972). Isolation and characterization of AS-1, a phycovirus infecting the blue-green algae, *Anacystis nidulans* and *Synechococcus cedrorum*. *Virology* **47**, 105-113.

Safferman, R. S., Cannon, R. E., Desjardins, P. R., Gromov, B. V., Haselkorn, R., Sherman, L. A. & Shilo, M. (1983). Classification and nomenclature of viruses of cyanobacteria. *Intervirology* **19**, 61-66.

Schroeder, D. C., Oke, J., Malin, G. & Wilson, W. H. (2002). Coccolithovirus (Phycodnaviridae): characterisation of a new large dsDNA algal virus that infects *Emiliana huxleyi*. *Archives of Virology* **147**, 1685-1698.

Schroeder, D. C., Oke, J., Hall, M., Malin, G. & Wilson, W. H. (2003). Virus succession observed during an *Emiliania huxleyi* bloom. *Applied and Environmental Microbiology* **69**, 2484-2490.

Short, S. M. & Suttle, C. A. (2002). Sequence analysis of marine virus communities reveals that groups of related algal viruses are widely distributed in nature. *Applied and Environmental Microbiology* **68**, 1290-1296.

Sicko-Goad, L. & Walker, G. (1979). Viroplasm and large virus like particles in the dinoflagellate *Gymnodinium uberrimum*. *Protoplasma* **99**, 203–210.

Silva, E. S. (1982). Relationship between dinoflagellates and intracellular bacteria. *Marine Algae in Pharmaceutical Science* **2**, 269-288.

Smyth, T. J., Tyrrell, T. & Tarrant, B. (2004). Time series of coccolithophore activity in the Barents Sea, from twenty years of satellite imagery. *Geophysical Research Letters* **31**, L11302.

Solé, J., Estradaa, M. & Garcia-Ladona, E. (2006). Biological control of harmful algal blooms: A modelling study. *Journal of Marine Systems* **61**, 165-179

Steward, G. F., Montiel, J. L. & Azam, F. (2000). Genome size distributions indicate variability and similarities among marine viral assemblages from diverse environments. *Limnology and Oceanography* **45**, 1697-1705.

Stockwell, D. A., Whitledge, T. E., Zeeman, S. I., Coyle, K. O., Napp, J. M., Brodeur, R. D., Pinchuk, A. I. & Hunt, G. L., Jr. (2001). Anomalous conditions in the southeastern Bering Sea, 1997: Nutrients, phytoplankton, and zooplankton. *Fisheries Oceanography* **10**, 99-116.

Strauss, J. H. & Strauss, E. G. (2001). *Viruses and Human Disease*. San Diego, California: Academic Press.

Strychara, K. B., Coatesa, M., Sammarcob, P. W. & Pivac, T. J. (2004). Bleaching as a pathogenic response in scleractinian corals, evidenced by high concentrations of apoptotic and necrotic zooxanthellae. *Journal of Experimental Marine Biology and Ecology* **304**, 99-121.

Sullivan, M. B., Coleman, M. L., Weigele, P., Rohwer, F. & Chisholm, S. W. (2005). Three *Prochlorococcus* cyanophage genomes: signature features and ecological interpretations. *PLoS Biology* **3**, e144.

Sullivan, M. B., Lindell, D., Lee, J. A., Thompson, L. R., Bielawski, J. P. & Chisholm, S. W. (2006). Prevalence and evolution of core photosystem II genes in marine cyanobacterial viruses and their hosts. *PLoS Biology* **4**, e234.

Suttle, C. A. (1999). Do viruses control the oceans? *Natural History* **108**, 48-51.

Suttle, C. A. (2000). *Viral Ecology*. New York, New York: C.J. Hurst Academic Press.

Suttle, C. A. (2005). Viruses in the sea. *Nature* **437**, 356-361.

Suttle, C. A. & Chan, A. M. (1993). Marine cyanophages infecting oceanic and coastal strains of *Synechococcus*: abundance, morphology, cross-infectivity and growth characteristics. *Marine Ecology Progress Series* **92**, 99-109.

Suttle, C. A. & Chan, A. M. (1995). Viruses infecting the marine prymnesiophyte *Chrysochromulina* spp.: isolation, preliminary characterization and natural abundance. *Marine Ecology Progress Series* **118**, 275-282.

Suttle, C. A., Chan, A. M. & Cottrell, M. T. (1991). Use of ultrafiltration to isolate viruses from seawater which are pathogens of marine phytoplankton. *Applied and Environmental Microbiology* **57**, 721-726.

Szmant, A. & Gassman, N. J. (1990). The effects of prolonged bleaching on the tissue biomass and reproduction of the reef coral *Monastrea annularis*. *Coral Reefs* **8**, 217–224.

Tai, V., Lawrence, J. E., Lang, A. S., Chan, A. M., Culley, A. I. & Suttle, C. A. (2003). Characterization of HaRNAV, a single-stranded RNA virus causing lysis of *Heterosigma akashiwo* (Raphidophyceae). *Journal of Phycology* **39**, 343-352.

Tanaka, S., Kerfeld, C. A., Sawaya, M. R., Cai, F., Heinhorst, S., Cannon, G. C. & Yeates, T. O. (2008). Atomic-level models of the bacterial carboxysome shell. *Science* **319**, 1083-1086.

Tapper, M. A. & Hicks, R. E. (1998). Temperate viruses and lysogeny in Lake Superior bacterioplankton. *Limnology and Oceanography* **43**, 95-103.

Tarutani, K., Nagasaki, K., Itakura, S. & Yamaguchi, M. (2001). Isolation of a virus infecting the novel shellfish-killing dinoflagellate *Heterocapsa circularisquama*. *Aquatic Microbial Ecology* **23**, 103-111.

Tomaru, Y., Katanozaka, N., Nishida, K., Shirai, Y., Tarutani, K., Yamaguchi, M. & Nagasaki, K. (2004). Isolation and characterization of two distinct types of HcRNAV, a single-stranded RNA virus infecting the bivalve-killing microalga *Heterocapsa circularisquama*. *Aquatic Microbial Ecology* **34**, 207-218.

Toren, A., Landau L., Kushmaro A., Loya Y. & Rosenberg, E. (1998). Effect of temperature on adhesion of Vibrio strain AK-1 to *Oculina patagonica* and on coral bleaching. *Applied and Environmental Microbiology* **64**, 1379-1384.

Trench, R. K. (1993). Microalgal-invertebrate symbioses: a review. *Endocytobiology and Cell Research* **9**, 135-175.

Tucker, S. & Pollard, P. (2005). Identification of cyanophage Ma-LBP and infection of the cyanobacterium *Microcystis aeruginosa* from an Australian subtropical lake by the virus. *Applied and Environmental Microbiology* **71**, 629-635.

Tyrell, T. (1999). The relative influences of nitrogen and phosphorous on oceanic primary productivity. *Nature* **400**, 525-531.

van den Hoek, C., Mann, D. G. & Jahns, H. M. (1995). *Algae An Introduction to Phycology*. New York, New York: Cambridge University Press.

van Etten, J. L. & Meints, R. H. (1999). Giant viruses infecting algae. *Annual Review of Microbiology* **53**, 447-494.

van Etten, J. L., Lane, L.C. & Meints, R. H. (1991). Viruses and virus-like particles of eukaryotic algae. *Microbiological Reviews* **55**, 586-620.

van Etten, J. L., Meints, R. H., Kuczmarski, D., Burbank, D. E. & Lee, K. (1982). Viruses of symbiotic Chlorella-like algae isolated from *Paramecium bursaria* and *Hydra viridis*. *Proceedings of the National Academy of Sciences of the United States of America* **79**, 3867-3871.

van Etten, J. L., Graves, M. V., Müller, D. G., Boland, W. & Delaroque, N. (2002). Phycodnaviridae - large DNA algal viruses. *Archives of Virology* **147**, 1479-1516.

van Oppen, M. J. H., Palstra, F. P., Piqet, A. M. T. & Miller, D. J. (2001). Patterns of coral-dinoflagellate associations in *Acropora*: significance of local availability and physiology of *Symbiodinium* strains and host-symbiont selectivity. *Proceedings of the Royal Society of London Series B-Biological Sciences* **268**, 1579-1767.

van Regenmortel, M. H. V. (1990). Virus species, a much overlooked but essential concept in virus classification. *Intervirology* **31**, 241-254.

van Regenmortel, M. H. V., Fauquet, C. M., Bishop, D. H. & other authors (2000). *Virus taxonomy: classification and nomenclature of viruses: seventh report of the international committee on tamonomy of viruses*. San Diego, California: Academic Press Inc.

Vance, B. D. (1977). Prophage induction in toxic *Microcystis acruginosa* NRC-1. *Journal of Phycology* **13**, 70.

Villarreal, L. P. & DeFilippis, V. R. (2000). A hypothesis for DNA viruses as the origin of eukaryotic replication proteins. *Journal of Virology* **74**, 7079-7084.

Visviki, I. & Rachlin, J. W. (1991). The toxic action and interactions of copper and cadmium to the marine Alga *Dunaliella minuta*, in both acute and chronic exposure. *Archives of Environmental Contamination and Toxicology* **20**, 271-275.

Wagner, E. K. & Hewlett, M. J. (2004). *Basic Virology*, Second edn. New York, New York: Blackwell Publishing.

Wang, J. & Douglas, A. E. (1998). Nitrogen recycling or nitrogen conservation in an alga-invertebrate symbiosis? *Journal of Experimental Biology* **201**, 2445–2453.

Weigele, P. R., Pope, W. H., Pedulla, M. L. & other authors (2007). Genomic and structural analysis of Syn9, a cyanophage infecting marine *Prochlorococcus* and *Synechococcus*. *Environmental Microbiology* **9**, 1675-1695.

Weinbauer, M. G. & Suttle, C. A. (1996). Potential significance of lysogeny to bacteriophage production and bacterial mortality in coastal waters of the Gulf of Mexico. *Applied and Environmental Microbiology* **62**, 4374-4380.

Weinbauer, M. G. (2004). Ecology of prokaryotic viruses. *FEMS Microbiology Reviews* **28**, 127-181.

Weinbauer, M. G. & Rassoulzadegan, F. (2004). Are viruses driving microbial diversification and diversity? *Environmental Microbiology* **6**, 1-11.

Wen, K., Ortmann, A. C. & Suttle, C. A. (2004). Accurate estimation of viral abundance by epifluorescence microscopy. *Applied and Environmental Microbiology* **70**, 3862-3867.

Wiegand, C. & Pflugmacher, S. (2005). Ecotoxicological effects of selected cyanobacterial secondary metabolites: a short review. *Toxicology and Applied Pharmacology* **203**, 201-218.

Wilhelm, S. W. & Suttle, C. A. (1999). Viruses and nutrient cycles in the sea - Viruses play critical roles in the structure and function of aquatic food webs. *Bioscience* **49**, 781-788.

Wilkinson, C. (1998). Status of Coral Reefs of the World. Townsville, Australia: Australian Institute of Marine Science.

Williamson, S. J., McLaughlin, M. R. & Paul, J. H. (2001). Interaction of the PhiHSIC virus with its host: lysogeny or pseudolysogeny? *Applied and Environmental Microbiology* **67**, 1682-1688.

Wilson, W. H., Francis, I., Ryan, K. & Davy, S. K. (2001). Temperature induction of viruses in symbiotic dinoflagellates. *Aquatic Microbial Ecology* **25**, 99-102.

Wilson, W. H., Dale, A. L., Davy, J. E. & Davy, S. K. (2005). An enemy within? Observations of virus-like particles in reef corals. *Coral Reefs* **24**, 145-148.

Wilson, W. H., Tarran, G. A., Schroeder, D. C., Cox, M., Oke, J. & Malin, G. (2002). Isolation of viruses responsible for the demise of an *Emiliania huxleyi* bloom in the English Channel. *Journal of the Marine Biological Association of the UK* **82**, 369-377.

Wilson, W. H., Schroeder, D.C., Allen, M.J., Holden, M.T., Parkhill, J., Barrell, B.G., Churcher, C., Hamlin, N., Mungall, K., Norbertczak, H., Quail, M.A., Price, C., Rabbinowitsch, E., Walker, D., Craigon, M., Roy, D., Ghazal, P.. (2005). Complete genome sequence and lytic phase transcription profile of a Coccolithovirus. *Science* **309**, 1090-1092.

Wommack, K. E. & Colwell, R. R. (2000). Virioplankton: viruses in aquatic ecosystems. *Microbiology and Molecular Biology Reviews* **64**, 69-114.

Wommack, K. E., Bhavsar, J. & Ravel, J. (2008). Metagenomics: read length matters. *Applied and Environmental Microbiology* **74**, 1453-1463.

Wommack, K. E., Ravel, J., Hill, R. T., Chun, J. & Colwell, R. R. (1999). Population dynamics of Chesapeake bay virioplankton: total-community analysis by pulsed-field gel electrophoresis. *Applied and Environmental Microbiology* **65**, 231-240.

Yamada, T., Onimatsu, H. & van Etten, J. L. (2006). Chlorella viruses. *Advances in Virus Research* **66**, 293-336.

Zingone, A., Natale, F., Biffali, E., Borra, M., Forlani, G. & Sarno, D. (2006). Diversity in morphology, infectivity, molecular characteristics and induced host resistance between two viruses infecting *Micromonas pusilla*. *Aquatic Microbial Ecology* **45**, 1-14.

APPLIED AND ENVIRONMENTAL MICROBIOLOGY, May 2007, p. 2976–2981 Vol. 73, No. 9
0099-2240/07/$08.00+0 doi:10.1128/AEM.02449-06

Characterization of a Latent Virus-Like Infection of Symbiotic Zooxanthellae[▽]

Jayne Lohr,[1,2] Colin B. Munn,[2] and William H. Wilson[1,3]*

Plymouth Marine Laboratory, Prospect Place, The Hoe, Plymouth PL1 3DH, United Kingdom[1]; School of Biological Sciences, University of Plymouth, Drake Circus, Plymouth PL4 8AA, United Kingdom[2]; and Bigelow Laboratory for Ocean Sciences, 180 McKown Point Road, P.O. Box 475, W. Boothbay Harbor, Maine 04575-0475[3]

Received 19 October 2006/Accepted 28 February 2007

A latent virus-like agent, which we designated zooxanthella filamentous virus 1 (ZFV1), was isolated from *Symbiodinium* sp. strain CCMP 2465 and characterized. Transmission electron microscopy and analytical flow cytometry revealed the presence of a new group of distinctive filamentous virus-like particles after exposure of the zooxanthellae to UV light. Examination of thin sections of the zooxanthellae revealed the formation and proliferation of filamentous virus-like particles in the UV-induced cells. Assessment of *Symbiodinium* sp. cultures was used here as a model to show the effects of UV irradiance and induction of potential latent viruses. The unique host-virus system described here provides insight into the role of latent infections in zooxanthellae through environmentally regulated viral induction mechanisms.

The frequency and intensity of coral bleaching have increased in the last two decades, leading to mass mortality of corals and a resulting reduction in the biodiversity of reefs (7, 33). Bleaching has been observed in more than 50 countries and in the three major oceans (31). Many environmental factors have been linked to coral bleaching; these factors include elevated and reduced temperatures (13), exposure to UV radiation (17), and bacterial infections (5, 19). However, the underlying causes of bleaching and the mechanisms involved remain largely unknown.

Reef-building corals associate with a diverse array of eukaryotic and prokaryotic microbes. The coral colony has been modeled as a holobiont comprising multispecies mutualisms consisting of the coral animal, endosymbiotic dinoflagellates (zooxanthellae), bacteria, fungi, protozoans, endolithic algae, and other unknown components (27). Disruption of any of these components may cause physiological changes that result in coral disease or death.

Zooxanthellae (genus *Symbiodinium*) are now known to comprise numerous clades (2). Zooxanthellae form a symbiotic relationship with many Cnidaria species and are by far the best-understood microbial associates of corals, and they have a clearly beneficial relationship with the coral. They release photosynthetic products to their hosts, providing an important source of organic carbon and nitrogen for host metabolism, growth, and reproduction (12, 24, 40). The symbiosis with zooxanthellae is believed to explain the success of reef-building corals in nutrient-poor tropical seas (15). Disruption of the zooxanthella-host symbiosis (bleaching) can lead to expulsion of zooxanthellae from the host and/or a decrease in the amount of the zooxanthella photosynthetic pigment (15, 18). Zooxanthellae have been shown to undergo necrosis, apoptosis, and lysis during bleaching (4, 31). The expulsion of *Symbiodinium* cells may help corals adapt to changing environmental conditions by allowing symbiont populations to redistribute themselves (3, 10). If the symbiont-host relationship is not recovered, the coral does not survive (33). It has been argued that the random mosaic patterns of bleaching are difficult to attribute to the effect of temperature stress alone as neighboring regions of a colony must be exposed to the same conditions (16). One explanation for the patchy spatial distribution of coral bleaching involves localized infections. Bacterial infection by *Vibrio* sp. has been shown to be responsible for some types of coral bleaching (5, 28, 37). Given the great abundance of viruses in marine systems, in which concentrations reach $>10^8$ particles ml^{-1} (6, 44), it is likely that viruses are also involved as agents of coral disease (11), and involvement of viruses in the coral bleaching process must be considered. It has been established that the majority of marine viruses infect bacteria, but viruses that infect eukaryotic algae have also been shown to be abundant in the marine environment (8). Virus-like particles (VLPs) have been found in cells of about 50 different algal species representing nearly all major algal classes (26, 38), and evidence suggests that viruses play a significant role in the population dynamics and community composition of marine phytoplankton (8, 22, 29, 32). Despite this, there have been relatively few reports on viruses of dinoflagellates (14, 30, 35) and fewer still on the presence of viruses in zooxanthellae. Previous studies in our laboratory have shown that zooxanthellae and corals produce VLPs when they are exposed to stress and elevated temperatures (11, 42, 43), suggesting that zooxanthellae harbor latent viruses. In order to determine whether VLPs are induced by exposure of the zooxanthellae to UV light, we utilized *Symbiodinium* sp. cultured in vitro to simplify the complexity found in whole organisms containing symbionts.

MATERIALS AND METHODS

Zooxanthella cultures. During this study, 16 strains of *Symbiodinium* species isolated from a variety of cnidarian hosts were maintained in culture (non-axenic).

* Corresponding author. Mailing address: Bigelow Laboratory for Ocean Sciences, 180 McKown Point Road, P.O. Box 475, W. Boothbay Harbor, ME 04575-0475. Phone: (207) 633-9666. Fax: (207) 633-9641. E-mail: wwilson@bigelow.org.

▽ Published ahead of print on 9 March 2007.

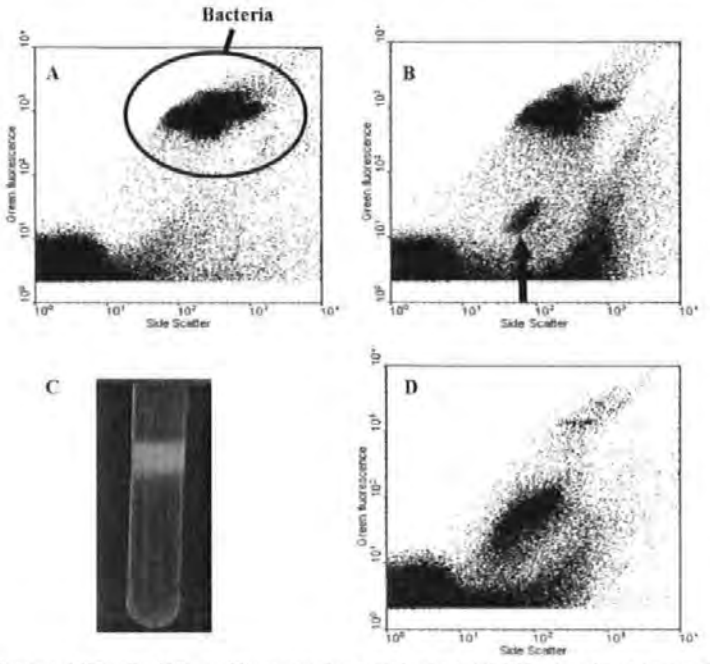

FIG. 1. APC analysis of VLPs induced following UV treatment of zooxanthella cultures. (A) APC analysis of control culture of zooxanthellae, showing bacteria (cultures were axenic). (B) APC analysis of UV-treated culture (after 96 h), showing a new VLP group with high SSC (indicated by arrow). (C) CsCl gradient of the VLPs with a translucent white band at ca. 1.05 g ml^{-1}. (D) APC analysis of concentrated VLPs taken from the 1 to 1 gradient, showing the presence of the high-SSC VLP group.

Strains 12, 61, 104,133, 135, 141, 152, 154, 208, 292, 368, 379, 382, and 385 were obtained from a collection at the Marine Biological Association and have been described in a previous study (20). Strains 200X and 200Y were isolated from *Aurelia aurita*. The zooxanthellae were grown in ASP-8A medium with antibiotics (25) and were subcultured monthly. Algal cultures were grown by using a cycle consisting of 16 h of light and 8 h of darkness at 26°C. The light intensity used was 40 to 50 mol quanta m^{-2} s^{-1}. Zooxanthella isolate 200 used in this study has been deposited in the Center for Culture of Marine Phytoplankton (http://ccmp.bigelow.org) as strain CCMP 2466.

Experimental treatments. Triplicate exponentially growing cultures (50 ml, approximately 10^6 cells ml^{-1}) were exposed for 2 min in open petri dishes to UV light (254 nm) from a Chromato-Vue transilluminator (model TM-20) which was placed upside down 12 cm above the petri dishes to allow down radiation. After exposure, the cultures were transferred back into 50-ml flasks and maintained at 20°C with illumination using a cycle consisting of 16 of light and 8 h of darkness. Samples used for enumeration of zooxanthellae and VLPs were collected daily for 1 week. Zooxanthellae were enumerated immediately and 1-ml aliquots were fixed in 0.5% glutaraldehyde, stored at 4°C for 30 min, snap frozen in liquid nitrogen, and stored at −80°C until they were processed for enumeration of VLPs and bacteria.

Enumeration of zooxanthellae, VLPs, and bacteria by analytical flow cytometry (APC). All analyses were performed with a Becton Dickinson FACSCalibur flow cytometer using the CellQuest software. For enumeration of live zooxanthellae, undiluted samples were examined for 2 min using a high flow rate (ca. 50 to 70 µl min^{-1}) with the discriminator set on red fluorescence. For enumeration of VLPs and bacteria, counting was performed using fixed samples diluted 1:10 to 1:1,000 in TE buffer (10 mM Tris, 1 mM EDTA, pH 8.0), filtered with a 30-kDa filter using tangential flow filtration (Vivaflow dip flow), and stained for 10 to 15 min at 80°C with a 10^{-4} dilution of SYBR green I stain (Molecular Probes). The samples were analyzed for 2 min at a low flow rate (ca. 10 µl min^{-1}) with the discriminator set on green fluorescence (13). VLPs and bacteria were enumerated using plots of side scatter (SSC) versus green fluorescence. All 16 zooxanthella strains were screened and exhibited differential sensitivity to UV induction. Strain CCMP 2465 exhibited the strongest response and was therefore utilized for further assessment.

TEM. Samples potentially containing VLPs were filtered through 0.45-µm filter units (Whatman) with a BD Plastipak sterile 20-ml syringe to remove debris and large cells. Aliquots were fixed in 0.5% glutaraldehyde, stored at 4°C for 30 min, and snap frozen in liquid nitrogen. "Spot" grids were prepared by placing grids onto 15 to 30 µl of a fixed suspension for 30 min. The excess liquid was removed with filter paper, and each preparation was negatively stained with uranyl acetate (2% [wt/vol] in water). For preparation of thin sections, UV-induced zooxanthellae were pelleted by centrifugation at 14,000 rpm in 1.5-ml Eppendorf tubes for 2 min. The pellets were resuspended, washed, and repelleted twice in filtered seawater (pore size, 0.2 µm). Molten agar (3% Fisher agar in distilled H_2O, 0.5 ml) was added to each washed pellet and allowed to set; the excess agar was trimmed from the agar plugs. A 4% solution of osmium solution was mixed 1:1 with filtered seawater and added to cover the agar plugs. The preparations were left for 1 h at room temperature, and this was followed by two washes in filtered seawater (pore size, 0.2 µm). Dehydration with a graded ethanol series, and infiltration with Spurr's resin is presently underway. Dried (48 h, 35°C) blocks were mounted and ultrathin sections that were 70 to 80 nm thick

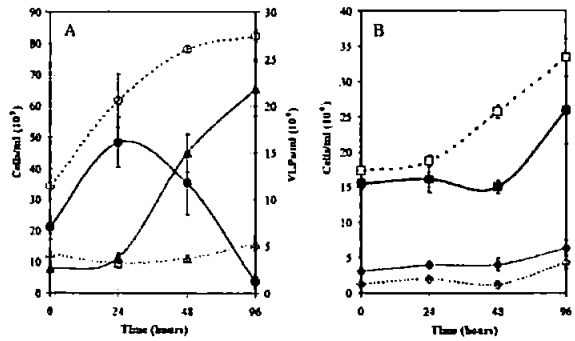

FIG. 2. (A) Growth curves showing numbers of cells of zooxanthella strain CCMP 2465 ml^{-1} in control cultures (○) and UV-treated cultures (●), together with the numbers of the high-SSC VLPs ml^{-1} in the unirradiated control cultures (△) and the UV-treated cultures (▲). (B) Concentrations of bacteria in the control cultures (□) and the UV-treated cultures (■), together with the numbers of bacteriophage particles ml^{-1} (10^6) in the control cultures (◇) and the UV-treated cultures (◆). The error bars indicate the standard errors for measurements from triplicate cultures.

with a Reichert-Jung Ultracut microtome; the sections were floated onto transmission electron microscopy (TEM) grids, stained with 2% uranyl acetate in 70% ethanol (15 min), washed in double-distilled H_2O, stained with Reynolds lead citrate for 15 min, and then rinsed in double-distilled H_2O. Prepared grids and thin sections were examined with a JEOL 2000 CX TEM (magnification, 80 to 500,000) at 160 kV. Photographs were taken at magnifications between ×5,000 and ×50,000.

Concentration of VLPs. Zooxanthellae were grown to a density of ca. 10^5 cells ml^{-1} in 3 liters of ASP 8A medium and exposed to UV light (254 nm) for 2 min in open petri dishes. VLPs were isolated from the growth media 96 h after exposure to UV. Debris, bacteria, and algal cells were removed by filtration through 0.45-μm-pore size, 47-mm-diameter filters (PALL Corp.). VLPs in the supernatant were concentrated by tangential flow filtration (Virasflow flip flow) with a 50-kDa cutoff to obtain ca. 50 ml. Further concentration to ca. 3 ml was accomplished by ultracentrifugation, with a Beckman L8-M at 100,000 × *g* for 2 h. VLPs were further purified and concentrated on a CsCl gradient prepared with CsCl in TE buffer at densities of 1.0, 1.2, 1.4, and 1.6 g cm^{-3}, and the pelleted VLPs were added to the 1.0-g cm^{-3} layer. This preparation was then centrifuged at 100,000 × *g* for 2 h at 20°C with the deceleration set at 8. A translucent white band was removed by piercing the ultracentrifuge tube just below the band, which allowed aliquots to be separated. Aliquots were dialyzed (Fisher, diameter, 0.32 mm; 12- to 14-kDa molecular mass cutoff) overnight against 1 liter of TE buffer at 4°C, and the TE buffer was changed twice in this time. The dialyzed VLP concentrate was stored at 4°C until it was analyzed.

RESULTS AND DISCUSSION

Induction of VLPs by UV irradiation of zooxanthellae. AFC analysis of UV-induced zooxanthella cultures revealed the presence of a separate group of high-SSC, low-green-fluorescence (GFL) particles which were visible ca. 24 h after UV induction. By 96 h, this group was clearly distinguishable (Fig. 1B). It was likely that this group contained VLPs, despite the fact that it had a unique SSC-versus-GFL signal with the SSC higher than that of previously described bacteriophages and viruses (9). The higher SSC suggested that the particles might be filamentous, since SSC is influenced by internal structure and its refractive index (9). Of the zooxanthella isolates screened for UV induction of potential latent viruses, 38% showed proliferation of a group of VLPs similar to that shown in Fig. 1B. VLPs in this high-SSC group were concentrated from a 3-liter culture of zooxanthella strain CCMP 2465. CsCl gradient centrifugation produced a discrete white band at a density of 1.25 g cm^{-3} (Fig. 1C). AFC analysis of this band revealed that it was dominated by the same high-SSC group of VLPs (Fig. 1D).

In UV induction experiments, a decline in the zooxanthella concentration was observed starting 24 h after UV induction, which correlated with the appearance and rapid increase in the concentration of the high-SSC VLP group (Fig. 2A). The concentration of the VLPs continued to increase to just over 2×10^6 particles ml^{-1} at 96 h after UV treatment, at which point the UV-induced zooxanthella culture had lysed.

Since the zooxanthella cultures were nonaxenic, a group with a signal characteristic of bacteria was present in the control (Fig. 1A), as well as in the UV-treated zooxanthella cultures (Fig. 1B). To rule out the possibility that lysogenic bacteria were the source of the high-SSC VLPs, bacterial concentrations were also monitored in the induction experiments. The temporal changes in bacterial concentrations were similar in the control and UV-treated cultures, although there was a slight decrease in the UV-treated cultures between 24 and 48 h, before they again exhibited the same growth rate as the control (Fig. 2B). This initial decrease in bacterial concentrations could have been caused by several factors, such as lysis of UV-sensitive bacteria and/or induction of lysogenic bacteriophage, although there was no apparent increase in the number of bacteriophage particles compared to the control during the induction experiment (Fig. 2B). Bacteriophages usually group in the area above the instrument noise in the bottom left corner of a GFL-versus-SSC plot (Fig. 1A) (9). This group was analyzed, and the number of events remained consistent for the controls and the experimental samples throughout the experiment. While the experimental treatment appeared to have an effect on the numbers of bacteria present in the nonaxenic zooxanthella culture, the clear correlation between the decrease in the size of the zooxanthella population and the con-

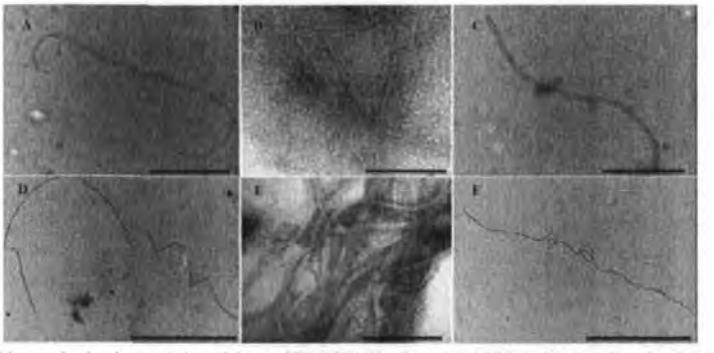

FIG. 3. TEM images showing the morphology of the new VLP, ZFV1. The filamentous VLP is ca. 2 to 3 μm long. (A, C, D, and F) Images from spot grids containing unconcentrated lysate. Scale bars = 1 μm. (B and E) Images of VLPs concentrated on a CsCl gradient (shown in Fig. 1C). Scale bars = 200 nm.

current increase in the VLP concentration suggests that bacterial contaminants were not the source of the new VLP group observed by AFC.

Identification of VLPs. After induction free VLPs in the UV-treated supernatants and concentrates were observed by TEM as *long flexible filaments* that were 2 to 3 μm long and approximately 30 nm wide (Fig. 3). In VLPs purified by CsCl gradient centrifugation there was an increase in the density of the filamentous VLPs after concentration (3×10^7 VLPs ml^{-1}) (Fig. 3B and E). Thin sections of UV-treated zooxanthellae

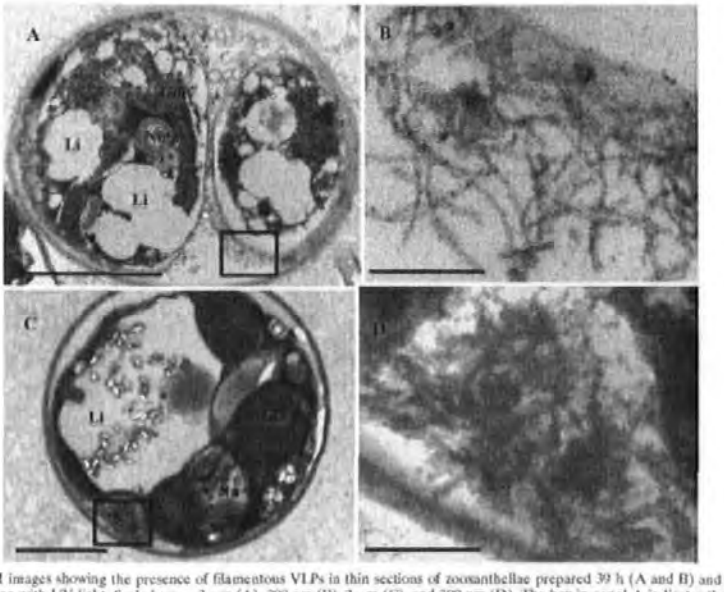

FIG. 4. TEM images showing the presence of filamentous VLPs in thin sections of zooxanthellae prepared 39 h (A and B) and 46 h (C and D) after induction with UV light. Scale bars = 3 μm (A), 200 nm (B), 2 μm (C), and 300 nm (D). The box in panel A indicates the area shown in panel B, and the box in panel C indicates the area shown in panel D. Chl, chloroplast; Nu, nucleus; Li, lipid vacuole.

revealed pockets of filamentous VLPs with similar morphology in the cytoplasm on the periphery of zooxanthella cells (Fig. 4); filamentous VLPs were not seen in controls. The incidence of VLPs observed in the thin sections increased markedly between 39 and 46 h postinduction compared to the incidence in noninduced controls (in which no filaments were observed). The presence of intracellular VLPs provides further evidence that the particles observed were actually infecting the zooxanthellae and not the bacteria present in the cultures. Therefore, we designated the new group of VLPs "zooxanthella filamentous virus 1" (ZFV1).

The majority of algal viruses described to date are members of the *Phycodnaviridae*, which is a family of large double-stranded DNA viruses that have an icosahedral shape (38, 44), although more recently a number of algal RNA viruses have also been isolated and characterized (21, 34, 36). ZFV1 is morphologically similar to RNA viruses which are known to infect plants, in particular viruses belonging to the family *Closteroviridae*. Members of this family are filamentous and flexuous, and they are 1,500 to 2,200 nm long (1, 39). However, determination of the taxonomic affiliation of ZFV1 will require further molecular characterization, and this certainly warrants further investigation.

Implications for the mechanism of coral bleaching. Wilson et al. (43) first suggested that zooxanthellae may harbor a latent infection, after showing that VLPs were present in zooxanthellae of thermally stressed anemones and that isolated VLPs could reinfect zooxanthellae. Further studies have shown that VLPs are present in three species of tropical coral (11). While the hosts of the numerous VLPs remain unknown, the abundance of VLPs and their close association with corals and the symbiotic zooxanthellae is evident. A variety of VLP forms have been observed, and while most of VLPs are hexagonal, it is notable that a filamentous VLP (up to 3 μm long) whose morphology is similar to that of ZFV1 has been observed in seawater following exposure of the coral *Acropora formosa* to heat stress (11). Although in our experiments we utilized nonaxenic cultures, our results clearly indicate that zooxanthellae contain a latent virus that is induced by UV treatment, leading to the lysis of the zooxanthellae. Extrapolation from this virus-host interaction and its effects on zooxanthella viability provides a novel link to the impact of latent infection on symbiotic dinoflagellates and the subsequent disruption of reef ecosystems. If stress-induced viral induction in zooxanthellae occurs in the natural reef environment, the presence of this new group of filamentous VLPs is clearly important.

ACKNOWLEDGMENTS

We acknowledge help and advice provided by Roy Moate, Peter Bond, and Glen Harper from the Plymouth Electron Microscopy Centre, University of Plymouth.

W.H.W. was supported through the NERC-funded core strategic research program of the Plymouth Marine Laboratory.

REFERENCES

1. Agranovsky, A. A., D. E. Lesemann, R. Maiss, R. Hull, and J. G. Atabekov. 1995. "Rattlesnake" structure of a filamentous plant RNA virus built of two capsid proteins. Proc. Natl. Acad. Sci. USA 92:2170–2173.
2. Baker, A. C. 2003. Flexibility and specificity in coral algal symbiosis: diversity, ecology, and biogeography of *Symbiodinium*. Annu. Rev. Ecol. Evol. Syst. 34:661–689.
3. Baker, A. C. 2001. Reef corals bleach to survive change. Nature 411:765–766.
4. Banin, E., Y. Ben-Haim, T. Israely, Y. Loya, and E. Rosenberg. 2000. Effect of the environment on the bacterial bleaching of corals. Water Air Soil Pollut. 123:337–352.
5. Ben-Haim, Y., M. Zicherman-Keren, and E. Rosenberg. 2003. Temperature-regulated bleaching and lysis of the coral *Pocillopora damicornis* by the novel pathogen *Vibrio coralliilyticus*. Appl. Environ. Microbiol. 69:4236–4242.
6. Bergh, O., K. Y. Børsheim, G. Bratbak, and M. Heldal. 1989. High abundance of viruses found in aquatic environments. Nature 340:467–468.
7. Brown, B. E. 1997. Coral bleaching: causes and consequences. Coral Reefs 16:129–138.
8. Brussaard, C. 2004. Viral control of phytoplankton populations—a review. J. Eukaryot. Microbiol. 51:125–138.
9. Brussaard, C. P. D. 2004. Optimization of procedures for counting viruses by flow cytometry. Appl. Environ. Microbiol. 70:1506–1513.
10. Buddemeier, R. W., and D. G. Fautin. 1993. Coral bleaching as an adaptive mechanism—a testable hypothesis. BioScience 43:320–326.
11. Davy, S. K., S. G. Burchett, A. L. Dale, P. Davies, J. E. Davy, C. Muncke, O. Hoegh-Guldberg, and W. H. Wilson. 2006. Viruses: agents of coral disease? Dis. Aquat. Org. 69:101–110.
12. Davy, S. K., L. A. N. Lucas, and J. R. Turner. 1996. Carbon budgets in temperate anthozoan-dinoflagellate symbioses. Mar. Biol. 126:773–783.
13. Fitt, W. K., B. E. Brown, M. E. Warner, and R. P. Dunne. 2001. Coral bleaching: interpretation of the thermal tolerance limits and thermal thresholds in tropical corals. Coral Reefs 20:51–65.
14. France, S. 1976. On the presence of virus-like particles in the dinoflagellate *Gyrodinium resplendens* (Hulburt). Protistologica 12:425–430.
15. Glynn, P. W., N. J. Gassman, C. M. Eakin, J. Cortes, D. B. Smith, and H. M. Guzman. 1991. Reef coral reproduction in the eastern Pacific: Costa Rica, Panama, and Galapagos Islands (Ecuador). I. Pocilloporidae. Mar. Biol. 109:355–368.
16. Hayes, R. L., and P. G. Bush. 1990. Microscopic observations of recovery in the reef building scleractinian coral, *Montastrea annularis*, after bleaching on a Cayman reef. Coral Reefs 9:203–209.
17. Jokiel, P. L., and S. L. Coles. 1990. Response of Hawaiian and other Indo Pacific reef corals to elevated temperatures. Coral Reefs 8:155–162.
18. Jones, R. J. 1997. Changes in zooxanthellar densities and chlorophyll concentrations in corals during and after a bleaching event. Mar. Ecol. Prog. Ser. 158:51–59.
19. Kushmaro, A., E. Rosenberg, M. Fine, and Y. Loya. 1997. Bleaching of the coral *Oculina patagonica* by Vibrio AK-1. Mar. Ecol. Prog. Ser. 147:159–165.
20. LaJeunesse, T. 2001. Investigating the biodiversity, ecology, and phylogeny of endosymbiotic dinoflagellates in the genus *Symbiodinium* using the ITS region: In search of a "species" level marker. J. Phycol. 37:866–880.
21. Lang, A. S., A. I. Culley, and C. A. Suttle. 2004. Genome sequence and characterization of a virus (HaRNAV) related to picorna-like viruses that infects the marine toxic bloom-forming alga *Heterosigma akashiwo*. Virology 320:206–217.
22. Larsen, A., T. Castberg, R. A. Sandaa, C. P. D. Brussaard, J. Egge, M. Heldal, A. Paulino, R. Thyrhaug, van B. J. Hannen, and G. Bratbak. 2001. Population dynamics and diversity of phytoplankton, bacteria and viruses in a seawater enclosure. Mar. Ecol. Prog. Ser. 221:47–57.
23. Marie, D., C. P. D. Brussaard, R. Thyrhaug, G. Bratbak, and D. Vaulot. 1999. Enumeration of marine viruses in culture and natural samples by flow cytometry. Appl. Environ. Microbiol. 65:45–52.
24. Muscatine, L. 1990. The role of symbiotic algae in carbon and energy flux in reef corals, p. 75–87. *In* Z. Dubinsky (ed.), Ecosystems of the world: coral reefs, vol. 25. Elsevier, Amsterdam, The Netherlands.
25. Provasoli, L., J. J. A. McLaughlin, and M. R. Droop. 1957. The development of artificial media for marine algae. Arch. Microbiol. 25:392–428.
26. Reisser, W. 1993. Viruses and virus-like particles of freshwater and marine eucaryotic algae—a review. Arch. Protistenkd. 143:257–265.
27. Rohwer, F., V. Segritsan, P. Azam, and N. Knowlton. 2002. Diversity and distribution of coral-associated bacteria. Mar. Ecol. Prog. Ser. 243:1–10.
28. Rosenberg, E., and Y. Ben-Haim. 2002. Microbial diseases of corals and global warming. Environ. Microbiol. 4:318–326.
29. Schroeder, D. C., J. Oke, M. Hall, G. Malin, and W. H. Wilson. 2003. Virus succession observed during an *Emiliania huxleyi* bloom. Appl. Environ. Microbiol. 69:2484–2490.
30. Sicko-Goad, L., and G. Walker. 1979. Viroplasm and large virus-like particles in the dinoflagellate *Gymnodinium uberrimum*. Protoplasma 99:203–210.
31. Snyshura, K. R., M. Coasera, P. W. Sammarco, and T. J. Pivac. 2004. Bleaching as a pathogenic response in scleractinian corals, evidenced by high concentrations of apoptotic and necrotic zooxanthellae. J. Exp. Mar. Biol. Ecol. 304:99–121.
32. Suttle, C. A. 2000. The ecological, evolutionary, and geochemical consequences of viral infection of cyanobacteria and eukaryotic algae, p. 248–296. *In* C. J. Hurst (ed.), Viral ecology. Academic Press, New York, N.Y.
33. Szmant, A., and N. J. Gassman. 1990. The effects of prolonged bleaching on the tissue biomass and reproduction of the reef coral *Montastrea annularis*. Coral Reefs 8:217–224.
34. Tai, V., J. E. Lawrence, A. S. Lang, A. M. Chan, A. I. Culley, and C. A. Suttle.

2003. Characterization of HaRNAV, a single-stranded RNA virus causing lysis of Heterosigma akashiwo (Raphidophyceae). J. Phycol. 39:343–352.
35. Tarutani, K., K. Nagasaki, S. Itakura, and M. Yamaguchi. 2001. Isolation of a virus infecting the novel shellfish killing dinoflagellate *Heterocapsa circularisquama*. Aquat. Microb. Ecol. 23:103–111.
36. Tomaru, Y., N. Katanozaka, K. Nishida, Y. Shirai, K. Tarutani, M. Yamaguchi, and K. Nagasaki. 2004. Isolation and characterization of two distinct types of HcRNAV, a single-stranded RNA virus infecting the bivalve-killing microalga Heterocapsa circularisquama. Aquat. Microb. Ecol. 34:207–218.
37. Toren, A., L. Landau, A. Kushmaro, Y. Loya, and E. Rosenberg. 1998. Effect of temperature on adhesion of *Vibrio* strain AK-1 to *Oculina patagonica* and on coral bleaching. Appl. Environ. Microbiol. 64:1379–1384.
38. Van Etten, J. L., and R. H. Meints. 1999. Giant viruses infecting algae. Annu. Rev. Microbiol. 53:447–494.
39. van Regenmortel, M. H. V., C. M. Fauquet, D. H. Bishop, E. B. Carsten, M. K. Estes, S. M. Lemon, J. Maniloff, M. A. Mayo, D. J. McGeoch, C. R. Pringle, and R. B. Wickner (ed.). 2000. Virus taxonomy: classification and nomenclature of viruses: seventh report of the international committee on taxonomy of viruses. Academic Press Inc., San Diego, CA.
40. Wang, J., and A. E. Douglas. 1998. Nitrogen recycling or nitrogen conservation in an alga-invertebrate symbiosis? J. Exp. Biol. 201:2445–2453.
41. Wilkinson, C. 1998. Status of coral reefs of the world. Australian Institute of Marine Science, Townsville, Australia.
42. Wilson, W. H., A. L. Dale, J. E. Davy, and S. K. Davy. 2005. An enemy within? Observations of virus-like particles in reef corals. Coral Reefs 24: 145–146.
43. Wilson, W. H., I. Francis, K. Ryan, and S. K. Davy. 2001. Temperature induction of viruses in symbiotic dinoflagellates. Aquat. Microb. Ecol. 25: 99–102.
44. Wommack, K. E., and R. R. Colwell. 2000. Virioplankton: viruses in aquatic ecosystems. Microbiol. Mol. Biol. Rev. 64:69–114.